

Fundamental solubility study of polycyclic aromatic hydrocarbons in subcritical water and ethanol mixtures

Author:

Teoh, Wen Hui

Publication Date:

2012

DOI:

<https://doi.org/10.26190/unsworks/15691>

License:

<https://creativecommons.org/licenses/by-nc-nd/3.0/au/>

Link to license to see what you are allowed to do with this resource.

Downloaded from <http://hdl.handle.net/1959.4/52135> in <https://unsworks.unsw.edu.au> on 2024-05-03



**FUNDAMENTAL SOLUBILITY STUDY OF
POLYCYCLIC AROMATIC HYDROCARBONS IN
SUBCRITICAL WATER AND ETHANOL MIXTURES**

by

Wen Hui TEOH, B.E. (Chemical Engineering), MPhil (Engineering)

A thesis submitted to the School of Chemical Engineering in partial fulfilment of the
requirements of the degree

Doctor of Philosophy (PhD)

The University of New South Wales

October 2012

PLEASE TYPE**THE UNIVERSITY OF NEW SOUTH WALES
Thesis/Dissertation Sheet**

Surname or Family name: TEOH

First name: WEN HUI

Other name/s:

Abbreviation for degree as given in the University calendar: PHD

School: CHEMICAL ENGINEERING

Faculty: ENGINEERING

Title:

FUNDAMENTAL SOLUBILITY STUDY OF POLYCYCLIC AROMATIC HYDROCARBONS IN SUBCRITICAL WATER AND ETHANOL MIXTURES

Abstract 350 words maximum: (PLEASE TYPE)

Water is increasingly being used as a processing medium as a consequence of the current emphasis for sustainable processes. At relatively high temperatures and pressures, water acts as a good solvent, resulting in a number of potential applications. A lack of fundamental data, however, has limited the development of subcritical water technologies. Hence, solubility studies are essential to quantify the solvating power of subcritical water and to determine the thermodynamic limit of a process.

A static analytical equilibrium method was used to measure the binary and ternary solubilities of anthracene and *p*-terphenyl in subcritical water and ethanol mixtures between 393 K and 473 K, and at 50 bar and 150 bar. Temperature was found to have the most significant effect on the solubility of polycyclic aromatic hydrocarbons (PAHs) in subcritical water. The effect of pressure, and the combined effect of temperature and pressure on solubility were found to be insignificant, particularly when the range of pressure considered is relatively small. It was also found in this work that the solubilities of PAHs are governed primarily by sublimation pressure, and only secondarily by the dielectric constant of water. The use of small amounts of ethanol in subcritical water systems was found to greatly enhance the solubility of hydrophobic solutes and thus, is able to expand the range of applications of subcritical water technologies, while enabling relatively mild operating conditions to be maintained.

The UNIQUAC, O-UNIFAC, and M-UNIFAC models were used to correlate the solubilities of PAHs in subcritical conditions. The UNIQUAC model best represents the solubilities of anthracene and *p*-terphenyl in binary and ternary systems while the O-UNIFAC and M-UNIFAC models perform poorly. The poor performance of the O-UNIFAC and the M-UNIFAC models were mainly due to the inadequacy of the residual component of the activity coefficient. All three models show increasing deviations from experimental data as ethanol concentration increases.

Declaration relating to disposition of project thesis/dissertation

I hereby grant to the University of New South Wales or its agents the right to archive and to make available my thesis or dissertation in whole or in part in the University libraries in all forms of media, now or here after known, subject to the provisions of the Copyright Act 1968. I retain all property rights, such as patent rights. I also retain the right to use in future works (such as articles or books) all or part of this thesis or dissertation.

I also authorise University Microfilms to use the 350 word abstract of my thesis in Dissertation Abstracts International (this is applicable to doctoral theses only).

Teoh Wen Hui

Signature

Jane Beh

Witness

12/10/2012

Date

The University recognises that there may be exceptional circumstances requiring restrictions on copying or conditions on use. Requests for restriction for a period of up to 2 years must be made in writing. Requests for a longer period of restriction may be considered in exceptional circumstances and require the approval of the Dean of Graduate Research.

FOR OFFICE USE ONLY

Date of completion of requirements for Award:

COPYRIGHT STATEMENT

'I hereby grant the University of New South Wales or its agents the right to archive and to make available my thesis or dissertation in whole or part in the University libraries in all forms of media, now or here after known, subject to the provisions of the Copyright Act 1968. I retain all proprietary rights, such as patent rights. I also retain the right to use in future works (such as articles or books) all or part of this thesis or dissertation.

I also authorise University Microfilms to use the 350 word abstract of my thesis in Dissertation Abstract International (this is applicable to doctoral theses only).

I have either used no substantial portions of copyright material in my thesis or I have obtained permission to use copyright material; where permission has not been granted I have applied/will apply for a partial restriction of the digital copy of my thesis or dissertation.'

Signed *Teoh Wen Hui*

Date 12/10/2012

AUTHENTICITY STATEMENT

'I certify that the Library deposit digital copy is a direct equivalent of the final officially approved version of my thesis. No emendation of content has occurred and if there are any minor variations in formatting, they are the result of the conversion to digital format.'

Signed *Teoh Wen Hui*

Date 12/10/2012

Abstract

Water is increasingly being used as a processing medium as a consequence of the current emphasis for sustainable processes. At relatively high temperatures and pressures, water acts as a good solvent, resulting in a number of potential applications. A lack of fundamental data, however, has limited the development of subcritical water technologies. Hence, solubility studies are essential to quantify the solvating power of subcritical water and to determine the thermodynamic limit of a process.

A static analytical equilibrium method was used to measure the binary and ternary solubilities of anthracene and *p*-terphenyl in subcritical water and ethanol mixtures between 393 K and 473 K, and at 50 bar and 150 bar. Temperature was found to have the most significant effect on the solubility of polycyclic aromatic hydrocarbons (PAHs) in subcritical water. The effect of pressure, and the combined effect of temperature and pressure on solubility were found to be insignificant, particularly when the range of pressure considered is relatively small. It was also found in this work that the solubilities of PAHs are governed primarily by sublimation pressure, and only secondarily by the dielectric constant of water. The use of small amounts of ethanol in subcritical water systems was found to greatly enhance the solubility of hydrophobic solutes and thus, is able to expand the range of applications of subcritical water technologies, while enabling relatively mild operating conditions to be maintained.

The UNIQUAC, O-UNIFAC, and M-UNIFAC models were used to correlate the solubilities of PAHs in subcritical conditions. The UNIQUAC model best represents the solubilities of anthracene and *p*-terphenyl in binary and ternary systems while the O-UNIFAC and M-UNIFAC models perform poorly. The poor performance of the O-UNIFAC and the M-UNIFAC models were mainly due to the inadequacy of the residual component of the activity coefficient. All three models show increasing deviations from experimental data as ethanol concentration increases.

In memory of my grandmother

*...whose imaginative storytelling
fuelled many of my own...*

Acknowledgement

To God be the glory, great things He has done – for He has so loved me, and delivered me. He is a faithful comforter and a tower of refuge, without Whom nothing could be accomplished.

I would like to thank Prof. Neil Foster for the opportunity to learn and grow under his supervision. It has been a privilege to work under a generous scientist who looks at the potential in others, and whose generosity means that he is always looking for opportunities to impart unto others so that transformations can take place. It would be challenging to follow in the footsteps of an agent who goes with a forward reaction rather than stays at equilibrium.

I am very grateful to Dr. Raffaella Mammucari, whose intellect, kindness, gentleness and patience meant that she became the sounding board for ideas and problems. You are the “steady state” in the ever-changing research environment.

I am indebted to Dr. Silvio A. B. Vieira de Melo who helped me navigate through the myriad and complex world of thermodynamics. You are God-sent and the catalyst to a big portion of this work. While not contributing directly to this work, I would like to acknowledge Dr. Ronald Pratt who first instilled my love for thermodynamics and built the foundation with which I could work upon.

I am grateful to God for the gift of a lifelong friend – Jane Beh – whose shared laughter became a comfort in a grueling PhD process. Our friendship is surely stronger than the hydrogen-bonds! I would like to thank Danh for his timely reminders and constant motivations that pushed me to finish the race. I am grateful to Ruth for her friendship, assistance and her curries throughout the course of this PhD. A well-fed student is a happy student. I am glad I met the group of Taïdo martial artists. The shared camaraderie and constant workout had kept me fit, happy and focused; yielding the right balance in my PhD life.

I am indebted to Mr. Van Bong Dang, Ms. Ik Ling Lau, Dr. Robert Chan, Ms. Ee Meen Iliffe, Phil, Paul, Rama, Jim, Ian, Ann, and Sandra for their assistance throughout the years. I am

thankful to all former colleagues – Roshan, Wendy and Adam – whose footprints paved the way that left testaments to God’s sustaining grace.

Lastly, I am eternally grateful to my family and friends whose constant prayers, love and encouragements had gotten me through this tough process. To my greatest supporters – my parents – both of you will always have my love and gratitude.

This thesis is not just a book that peers into solubility. Rather, it is also a reflection on the journey itself, where knowledge was gained and bonds established – much like a warm solution in a mixing pot with an activity coefficient that approaches unity (ideal solution). For all the big and small “molecules” that were in the little mixing pot, this thesis is as much yours as it is in my name.

List of publications

Conference papers

1. Wen Hui Teoh, Raffaella Mammucari, Neil R. Foster. *Measuring solubility in subcritical water*. International Conference on Process Intensification for Sustainable Chemical Industries (ICPI 2011). Beijing, China. 26-29 June 2011
2. Wen Hui Teoh, Raffaella Mammucari, Neil R. Foster. *Ternary solubilities of anthracene in binary water/ethanol mixtures at temperatures ranging from 393 K to 473 K*. Chemeca 2011. Sydney, 18-21 Sept., 2011

Articles

1. Wen H. Teoh, Raffaella Mammucari, Silvio A. B. Vieira de Melo, Neil R. Foster. *Solubility and solubility modeling of polycyclic aromatic hydrocarbons in subcritical water*. [submitted to the Industrial and Engineering Chemistry Research]
2. Wen H. Teoh, Raffaella Mammucari, Silvio A. B. Vieira de Melo, Neil R. Foster. *Solubility and solubility modeling of polycyclic aromatic hydrocarbons in ethanol-modified subcritical water*. [in preparation]
3. Wen H. Teoh, Silvio A. B. Vieira de Melo, Raffaella Mammucari, Neil R. Foster. *Activity coefficient based solubility modeling of polycyclic aromatic hydrocarbons in subcritical water and ethanol mixtures*. [in preparation]

Table of contents

Chapters	#
1 Introduction	1
1.1 Bibliography	6
2 Solubility and factors that affect solubility in subcritical water	9
2.1 Introduction	9
2.2 The effects of intermolecular forces on solubility	11
2.3 The effects of the free volume difference on solubility	13
2.4 Solute effects on solubility in subcritical water	14
2.5 Co-solvent and co-solute effects on solubility	17
2.6 Conclusion	18
2.7 Bibliography	19
3 Solubility measurement of solid PAHs in subcritical water	21
3.1 Introduction	21
3.1.1 Dynamic extractive equilibrium method	22
3.1.2 Static analytical equilibrium method	24
3.2 Preparation for solubility measurement: water and solutes characterization at subcritical conditions	26
3.2.1 Vapor-liquid equilibria of water, solid-vapor equilibria of the solutes at subcritical conditions	26
3.2.2 Phase behavior of organic solutes in subcritical water	27

3.2.3	Temperature and pressure profiles of liquid solvents in an equilibrium vessel	30
3.2.4	Stability of solid solutes at experimental conditions	35
3.3	Solubility measurement	36
3.3.1	Materials	36
3.3.2	Apparatus and experimental method	36
3.3.3	Rig validation	40
3.3.4	Preliminary study on the effect of temperature and pressure on the solubility of a PAH in subcritical water	44
3.3.5	The effect of temperature on the solubility of PAHs in subcritical water: binary systems	46
3.3.6	The effect of temperature on the solubility of PAHs in subcritical water: ternary systems	51
3.4	Conclusion	54
3.5	Bibliography	55
4	Solubility measurement of PAHs in ethanol-modified subcritical water and subcritical ethanol	57
4.1	Solubility measurement of PAHs in ethanol-modified subcritical water	57
4.2	Preparation for solubility measurement: solvents and solutes behaviour at subcritical conditions	58
4.2.1	Vapor-liquid equilibria at subcritical conditions	59
4.2.2	Phase behavior of PAHs in ethanol-modified subcritical water	60
4.3	Solubility measurement	61
4.3.1	Materials	61

4.3.2	Apparatus and experimental method	62
4.3.3	Preliminary study on the effect of temperature, pressure and the addition of ethanol on the solubility of a PAH in modified subcritical water system	62
4.3.4	The effect of temperature and ethanol mole fraction on the solubility of PAHs in modified subcritical water systems	66
4.4	Solubility measurement of solid PAHs in subcritical ethanol	77
4.4.1	Ethanol VLE and the phase behavior of solutes at subcritical conditions	77
4.4.2	Solubility measurement in subcritical ethanol	80
4.4.3	The effect of temperature on the solubility of PAHs in subcritical ethanol	81
4.5	Conclusion	83
4.6	Bibliography	84
5	Thermodynamic modelling	85
5.1	Introduction	85
5.2	Thermodynamic framework	88
5.2.1	The UNIQUAC model	89
5.2.2	The O-UNIFAC model	91
5.2.3	The M-UNIFAC model	91
5.3	Results and discussion	94
5.3.1	Empirical model: variation of solubility with temperature	94
5.3.2	Correlation via the UNIQUAC model	99
5.3.3	Correlation via the O-UNIFAC model	126
5.3.4	Correlation via the M-UNIFAC model	141

5.3.5 Comparing the UNIQUAC, O-UNIFAC and M-UNIFAC models	156
5.4 Conclusion	177
5.5 Bibliography	178
6 Conclusion and recommendation	180
Appendix A	182
Appendix B	189

List of figures

Figures	#
Figure 1.1 The dielectric constant of water at various temperatures and pressures	2
Figure 2.1 Factors that contribute to the solubility of a solute in a solvent	10
Figure 2.2 Dielectric constant of water and water-ethanol mixtures at various temperatures	18
Figure 3.1 Dynamic extractive equilibrium experimental set-up for solubility study by Miller and Hawthorne (1998)	23
Figure 3.2 General schematic diagram of solubility determination based on the static equilibrium method	24
Figure 3.3 Schematic diagram of the phase behaviour study	28
Figure 3.4 Schematic diagram of temperature profiling in an equilibrium vessel	30
Figure 3.5 Schematic diagram of high pressure profiling in an equilibrium vessel	32
Figure 3.6 Pressure profile at 100 °C, 150 °C and 200 °C	32
Figure 3.7 Pressure and temperature profiles of subcritical water in an equilibrium vessel at 100 °C	33
Figure 3.8 Pressure and temperature profiles of subcritical water in an equilibrium vessel at 150 °C	34
Figure 3.9 Pressure and temperature profiles of subcritical water in an equilibrium vessel at 200 °C	34
Figure 3.10 Schematic diagram of the solubility apparatus	37
Figure 3.11 (a) Front view of equilibrium vessel	37
(b) Cross-section view of filter stone set-up	37

Figure 3.12	Heating and equilibration times required for solubility measurements at various temperatures	38
Figure 3.13	Front view of the collection vessel	39
Figure 3.14	Solubility data of anthracene in subcritical water at various temperatures from various sources	42
Figure 3.15	Interaction plots: the effects of temperature and pressure on the solubility of anthracene in subcritical water	45
Figure 3.16	Binary solubility data of anthracene and <i>p</i> -terphenyl in subcritical water at 50 bar and various temperatures	47
Figure 3.17	The variation of the sublimation pressure of solid PAHs with temperature	48
Figure 3.18	Dielectric constant of subcritical water at 50 bar and various temperatures	48
Figure 3.19	The variation in the density of subcritical water with temperature at 50 bar	50
Figure 3.20	Solubility of ternary anthracene and <i>p</i> -terphenyl in subcritical water as a function of temperature	53
Figure 3.21	Natural logarithmic solubility of anthracene and <i>p</i> -terphenyl in binary and ternary subcritical water systems	53
Figure 4.1	<i>P</i> - <i>x</i> - <i>y</i> diagram of ethanol-water VLE at 200 °C	60
Figure 4.2	Interaction plots: the effects of temperature and pressure on the solubility of anthracene in subcritical water/ethanol system at $f = 0.06$	63
Figure 4.3	Interaction plots: the effects of temperature and ethanol mole fractions on the solubility of anthracene in subcritical water/ethanol systems at 50 bar	65
Figure 4.4	Solubility of anthracene as a function of temperature in subcritical water (1) – ethanol (2) – anthracene (3) systems	70

Figure 4.5	Solubility of <i>p</i> -terphenyl as a function of temperature in subcritical water (1) – ethanol (2) – <i>p</i> -terphenyl (3) systems	71
Figure 4.6	Solubility of anthracene as a function of ethanol mole fraction in subcritical water(1) – ethanol (2) – anthracene systems	72
Figure 4.7	Solubility of <i>p</i> -terphenyl as a function of ethanol mole fraction in subcritical water (1) – ethanol (2) – <i>p</i> -terphenyl (3) systems	73
Figure 4.8	Plot of $\ln(x_3)$ versus temperature for anthracene in subcritical water/ethanol	74
Figure 4.9	Plot of $\ln(x_3)$ versus temperature for <i>p</i> -terphenyl in subcritical water/ethanol	74
Figure 4.10	Plot of $\ln(x_3)$ versus ethanol mole fractions for anthracene in subcritical water/ethanol	75
Figure 4.11	Plot of $\ln(x_3)$ versus ethanol mole fractions for <i>p</i> -terphenyl in subcritical water/ethanol	75
Figure 4.12	Plot of $\ln(x_3)$ against ethanol mole fraction and temperature for anthracene	76
Figure 4.13	Plot of $\ln(x_3)$ versus ethanol mole fraction and temperature for <i>p</i> -terphenyl	76
Figure 4.14	The dielectric constant of ethanol at various temperatures	78
Figure 4.15	Schematic diagram of the solubility apparatus for measurement in subcritical ethanol	81
Figure 4.16	Solubility data of anthracene and <i>p</i> -terphenyl in subcritical ethanol at 50 bar and various temperatures	82
Figure 5.1	$\ln(x_2)$ as a function of temperature for subcritical water (1) – anthracene (2) and subcritical water (1) – <i>p</i> -terphenyl (2) systems	95
Figure 5.2	$\ln(x_2)$ as a function of temperature for subcritical ethanol (1) – anthracene (2) and subcritical ethanol (1) – <i>p</i> -terphenyl (2) systems	95

Figure 5.3	$\ln(x_3)$ as a function of temperature for subcritical water (1) – ethanol (2) – anthracene (3) systems	96
Figure 5.4	$\ln(x_3)$ as a function of temperature for subcritical water (1) – ethanol (2) – <i>p</i> -terphenyl (3) systems	96
Figure 5.5	Sublimation pressure ratio of anthracene relative to <i>p</i> -terphenyl	98
Figure 5.6	Sensitivity analysis conducted on subcritical water (1) - anthracene (3) system to obtain global minima [$a_{ji} = (u_{ji} - u_{ii})/R$]	101
Figure 5.7	Sensitivity analysis conducted on subcritical ethanol (2) - anthracene (3) system to obtain global minima [$a_{ji} = (u_{ji} - u_{ii})/R$]	102
Figure 5.8	Sensitivity analysis conducted on subcritical water (1) - <i>p</i> -terphenyl (3) system to obtain global minima [$a_{ji} = (u_{ji} - u_{ii})/R$]	103
Figure 5.9	Sensitivity analysis conducted on subcritical ethanol (2) - <i>p</i> -terphenyl (3) system to obtain global minima [$a_{ji} = (u_{ji} - u_{ii})/R$]	104
Figure 5.10	Experimental and UNIQUAC calculated solubility at various temperatures in ethanol (1) – anthracene (2) system with $(u_{ji} - u_{ii})/R = a_{ji}$	106
Figure 5.11	Experimental and UNIQUAC calculated solubility at various temperatures in ethanol (1) – <i>p</i> -terphenyl (2) system with $(u_{ji} - u_{ii})/R = a_{ji}$	106
Figure 5.12	Experimental and UNIQUAC calculated solubility at various temperatures in water (1) – anthracene (2) system with $(u_{ji} - u_{ii})/R = a_{ji}$	107
Figure 5.13	Experimental and UNIQUAC calculated solubility at various temperatures in water (1) – <i>p</i> -terphenyl (2) system with $(u_{ji} - u_{ii})/R = a_{ji}$	107
Figure 5.14	Experimental and UNIQUAC calculated solubility at various temperatures with $(u_{ji} - u_{ii})/R = a_{ji}$ in water (1) – ethanol (2) – anthracene (3) system, $f = 0.01$	108

Figure 5.15	Experimental and UNIQUAC calculated solubility at various temperatures with $(u_{ji} - u_{ii})/R = a_{ji}$ in water (1) – ethanol (2) – anthracene (3) system, $f = 0.10$	108
Figure 5.16	Experimental and UNIQUAC calculated solubility at various temperatures with $(u_{ji} - u_{ii})/R = a_{ji}$ in water (1) – ethanol (2) – <i>p</i> -terphenyl (3) system, $f = 0.01$	109
Figure 5.17	Experimental and UNIQUAC calculated solubility at various temperatures with $(u_{ji} - u_{ii})/R = a_{ji}$ in water (1) – ethanol (2) – <i>p</i> -terphenyl (3) system, $f = 0.10$	109
Figure 5.18	Experimental and UNIQUAC calculated solubility as a function of temperature in subcritical water (1) – anthracene (2) system	118
Figure 5.19	Experimental and UNIQUAC calculated solubility as a function of temperature in subcritical ethanol (1) – anthracene (2) system	118
Figure 5.20	Experimental and UNIQUAC calculated solubility as a function of temperature in subcritical water (1) – ethanol (2) – anthracene (3) system, $f = 0.01$	119
Figure 5.21	Experimental and UNIQUAC calculated solubility as a function of temperature in subcritical water (1) – ethanol (2) – anthracene (3) system, $f = 0.10$	119
Figure 5.22	Experimental and UNIQUAC calculated solubility as a function of temperature in subcritical water (1) – <i>p</i> -terphenyl (2) system	120
Figure 5.23	Experimental and UNIQUAC calculated solubility as a function of temperature in subcritical ethanol (1) – <i>p</i> -terphenyl (2) system	120
Figure 5.24	Experimental and UNIQUAC calculated solubility as a function of temperature in subcritical water (1) – ethanol (2) – <i>p</i> -terphenyl (3) system, $f = 0.01$	121

Figure 5.25	Experimental and UNIQUAC calculated solubility as a function of temperature in subcritical water (1) – ethanol (2) – <i>p</i> -terphenyl (3) system, $f = 0.10$	121
Figure 5.26	Deviation between UNIQUAC calculated and experimental solubility data: anthracene in subcritical water, subcritical ethanol and ethanol-modified subcritical water	122
Figure 5.27	Deviation between UNIQUAC calculated and experimental data: <i>p</i> -terphenyl in subcritical water, subcritical ethanol and ethanol-modified subcritical water	123
Figure 5.28	Experimental and UNIQUAC calculated solubility as a function of temperature in subcritical water (1) – anthracene (2) – <i>p</i> -terphenyl (3) system	125
Figure 5.29	Experimental and O-UNIFAC calculated solubility as a function of temperature in subcritical water (1) – anthracene (2) system	133
Figure 5.30	Experimental and O-UNIFAC calculated solubility as a function of temperature in subcritical ethanol (1) – anthracene (2) system	133
Figure 5.31	Experimental and O-UNIFAC calculated solubility as a function of temperature in subcritical water (1) – ethanol (2) – anthracene (3) system, $f = 0.01$	134
Figure 5.32	Experimental and O-UNIFAC calculated solubility as a function of temperature in subcritical water (1) – ethanol (2) – anthracene (3) system, $f = 0.10$	134
Figure 5.33	Experimental and O-UNIFAC calculated solubility as a function of temperature in subcritical water (1) – <i>p</i> -terphenyl (2) system	135
Figure 5.34	Experimental and O-UNIFAC calculated solubility as a function of temperature in subcritical ethanol (1) – <i>p</i> -terphenyl (2) system	135

Figure 5.35	Experimental and O-UNIFAC calculated solubility as a function of temperature in subcritical water (1) – ethanol (2) – <i>p</i> -terphenyl (3) system, $f = 0.01$	136
Figure 5.36	Experimental and O-UNIFAC calculated solubility as a function of temperature in subcritical water (1) – ethanol (2) – <i>p</i> -terphenyl (3) system, $f = 0.10$	136
Figure 5.37	Deviation between O-UNIFAC calculated and experimental solubility data: anthracene in subcritical water, subcritical ethanol and ethanol-modified subcritical water	137
Figure 5.38	Deviation between O-UNIFAC calculated and experimental solubility data: <i>p</i> -terphenyl in subcritical water, subcritical ethanol and ethanol-modified subcritical water	138
Figure 5.39	O-UNIFAC calculated and experimental solubility values as a function of temperature in ternary system consisting of anthracene, <i>p</i> -terphenyl and subcritical water	140
Figure 5.40	Experimental and M-UNIFAC calculated solubility as a function of temperature in subcritical water (1) – anthracene (2) system	148
Figure 5.41	Experimental and M-UNIFAC calculated solubility as a function of temperature in subcritical ethanol (1) – anthracene (2) system	148
Figure 5.42	Experimental and M-UNIFAC calculated solubility as a function of temperature in subcritical water (1) – ethanol (2) – anthracene (3) system, $f = 0.01$	149
Figure 5.43	Experimental and M-UNIFAC calculated solubility as a function of temperature in subcritical water (1) – ethanol (2) – anthracene (3) system, $f = 0.10$	149
Figure 5.44	Experimental and M-UNIFAC calculated solubility as a function of temperature in subcritical water (1) – <i>p</i> -terphenyl (2) system	150

Figure 5.45	Experimental and M-UNIFAC calculated solubility as a function of temperature in subcritical ethanol (1) – <i>p</i> -terphenyl (2) system	150
Figure 5.46	Experimental and M-UNIFAC calculated solubility as a function of temperature in subcritical water (1) – ethanol (2) – <i>p</i> -terphenyl (3) system, $f = 0.01$	151
Figure 5.47	Experimental and M-UNIFAC calculated solubility as a function of temperature in subcritical water (1) – ethanol (2) – <i>p</i> -terphenyl (3) system, $f = 0.10$	151
Figure 5.48	Deviation between M-UNIFAC calculated and experimental values: anthracene in subcritical water, subcritical ethanol and ethanol-modified subcritical water	152
Figure 5.49	Deviation between M-UNIFAC calculated and experimental values: <i>p</i> -terphenyl in subcritical water, subcritical ethanol and ethanol-modified subcritical water	153
Figure 5.50	Comparisons between the M-UNIFAC calculated and experimental solubility values in ternary water (1) – anthracene (2) – <i>p</i> -terphenyl (3) system	155
Figure 5.51	Anthracene solubility in subcritical water calculated from various models and in comparison with experimental data	157
Figure 5.52	Anthracene solubility in subcritical ethanol calculated from various models and in comparison with experimental data	157
Figure 5.53	Anthracene solubility in ethanol-modified subcritical water calculated from various models and in comparison with experimental data, $f = 0.01$	158
Figure 5.54	Anthracene solubility in ethanol-modified subcritical water calculated from various models and in comparison with experimental data, $f = 0.02$	158
Figure 5.55	Anthracene solubility in ethanol-modified subcritical water calculated from various models and in comparison with experimental data, $f = 0.03$	159

Figure 5.56	Anthracene solubility in ethanol-modified subcritical water calculated from various models and in comparison with experimental data, $f = 0.04$	159
Figure 5.57	Anthracene solubility in ethanol-modified subcritical water calculated from various models and in comparison with experimental data, $f = 0.06$	160
Figure 5.58	Anthracene solubility in ethanol-modified subcritical water calculated from various models and in comparison with experimental data, $f = 0.10$	160
Figure 5.59	<i>p</i> -Terphenyl solubility in subcritical water calculated from various models and in comparison with experimental data	161
Figure 5.60	<i>p</i> -Terphenyl solubility in subcritical ethanol calculated from various models and in comparison with experimental data	161
Figure 5.61	<i>p</i> -Terphenyl solubility in ethanol-modified subcritical water calculated from various models and in comparison with experimental data, $f = 0.01$	162
Figure 5.62	<i>p</i> -Terphenyl solubility in ethanol-modified subcritical water calculated from various models and in comparison with experimental data, $f = 0.02$	162
Figure 5.63	<i>p</i> -Terphenyl solubility in ethanol-modified subcritical water calculated from various models and in comparison with experimental data, $f = 0.03$	163
Figure 5.64	<i>p</i> -Terphenyl solubility in ethanol-modified subcritical water calculated from various models and in comparison with experimental data, $f = 0.04$	163
Figure 5.65	<i>p</i> -Terphenyl solubility in ethanol-modified subcritical water calculated from various models and in comparison with experimental data, $f = 0.06$	164
Figure 5.66	<i>p</i> -Terphenyl solubility in ethanol-modified subcritical water calculated from various models and in comparison with experimental data, $f = 0.10$	164
Figure 5.67	Anthracene solubility in water (1) – anthracene (2) – <i>p</i> -terphenyl (3) system calculated from various models and in comparison with experimental data	165

Figure 5.68	<i>p</i> -Terphenyl solubility in water (1) – anthracene (2) – <i>p</i> -terphenyl (3) system calculated from various models and in comparison with experimental data	165
Figure 5.69	Natural logarithm of activity coefficient as a function of temperature for anthracene in various subcritical solvent systems	166
Figure 5.70	Natural logarithm of activity coefficient as a function of temperature for <i>p</i> -terphenyl in various subcritical solvent systems	167
Figure 5.71	Natural logarithm of activity coefficient as a function of anthracene solubility in various subcritical solvent systems	168
Figure 5.72	Natural logarithm of activity coefficient as a function of <i>p</i> -terphenyl solubility in various subcritical solvent systems	169
Figure 5.73	$\ln \gamma^C$ as a function of anthracene solubility in various subcritical solvent systems	170
Figure 5.74	$\ln \gamma^C$ as a function of <i>p</i> -terphenyl solubility in various subcritical solvent systems	171
Figure 5.75	$\ln \gamma^R$ as a function of anthracene solubility in various subcritical solvent systems	172
Figure 5.76	$\ln \gamma_2^R$ as a function of <i>p</i> -terphenyl solubility in various subcritical solvent systems	173
Figure A.1	FT-IR spectra of raw anthracene	183
Figure A.2	FT-IR spectra of anthracene post solubility measurement in subcritical water at 120 °C, 50 bar and 197 minutes	184
Figure A.3	FT-IR spectra of anthracene post solubility measurement in subcritical water at 180 °C, 50 bar and 63 minutes	184
Figure A.4	FT-IR spectra of anthracene post solubility measurement in subcritical water at 200 °C, 50 bar and 50 minutes	185

Figure A.5	FT-IR spectra of raw <i>p</i> -terphenyl	186
Figure A.6	FT-IR spectra of <i>p</i> -terphenyl post solubility measurement in subcritical water at 120 °C, 50 bar and 197 minutes	187
Figure A.7	FT-IR spectra of <i>p</i> -terphenyl post solubility measurement in subcritical water at 180 °C, 50 bar and 63 minutes	188
Figure A.8	FT-IR spectra of <i>p</i> -terphenyl post solubility measurement in subcritical water at 200 °C, 50 bar and 50 minutes	188
Figure B.1	Calibration curve of anthracene in methanol at 356 nm	190
Figure B.2	Calibration curve of <i>p</i> -terphenyl in methanol at 278 nm	191
Figure B.3	Calibration curve of anthracene in acetonitrile at 357 nm	192
Figure B.4	Calibration curve of <i>p</i> -terphenyl in acetonitrile at 279 nm	193

List of tables

Tables	#
Table 2.1 Solubilities (in mole fraction) of various organic compounds in subcritical water at 140 °C, and their corresponding molecular structure	15
Table 2.2 Solubilities (in mole fraction) of various organic compounds in subcritical water at 150 °C, and their corresponding molecular structure	16
Table 2.3 Solubility of atrazine in subcritical water and ethanol-modified subcritical water at 100 °C and 50 bar	17
Table 3.1 Vapor pressures for water, anthracene and <i>p</i> -terphenyl at various temperatures	27
Table 3.2 Phase behaviour of anthracene and <i>p</i> -terphenyl in subcritical water at 50 bar and various temperatures	29
Table 3.3 Average heating time to attain a required temperature in an equilibrium vessel	31
Table 3.4 Solubility (x_2) of anthracene (mole fraction) in subcritical water measured using various methods	41
Table 3.5 Solubility data of anthracene in subcritical water at 140 °C and 180 °C, and at pressures of 50 bar and 150 bar	45
Table 3.6 Main effects that contribute to the solubility of anthracene in subcritical water	46
Table 3.7 Solubility data (mole fraction) for binary water (1) – anthracene (2) and <i>p</i> -terphenyl (1) – water (2) systems	46
Table 3.8 Ratios of the dielectric constant (ϵ_r) of water, PAHs sublimation pressures (P_T^{sub}) and PAHs solubility (x_T) at various temperatures	49
Table 3.9 Solubility of anthracene in various solvents, temperatures and dielectric constants	50
Table 3.10 RP-HPLC mobile phase gradient with a flow rate of 1 ml/min	52

Table 3.11	Solubility data (mole fraction) in subcritical water (1) – anthracene (2) – <i>p</i> -terphenyl (3) system	52
Table 4.1	Vapor-liquid equilibrium of ethanol-water at 200 °C	59
Table 4.2	Phase behaviour of anthracene and <i>p</i> -terphenyl at 50 bar and various temperatures and mole fractions of ethanol	61
Table 4.3	Solubility data of anthracene in subcritical water/ethanol systems at 140 °C and 180 °C, and at pressures of 50 bar and 150 bar ($f = 0.06$)	63
Table 4.4	Main effects that contribute to the solubility of anthracene in subcritical water/ethanol system at 140 °C and 180 °C, and at pressures of 50 bar and 150 bar ($f = 0.06$)	63
Table 4.5	Solubility of anthracene in subcritical water/ethanol systems at 140 °C and 180 °C, and ethanol mole fractions, $f = 0.01$ and $f = 0.10$	64
Table 4.6	Main effects that contribute to the solubility of anthracene in subcritical water/ethanol system at 140 °C and 180 °C and ethanol mole fractions, $f = 0.01$ and $f = 0.10$	65
Table 4.7	Solubility data for ternary water (1) - ethanol (2) – anthracene (3) systems	68
Table 4.8	Solubility data for ternary water (1) - ethanol (2) – <i>p</i> -terphenyl (3) systems	69
Table 4.9	Saturated pressures of ethanol at various temperatures	78
Table 4.10	Phase behavior of anthracene and <i>p</i> -terphenyl at 50 bar and various temperatures and mole fractions of ethanol	79
Table 4.11	Solubility data for binary subcritical ethanol (1) – anthracene (2) and subcritical ethanol (1) – <i>p</i> -terphenyl (2)	82
Table 5.1	Parameters m and c derived from Equation (5.37) for anthracene and <i>p</i> -terphenyl in various subcritical solvent systems	97
Table 5.2	Parameters used in the UNIQUAC and O-UNIFAC models	99
Table 5.3	Values of a_{ij} for water (1) - ethanol (2) - PAH (3) systems obtained with $z = 10$ and $(u_{ji} - u_{ii})/R = a_{ji}$	105
Table 5.4	The a_{ij} , b_{ij} , and c_{ij} values in water (1) - ethanol (2) - PAH (3) systems obtained with $z = 10$ and $[(u_{ji} - u_{ii})/R = a_{ij} + b_{ij}T + c_{ij}T^2]$	111

Table 5.5	Experimental and UNIQUAC calculated solubility data and the corresponding activity coefficients for binary water (1) - anthracene (2) system	112
Table 5.6	Experimental and UNIQUAC calculated solubility data and the corresponding activity coefficients for binary water (1) - <i>p</i> -terphenyl (2) system	112
Table 5.7	Experimental and UNIQUAC calculated solubility data and the corresponding activity coefficients for binary ethanol (1) - anthracene (2) system	113
Table 5.8	Experimental and UNIQUAC calculated solubility data and the corresponding activity coefficients for binary ethanol (1) - <i>p</i> -terphenyl (2) system	113
Table 5.9	Experimental and UNIQUAC calculated solubility data and the corresponding activity coefficients for ternary water (1) – ethanol (2) – anthracene (3) systems [$f = 0.01-0.03$]	114
Table 5.10	Experimental and UNIQUAC calculated solubility data and the corresponding activity coefficients for ternary water (1) – ethanol (2) – anthracene (3) systems [$f = 0.04-0.06$]	115
Table 5.11	Experimental and UNIQUAC calculated solubility data and the corresponding activity coefficients for ternary water (1) – ethanol (2) – <i>p</i> -terphenyl (3) systems [$f = 0.01-0.03$]	116
Table 5.12	Experimental and UNIQUAC calculated solubility data and the corresponding activity coefficients for ternary water (1) – ethanol (2) – <i>p</i> -terphenyl (3) systems [$f = 0.04-0.06$]	117
Table 5.13	Experimental and UNIQUAC calculated solubility data and the absolute standard deviations for ternary water (1) - anthracene (2) - <i>p</i> -terphenyl (3) system with $a_{23} = -1000.03$ and $a_{32} = -1000.05$	124
Table 5.14	Experimental and UNIQUAC calculated activity coefficients for ternary water (1) - anthracene (2) - <i>p</i> -terphenyl (3) system	125
Table 5.15	O-UNIFAC calculated solubility data (mole fraction), the corresponding activity coefficients and the absolute standard deviations (ASD) from experimental data in subcritical water (1) – anthracene (2) system	127

Table 5.16	O-UNIFAC calculated solubility data (mole fraction), the corresponding activity coefficients and the absolute standard deviations (ASD) from experimental data in subcritical water (1) – <i>p</i> -terphenyl (2) system	127
Table 5.17	O-UNIFAC calculated solubility data (mole fraction), the corresponding activity coefficients and the absolute standard deviations (ASD) from experimental data in subcritical ethanol (1) – anthracene (2) system	128
Table 5.18	O-UNIFAC calculated solubility data (mole fraction), the corresponding activity coefficients and the absolute standard deviations (ASD) from experimental data in subcritical ethanol (1) – <i>p</i> -terphenyl (2) system	128
Table 5.19	O-UNIFAC calculated solubility data (mole fraction), the corresponding activity coefficients and the absolute standard deviations (ASD) from experimental data in subcritical water (1) – ethanol (2) – anthracene (3) system [$f = 0.01 - 0.03$]	129
Table 5.20	O-UNIFAC calculated solubility data (mole fraction), the corresponding activity coefficients and the absolute standard deviations (ASD) from experimental data in subcritical water (1) – ethanol (2) – anthracene (3) system [$f = 0.04 - 0.10$]	130
Table 5.21	O-UNIFAC calculated solubility data (mole fraction), the corresponding activity coefficients and the absolute standard deviations (ASD) from experimental data in subcritical water (1) – ethanol (2) – <i>p</i> -terphenyl (3) system [$f = 0.01 - 0.03$]	131
Table 5.22	O-UNIFAC calculated solubility data (mole fraction), the corresponding activity coefficients and the absolute standard deviations (ASD) from experimental data in subcritical water (1) – ethanol (2) – <i>p</i> -terphenyl (3) system [$f = 0.04 - 0.10$]	132
Table 5.23	The calculated solubility values and activity coefficients obtained from the O-UNIFAC model for water (1) – anthracene (2) – <i>p</i> -terphenyl (3) system at various temperatures	139
Table 5.24	Absolute standard deviation (ASD) obtained with the O-UNIFAC model for water (1) – anthracene (2) – <i>p</i> -terphenyl (3) system	139
Table 5.25	Physical properties of anthracene and <i>p</i> -terphenyl used in this study	141

Table 5.26	M-UNIFAC calculated solubility data (mole fraction), the corresponding activity coefficients and the absolute standard deviations (ASD) from experimental data in subcritical water (1) – anthracene (2) system	142
Table 5.27	M-UNIFAC calculated solubility data (mole fraction), the corresponding activity coefficients and the absolute standard deviations (ASD) from experimental data in subcritical water (1) – <i>p</i> -terphenyl (2) system	142
Table 5.28	M-UNIFAC calculated solubility data (mole fraction), the corresponding activity coefficients and the absolute standard deviations (ASD) from experimental data in subcritical ethanol (1) – anthracene (2) system	143
Table 5.29	M-UNIFAC calculated solubility data (mole fraction), the corresponding activity coefficients and the absolute standard deviations (ASD) from experimental data in subcritical ethanol (1) – <i>p</i> -terphenyl (2) system	143
Table 5.30	M-UNIFAC calculated solubility data (mole fraction), the corresponding activity coefficients and the absolute standard deviations (ASD) from experimental data in subcritical water (1) – ethanol (2) – anthracene (3) system [$f = 0.01 - 0.03$]	144
Table 5.31	M-UNIFAC calculated solubility data (mole fraction), the corresponding activity coefficients and the absolute standard deviations (ASD) from experimental data in subcritical water (1) – ethanol (2) – anthracene (3) system [$f = 0.04 - 0.10$]	145
Table 5.32	M-UNIFAC calculated solubility data (mole fraction), the corresponding activity coefficients and the absolute standard deviations (ASD) from experimental data in subcritical water (1) – ethanol (2) – <i>p</i> -terphenyl (3) system [$f = 0.01 - 0.03$]	146
Table 5.33	M-UNIFAC calculated solubility data (mole fraction), the corresponding activity coefficients and the absolute standard deviations (ASD) from experimental data in subcritical water (1) – ethanol (2) – <i>p</i> -terphenyl (3) system [$f = 0.04 - 0.10$]	147
Table 5.34	The calculated solubility values and activity coefficients obtained from the M-UNIFAC model for water (1) – anthracene (2) – <i>p</i> -terphenyl (3) system at various temperatures	154

Table 5.35 Absolute standard deviation (ASD) obtained with the M-UNIFAC model
for water (1) – anthracene (2) – *p*-terphenyl (3) system

154

NOMENCLATURE

Symbols

a	activity coefficient
a_{ij}	fitted energy parameter
a_{nm}, b_{nm}, c_{nm}	M-UNIFAC group interaction parameters between group n and m
C_p	heat capacity at constant pressure
f_i	fugacity of component i
\hat{f}_2^S	fugacity of a solid solute in a mixture
\hat{f}_2^L	fugacity of a liquid solute in a mixture
f	ethanol mole fraction [f = moles of ethanol/(moles of ethanol + water)]
G	Gibbs free energy
H	enthalpy
H-bond	hydrogen bond
N	total number of components
OB	objective function
P	pressure
r	correlation coefficient
R	gas constant
R_k	van der Waals group surface parameter
Q_k	van der Waals group volume parameter
S	entropy
T	temperature
T_m	melting temperature
x_i	solubility (in mole fraction) of solute i
V_i	surface fraction/mole fraction for component i [M-UNIFAC]
z	coordination number

Greek symbols

ε_r	dielectric constant or the relative permittivity
γ	activity coefficient
Φ	volume fraction [UNIQUAC]
μ	chemical potential
θ_i	area fraction [UNIQUAC]
τ_{ij}	binary adjustable parameters
Γ_k	group residual activity coefficient
$\Gamma_k^{(i)}$	group residual activity coefficient in a solution containing only molecule i
Θ	group area fraction [O-UNIFAC]

Abbreviation

ASD	absolute standard deviation
AASD	average absolute standard deviation
EtOH	ethanol
FID	flame Ionization Detection
FTIR	Fourier transform infra red spectroscopy
GC	gas chromatography
HPLC	high pressure liquid chromatography
LLE	liquid-liquid equilibria
N ₂	nitrogen gas
NRTL	non-random two liquid model
M-UNIFAC	Modified Universal Functional Activity Coefficient model
MW	molecular weight
O-UNIFAC	Original Universal Functional Activity Coefficient model
PI	pressure indicator
RP-HPLC	reversed-phase high pressure liquid chromatography
RSD	relative standard deviation
SLE	solid-liquid equilibria

SSLE	solid-solid-liquid equilibria
TI	temperature indicator
UNIQUAC	Universal Quasi-Chemical model
UV	ultraviolet
V	valve
VLE	vapour-liquid equilibria

Subscripts

f	fusion
i, j	component i or j
m	mixture
w	water
s	solution
tr	transfer

Superscripts

C	combinatorial
exp	experiment
cal	calculation
L	liquid
R	residual
PAH	polycyclic aromatic hydrocarbon
S	solid

1 Introduction

Water is pervasive on Earth; being present, and playing significant roles in many biological and colloidal systems. Water is also used in many reaction and separation processes, gaining further footholds in many processes as more chemical industries gear towards sustainability. One of the vital characteristics of liquid water is its cohesive energy, which is primarily a consequence of the hydrogen-bonds formed between water molecules. The hydrogen bond network plays a central role in the solvating power of water, inducing strong attraction between water molecules that becomes the main reason for the observed low solubilities of non-polar compounds in liquid water. However, at higher temperatures, the H-bonds in liquid water weaken. As a consequence, the solvating power of liquid water for hydrophobic compounds increases.

Liquid water heated to any temperature below its critical temperature and at sufficient pressure to maintain the liquid state is known as subcritical water (or pressurized hot water or superheated water). The solvating power of subcritical water has been observed to be considerably higher than at room temperature [2-6]. The solvating power of subcritical water, and the polarity thereof, is directly dependent upon temperature while the effect of pressure is relatively insignificant at moderate pressure ranges [2]. The change in the polarity of subcritical water with temperature is reflected in its dielectric constant (or relative permittivity) values, as shown in Figure 1.1. The dielectric constant of water at 25 °C and 1 atm is 78.5, limiting its solvating power to mostly polar compounds. However, as temperature increases, the dielectric constant of water decreases, thereby increasing its solvent power to a wider range of non-polar organic compounds.

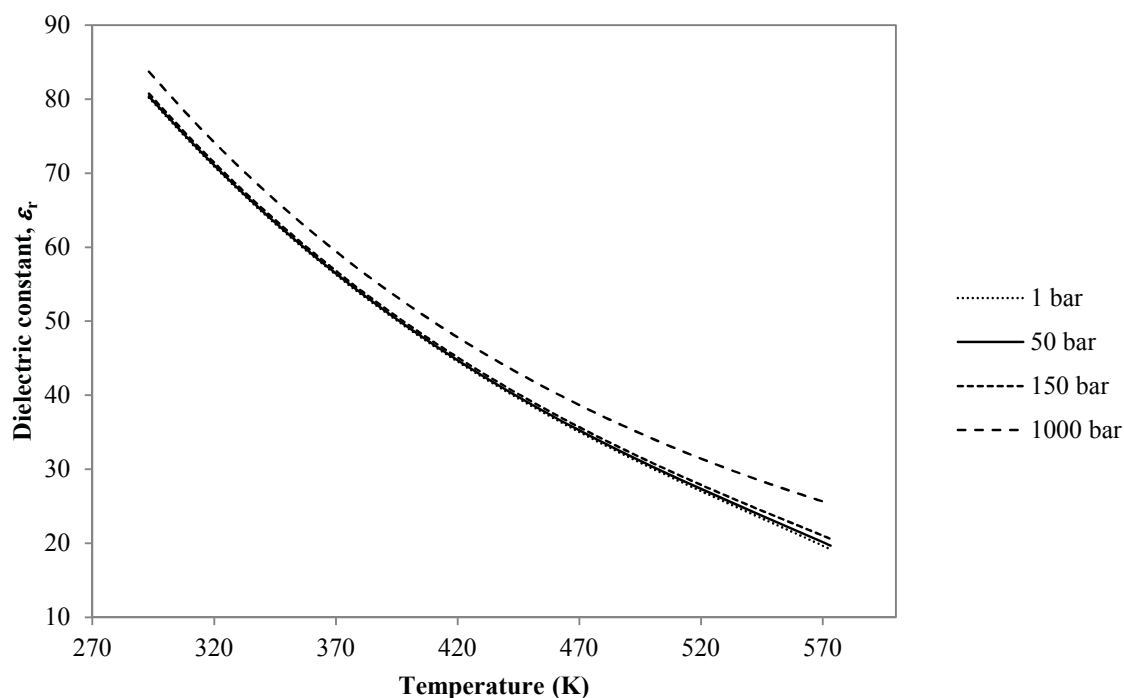


Figure 1.1: The dielectric constant of water at various temperatures and pressures (reproduced from Bradley and Pitzer [7])

The solubilities of a number of hydrophobic solid substances in water have been investigated in recent years, and found to be as low as 10^{-6} and even 10^{-7} mole fraction [8,9]. However, numerous studies have also shown that the solubilities of hydrophobic compounds in liquid water increase exponentially above 100 °C [2-4,6,10]. As a consequence of the dramatic increase in solvating power, subcritical water at relatively higher temperatures has been shown to be a good alternative solvent [10,11]. Subcritical water processing has its advantages in that water is non-toxic, inexpensive, readily available and easily disposed. In terms of the extraction process, subcritical water has the added advantage of not requiring the drying of samples prior to processing [11]. Subcritical water technologies have been applied to the removal and decomposition of pollutants, for the extraction of compounds such as polycyclic aromatic hydrocarbons (PAHs) and polychlorinated biphenyls from soils, and recently, to the micronization of hydrophobic drugs [3,6,10,12-16].

The extraction and remediation of PAHs using subcritical water have been conducted in small and pilot scales with much success, and in some cases, reducing the concentration of PAHs to below detectable levels [16-22]. PAHs are produced through incomplete combustion and pyrolysis of organic compounds. Their presence in soils becomes an environmental concern due to their mutagenic, teratogenic and carcinogenic properties. PAHs have been found around coal-mining areas, and in sediments from the extraction and transportation of oil [23-26]. Hydrophobic by nature, PAHs tend to absorb tightly to organic matter in soil. Prolonged aging time promotes the sequestration of PAHs into nanopores and their partitioning in organic matter [27]. Hence, PAHs are resistant to decomposition while the lipophilic nature of PAHs leads to accumulation in soil, sediment and vegetation [27]. Due to the strong sorption of PAHs in matrixes, the extraction process is often difficult and incomplete; requiring different techniques for different contamination levels [28]. A number of bioremediation and phytoremediation studies had been conducted on PAHs contaminated soil although the yield and the efficiency with which PAHs (particularly higher molecular weight compounds) are removed are generally poor [17,22,29-33]. The onward desire for sustainability through the reduction in the costs and usage of toxic organic solvents, the search for alternatives that are non-exhaustible, and the need for versatility in PAHs extraction techniques became the motivation for the development of subcritical water extraction [18,34].

Although the use of subcritical water to process materials is gaining increased interest, many potential applications of subcritical water processes remain undeveloped due to a lack of fundamental data. While the feasibility of a subcritical water process depends on the behaviors of subcritical water and the compounds involved, the complexity and the non-ideality of subcritical water characteristics make it difficult to predict its behavior and that of the solutes. Consequently, extensive, expensive and time-consuming experimental studies are required. Furthermore, accurate thermodynamic models for subcritical water systems are essential. An understanding of the thermodynamics of phase equilibrium is also important in the design of separation and extraction processes. A process optimized in terms of its equipment selection, configuration and operations can be rendered inoperable if the process simulation is based on inaccurate thermodynamic models. Thermodynamic models (in addition to the experimental data from which the models were derived from) can exhibit systematic and random errors that

affect their accuracy and precision while contributing to the uncertainty in the calculation of physical properties [35].

In light of the need for accurate thermodynamic data, fundamental solubility studies are necessary to facilitate decision-making processes as they provide potential operating conditions and give a key indication of the technical feasibility of a prospective process [36]. Solubility studies are essential as they quantify the ability of subcritical water to act as a solvent which consequently defines the feasibility of a particular process for a particular application [36,37]. Solubility studies play an important role in determining the economic effectiveness of a particular process since solubility provides the thermodynamic limit to a process [38]. As such, there is a need to investigate the factors that affect solubility in subcritical water to allow for a continual development in the many potential applications, as well as the design and scale up of subcritical water processes.

While a number of solubility studies have been conducted on PAHs in subcritical water, these studies are heavily based on binary systems consisting of a pure solute in subcritical water. However, the extraction or removal of pollutants from a matrix of compounds are intricate, and can rarely be depicted entirely by binary systems. Moreover, the solubilities of hydrophobic organic pollutants (HOPs) such as PAHs are known to be affected by the addition of co-solvents and co-solutes into water and are important in the treatment of industrial wastewater [39]. While many data are available for the solubilities of HOPs in water, their availability in water-cosolvent mixtures is lacking [39]. Hence, experimental data and the thermodynamic quantity which predicts the behavior of HOPs in aqueous solutions are necessary. Therefore, the aim of this study is to complement the available data on the solubility of polycyclic aromatic hydrocarbons (PAHs) in subcritical water, and in the presence of a co-solvent or a co-solute. In this study, the solubilities of anthracene and *p*-terphenyl were measured in subcritical water, subcritical ethanol, and ethanol-modified subcritical water. In the ethanol-modified subcritical water systems, solubilities were measured at ethanol mole fractions, f of 0.01, 0.02, 0.03, 0.04, 0.06 and 0.10. All measurements were conducted at 50 bar, between 393 K and 473 K. While the main focus of this thesis was to investigate the effects of temperature and the addition of a third compound on the solubility of a PAH, the effects from increasing processing pressure and the combined effects of these parameters were also investigated. The suitability of three activity

coefficient based models - UNIQUAC, O-UNIFAC and M-UNIFAC models - were also evaluated for such materials in subcritical water. The definition of solubility and the factors that affect solubility are discussed further in Chapter 2 while the methods by which solubility measurements are conducted in subcritical water are addressed in Chapter 3. The co-solvent effect on solubility in subcritical water is studied in Chapter 4. Meanwhile the suitability of thermodynamic models for the solute-solvent systems involved is discussed in Chapter 5.

1.1 Bibliography

- [1] Zhao H, Unhannanant P, Hanshaw W, Chickos JS. Enthalpies of vaporization and vapor pressures of some deuterated hydrocarbons. Liquid-vapor pressure isotope effects. *J. Chem. Eng. Data* 2008;53:1545-56.
- [2] Miller DJ, Hawthorne SB, Gizir AM, Clifford AA. Solubility of polycyclic aromatic hydrocarbons in subcritical water from 298 K to 498 K. *Journal of Chemical & Engineering Data* 1998;43 (6):1043-7.
- [3] Karasek P, Hohnova B, Planeta J, Roth M. Solubility of solid ferrocene in pressurized hot water. *Journal of Chemical & Engineering Data* 2010;55 (8):2866-9.
- [4] Karasek P, Planeta J, Roth M. Solubility of solid polycyclic aromatic hydrocarbons in pressurized hot water at temperatures from 313K to the melting point. *Industrial & Engineering Chemistry Research* 2006;45 (12):4454-60.
- [5] Andersson TA, Hartonen KM, Riekkola M-L. Solubility of acenaphthene, anthracene, and pyrene in water at 50 °C to 300 °C. *Journal of Chemical & Engineering Data* 2005;50 (4):1177-83.
- [6] Carr AG, Mammucari R, Foster NR. Solubility and micronization of griseofulvin in subcritical water. *Industrial & Engineering Chemistry Research* 2010;49 (7):3403-10.
- [7] Bradley DJ, Pitzer KS. Thermodynamics of electrolytes. 12. Dielectric properties of water and Debye-Hueckel parameters to 350.degree.C and 1 kbar. *The Journal of Physical Chemistry* 1979;83 (12):1599-603.
- [8] Bennett D, Canady WJ. Thermodynamics of solution of naphthalene in various water-ethanol mixtures. *Journal of the American Chemical Society* 1984;106 (4):910-5.
- [9] Zhou B, Cai W, Zou L. Thermodynamic functions for transfer of anthracene from water to (water + alcohol) mixtures at 298.15 K. *Journal of Chemical & Engineering Data* 2003;48 (3):742-5.
- [10] Miller DJ, Hawthorne SB. Method for determining the solubilities of hydrophobic organics in subcritical water. *Analytical Chemistry* 1998;70 (8):1618-21.
- [11] Curren MSS, King JW. Solubility of triazine pesticides in pure and modified subcritical water. *Analytical Chemistry* 2001;73 (4):740-5.
- [12] Yang Y, Bowadt S, Hawthorne SB, Miller DJ. Subcritical water extraction of polychlorinated biphenyls from soil and sediment. *Analytical Chemistry* 1995;67 (24):4571-6.
- [13] Carr AG, Branch A, Mammucari R, Foster NR. The solubility and solubility modelling of budesonide in pure and modified subcritical water solutions. *The Journal of Supercritical Fluids* 2010;55 (1):37-42.
- [14] Carr AG, Mammucari R, Foster NR. Solubility, solubility modeling, and precipitation of naproxen from subcritical water solutions. *Industrial & Engineering Chemistry Research* 2010;49 (19):9385-93.
- [15] Carr AG, Mammucari R, Foster NR. Particle formation of budesonide from alcohol-modified subcritical water solutions. *International Journal of Pharmaceutics* 2011;405 (1-2):169-80.
- [16] Hawthorne SB, Yang Y, Miller DJ. Extraction of organic pollutants from environmental solids with sub- and supercritical water. *Analytical Chemistry* 1994;66 (18):2912-20.
- [17] Islam MN, Jo YT, Park JH. Remediation of PAHs contaminated soil by extraction using subcritical water. *Journal of Industrial and Engineering Chemistry* 2012.

- [18] Latawiec AE, Reid BJ. Sequential extraction of polycyclic aromatic hydrocarbons using subcritical water. *Chemosphere* 2010;78 (8):1042-8.
- [19] Soltanali S, Hagani ZS, Rouzbahani V. Investigation of operating conditions for soil remediation by subcritical water. *Chemical Industry and Chemical Engineering Quarterly* 2009;15 (2):89-94.
- [20] Dadkhah AA, Akgerman A. Hot water extraction with in situ wet oxidation: PAHs removal from soil. *Journal of Hazardous Materials* 2002;93 (3):307-20.
- [21] Hawthorne SB, Trembley S, Moniot CL, Grabanski CB, Miller DJ. Static subcritical water extraction with simultaneous solid-phase extraction for determining polycyclic aromatic hydrocarbons on environmental solids. *Journal of Chromatography A* 2000;886 (1-2):237-44.
- [22] Lagadec AJM, Miller DJ, Lilke AV, Hawthorne SB. Pilot-scale subcritical water remediation of polycyclic aromatic hydrocarbon- and pesticide-contaminated soil. *Environmental Science & Technology* 2000;34 (8):1542-8.
- [23] Ruiz-Fernández AC, Sprovieri M, Frignani M, Sanchez-Cabeza JA, Feo ML, Bellucci LG, Pérez-Bernal LH, Preda M, Machain-Castillo ML. Reconstruction of hydrocarbons accumulation in sediments affected by the oil refinery industry: the case of Tehuantepec Gulf (Mexico). *Environmental Earth Sciences* 2012:1-16.
- [24] Yang C, Zhong NN, Chen DY, Li Y, Liu S. Distribution characteristics of aromatic hydrocarbons pollution in dustfall samples from a coal-mining area, China. *Zhongguo Kuangye Daxue Xuebao/Journal of China University of Mining and Technology* 2007;36 (3):415-20.
- [25] Wang R, Liu G, Chou CL, Liu J, Zhang J. Environmental assessment of PAHs in soils around the Anhui Coal District, China. *Archives of environmental contamination and toxicology* 2010;59 (1):62-70.
- [26] Hadjizadeh Zaker N, Rahmani I, Shadi R, Moghaddam M, Abessi O. Concentrations and sources of petroleum hydrocarbons in the sediments of Anzali Port in the Caspian Sea in Iran. *Journal of Environmental Studies* 2012;37 (60):99-106.
- [27] Hatzinger PB, Alexander M. Biodegradation of organic compounds sequestered in organic solids or in nanopores within silica particles. *Environmental Toxicology and Chemistry* 1997;16 (11):2215-21.
- [28] Hollender J, Koch B, Lutermann C, Dott W. Efficiency of different methods and solvents for the extraction of polycyclic aromatic hydrocarbons from soils. *International Journal of Environmental Analytical Chemistry* 2003;83 (1):21-32.
- [29] Wang X, Yu X, Bartha R. Effect of bioremediation on polycyclic aromatic hydrocarbon residues in soil. *Environmental Science and Technology* 1990;24 (7):1086-9.
- [30] Chang BV, Shiung LC, Yuan SY. Anaerobic biodegradation of polycyclic aromatic hydrocarbon in soil. *Chemosphere* 2002;48 (7):717-24.
- [31] Mueller KE, Shann JR. PAH dissipation in spiked soil: Impacts of bioavailability, microbial activity, and trees. *Chemosphere* 2006;64 (6):1006-14.
- [32] Parrish ZD, Banks MK, Schwab AP. Assessment of contaminant lability during phytoremediation of polycyclic aromatic hydrocarbon impacted soil. *Environmental Pollution* 2005;137 (2):187-97.
- [33] Cofield N, Banks MK, Schwab AP. Lability of polycyclic aromatic hydrocarbons in the rhizosphere. *Chemosphere* 2008;70 (9):1644-52.

- [34] Yang Y, Hawthorne SB, Miller DJ. Class-selective extraction of polar, moderately polar, and nonpolar organics from hydrocarbon wastes using subcritical water. *Environmental Science & Technology* 1997;31 (2):430-7.
- [35] Vasquez VR, Whiting WB. Effect of systematic and random errors in thermodynamic models on chemical process design and simulation: a Monte Carlo approach. *Industrial & Engineering Chemistry Research* 1999;38 (8):3036-45.
- [36] Lucien FP. Solubility behavior of solid mixtures in supercritical carbon dioxide. Sydney: The University of New South Wales, 1996. pp. 46.
- [37] Macnaughton SJ, Tomasko DL, Foster NR, Eckert CA. Design considerations for soil remediation using supercritical fluid extraction. *Trans. IChemE* 1993;71(B).
- [38] Domanska U. Chapter 8: Solubility of organic solids for industry. In: Letcher TM, editor. *Developments and applications in solubility*. UK: RSC Publishing, 2007.
- [39] Ruckenstein E, Shulgin I. Solubility of hydrophobic organic pollutants in binary and multicomponent aqueous solvents. *Environmental Science & Technology* 2005;39 (6):1623-31.

Chapter 2 Solubility and Factors that Affect Solubility in Subcritical Water

2.1 Introduction

Solubility is the analytical composition of a solution saturated under equilibrium with one of the components of the solution at a particular temperature and pressure [1,2]. It quantifies the dynamic equilibrium state achieved where the dissolution rate equals that of the precipitation rate in a solid-liquid system. Solubility is very dependent on the inter-molecular forces between solute-solvent, solute-solute and solvent-solvent [3]. For a system consisting of a solute, i and a solvent, j , the ability of i to dissolve in j is given by the strength of interactions between i and j . If the attractive forces of i - j are higher than that of i - i and j - j , then the solute i would dissolve in the solvent j . The ancient heuristic of "like dissolves like" is still applicable in many solute-solvent systems since intermolecular forces between similar chemical compounds lead to smaller endothermic enthalpy of solution than dissimilar compounds [3]. The factors that contribute to the solubility of a given solute in a solvent are summarized in Figure 2.1.

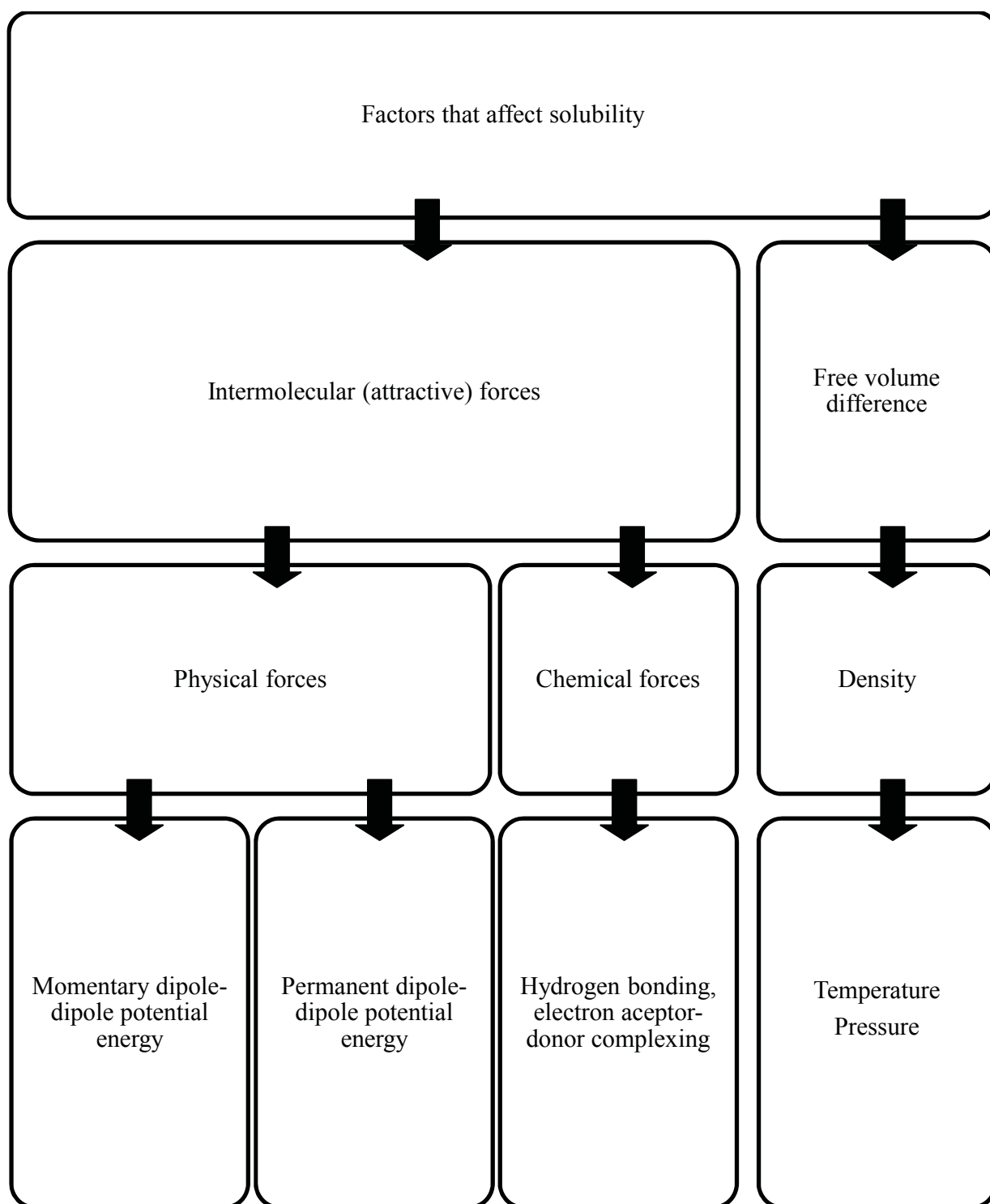


Figure 2.1: Factors that contribute to the solubility of a solute in a solvent

2.2 The effects of intermolecular forces on solubility

The fundamental source of most physical *properties* of a molecule is its intermolecular forces [4]. Intermolecular forces in operation between molecules are governed by the physical and chemical forces existing between the molecules in the solution. The physical forces of attraction between molecules are governed by the *momentary* (induced) dipole-dipole potential energy and the *permanent* dipole-dipole potential energy. In the momentary dipole-dipole potential energy interaction, a molecule with a momentary dipole causes a dipole in neighboring molecules, producing net attractive forces between the molecules that subsequently governs the solubility of a *non-polar* solute in a *non-polar* solvent [5]. The momentary dipole-dipole potential energy depends on the polarizability of a molecule and the distance between two molecules. The polarizability of a solvent (which increases with its molecular size) indicates the strength of the solvent [5]. The momentary dipole-dipole potential energy is, however, not affected by temperature changes.

The permanent dipole-dipole potential energy attributed to the structure and size of a molecule provides an additional force of attraction between molecules. Large, complex molecules generally have weakened dipole interactions due to the large volume of the molecules [6]. A molecule with high polar moments and high dielectric constant is considered polar. The permanent dipole-dipole potential energy changes with intermolecular distance while it decreases with increasing temperature. Hence, a polar liquid solvent exhibits non-polarity at higher temperatures, such as that observed in water. At very high pressures and densities, repulsive intermolecular forces could also dominate and reduce the solubility of a solute [7]. Higher-order polar moments also affect the solvating power of a solvent although these effects are less significant than a dipole moment [5]. A good example is carbon dioxide which has a large quadrupole moment that greatly enhances the solubility of a number of polar solutes in supercritical carbon dioxide [8].

Chemical forces of attraction such as hydrogen bonding and electron acceptor-donor complexing also play important roles in solubility, although these are harder to quantify [5]. The effects of chemical forces in a solution are generally categorized as solvation, where the molecules of the solutes and solvents tend to form complexes [9]. In contrast to physical forces, chemical forces can become saturated and are very dependent on temperature [9]. Chemical

forces generally decrease with increasing temperature such as the observed weaker H-bonds in subcritical and supercritical water. Generally, H-bonds are easily broken at higher temperatures when the molecules involved have sufficient energy to break loose as the strength of H-bonds are lower than that of covalent bonds [9].

In liquid water, the hydrogen bond network plays a central role in the solvating power of water while the electric dipole moment is of secondary importance. The strong attraction between water molecules due to the hydrogen bonds is also the main reason for the observed low solubilities of non-polar compounds in liquid water. Water molecules in liquid water tend to self-associate as a consequence of the hydrogen bonds (H-bonds) and at room temperature water molecules in liquid water form tetrahedral clusters; averaging about 4.5 molecules per cluster [10]. Increased temperature and pressure, however, elicit changes in the structure of water. The H-bonds in water tend to break or distort, with the tetrahedral ordering of liquid water diminishing gradually as temperature increases [11]. Elevated pressure also weakens the tetrahedral ordering and increases the non-hydrogen bonded water molecules of liquid water [11]. Hence, at subcritical conditions, bulk water is considered to consist of a mixture of small H-bonded clusters and smaller aggregates consisting of oligomers and monomers [11]. The weakening of the H-bonds also explains the decrease in the polarity of water with temperature, which is reflected in its dielectric constant values.

While H-bonds are traditionally defined to be between proton and electron donors, H-bonds are electrostatic by nature. Hence, other sources of electrons such as the hybridized π -bonds from an aromatic ring could also act as H-bonds acceptors although these bonds are generally weaker [12-14]. The H-bond between benzene and amino acid have been found to be half the strength of a normal H-bond while the H-bond for ethanol-toluene and ethanol-xylene were found to be 300 times weaker than that of alcohol-alcohol [12,13]. π -Hydrogen bonding between water and aromatic molecules were found to exist even at higher temperatures and pressures [15]. Experimental studies on the solvation of benzene in water has been conducted with the general consensus that the water molecule is on one side of the benzene molecule having one or two hydrogen atoms facing the π -cloud of the benzene molecule [16].

2.3 The effects of the free volume difference on solubility

Free volume is defined as the total integral over the part of the potential energy due to the thermal displacements of the center of gravity of the molecule from its equilibrium [17]. It is the “empty” volume available to the molecule after subtracting the hard-core volume of the molecule itself [18]. Therefore, free volume reflects the compressibility or expansivity of a substance [5]. The free volume difference between the solute and the solvent is related to the density of the solvent as this affects the interaction level between molecules in a solution. In general, the solubility of a solute in subcritical water decreases with increasing density at constant temperature. In an investigation conducted by Rossling and Franck (1983) at temperatures and pressures between 75 – 280 °C and 20 – 2850 bar, the isothermal solubility of anthracene in subcritical water was found to decrease with increasing water density.

Pressure has a direct influence on the density of solvents and thus, affects the solubility of solids in subcritical water. The isothermal solubility of solids in subcritical water has been shown to decrease with *large* increase in pressure although pressure *differences* of up to 100 bar were found to elicit negligible solubility changes [19-21]. Thus, small pressure differences generally do not have a significant effect on the phase behavior of solid-liquid systems [3].

An increase in temperature decreases the density of the solvent. While a decrease in solvent density is usually linked to a decrease in solubility, the opposite trend is observed when temperature is raised in subcritical water. An example is that the solubility of anthracene in subcritical water that was observed to increase with temperature at constant density [21]. The reason for such behavior is the temperature effect on other physico-chemical properties of the solvent and solute, such as the H-bonding and vapor pressure that present a contrasting trend to that of density. Since decreasing density does not correspond with increased temperature and solubility behavior, and the effect of small pressure changes to density and solubility is small, it can be construed that density has a minor influence on solubility in subcritical water at moderate pressure range.

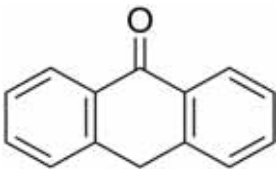
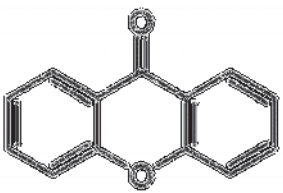
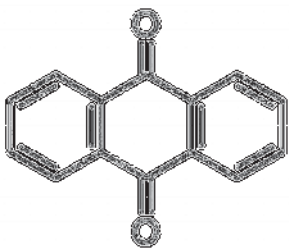
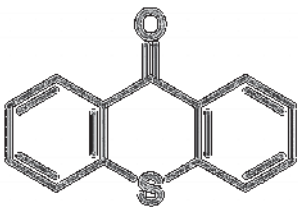
2.4 Solute effects on solubility in subcritical water

For a given binary solid-solvent system, comparison between two solid solutes with similar enthalpy of fusion would yield a higher solubility for the solute with a lower melting temperature [22]. Likewise, if two solutes with similar melting temperatures are compared, the solute with the higher enthalpy of fusion would have a higher solubility. Generally the solubility of a hydrophobic compound in subcritical water increases with a decrease in molecular size. For example, the solubilities of anthracene (molecular weight, MW = 178), chrysene (MW = 228) and perylene (MW = 252) were found to increase in the order of perylene < chrysene < anthracene [20].

The added presence of oxygen, sulfur, chlorine or aliphatic side-chains in a solute also decreases its solubility in subcritical water. In Tables 2.1 – 2.2, the molecular structure and the solubility values of anthrone, xanthone, 9,10-anthraquinone, thioxanthone, benzene, ethylbenzene, *m*-xylene, toluene, 1,2-dichlorobenzene, benzoic acid and salicylic acid in subcritical water are compared. Table 2.1 shows that the influence of the functional groups can be rated in the order of: carbonyl (=O) < thiane (–S–) < oxane (–O–). The presence of methyl, ethyl or chlorine functional groups in a solute also decreases its solubility in subcritical water while the presence of a carboxyl group enhances solute solubility (as shown in Table 2.2).


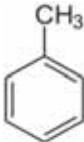
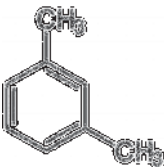

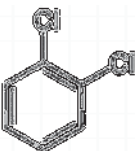
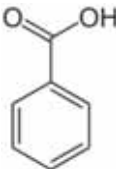
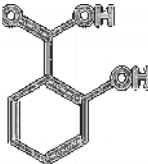
Generally, the addition of a hydroxyl group increases the solubility of a solute in water; the most obvious being the higher solubility of phenol than benzene in water [23,24]. However, Table 2.2 shows that the solubility of benzoic acid is higher than the solubility of salicylic acid in subcritical water, even with the addition of a hydroxyl group in salicylic acid. One contributing factor to the lower solubility of salicylic acid is the intramolecular H-bonding that occurs in salicylic acid [25]. It is to be noted, however, that the presence of the different functional groups increases the size of the solute, which consequently also contributes to the lower solubility values. While the solute effect is given in this section, generalization of the contributing effects from different functional groups can only be fully realized when solute solubility studies are extended to a wider range of compounds. The type of solutes investigated in subcritical water is currently limited to a small number.

Table 2.1: Solubilities (in mole fraction) of various organic compounds in subcritical water at 140 °C, and their corresponding molecular structure

Compound	Molecular structure	Solubility at 140 °C and 50 ± 3 bar	Reference
Anthrone MW = 194.23		9.89×10^{-5}	[26]
Xanthone MW = 196.19		9.13×10^{-5}	[26]
9,10-Anthraquinone MW = 208.21		1.06×10^{-5}	[26]
Thioxanthone MW = 212.27		1.98×10^{-5}	[26]

Note: MW = molecular weight

Table 2.2: Solubilities (in mole fraction) of various organic compounds in subcritical water at 150 °C, and their corresponding molecular structure

Compound	Molecular structure	Solubility at 150 °C and 50 bar	Reference
Benzene MW = 78.11		1.7×10^{-3}	[27]
Toluene MW = 92.14		8.7×10^{-4}	[27]
<i>m</i> -Xylene MW = 106.16		2.7×10^{-4}	[27]
Ethylbenzene MW = 106.17		2.4×10^{-4}	[27]
1,2-dichlorobenzene MW = 147.01		1.8×10^{-4}	[27]
Benzoic acid MW = 122.12		0.131	[28]
Salicylic acid MW = 138.12		0.102	[28]

Note: MW = molecular weight

2.5 Co-solvent and co-solute effects on solubility

The addition of a third component into a binary system brings about synergistic effects (positive and negative) on solubility. Hence, chemical compounds behave differently in pure and modified solvents at subcritical conditions. The varying solubilities of atrazine in subcritical water and ethanol-modified subcritical water are shown in Table 2.3. Solubilities were found to increase with increased ethanol concentrations. The varying solubilities were attributed to decreases in the dielectric constant that resulted from the addition of ethanol to the solvent mixtures [29], shown in Figure 2.2. Studies on co-solute effects in subcritical water are scarce. In a study conducted by Miller and Hawthorne [20], the solubility of anthracene, carbazole and chrysene mixtures in subcritical water was determined; yielding solubility depressions in all three solutes at temperatures above 100 °C.

Table 2.3: Solubility of atrazine in subcritical water and ethanol-modified subcritical water at 100 °C and 50 bar (data extracted from Curren and King [29])

Mole fraction of ethanol in solvent mixture	Solubility of atrazine (mole fraction)
0	5.00×10^{-4}
8	1.90×10^{-3}
12	3.56×10^{-3}
20	6.24×10^{-3}

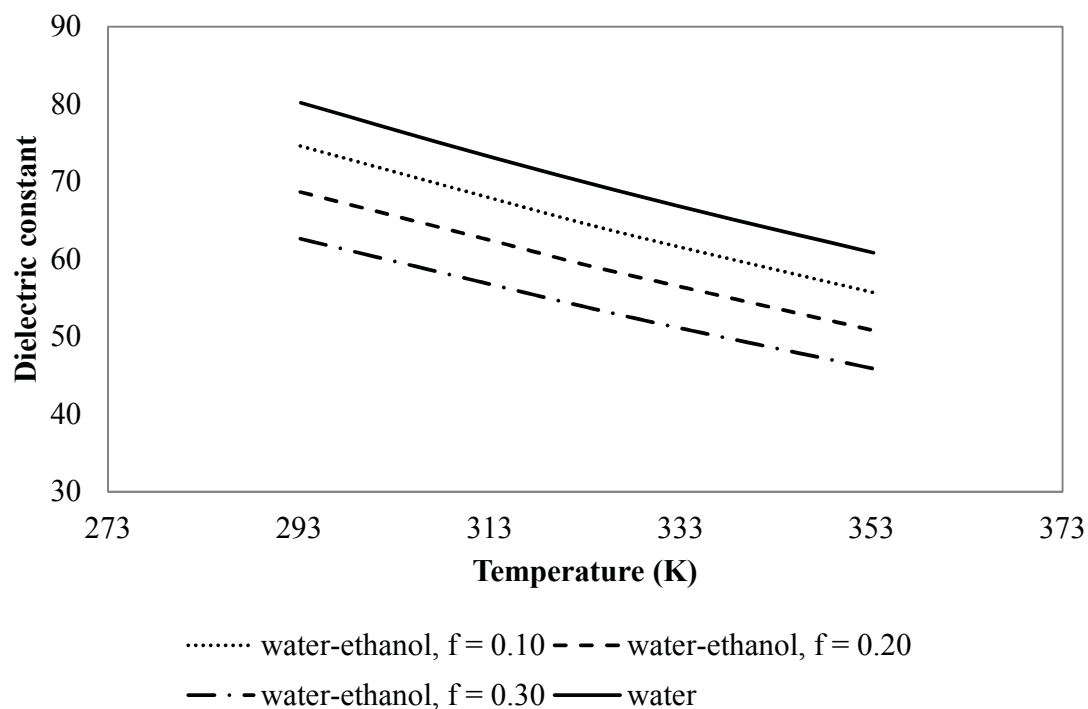


Figure 2.2: Dielectric constant of water and water-ethanol mixtures at various temperatures. (Data for water-ethanol mixtures were extracted from [30] while data for water was extracted from [31])

2.6 Conclusion

The present chapter highlights the factors that contribute to the solubility of solid solutes in subcritical water. Temperature and pressure changes affect the physico-chemical properties of both the solute and the solvent, consequently influencing the solubility of the solute in the solvent involved. H-bonding plays a dominant role in water; further influencing solute-water behavior at subcritical conditions.

2.7 Bibliography

- [1] Özel MZ, Bartle KD, Clifford AA, Burford MD. Extraction, solubility and stability of metal complexes using stainless steel supercritical fluid extraction system. *Analytica Chimica Acta* 2000;417 (2):177-84.
- [2] Gamsjager H, Lorimer JW, Scharlin P, Shaw DG. Glossary of terms related to solubility (IUPAC Recommendations 2008). *Pure and applied chemistry* 2008;80 (2):233-76.
- [3] Domanska U. Chapter 8: Solubility of organic solids for industry. In: Letcher TM, editor. *Developments and applications in solubility*. UK: RSC Publishing, 2007.
- [4] Allada SR. Solubility parameters of supercritical fluids. *Industrial & Engineering Chemistry Process Design and Development* 1984;23 (2):344-8.
- [5] McHugh MA, Krukonis VJ. *Supercritical fluid extraction: principles and practice*: Butterworth, Stoneham, Mass., 1986.
- [6] Castellan GW. *Physical chemistry*. Reading, MA: Addison-Wesley Publishing, 1971.
- [7] Lira CT. Physical chemistry of supercritical fluids: a tutorial. In: Charpentier BA, Sevenants, M.R., editor. *Supercritical Fluid Extraction and Chromatography: Techniques and Applications*, ACS Symposium Series, 1988. pp. 1-25.
- [8] Yee GG, Fulton JL, Smith RD. Fourier transform infrared spectroscopy of molecular interactions of heptafluoro-1-butanol or 1-butanol in supercritical carbon dioxide and supercritical ethane. *The Journal of Physical Chemistry* 1992;96 (15):6172-81.
- [9] Prausnitz JM, Lichtenthaler RN, de Azevedo EG. *Molecular thermodynamics of fluid-phase equilibria*. Englewood Cliffs, N.J.: Prentice-Hall Inc., 1969.
- [10] van Oss CJ, editor. *The properties of water and their role in colloidal and biological systems*. Netherlands: Elsevier Ltd., 2008.
- [11] Ohtaki H, Radnai T, Yamaguchi T. Structure of water under subcritical and supercritical conditions studied by solution X-ray diffraction. *Chemical Society Reviews* 1997;26 (1):41-51.
- [12] Brinkley RL, Gupta RB. Hydrogen bonding with aromatic rings. *AIChE Journal* 2001;47 (4):948-53.
- [13] Levitt M, Perutz MF. Aromatic rings act as hydrogen bond acceptors. *Journal of Molecular Biology* 1988;201 (4):751-4.
- [14] Scheiner S, Kar T, Pattanayak J. Comparison of various types of hydrogen bonds involving aromatic amino acids. *Journal of the American Chemical Society* 2002;124 (44):13257-64.
- [15] Furutaka S, Ikawa S-i. pi-hydrogen bonding between water and aromatic hydrocarbons at high temperatures and pressures. *The Journal of Chemical Physics* 2002;117 (2):751-5.
- [16] Tarakeshwar P. A theoretical investigation of the nature of the π -H interaction in ethene-H₂O, benzene-H₂O, and benzene-(H₂O)₂. *J. Chem. Phys.* 1999;111 (13):5838.
- [17] Kincaid JF, Eyring H. Free volumes and free angle ratios of molecules in liquids. *The Journal of Chemical Physics* 1938;6 (10):620-9.
- [18] Kontogeorgis GM. The Hansen solubility parameters (HSP) in thermodynamic models for polymer solutions. In: Hensen CM, editor. *Hansen Solubility Parameters: A User's Handbook*. Boca Raton: CRC Press, 2007. pp. 77-94.
- [19] Khuwijitjaru P, Adachi S, Matsuno R. Solubility of saturated fatty acids in water at elevated temperatures. *Biosci. Biotechnol. Biochem*, 2002;66 (8):1723-6.

- [20] Miller DJ, Hawthorne SB, Gizir AM, Clifford AA. Solubility of polycyclic aromatic hydrocarbons in subcritical water from 298 K to 498 K. *Journal of Chemical & Engineering Data* 1998;43 (6):1043-7.
- [21] Rössling GL, Franck EU. Solubility of anthracene in dense gases and liquids to 200°C and 2000 bar. *Berichte der Bunsengesellschaft für physikalische Chemie* 1983;87 (10):882-90.
- [22] Poling BE, Prausnitz JM, O'Connell JP. *The properties of gases and liquids*. New York: McGraw-Hill, 2001.
- [23] Arnold DS, Plank CA, Erickson EE, Pike FP. Solubility of benzene in water. *Journal of Chemical and Engineering Data* 1958;3 (2):253-6.
- [24] Kralj F, Sincic D. Mutual solubilities of phenol, salicylaldehyde, phenol-salicylaldehyde mixture, and water with and without the presence of sodium chloride or sodium chloride plus sodium sulfate. *Journal of Chemical & Engineering Data* 1980;25 (4):335-8.
- [25] Diebler H, Secco F, Venturini M. The influence of intramolecular hydrogen bonding on proton-transfer reactions. A temperature-jump study of acid-base reactions involving substituted salicylic acids. *The Journal of Physical Chemistry* 1984;88 (19):4229-32.
- [26] Karasek P, Planeta J, Roth M. Solubilities of oxygenated aromatic solids in pressurized hot water. *Journal of Chemical & Engineering Data* 2009;54 (5):1457-61.
- [27] Mathis J, Gizir AM, Yang Y. Solubility of alkylbenzenes and a model for predicting the solubility of liquid organics in high-temperature water. *Journal of Chemical & Engineering Data* 2004;49 (5):1269-72.
- [28] Kayan B, Yang Y, Lindquist EJ, Gizir AM. Solubility of benzoic and salicylic acids in subcritical water at temperatures ranging from (298 to 473) K. *Journal of Chemical & Engineering Data* 2009;55 (6):2229-32.
- [29] Curren MSS, King JW. Solubility of triazine pesticides in pure and modified subcritical water. *Analytical Chemistry* 2001;73 (4):740-5.
- [30] Akerlof G. Dielectric constants of some organic solvent-water mixtures at various temperatures. *Journal of the American Chemical Society* 1932;54 (11):4125-39.
- [31] Bradley DJ, Pitzer KS. Thermodynamics of electrolytes. 12. Dielectric properties of water and Debye-Hueckel parameters to 350.degree.C and 1 kbar. *The Journal of Physical Chemistry* 1979;83 (12):1599-603.

3 Solubility Measurement of Solid PAHs in Subcritical Water

3.1 Introduction

The conduct of solubility experiments can primarily be divided into dynamic or static equilibrium methods. The dynamic method can be divided into the dynamic continuous method and the dynamic extractive method. The dynamic continuous method is used solely for *liquid* solute solubility measurement while the dynamic extractive method is used for *solid* solutes. A dynamic extractive method involves the use of a pump to provide continuous subcritical water flow through a bed of solute. The main issue with a dynamic extractive equilibrium technique is the mass transfer rate between the liquid and the solute matrix, where the possibility of the solute solution not attaining saturation needs to be taken into account [1]. Generally, the concentration of a solute solution at the exit of the equilibrium cell must be independent of the length of the cell and the superficial velocity of the liquid solvent [1,2]. These characteristics are material-specific and, therefore, it is vital to distinguish the conditions for each solute at which equilibrium is achieved [1]. Also, in a dynamic method where a solid *mixture* is involved (instead of a pure solid), one or more components can be selectively extracted and, consequently, the solid mixture composition would change with time. Thus, the dynamic extractive method is suitable for pure solid solubility studies rather than for mixed solids solubility studies.

A static equilibrium method can be divided into a static synthetic method and a static analytical method. Static synthetic methods are employed when the global initial composition of the system is known, and when the equilibrium phase composition can be obtained directly. However, the static synthetic method is only confined to binary systems. A static analytical method differs from the synthetic method in that samples are taken from the equilibrium phases for analysis. While the analytical method requires more effort and time, it can be applied to mixtures containing more than two compounds. Generally, a static equilibrium method has a fixed amount of solvent in contact with the solute and is relatively slow to reach equilibrium when solubility is very low. The equilibration time, i.e. the minimum amount of time required to achieve a saturated solution in an equilibrium cell, is of primary concern in a static extraction

method. The dynamic extractive method and the static analytical method are discussed in detail in the following sections.

3.1.1 Dynamic extractive equilibrium method

The significant solvent power of water for a number of hydrophobic compounds at temperatures above 373K was first reported by Miller and Hawthorne [2] who used a dynamic equilibrium method, shown schematically in Figure 3.1. Solutes were packed together with clean sand into a saturation cell while water was supplied in constant flow mode with an ISCO pump through a preheating coil. Pressures in the 30-70 bars range were maintained with an outlet valve and temperature was measured with a thermocouple placed in a tee before the saturation cell. Chloroform was injected with an ISCO pump into a fused-silica-lined tee to prevent deposition of the solute from water as it cooled during collection. A stainless steel cooling coil was immersed in an ice bath to cool the solute-water-chloroform mixture to room temperature. After an initial equilibration period of 30 minutes, water at a certain flow rate was passed through the saturation cell and 5 – 10 3-min fractions for each condition were collected. In order to ensure that equilibrium was achieved while water was flowing through the saturation cell, saturation cells of different volumes were tested. The residence time of the water in the cell was found to be sufficient to achieve saturation. Samples were then analyzed with either a GC/FID (gas chromatograph with flame ionization detection) or a GC/MS (gas chromatograph with mass spectroscopy).

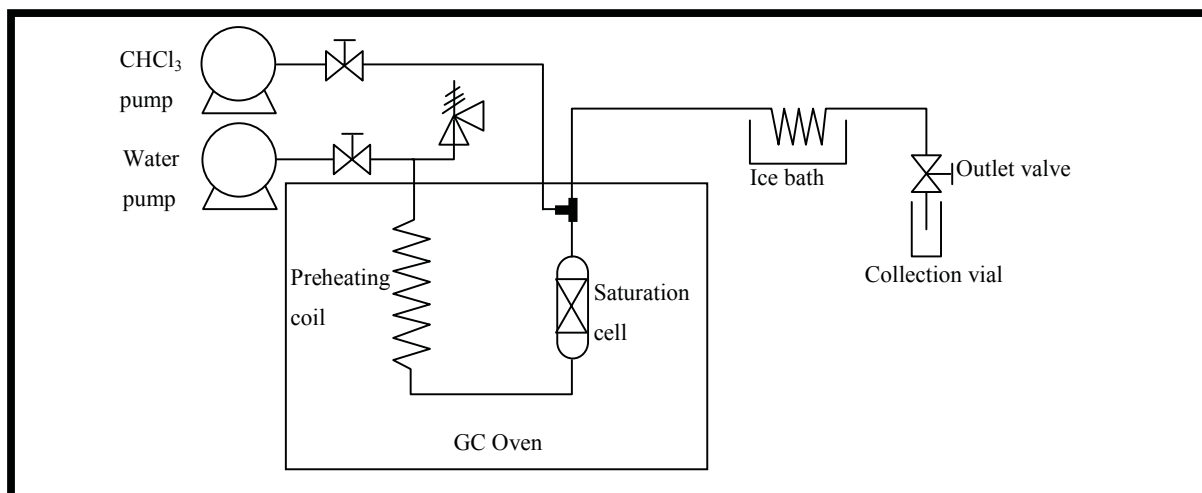


Figure 3.1: Dynamic extractive equilibrium experimental set-up for solubility study by Miller and Hawthorne [2]

Since the publication of the dynamic extractive equilibrium method by Miller and Hawthorne [2], a number of experiments with slight modifications to the dynamic method have also been conducted by Andersson et al. [3], Karasek et al. [4,5] and Kayan et al. [6]. In the experiments conducted by Andersson et al. [3], toluene was used as a collection solvent rather than chloroform. The main reason for the choice of collection solvent was that the authors could obtain a lower RSD (relative standard deviation) with toluene. The RSD obtained for polycyclic aromatic hydrocarbons (PAHs) with toluene at 50 °C and 50 bar was 23% while the RSD obtained with chloroform was 109%.

In the solubility study conducted by Karasek et al. [4], water was fed into an equilibrium cell encased in an aluminum block covered with a heavy thermal insulation coat. The equilibrium cell was filled with PAH mixed with glass beads. The system was then heated and pressurized, and allowed to stabilize for 20 minutes. A water flow rate of 0.010 – 0.017 g/s was then employed to collect 5 fractions of samples for each condition. Collection was conducted in vials capped with Teflon-lined silicone rubber. The sample in the vial was then kept at 5 °C for 24 hours, then mixed with toluene to create an emulsion and equilibrated for 72 hours. The emulsion was subsequently separated and analyzed with CG/MS.

3.1.2 Static analytical equilibrium method

In the static equilibrium method, water and solute are loaded into an equilibrium vessel and heated to a desired temperature and pressure. Stirrers are used to ensure that both the solute and water are properly mixed to saturation. When equilibrium is attained, the water saturated with the solute is pushed out of the system with gas or an organic solvent [7,8]. A schematic diagram depicting the static equilibrium method is shown in Figure 3.2.

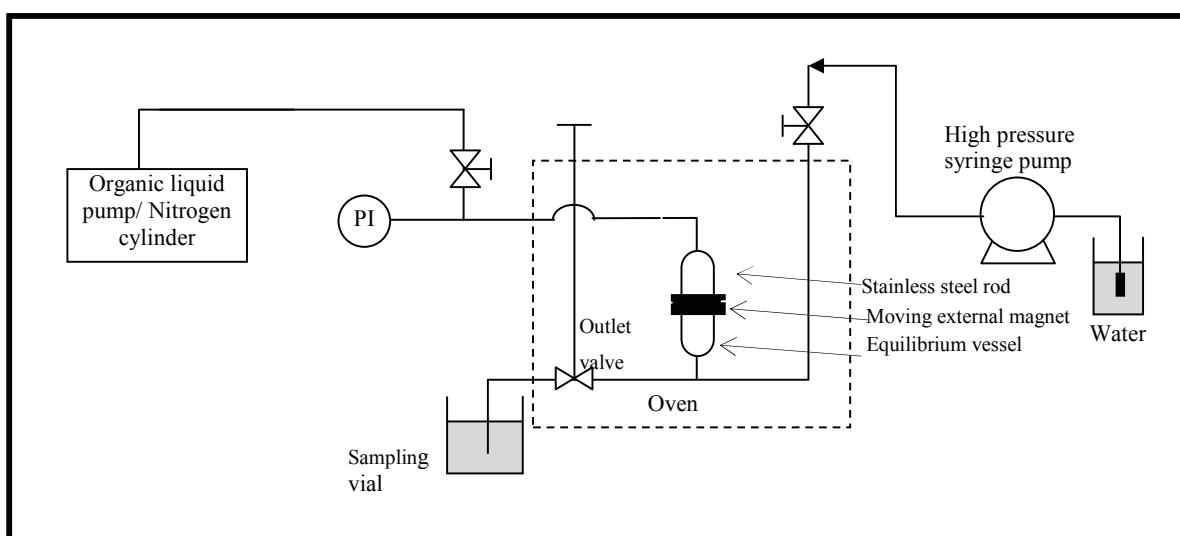


Figure 3.2: General schematic diagram of solubility determination based on the static equilibrium method

In the study conducted by Mathis et al. [8], solubilities of liquid organic solutes were determined with the static equilibrium method. Water was first filled into a 10ml equilibrium cell. The cell was then connected to the system, placed in an oven, and the oven was heated up. During the heating process, approximately 5 ml of a pure liquid organic solute was loaded into the equilibrium cell by pushing out the preloaded water through the outlet of the cell. Approximately 10 min after the oven reached the desired temperature, mixing was conducted for another 10 min. The system was then allowed to equilibrate without any mixing for a further 10 min before the collection of the aqueous phase. The pressure of the system was maintained

at 50 bar. After the equilibration step, approximately 2 ml of the saturated aqueous solution was decanted into a vial that contained 2 ml of methylene chloride. GC/FID was used to measure the amount of solute dissolved. The RSD obtained in the solubility study conducted by Mathis et al. [8] ranged between 3.7 % and 19.5 %.

A solubility study on solid organic compounds via the static equilibrium method was conducted by Carr [9] where solid solutes were preloaded into an equilibrium cell. The cell was then placed in a GC oven. A syringe pump was used to deliver water into the system. The system was then heated to a required temperature. When the desired temperature was achieved, the system was equilibrated for 10 min while being stirred by a magnetic bar. The pressure of the system was maintained at 70 bar. After 10 min of mixing, the magnetic stirrer was stopped while nitrogen at 72 bar was allowed to contact the solution. The solution was then decanted into a collection vial with the N₂ acting as the force to push the solution into the vial while maintaining the liquid state of the solution. The solution collected was weighed, washed with acetone, and dried. The outlet valve was also washed with acetone and dried. Gravimetric and/or UV analyses were conducted on the samples to measure the amount of solute collected. The solubility data obtained for griseofulvin was found to have RSDs between 4.1% and 39.4% [7].

In the present study, a static analytical equilibrium method was employed to measure the solubilities of anthracene and *p*-terphenyl. This work follows from the experimental work conducted by Carr [9] with a number of modifications incorporated to improve the reliability and the RSD of the solubility data obtained. A detailed discussion is given in the following sections.

3.2 Preparation for solubility measurement: Water and solutes characterization at subcritical conditions

Prior to the start of measuring solubility in subcritical water, an understanding of the behavior of the solvent, as well as the behavior of the organic compounds in the solvent involved are of importance. Considerations that need to be factored in prior to a solubility measurement include:

- a) vapor-liquid equilibria (VLE) of the solvents and solid-vapor equilibria (SVE) of the solutes at subcritical conditions
- b) phase behavior of organic compounds in the solvents involved at subcritical conditions
- c) temperature and pressure profiles of the liquid solvents in an equilibrium vessel
- d) mixing time required for solutes to reach saturation (equilibration time)
- e) stability of solutes at operating conditions

3.2.1 Vapor-liquid equilibria of water and solid-vapor equilibria of solutes at subcritical conditions

Solubility measurements conducted in this study are above the normal boiling points of the solvents. Sufficient pressure must be applied to maintain the liquid state of the solvents used. Therefore, an understanding of the VLE of the solvents involved is essential. The saturated vapor pressures of water at various temperatures are shown in Table 3.1. The data from Table 3.1 shows that a minimum pressure of 16 bar is required to ensure water is in the liquid state at temperatures between 120 - 200 °C. The sublimation pressure of anthracene and *p*-terphenyl are also shown in Table 3.1, and are lower than the vapor pressure of water. All solubility measurements in the present study were conducted at a pressure of 50 bar to keep a safe range away from the minimum 16 bar.

Table 3.1: Vapor pressures for water, anthracene and *p*-terphenyl at various temperatures

Temperature (°C)	Water Saturated vapor pressure ^a (bar)	Anthracene Sublimation pressure ^b (bar)	<i>p</i> -Terphenyl Sublimation pressure ^b (bar)
120	1.99	8.97×10^{-4}	8.59×10^{-5}
140	3.61	2.50×10^{-3}	3.15×10^{-4}
150	4.76	3.99×10^{-3}	5.70×10^{-4}
160	6.18	6.22×10^{-3}	9.33×10^{-4}
170	7.92	9.45×10^{-3}	1.68×10^{-3}
180	10.02	1.40×10^{-2}	2.75×10^{-3}
200	15.54	2.92×10^{-2}	6.81×10^{-3}

Data obtained from: ^a Parry et al. [10], ^b Zhao et al. [11]

3.2.2 Phase behavior of organic solutes in subcritical water

Fundamental to the study on solubility is an understanding of the phase behavior of a system to ensure proper use and design of an experimental set-up. Phase behavioral studies are important in solubility experiments conducted at elevated pressures since solutes may undergo melting point depression. Therefore, a preliminary phase behavior study is required since the solubility measurement method utilized in this study can only measure the solubility of *solid* solutes in *liquid* solvents. Therefore, it was vital that phase behaviors of the solutes were known prior to the solubility study. The experimental method and results for a phase behavioral study is given in the following sections.

3.2.2.1 Phase behavior study: Apparatus and experimental methodology

The experimental set-up for a phase behavior study is shown in Figure 3.3. Solute and solvents were packed into a glass pipette tapered at one end. The pipette was then put into a Jergusen gauge and the Jergusen gauge (with the pipette inside) was placed in a GC oven. A K-type thermocouple attached to a Jenco temperature indicator (model 7000CH) was inserted into the pipette through the Jergusen gauge. Nitrogen at 50 bar was regulated into the Jergusen gauge. Once the system reached 50 bar, the valve connected to the N₂ supply line was closed. Nitrogen at 50 bar was used to maintain the solvents in liquid form. The temperature of the oven was first raised to the lowest desired temperature. As the oven was heated up, the pressure in the system increased. Nitrogen was released via valve V3 to maintain the pressure of the system at 50 bar. When the system had reached the required temperature and pressure, the system was allowed to equilibrate for 30 minutes. Any physical changes to the sample were observed. The temperature was then raised to the next designated temperature and the steps were repeated until the maximum desired temperature.

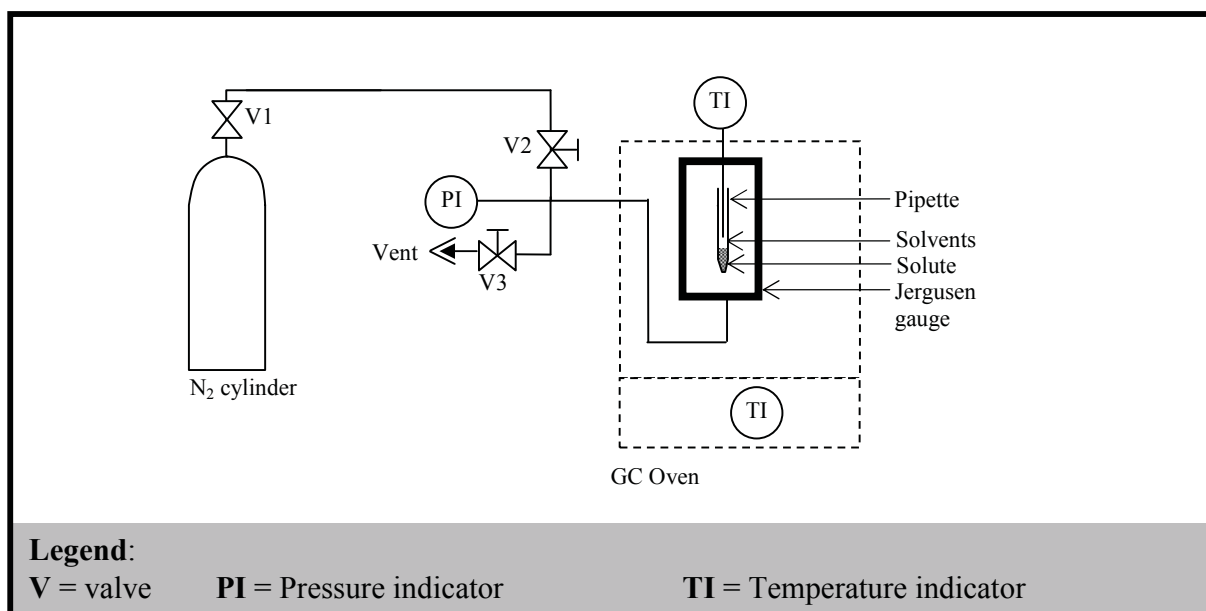


Figure 3.3: Schematic diagram of the phase behavior study

3.2.2.2 Results and Discussion

The phase behavior of anthracene and *p*-terphenyl in subcritical water at 50 bar and various temperatures are shown in Table 3.2. Both compounds were found to be solid in subcritical water between 120 °C and 200 °C. Thus, melting point depression was not observed for anthracene and *p*-terphenyl in water at temperatures as high 200 °C.

Table 3.2: Phase behavior of anthracene and *p*-terphenyl in subcritical water at 50 bar and various temperatures

	Temperature (°C)	Phase behavior
Anthracene	120	Solid-liquid
	140	Solid-liquid
	150	Solid-liquid
	160	Solid-liquid
	170	Solid-liquid
	180	Solid-liquid
	200	Solid-liquid
<i>p</i> -terphenyl	120	Solid-liquid
	140	Solid-liquid
	150	Solid-liquid
	160	Solid-liquid
	170	Solid-liquid
	180	Solid-liquid
	200	Solid-liquid

3.2.3 Temperature and pressure profiles of liquid solvents in an equilibrium vessel

3.2.3.1 Temperature profile

Solubility measurement in this study was conducted in an equilibrium vessel with a volume of approximately 6 ml. During a solubility run, the determination of solvent temperature in the equilibrium vessel became impossible due to the presence of filter stones fitted to each end of the equilibrium vessel. While the filter stones prevented physical entrainment of solid solutes in the liquid phase, these stones also prevented a thermocouple from being inserted into the equilibrium vessel. Consequently, the average time for solvent in the equilibrium vessel to reach a required temperature was measured. A schematic diagram of the experimental set-up is given in Figure 3.4. In profiling the temperature of liquid water in the equilibrium vessel, a filter stone was removed from the top-end of the equilibrium vessel. In this study, the average time taken for pure water to reach a designated temperature in the equilibrium vessel was used as the heating time required to heat liquid water, and is shown in Table 3.3.

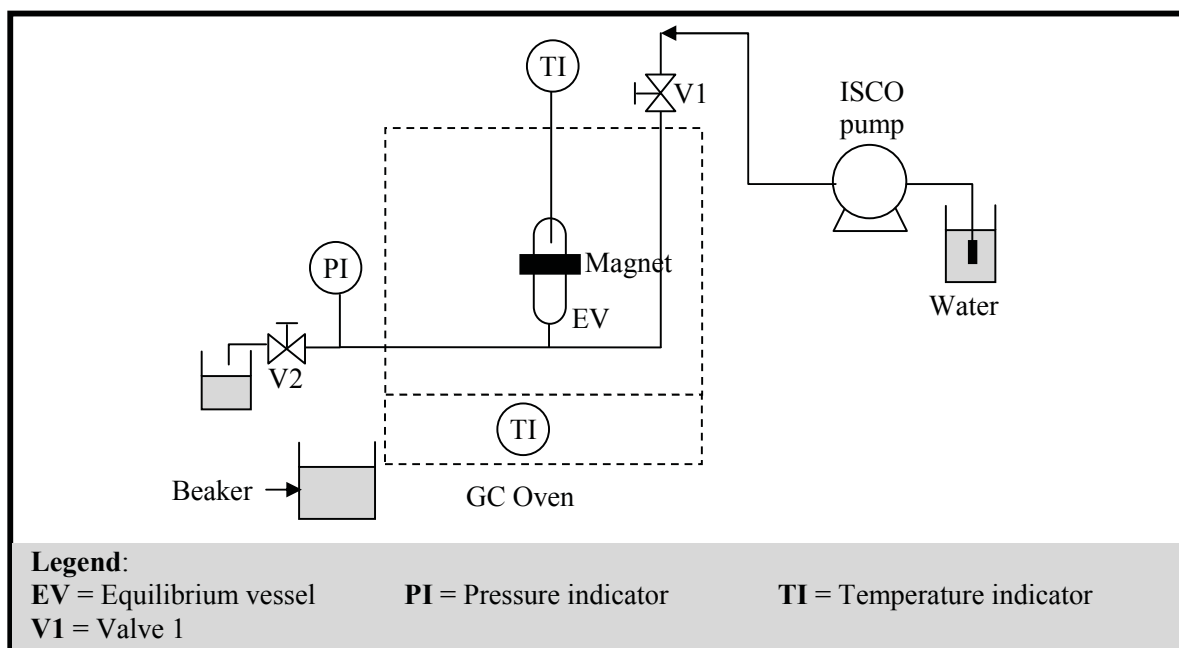


Figure 3.4: Schematic diagram of temperature profiling in an equilibrium vessel

Table 3.3: Average heating time to attain a required temperature in an equilibrium vessel

Temperature (°C)	Time (min)	Temperature (°C)	Time (min)
120	17 ± 1	170	22 ± 2
140	19 ± 1	180	23 ± 2
150	20 ± 1	200	25 ± 2
160	21 ± 1		

3.2.3.2 Pressure profile

A preliminary study on the pressure profiles of the liquid solvent in the equilibrium vessel was conducted to verify the ability of the rig to sustain the pressure of the system without any external input at a constant designated pressure. The investigation into the ability of the system to maintain its pressure was necessary to ensure both steady state and equilibrium were attained. The experimental set-up is shown in Figure 3.5. Water, heated to 100 °C, 150 °C and 200 °C, was allowed to reach a pressure of 50 bar. Once the required temperature was attained, the pressure of the system was observed. The change in the pressure of the system (while temperature was maintained, and V1 closed) is shown in Figure 3.6. Pressures were measured with a Druck pressure transducer (PDCR 911), coupled with a Druck DPI 260 pressure indicator calibrated with a Hydraulic Deadweight Tester (Pressurements Model M2200). It was observed that pressure increased rapidly in the first 20 to 30 min of heating, and decreased slowly thereafter. At 150 °C and 200 °C, constant pressures were observed after 85 min and 65 min respectively, while at 100 °C, water pressure was observed to decrease slowly without reaching steady state up to the 125th min of heating. These profiles were attributed to a difference in the rate of thermal expansion between water and the equilibrium vessel. While solubility measurements could be conducted for a long period of time to ensure that a constant pressure was maintained, it was decided that each solubility run should be conducted at as short an interval as possible to prevent thermal degradation of solutes. As such, the equilibrium vessel was pre-expanded in a 50 °C oven prior to the start of the experiment, and an ISCO model 260D syringe pump was used to maintain the pressure of liquid solvents in the system.

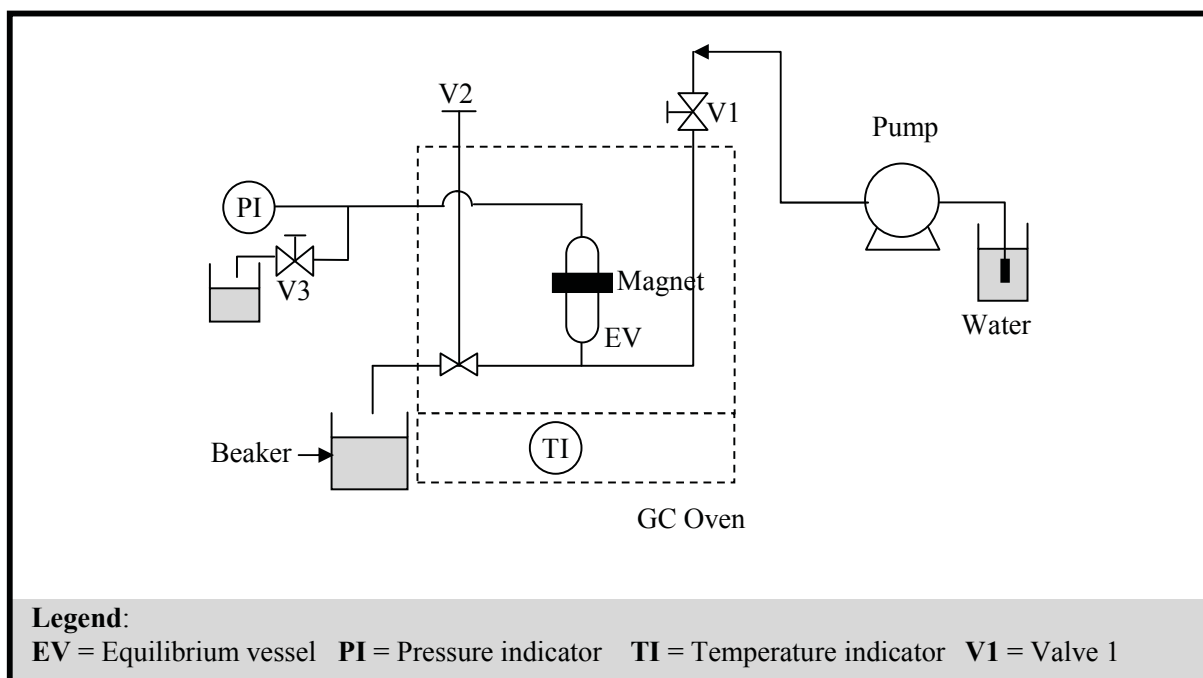


Figure 3.5: Schematic diagram of high pressure profiling in an equilibrium vessel

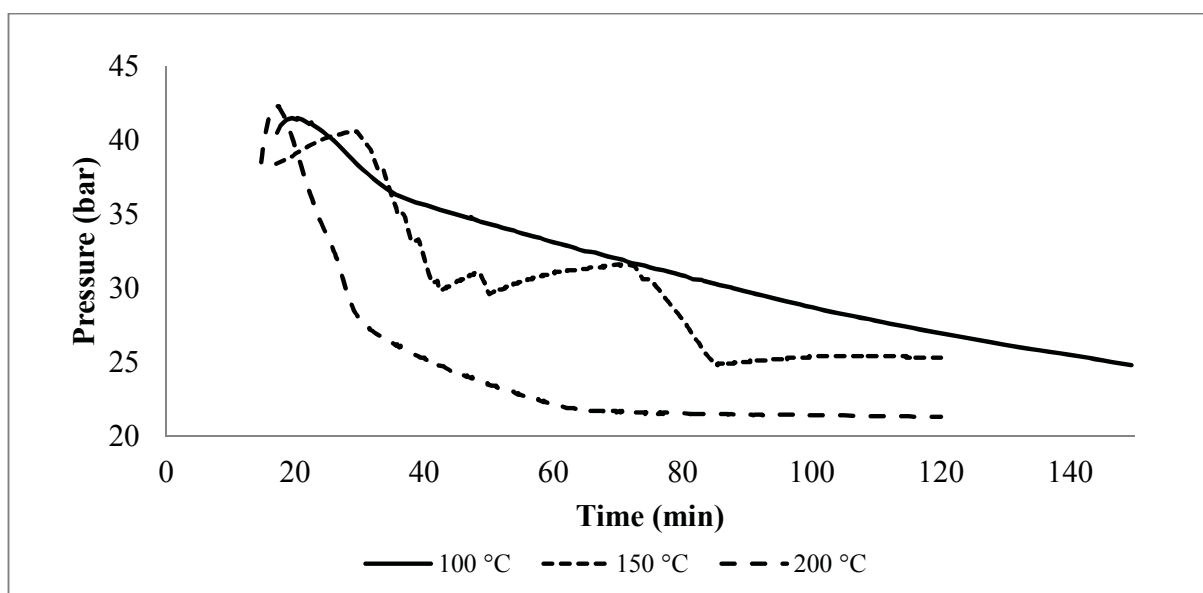


Figure 3.6: Pressure profile at 100 °C, 150 °C and 200 °C. [Note that the pressure profile is not given in the first 15-20 min due to the rapid increase in the water pressure and the continuous manual depressurization of the system via valve V3]

The temperature and pressure profiles obtained for subcritical water at 100 °C, 150 °C and 200 °C were superimposed and are shown in Figures 3.7 – 3.9. These diagrams show that observance of a maximum pressure was not an indication of the system reaching thermal equilibrium. Hence, the diagrams in Figures 3.7 – 3.9 substantiate the need to pre-measure the heating time required for solvents to reach a designated temperature.

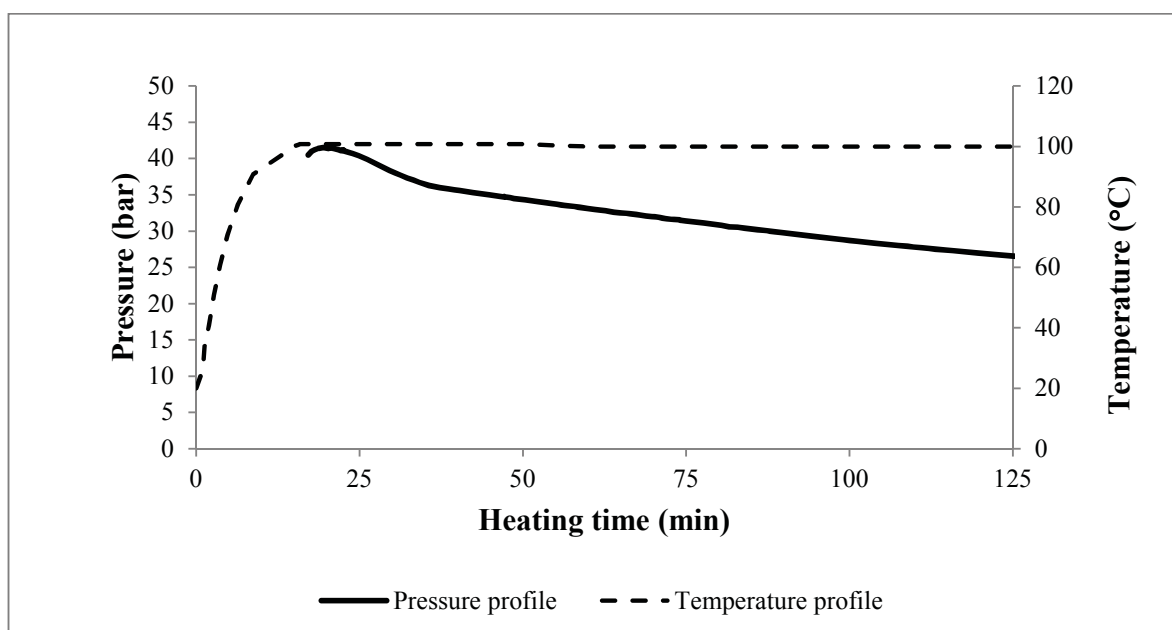


Figure 3.7: Pressure and temperature profiles of subcritical water in an equilibrium vessel at 100°C

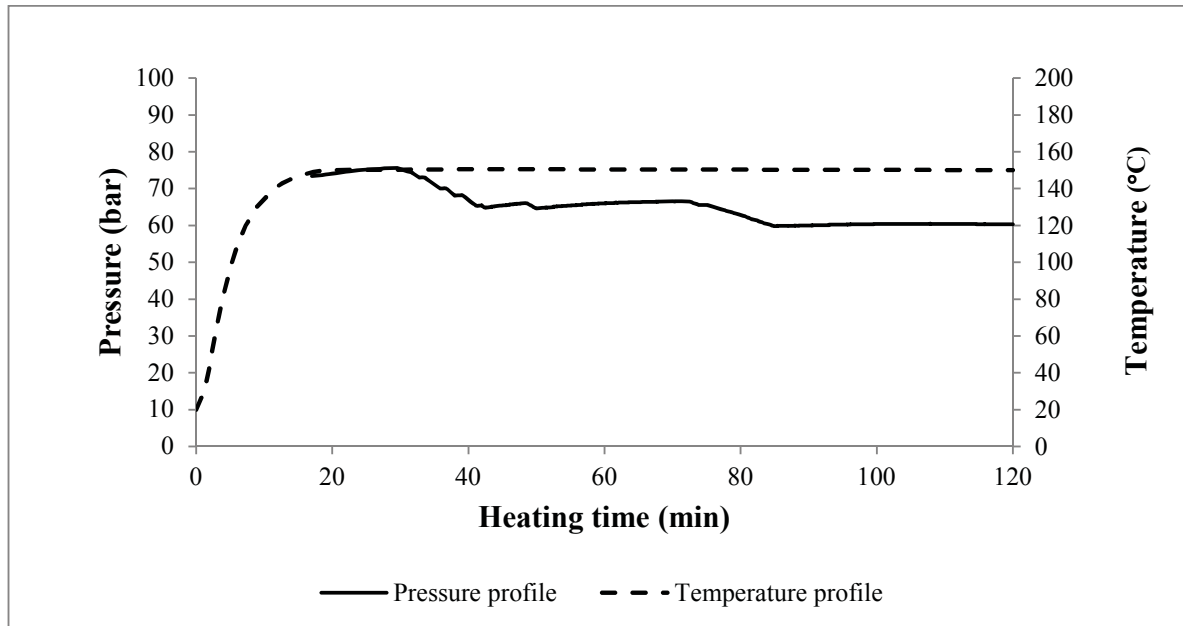


Figure 3.8: Pressure and temperature profiles of subcritical water in an equilibrium vessel at 150°C

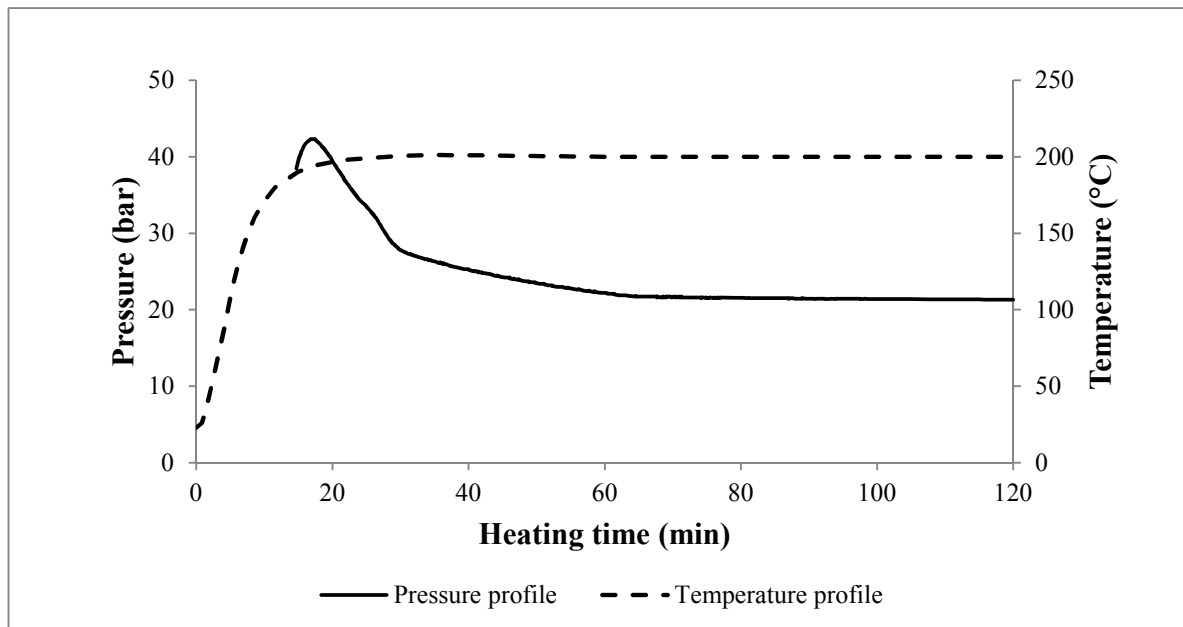


Figure 3.9: Pressure and temperature profiles of subcritical water in an equilibrium vessel at 200°C

3.2.4 Stability of solid solutes at experimental conditions

Solubility measurements at relatively high temperatures for an extended amount of time necessitate a stability study on the investigated solutes. Solute reaction and/or degradation in subcritical water would render experimentally determined solubility data inaccurate. Literature surveys on the stability of PAHs in subcritical water reveal contrasting results [3,4,6,9,12]. In the solubility study by Karasek et al. [4], analysis of PAHs extracted at temperatures between 40 °C and 210 °C did not reveal noticeable degradation. However, in a study by Yang and Hildebrand [12], a portion of phenanthrene in subcritical water was degraded to several organic compounds that include phenol, naphthalene and benzoic acid [12]. Degradation and reduced recovery of extracted PAHs using water at high temperatures and pressures have also been observed [13,14].

The detailed study by Yang and Hildebrand [12] showed that temperature and concentrations of phenanthrene and dissolved oxygen in subcritical water played significant roles in phenanthrene degradation. The proportion of degraded phenanthrene was found to be higher at higher temperatures. For a relatively high concentration of phenanthrene in subcritical water, insignificant amount of degradation was obtained with the proportion of phenanthrene that degraded ranged from 0.2 % to 5.6 % between 150 °C and 350 °C [12]. At lower concentrations of phenanthrene, the proportion of phenanthrene that degraded increased to 61.9% at 350 °C [12]. Compounds obtained from the degradation of phenanthrene were found to be mostly byproducts of oxidation. The oxidizing power of subcritical water in the investigated phenanthrene-water system was attributed by the authors to the presence of dissolved oxygen in water [12]. Therefore, in solubility/extraction studies where the degassing of water was carried out, no significant degradation was observed. The reduction in the amount of dissolved oxygen, thus, reduces the oxidizing power of water. Also, in most literature studies, relatively large quantities of organic compounds are used. The small quantity of oxygen available in the degassed water could only oxidize a small fraction of the large quantity of organic compounds present; reducing the degradation percentage to unnoticeable levels [12].

In order to reduce solute degradation in the present study, water was degassed prior to the conduct of solubility measurements while substantial amount of solutes was added into the

equilibrium vessel. FTIR (Fourier transformed infra-red spectroscopy) recorded with a Thermo Nicolet 370 FTIR spectrometer on a KBr disc was used to observe for degradation of anthracene and *p*-terphenyl under the experimental conditions used in this study. No noticeable degradation was found in both anthracene and *p*-terphenyl from the IR spectra obtained. The IR spectra for both solutes are shown in Appendix A.

3.3 Solubility measurement

3.3.1 Materials

Anthracene (99 mole %) and *p*-terphenyl (99 mol %) were purchased from Sigma-Aldrich. Both compounds were used as received. Deionised water was used in all experiments.

3.3.2 Apparatus and experimental method

A static equilibrium experimental set-up was utilized in this study and is shown in Figure 3.10. Solute was packed into a 6 ml stainless steel equilibrium vessel together with a magnetic stirrer. A front view diagram of the equilibrium vessel is shown in Figure 3.11(a). The amount of solute loaded into the vessel was higher than the amount solubilized during the experiment, and at all times there was an excess of solute. An external oscillating iron ring magnet attached to a motor via stainless steel rods, guided the internal magnet. Filter stones of 2 μm porosity were fitted to each end of the vessel to prevent physical entrainment of the solute in the liquid phase. A cross-section diagram of the filter stone set-up is shown in Figure 3.11(b). A Shimadzu GC-8A chromatography oven was used for heating. The temperature indicator in the GC oven was calibrated with a GMC-calibrated K-type thermocouple attached to a Jenco (model 7000CH) temperature indicator.

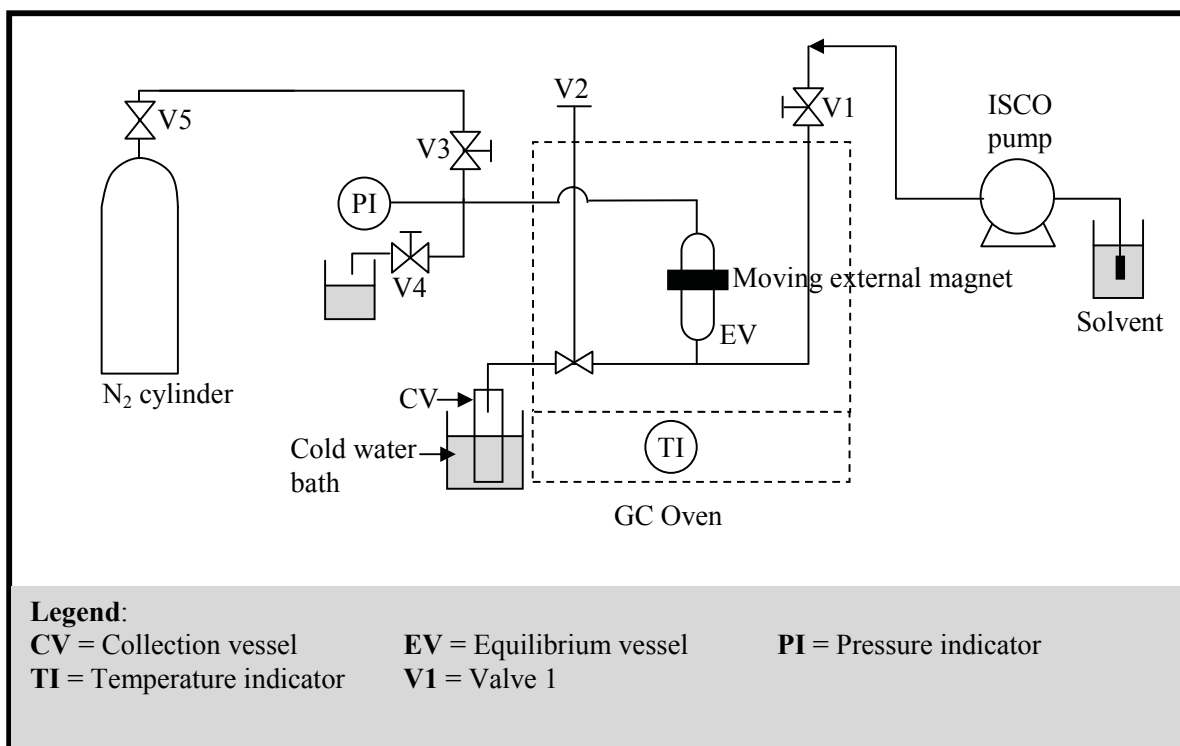


Figure 3.10: Schematic diagram of the solubility apparatus

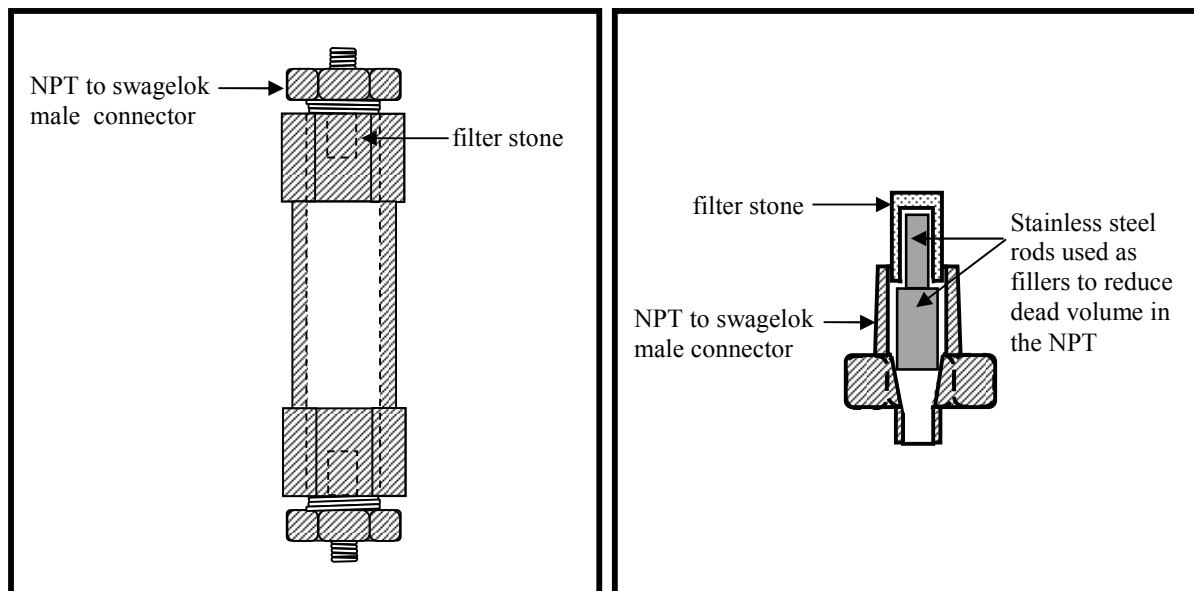


Figure 3.11: (a) Front view of equilibrium vessel (b) Cross section view of filter stone set-up

At the commencement of an experiment, an ISCO model 260D syringe pump was used to supply water to the system. Water was *not* heated and set to the required temperature prior to being pumped into the rig due to the limitations in the equipment available. Valves V1, V2 and V4 were opened. Valve V2 and subsequently, V4, were closed once water dripped out. At the onset of heating, valve V4 was occasionally opened to relieve pressure generated from thermal expansion. Pressure was kept at 50 bar throughout the experiment with an ISCO syringe pump operating in constant pressure mode. Pressures were measured with a Druck pressure transducer (PDCR 911), coupled with a Druck DPI 260 pressure indicator calibrated with a Hydraulic Deadweight Tester (Pressurements Model M2200). Stirring commenced at the onset of heating. The average time for water in the equilibrium vessel to reach a required temperature is described in Section 3.2.3. Once the system had reached the required temperature, the system was left to equilibrate for a designated amount of time while being stirred by the magnetic stir bar. Equilibration times for each condition were measured by measuring the concentration of solute into aliquots of subcritical water solutions sampled at fixed time intervals. Equilibration time for each condition is shown in Figure 3.12. Low solubilities and lower temperatures required longer mixing time to reach equilibrium than high solubilities and high temperatures.

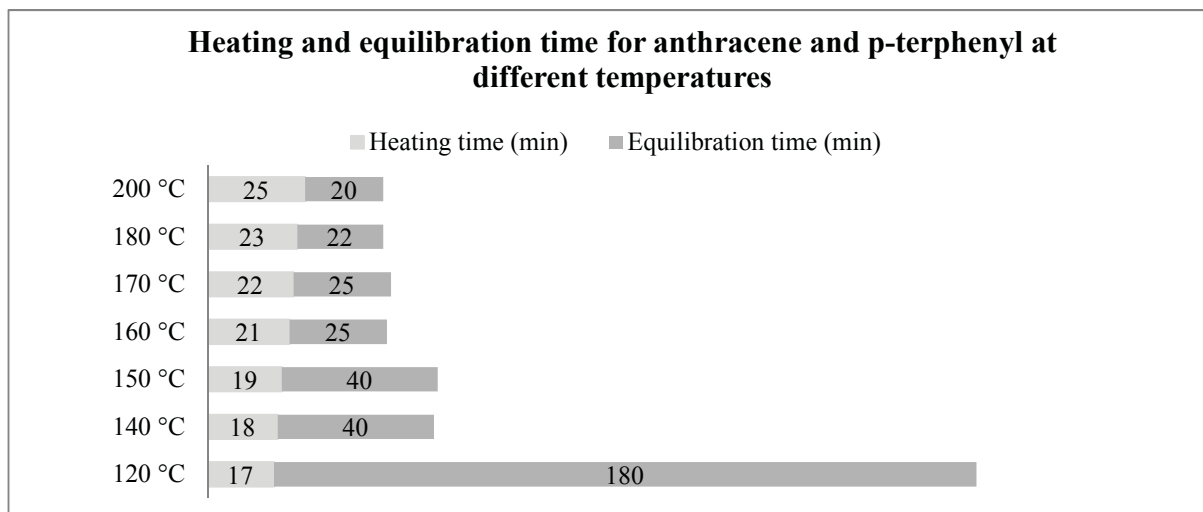


Figure 3.12: Heating and equilibration times required for solubility measurement at various temperatures

Near the end of the equilibration time, a weighed collection vessel (CV) dipped into a cold water bath was connected to valve V2 (Figure 3.13). The collection vessel was made of a 1/2-inch tube fitted with a 1/2-inch cap at the bottom, and a 1/2-inch to 1/8-inch reducer at the top, with the 1/8-inch part of the reducer being connected to the collection vessel. All fittings and tubing were made of stainless steel type 316. At the end of equilibration, the magnetic stirrer was stopped. Nitrogen gas preset to 54 bar was allowed to contact the solution in the equilibrium vessel via valve V3. Nitrogen was used to maintain the pressure of the solution in the equilibrium vessel to prevent premature vaporization of the solution. In this way it is possible to withdraw samples without disturbing the equilibrium condition (constant pressure, temperature and phase composition). Once V3 was fully opened, V2 was opened for the decanting of solution into the collection vessel (CV). When N₂ started to flow into the collection vessel, V2 and V3 were shut and the oven was turned off.

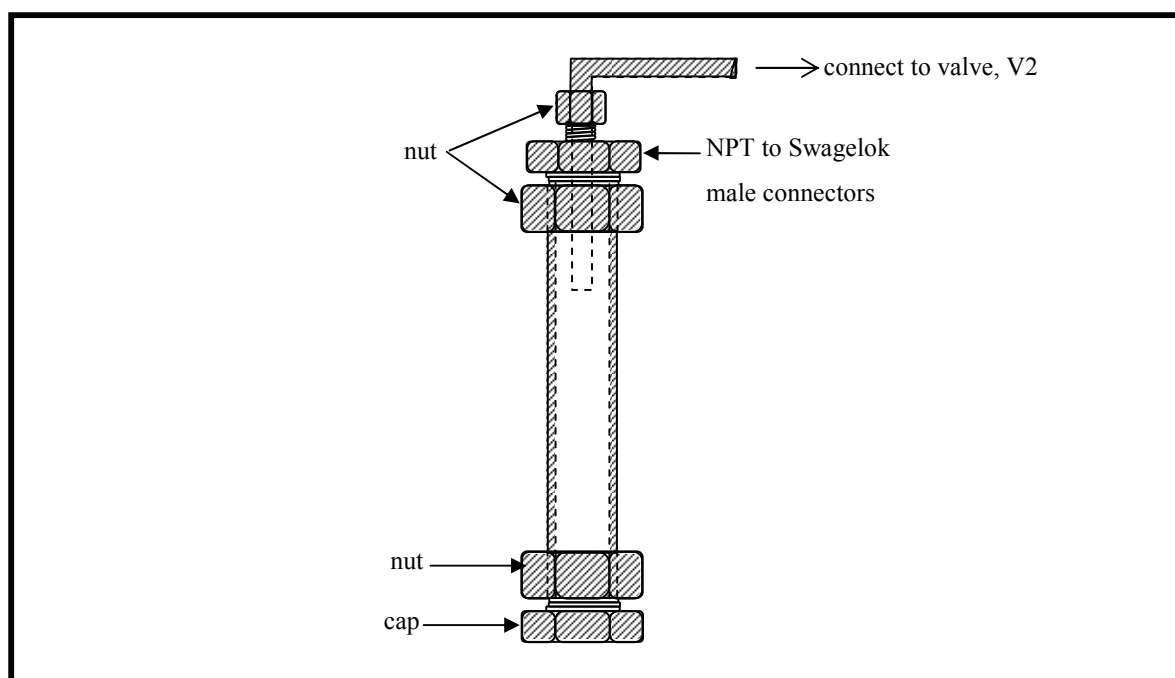


Figure 3.13: front view of the collection vessel

When the collection vessel had cooled, it was removed, externally dried and weighed. The solvent and the precipitated solutes in the collection vessel were collected in a glass vial. Further washings with acetone were conducted to ensure all solutes were collected in the glass vial. Valve V2 was also washed with acetone. The liquid was collected in a glass vial and dried. The solutes were then dissolved in analytical grade methanol and analyzed by UV. Five-point calibration curves were generated for each solute, and shown in Appendices B1 and B2. Three experimental runs were conducted on each solubility data point with a maximum of 5% relative standard deviation (RSD) obtained. The reported solubility data is expressed as the mean values of three experimental runs and given as mole fractions of the solute in water. The results were compared against the solubility of anthracene in subcritical water from published literature and are discussed in the following sections.

3.3.3 Rig validation

The ability of the apparatus designated for solubility study in this work, to accurately measure solubility, was validated by measuring and comparing the solubility of anthracene in subcritical water with published literature data. Solubility data of anthracene in subcritical water measured at 50 bar was compared with various authors as shown in Table 3.4 and Figure 3.14.

Table 3.4: Solubility (x_2) of anthracene (mole fraction) in subcritical water measured using various methods

Temperature		100 °C	150 °C	160 °C	200 °C
Miller et al. [15] [dynamic]	x_2	$(3.20 \pm 0.50) \times 10^{-7}$ [P = 45 bar]	$(9.2 \pm 0.60) \times 10^{-6}$ [P = 47 bar]	-	$(2.10 \pm 0.25) \times 10^{-4}$ [P = 48 bar]
	RSD	15.6 %	6.5 %	-	11.9 %
Andersson et al. [3] [dynamic]	x_2	$(3.25 \pm 0.34) \times 10^{-7}$ [P = 50 bar]	$(1.02 \pm 0.13) \times 10^{-5}$ [P = 50 bar]	-	$(1.38 \pm 0.19) \times 10^{-4}$ [P = 50 bar]
	RSD	10.5 %	12.7 %	-	13.8 %
Karasek et al. [4] [dynamic]	x_2	$(4.57 \pm 0.32) \times 10^{-7}$ [P = 39 bar]	-	$(1.59 \pm 0.04) \times 10^{-5}$ [P = 54 bar]	$(1.30 \pm 0.03) \times 10^{-4}$ [P = 77 bar]
	RSD	7.0 %	-	2.5 %	2.3%
Carr [9] [static]	x_2	2.40×10^{-7} [P = 70 bar]	9.00×10^{-6} [P = 70 bar]	1.85×10^{-5} [P = 70 bar]	2.30×10^{-4} [P = 70 bar]
	RSD	Not available	Not available	Not available	Not available
This work [static]	x_2	-	$(8.75 \pm 0.24) \times 10^{-6}$ [P = 50 bar]	$(1.55 \pm 0.02) \times 10^{-5}$ [P = 50 bar]	$(1.53 \pm 0.01) \times 10^{-4}$ [P = 50 bar]
	RSD	-	2.74 %	1.90 %	0.88 %

x_2 = solubility in mole fraction, RSD = relative standard deviation

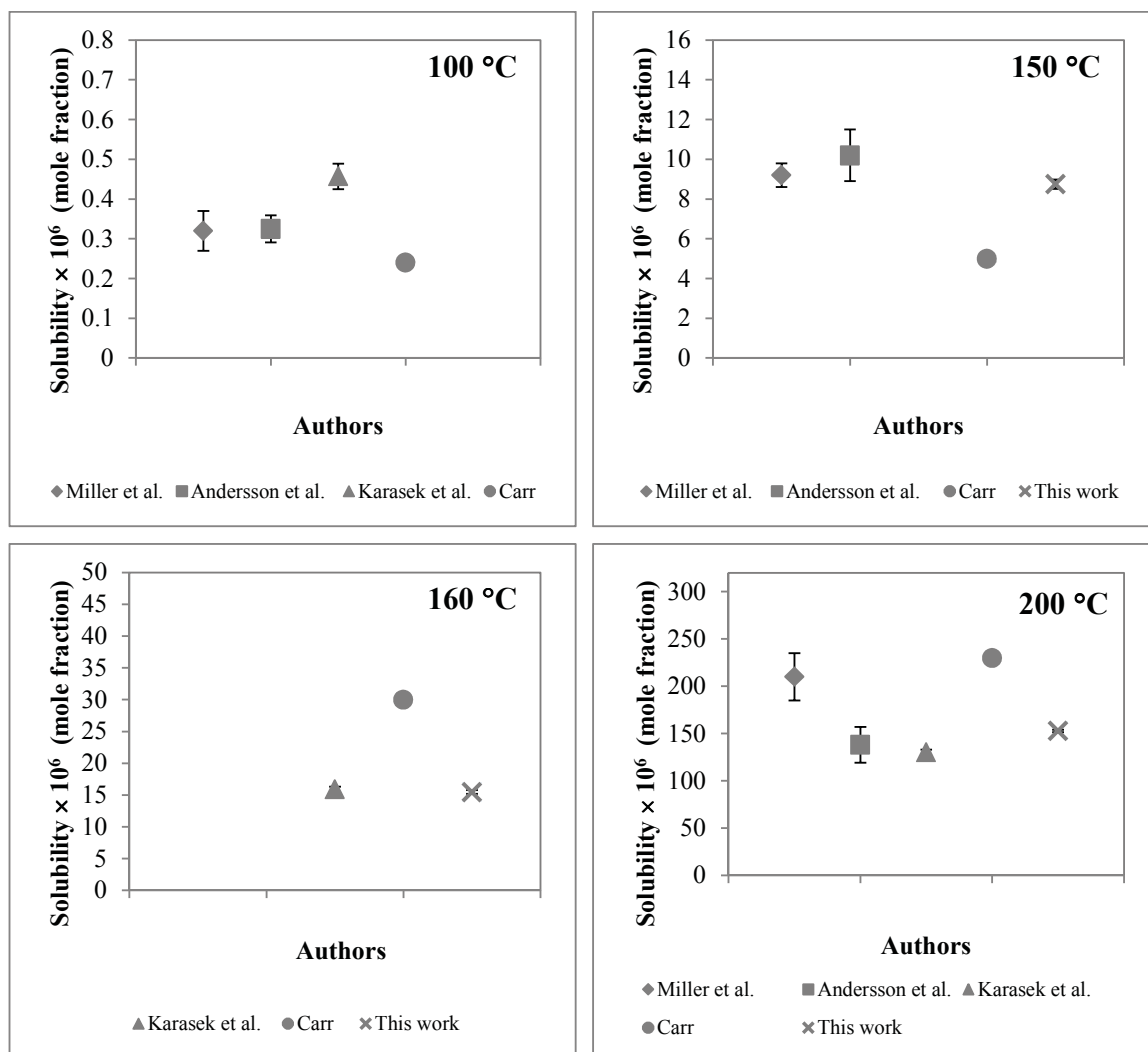


Figure 3.14: Solubility data of anthracene in subcritical water at various temperatures from various sources [note: standard deviations not available for Carr]

Table 3.4 and Figure 3.14 show that most of the solubility data were in reasonably moderate agreement with each other. The variations found in measured data by various authors range from 6% to 90% although most data are of the same order of magnitude. The RSDs for most of the anthracene solubility data, apart from the work of Karasek et al. [4] and this study, were mostly above 10%. The fairly high RSDs reflect moderate reproducibility of the data.

The solubility data of anthracene at 200 °C shows high variability among authors. The solubility data obtained by Andersson et al. [3] and Karasek et al. [4] were in very good

agreement. However, the work of Andersson et al. showed a high RSD at 13.8%. Low reproducibility (high RSD) was reported by Andersson et al. when various collection solvents were used in the analytical step required for quantification. Thus, the analytical step in solute-solvent quantifications could be a source of error and may have contributed to the high RSD obtained. Nevertheless, a high RSD may also indicate that saturation was not fully achieved in the solute solution at 200 °C. Miller et al. [15] also obtained a fairly high RSD for their solubility data at 200 °C. The 11.9% RSD obtained by Miller et al. could also represent a degree of unsaturation in the solution collected. The results from the experiments conducted in this study found that the solubility of anthracene at 200 °C is 15% higher than the value reported in the work of Karasek et al.. While the system used in this study was similar to that of Carr [9], the value obtained by Carr 33% higher at 200 °C. The higher value is attributed to the fact that Carr collected the saturated aqueous solutions in an unsealed collection vial where water may have been lost in the form of steam which could consequently lead to a higher estimate of solute concentration; whereas in this study, a closed collection vessel was used.

At 100 °C, the solubility data of Miller et al. and Andersson et al. were found to be in good agreement. However, the value obtained by Karasek et al. was approximately 40% higher than Miller et al. and Andersson et al.. While the data obtained by Miller et al. and Andersson et al. are similar, the high RSDs found in their work and the lower solubility values when compared to Karasek et al., may point to a degree of unsaturation in their solutions. In the case of Carr, the solubility data obtained at 100 °C was much lower than the data obtained by other works. The primary reason was found to be the equilibration time used. In its infancy, the static equilibrium technique utilized by Carr included a 10 min equilibration time. However, it was found in this study that at 100 °C, an equilibration time of more than 8 hours is required.

In this study, it was also found that, at relatively low solubility and low temperature, longer equilibration time is required for a static equilibrium solubility study. In fact, the equilibration time required for anthracene at 120 °C was 7 times longer than that at 200 °C. It was also found in this study that for a static equilibrium technique, verifying the difference in solute concentrations at an interval of 20 or 30 minutes to determine an equilibration time may not work well at very low solubilities and low temperatures. At very low solubilities, and particularly at 100 °C and 120 °C, an interval of at least 1 hour is necessary to compare

concentrations and determine equilibration time, as the differences found in solute concentrations at 20-30 min intervals may well fall within 5% of each other. An experimenter may misconstrue the 5% difference as experimental error and deem the solute solution saturated. Hence, the equilibration time of 10 minutes used by both Mathis et al. [8] and Carr [9] may have been insufficient at lower temperatures. Insufficient mixing time to achieve saturation in a solution would be reflected in high RSDs and lower observed solubility values.

Despite the fact that the solubility values were compiled at similar temperatures, the pressures of the system used by different authors to keep water in the liquid state were dissimilar. However, such a relatively small range of pressures has been found to have no major effects on the solubility of a solute in subcritical water [15]. Hence, the comparisons made among the five studies in this paper are still relevant and valid.

3.3.4 Preliminary study on the effect of temperature and pressure on the solubility of a PAH in subcritical water

In a preliminary solubility study, the effects of pressure and temperature, and the joint effect of the two factors on the solubility of anthracene in water were studied. Solubility measurements were conducted at 140 °C and 180 °C and at pressures of 50 bar and 150 bar. The results of the solubility measurements are shown in Table 3.5. The interaction plots between the two factors are shown in Figure 3.15 (a) and (b). The interaction plots indicate a strong interaction between temperature and the solubility of anthracene in subcritical water. The calculation of the main effects, shown in Table 3.6, confirms that temperature has the most significant effect on solubility in subcritical water, while pressure, and the combined effect of temperature and pressure (i.e. density), are not significant. The results shown in Table 3.6 are consistent with observations made in the literature, in that the effect of pressure on the solubility of organic compounds in subcritical water is minimal, particularly when the range of pressure considered is relatively small. The preliminary 2-factor experimental design was not extended to *p*-terphenyl as the PAH solute is expected to exhibit the same cause and effect behavior as anthracene. The similarity in the solubility behavior observed between *p*-terphenyl and anthracene can be found in a solubility study by Karasek et al. via the dynamic equilibrium

method [4], and confirmed by the results obtained in the present study, described in Section 3.3.5.

Table 3.5: Solubility data of anthracene in subcritical water at 140 °C and 180 °C and at pressures of 50 bar and 150 bar

Factor: Temperature, T	Factor: Pressure, P	
	P low (50 bar)	P high (150 bar)
T low (140 °C)	4.41×10^{-6}	4.87×10^{-6}
T high (180 °C)	5.48×10^{-5}	5.83×10^{-5}

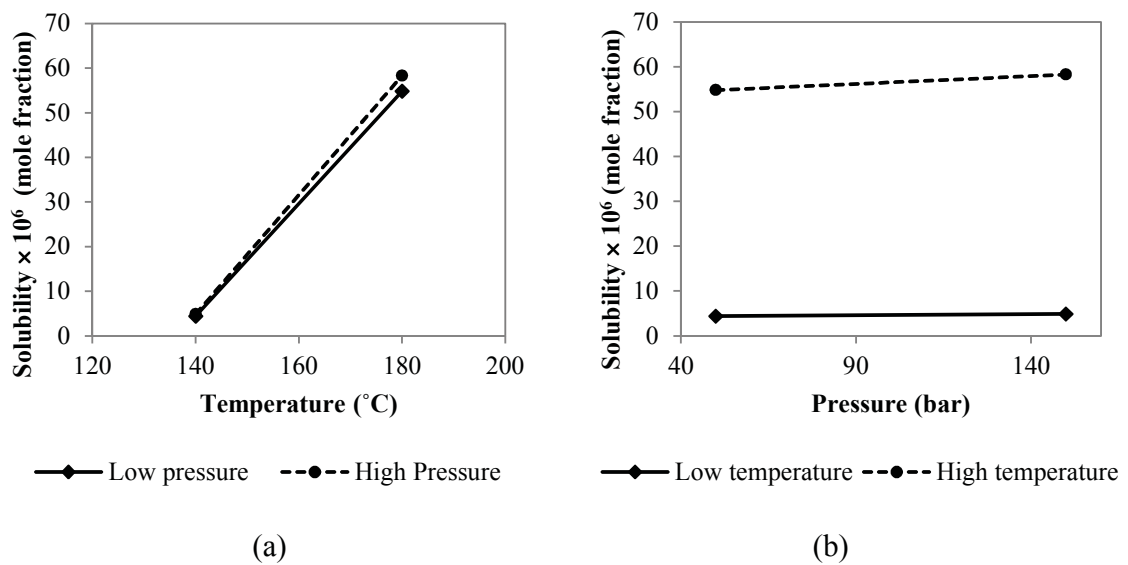


Figure 3.15: Interaction plots: the effects of temperature and pressure on the solubility of anthracene in subcritical water

Table 3.6: Main effects that contribute to the solubility of anthracene in subcritical water

Parameter	Main effect	Sum of squares
Temperature	5.19×10^{-5}	2.69×10^{-9}
Pressure	1.97×10^{-6}	3.89×10^{-12}
Combined pressure and temperature	-1.51×10^{-6}	2.29×10^{-12}

3.3.5 The effect of temperature on the solubility of PAHs in subcritical water: binary systems

In the preliminary study discussed in Section 3.3.4, solubility measurements were conducted at high and low temperatures of 140 °C and 180 °C. In a more detailed investigation of the effect of temperature, temperature measurements were extended to 120 °C and 200 °C. The pressure of the system was kept constant at 50 bar. The solubilities of pure anthracene and *p*-terphenyl in subcritical water are shown in Table 3.7 and Figure 3.16. The relative standard deviations for all solubility data were found to be less than 5%.

Table 3.7: Solubility data (mole fraction) for binary water (1) – anthracene (2) and *p*-terphenyl (1) – water (2) systems

T (°C)	Anthracene x_2	<i>p</i> -Terphenyl x_2
120	$(1.59 \pm 0.04) \times 10^{-6}$	$(1.95 \pm 0.08) \times 10^{-7}$
140	$(5.34 \pm 0.08) \times 10^{-6}$	$(5.90 \pm 0.05) \times 10^{-7}$
150	$(8.75 \pm 0.24) \times 10^{-6}$	$(1.05 \pm 0.03) \times 10^{-6}$
160	$(1.55 \pm 0.03) \times 10^{-5}$	$(1.96 \pm 0.06) \times 10^{-6}$
170	$(3.04 \pm 0.16) \times 10^{-5}$	$(3.71 \pm 0.12) \times 10^{-6}$
180	$(5.29 \pm 0.10) \times 10^{-5}$	$(7.14 \pm 0.24) \times 10^{-6}$
200	$(1.53 \pm 0.01) \times 10^{-4}$	$(2.43 \pm 0.03) \times 10^{-5}$

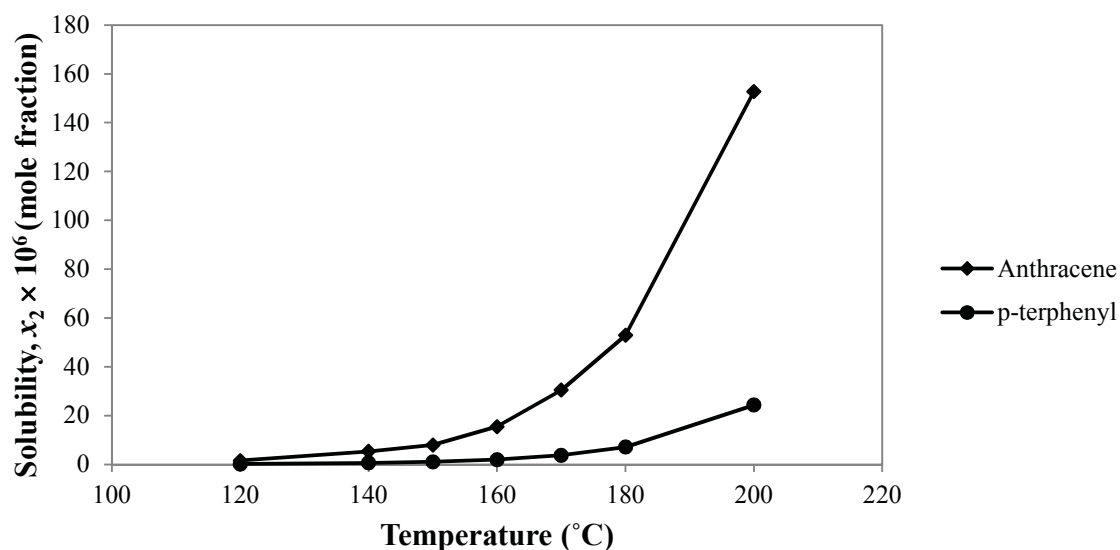


Figure 3.16: Binary solubility data of anthracene and *p*-terphenyl in subcritical water at 50 bar and various temperatures

In accordance with previous reports [2-5,15], the solubilities of anthracene and *p*-terphenyl were found to increase exponentially with temperature. The dramatic increase is generally attributed, in the literature, to the reduced dielectric constant of water as a consequence of temperature increase. However, the exponential increase observed in PAHs solubility with temperature does not correspond to the rate of decrease in the dielectric constant of water, particularly the sharp increase in solubility observed above 150 °C. In fact, the observed exponential solubility trend shown in Figure 3.16 is more similar to the change in sublimation pressure with temperature for both PAHs, as shown in Figure 3.17. The change in the dielectric constant of water with temperature is shown in Figure 3.18, to provide a comparison with the change in sublimation pressure. Attributing the increase in PAH solubilities in subcritical water to the change in their sublimation pressure is reasonable since the solubilities of solid hydrocarbons in supercritical fluids have also been shown to be heavily influenced by their sublimation pressures [16,17]. The ratios of the dielectric constant, the sublimation pressures and the PAHs solubilities at various temperatures are shown in Table 3.8. The increment change in solubility mirrors that of the sublimation pressures of the solid solutes, rather than that of the dielectric constant.

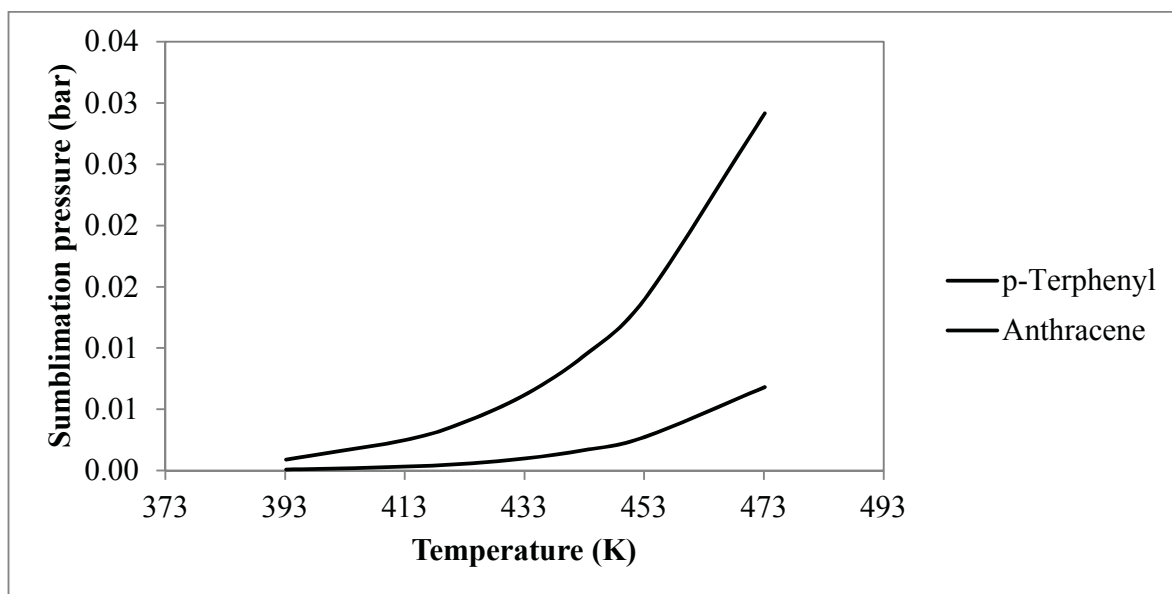


Figure 3.17: The variation of sublimation pressure of solid PAHs with temperature (data reproduced from Zhao et al. [11])

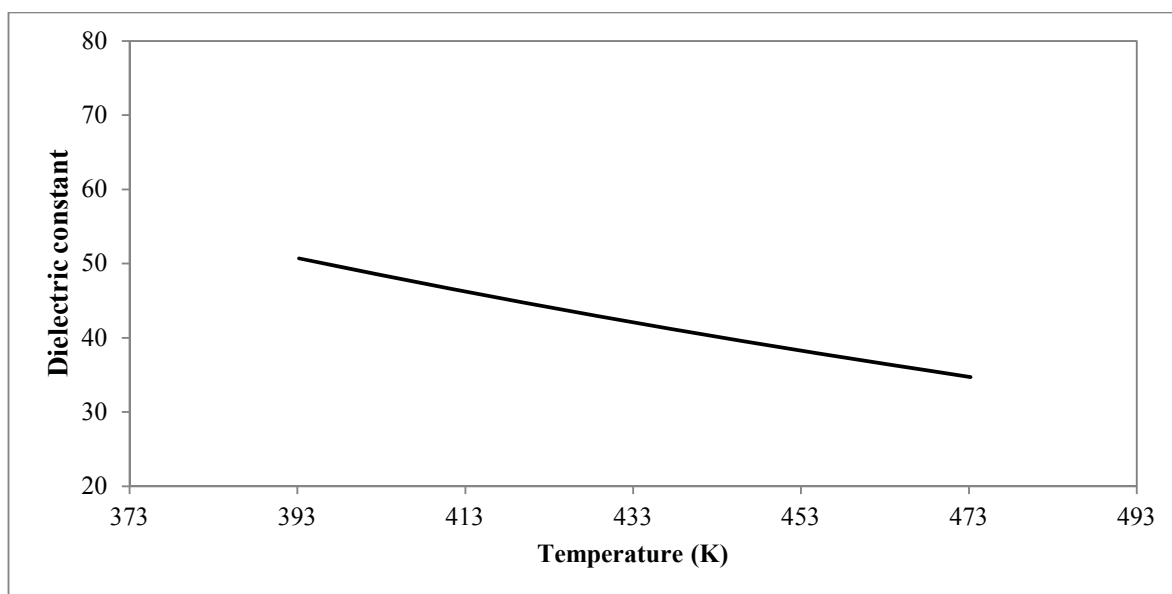


Figure 3.18: Dielectric constant of subcritical water at 50 bar and various temperatures (reproduced from Bradley and Pitzer [18])

Table 3.8: Ratios of the dielectric constant (ϵ_r) of water, PAHs sublimation pressures (P_T^{sub}) and PAHs solubility (x_T) at various temperatures

T_1 (°C)	T_2 (°C)	$\left(\frac{\epsilon_{r,T1}}{\epsilon_{r,T2}}\right)_{\text{water}}$	$\left(\frac{P_{T2}^{\text{sub}}}{P_{T1}^{\text{sub}}}\right)_{\text{PAH}}$		$\left(\frac{x_{T2}}{x_{T1}}\right)_{\text{PAH}}$	
			Anthracene	<i>p</i> -Terphenyl	Anthracene	<i>p</i> -Terphenyl
120	140	1.10	2.79	3.67	3.36	3.03
140	150	1.05	1.60	1.81	1.64	1.78
150	160	1.05	1.56	1.74	1.77	1.87
160	170	1.05	1.52	1.69	1.96	1.89
170	180	1.05	1.49	1.64	1.74	1.92
180	200	1.05	2.08	2.48	2.89	3.40

With regard to the dielectric constant playing a smaller role in solubility, a further observation can be made by comparing the solubility of anthracene in subcritical water with that in nitrobenzene, as shown in Table 3.9. While both solvents exhibit similar dielectric constant values, the solubility of anthracene in nitrobenzene is approximately 670 times higher. Moreover, the solubility of anthracene in nitrobenzene is 31 times higher than in methanol even though methanol bears a lower dielectric constant. It is evident, therefore, that the dielectric constant is not the main determinant of PAHs solubility in solvents. Although temperature bears considerable influence on both the dielectric constant of water and the sublimation pressure of the solutes, the contrast in the trends observed points to solubility in subcritical water being predominantly governed by the solute sublimation pressures. The effect from mixture density has been established (in Section 3.3.4) as insignificant within the temperature and pressure range considered in this study. The change in solvent density with temperature is shown in Figure 3.19 to provide a comparison with Figure 3.17.

Table 3.9: Solubility of anthracene in various solvents, temperatures and dielectric constants

Solvent	Dielectric constant	Conditions	Anthracene Solubility	References
Nitrobenzene	^a 34.8	25 °C	^b 1.03×10^{-2}	^a [19], ^b [20]
Methanol	^c 32.6	25 °C	^d 3.26×10^{-4}	^c [21], ^d [22]
Water	^e 34.7	200 °C, 50 bar	1.53×10^{-5}	^e [18]

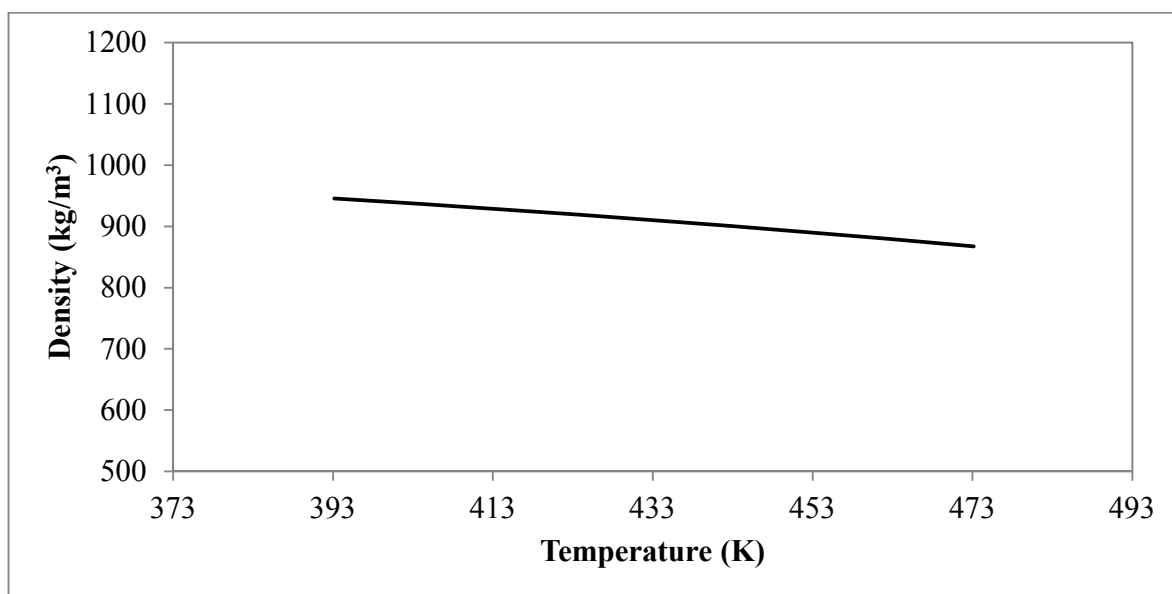


Figure 3.19: The variation in the density of subcritical water with temperature at 50 bar (reproduced from Parry et al. [10])

3.3.6 The effect of temperature on the solubility of PAHs in subcritical water: ternary systems

Subcritical water has been used to remove or decompose pollutants such as PAHs, pesticides and polychlorinated biphenyls from contaminated soils. While systematic solubility studies on PAHs in subcritical water has been widely conducted, most studies were carried out for binary systems and very few data are available for solvent-solid-solid systems [2-5,15,23,24]. However, as pollutants rarely exist as a single component, solubility studies conducted on multi-component systems would be beneficial. While the study on the effects of a co-solute on another solute in subcritical water is scarce, Miller et al. [15] studied the solubilities of mixed ternary PAHs in subcritical water. The solubilities of a mixture of carbazene, anthracene and chrysene in subcritical water were measured between 25 °C and 200 °C. Miller et al. [15] found that the PAHs behaved as separate solids at relatively lower temperatures as the solubilities of the PAHs in the quaternary system were found to be similar to their individual solubilities in subcritical water between 25 °C and 50 °C. However, as temperatures increased above 50 °C, solubility depressions were found to occur in the 3 solutes.

In the present study, additional experiments were conducted to determine the effects of a co-solute PAH on another PAH when the two solutes are mixed together in subcritical water. The work conducted in this thesis is a continuing study on solid-liquid equilibrium (SLE) in ternary systems consisting of solid-solid-solvent at different temperatures. This is the first known study conducted on a mixture of two solutes in subcritical water at the invariant point where the solution is saturated with both solutes. In this section, the solid-solid-liquid ternary systems of *p*-terphenyl-anthracene-water at temperatures between 120 °C and 170 °C are presented.

In the conduct of the solid-solid-liquid equilibrium (SSLE) experiments, an equimolar mixture of anthracene and *p*-terphenyl was packed into the equilibrium vessel prior to the start of the experiment. All other parts of the experiment were conducted similarly to the experiment conducted for binary systems. The amounts of solutes collected were dried and dissolved in acetonitrile. Separation and analysis of solutes were conducted using a Waters RP-HPLC (reversed-phase high pressure liquid chromatography) system. Chromatographic separations were conducted with a Lichrosorb RP18 analytical column. The RP-HPLC gradient profile used to separate anthracene and *p*-terphenyl is shown in Table 3.10, with a total separation run time

of 60 minutes. Five point calibration curves were generated for each solute and are shown in Appendices B3 and B4. The solubilities of the solutes in subcritical water at various temperatures are shown in Table 3.11 and Figure 3.20. The natural logarithms of both the binary and ternary solubilities of each PAH are shown in Figure 3.21.

Table 3.10: RP-HPLC mobile phase gradient with a flow rate of 1 ml/min

Time (min)	Water (%)	Acetonitrile (%)
0	50	50
20	50	50
30	30	70
45	30	70
50	50	50
60	50	50

Table 3.11: Solubility data (mole fraction) in subcritical water (1) – anthracene (2) – *p*-terphenyl (3) system

T (°C)	x_2	x_3
120	$(1.22 \pm 0.05) \times 10^{-8}$	$(1.82 \pm 0.07) \times 10^{-7}$
140	$(4.68 \pm 0.35) \times 10^{-6}$	$(5.60 \pm 0.35) \times 10^{-7}$
150	$(1.09 \pm 0.06) \times 10^{-6}$	$(1.83 \pm 0.05) \times 10^{-6}$
160	$(1.52 \pm 0.06) \times 10^{-5}$	$(1.89 \pm 0.03) \times 10^{-6}$
170	$(2.84 \pm 0.107) \times 10^{-5}$	$(8.67 \pm 0.54) \times 10^{-6}$

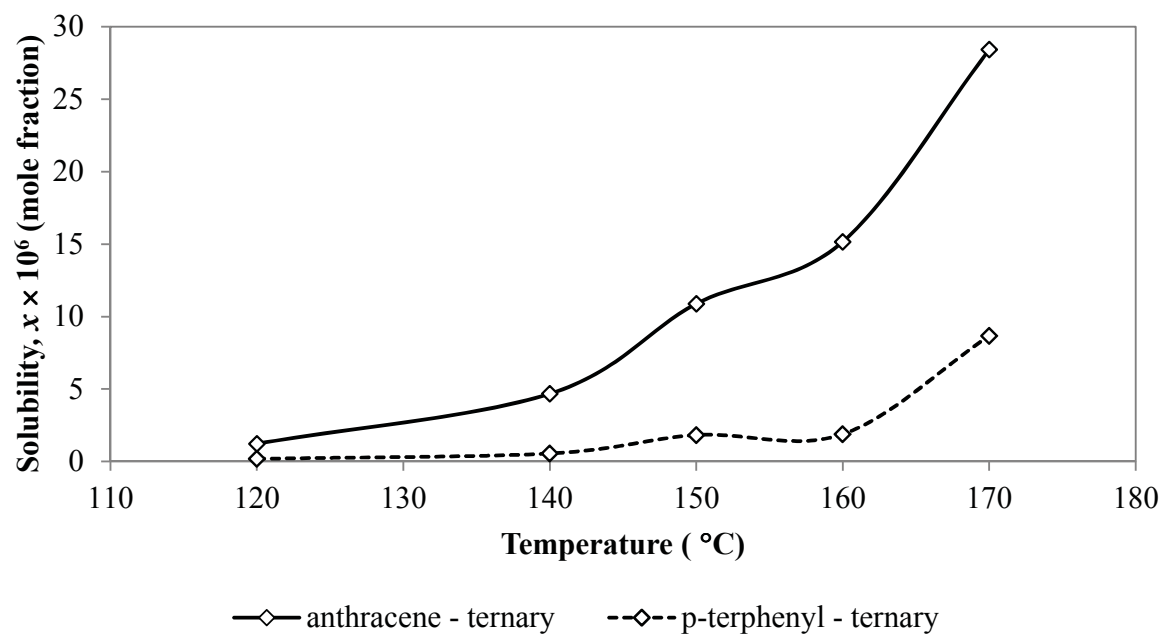


Figure 3.20: Solubility of ternary anthracene and *p*-terphenyl in subcritical water as a function of temperature

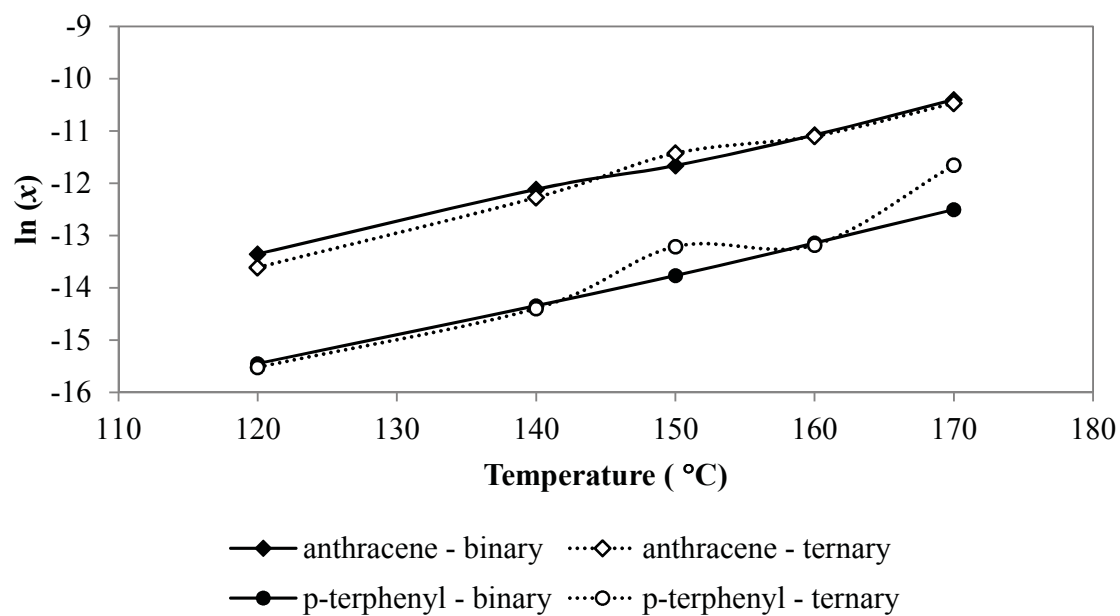


Figure 3.21: Natural logarithmic solubility of anthracene and *p*-terphenyl in binary and ternary subcritical water systems

Solubility depression was observed for anthracene at all temperatures, except at 150 °C, while depression was observed for *p*-terphenyl at 120 °C and 140 °C. While the solubility depressions observed are in agreement with the observations made by Miller et al. [15], the increased solubilities of mixed anthracene and *p*-terphenyl at several temperatures show the unpredictable effects of having a co-solute in subcritical water systems. In this study, it was assumed that the mixing in the equilibrium vessel was sufficient to make both solutes available to the solvent, and that there was no significant interaction between anthracene and *p*-terphenyl. Therefore, both anthracene and *p*-terphenyl were treated as two pure solids in the ternary mixtures. While it was assumed that two pure solid phases and a single liquid mixture exist in the ternary systems, the reasons for the augmented solubility values of *p*-terphenyl at 150 °C and 170 °C were unknown. It is possible that at these temperatures the dissolved anthracene acts as a co-solute that enhances the solubility of *p*-terphenyl.

3.4 Conclusion

The static and dynamic equilibrium methods to determine solute solubility in subcritical water are compared in this chapter. Both the static and dynamic equilibrium methods can yield reasonable solubility results. However, using a dynamic equilibrium method for ternary systems with two solid solutes could cause one component to be selectively extracted first and cause a change in the equilibrium conditions with time. Hence, the static equilibrium method is a more appropriate method to be utilized in this study even though it is a longer process. Precautions must also be taken to ensure that equilibration, steady-state operation and closed-capture solute collection are established in the static equilibrium method. The solubilities of anthracene and *p*-terphenyl in subcritical water were successfully measured and found to increase exponentially with temperature. The solubilities of PAHs in subcritical water were found to be governed primarily by sublimation pressures of the solutes and only secondarily by the dielectric constant of water.

3.5 Bibliography

- [1] Bristow S, Shekunov BY, York P. Solubility analysis of drug compounds in supercritical carbon dioxide using static and dynamic extraction systems. *Industrial & Engineering Chemistry Research* 2001;40 (7):1732-9.
- [2] Miller DJ, Hawthorne SB. Method for determining the solubilities of hydrophobic organics in subcritical water. *Analytical Chemistry* 1998;70 (8):1618-21.
- [3] Andersson TA, Hartonen KM, Riekkola M-L. Solubility of acenaphthene, anthracene, and pyrene in water at 50 °C to 300 °C. *Journal of Chemical & Engineering Data* 2005;50 (4):1177-83.
- [4] Karasek P, Planeta J, Roth M. Solubility of solid polycyclic aromatic hydrocarbons in pressurized hot water at temperatures from 313K to the melting point. *Industrial & Engineering Chemistry Research* 2006;45 (12):4454-60.
- [5] Karasek P, Hohnova B, Planeta J, Roth M. Solubility of solid ferrocene in pressurized hot water. *Journal of Chemical & Engineering Data* 2010;55 (8):2866-9.
- [6] Kayan B, Yang Y, Lindquist EJ, Gizir AM. Solubility of benzoic and salicylic acids in subcritical water at temperatures ranging from (298 to 473) K. *Journal of Chemical & Engineering Data* 2009;55 (6):2229-32.
- [7] Carr AG, Mammucari R, Foster NR. Solubility and micronization of griseofulvin in subcritical water. *Industrial & Engineering Chemistry Research* 2010;49 (7):3403-10.
- [8] Mathis J, Gizir AM, Yang Y. Solubility of alkylbenzenes and a model for predicting the solubility of liquid organics in high-temperature water. *Journal of Chemical & Engineering Data* 2004;49 (5):1269-72.
- [9] Carr AG. Thesis: Subcritical water as a tunable solvent for particle engineering. Chemical Engineering. Sydney: The University of New South Wales, 2010.
- [10] Parry WT, Bellows JC, Gallagher JS, Harvey AH. ASME international steam tables for industrial use: ASME Press, 2009.
- [11] Zhao H, Unhannanant P, Hanshaw W, Chickos JS. Enthalpies of vaporization and vapor pressures of some deuterated hydrocarbons. Liquid-vapor pressure isotope effects. *J. Chem. Eng. Data* 2008;53:1545-56.
- [12] Yang Y, Hildebrand F. Phenanthrene degradation in subcritical water. *Analytica Chimica Acta* 2006;555 (2):364-9.
- [13] Kronholm J, Desbands B, Hartonen K, Riekkola M-L. Environmentally friendly laboratory-scale remediation of PAH-contaminated soil by using pressurized hot water extraction coupled with pressurized hot water oxidation. *Green Chemistry* 2002;4 (3):213-9.
- [14] Kronholm J, Kuosmanen T, Hartonen K, Riekkola M-L. Destruction of PAHs from soil by using pressurized hot water extraction coupled with supercritical water oxidation. *Waste Management* 2003;23 (3):253-60.
- [15] Miller DJ, Hawthorne SB, Gizir AM, Clifford AA. Solubility of polycyclic aromatic hydrocarbons in subcritical water from 298 K to 498 K. *Journal of Chemical & Engineering Data* 1998;43 (6):1043-7.
- [16] Lucien FP, Foster NR. Phase behavior and solubility. In: P.G. J, Leitner W, editors. *Chemical synthesis using supercritical fluids*. Weinheim: Wiley-VCH, 1999.

- [17] Huang Z, Yang X-W, Sun G-B, Song S-W, Kawi S. The solubilities of xanthone and xanthene in supercritical carbon dioxide: Structure effect. *The Journal of Supercritical Fluids* 2005;36 (2):91-7.
- [18] Bradley DJ, Pitzer KS. Thermodynamics of electrolytes. 12. Dielectric properties of water and Debye-Hueckel parameters to 350.degree.C and 1 kbar. *The Journal of Physical Chemistry* 1979;83 (12):1599-603.
- [19] Riddick JA, Bunger WB, Sakano T. *Organic solvents: physical properties and methods of purification*: Wiley, 1986.
- [20] Mahieu J. La solubilité dans les mélanges de deux solvants miscibles. *Bulletin des Sociétés Chimiques Belges* 1936;45:667-75.
- [21] Shirke RM, Chaudhari A, More NM, Patil PB. Temperature dependent dielectric relaxation study of ethyl acetate — Alcohol mixtures using time domain technique. *Journal of Molecular Liquids* 2001;94 (1):27-36.
- [22] Merck Index: Rahway, NJ, 1989.
- [23] Miller DJ, Hawthorne SB. Solubility of liquid organics of environmental interest in subcritical (hot/liquid) water from 298 K to 473 K. *Journal of Chemical & Engineering Data* 1999;45 (1):78-81.
- [24] Domanska U, Groves FR, McLaughlin E. Solid-liquid phase equilibria of binary and ternary mixtures of benzene and polynuclear aromatic compounds. *Journal of Chemical & Engineering Data* 1993;38 (1):88-94.

4 Solubility Measurement of PAHs in Ethanol-Modified Subcritical Water and Subcritical Ethanol

4.1 Solubility measurement of PAHs in ethanol-modified subcritical water

The introduction of an organic co-solvent into a solution is one of the many methods that have been used to enhance the solubility of non-polar solutes. Organic co-solvents such as ethanol and acetone have been used in small amounts to modify the solvating power of other solvents such as water. While an increase in temperature decreases the polarity of water, the same can happen with the addition of a co-solvent (or modifier). Addition of 50 wt% of methanol into water at room temperature has been found to decrease the dielectric constant of water from 78.48 to 56.28 [1]. Subcritical water with ethanol as modifier has been used to remove nonylphenol polyethoxy carboxylates (NPECs) from industrial and municipal sludges, and has been used in combination with solid-phase microextraction to extract atrazine from beef [2,3]. Organic co-solvents have also been used to increase the solubility of active pharmaceutical ingredients (APIs) in subcritical water, and to control the particle morphologies of APIs in subcritical water micronization processes [4].

Systematic investigations into the solubility of hydrophobic organic compounds in subcritical water with organic modifiers are limited to a small number of studies. Solubility measurements of triazine pesticides and budesonide in subcritical water with ethanol as a modifier have been conducted, resulting in enhanced solubility for both compounds [5,6]. The solubility of atrazine in subcritical water at 100 °C was found to increase over an order of magnitude when 20 wt% of ethanol was added into the mixture [5].

In the present chapter, the solubilities of anthracene were measured for (1- f) water – f ethanol mixtures at ethanol mole fractions, $f = 0.01, 0.02, 0.03, 0.04, 0.06$ and 0.10 at 50 bar between 393 K and 473 K. The study on the solubility behavior of PAHs in water-ethanol mixtures is justified by the lack of available data on the effects of adding organic co-solvents to the aqueous solubility of hydrocarbons at subcritical conditions. Also, the effects of added organic solvents on the thermodynamics of solution for anthracene and the temperature dependence of the solution process is necessary, and might enlighten the process of solubilization of a fairly

bulky hydrocarbon compound. The solubility of anthracene in water-ethanol mixtures at relatively lower temperatures (25 – 40 °C) had been conducted by Zhou et al. [7].

A static equilibrium method was employed in the present study to measure the solubilities of anthracene and *p*-terphenyl. Solubility measurement in ethanol-modified subcritical water follows from the experimental work conducted in chapter 3. A detailed discussion is given in the following sections.

4.2 Preparation for solubility measurement: Solvents and solutes behavior at subcritical conditions

The behavior of solvents and solutes in a modified subcritical water system could potentially change with the addition of a co-solvent. The addition of a co-solvent changes the VLE of the solvents involved, as well as the phase behavior of the organic compounds at subcritical conditions. Therefore, an understanding of the vapor-liquid equilibria of the solvents involved is essential, while the phase behavior of anthracene and *p*-terphenyl would need to be re-examined. These two factors are discussed in the following sections. The addition of small amounts of ethanol did not change the mixing and equilibration time required for the solution to reach saturation.

4.2.1 Vapor-liquid equilibria at subcritical conditions

Knowledge of the VLE of water-ethanol mixtures is required in order to ensure sufficient pressure is applied to maintain the liquid state of the solvents. Saturated vapor pressure changes with temperature and ethanol composition; the higher the ethanol composition and temperature, the higher the vapor pressure. Hence, a literature research was conducted on saturated vapor pressures for various ethanol-water compositions, at the highest temperature with which solubility measurements were conducted. The vapor-liquid equilibrium of ethanol-water at 200 °C for various mole fraction of ethanol is shown in Table 4.1 and Figure 4.1. As the maximum mole fractions of ethanol used in this study was 10%, a minimum pressure of 23 bar was required to maintain the liquid state of the solvents involved. Hence, solubility measurement at a pressure of 50 bar was sufficient to maintain the liquid state of the solvents in this study.

Table 4.1: Vapor-liquid equilibrium of ethanol-water at 200 °C [8]

Mol % ethanol		Saturated Vapor Pressure (bar)
Vapor	Liquid	
13.4	2.3	17.9
17.5	3.2	18.7
26.2	6.6	20.7
33.7	11.2	22.7
42.4	21.4	24.8
71.9	68.9	29.1
92.9	93.4	29.5

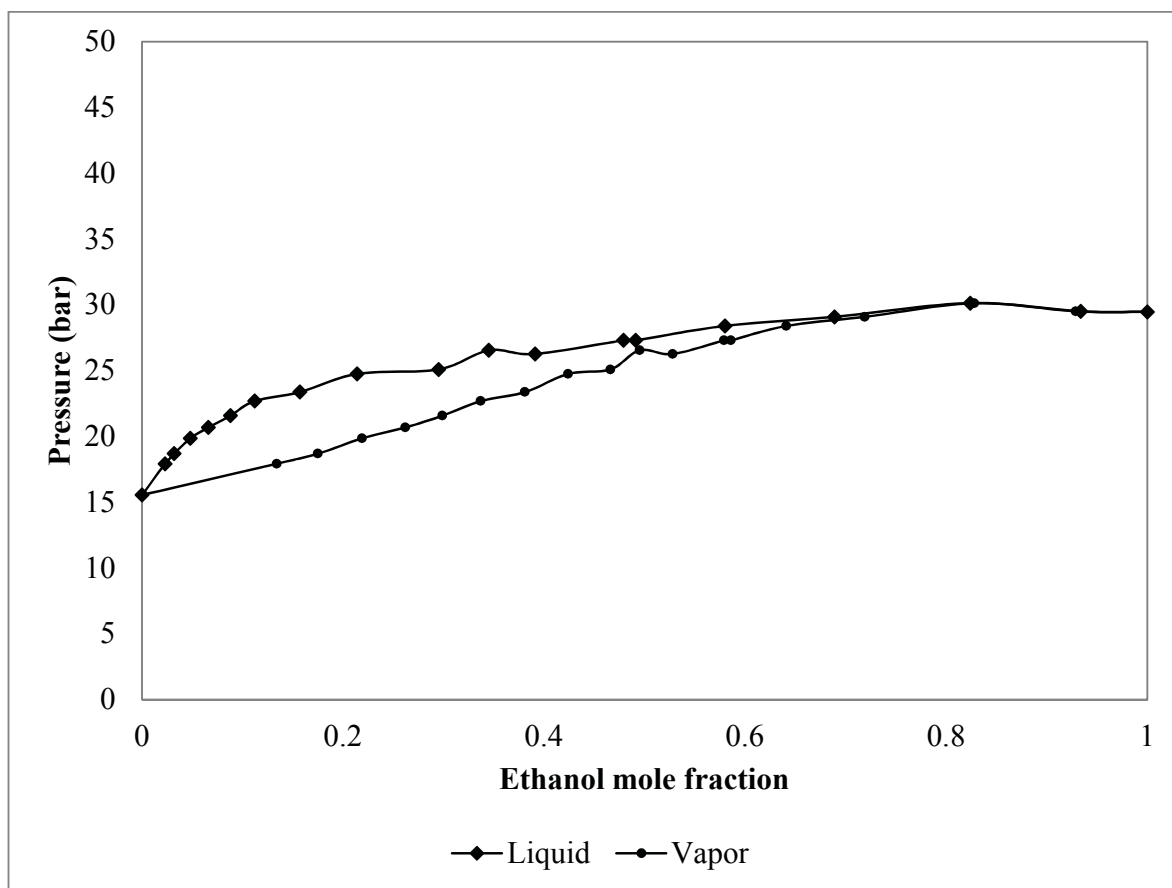


Figure 4.1: P - x - y diagram of ethanol-water VLE at 200 °C, reproduced from [8]

4.2.2 Phase behavior of PAHs in ethanol-modified subcritical water

A phase behavior study was conducted on anthracene and *p*-terphenyl in modified subcritical water systems. A detailed discussion of the experimental set-up and methodology has been presented in Chapter 3. The phase behavior of anthracene and *p*-terphenyl in several ethanol fractions at 50 bar and various temperatures are shown in Table 4.2. Melting point depression was observed for both anthracene and *p*-terphenyl. Hence, both compounds were found to be in liquid phases at certain temperatures and ethanol mole fractions, as shown in Table 4.2. Solubility measurements were *not* conducted for anthracene and *p*-terphenyl in water/ethanol mixtures where *liquid-liquid* equilibrium was observed.

Table 4.2: Phase behavior of anthracene and *p*-terphenyl at 50 bar and various temperatures and mole fractions of ethanol

Compound	Temperature (°C)	Mole fractions of ethanol in water, <i>f</i>					
		0.01	0.02	0.03	0.04	0.06	0.10
Anthracene	120	S-L	S-L	S-L	S-L	S-L	S-L
	140	S-L	S-L	S-L	S-L	S-L	S-L
	150	S-L	S-L	S-L	S-L	S-L	S-L
	160	S-L	S-L	S-L	S-L	S-L	S-L
	170	S-L	S-L	S-L	S-L	S-L	S-L
	180	S-L	S-L	S-L	S-L	S-L	S-L
	200	S-L	S-L	S-L	S-L	L-L	L-L
<i>p</i> -terphenyl	120	S-L	S-L	S-L	S-L	S-L	S-L
	140	S-L	S-L	S-L	S-L	S-L	S-L
	150	S-L	S-L	S-L	S-L	S-L	S-L
	160	S-L	S-L	S-L	S-L	S-L	S-L
	170	S-L	S-L	S-L	S-L	S-L	S-L
	180	S-L	S-L	S-L	S-L	S-L	S-L
	200	S-L	L-L	L-L	L-L	L-L	L-L

Note: S-L = solid-liquid equilibrium; L-L = liquid-liquid equilibrium

4.3 Solubility measurement

4.3.1 Materials

Anthracene (99 mole %) and *p*-terphenyl (99 mol %) were purchased from Sigma-Aldrich. Both compounds were used as received. Ethanol absolute (99.9%) was purchased from Scharlau Chemie. Deionised water was used in all experiments.

4.3.2 Apparatus and experimental method

A static equilibrium method was utilized to measure the solubility of PAHs in modified subcritical water. The performance, validation, experimental set-up and method utilized in this study have been discussed in Chapter 3 (section 3.3) and therefore, will not be discussed further in this section.

4.3.3 Preliminary study on the effect of temperature, pressure and the addition of ethanol on the solubility of a PAH in modified subcritical water system

The introduction of small amounts of ethanol could potentially change the “cause and effect” behavior of PAH in subcritical conditions. While the effects from pressure changes on the solubility of a PAH in subcritical water are almost negligible, the same could not be stated confidently for a modified subcritical water system. Hence, in a preliminary study, the effects of pressure and temperature, and their joint effect on the solvating power of modified subcritical water were studied. Solubility measurements were conducted in 6 mol% of ethanol, at 140 °C and 180 °C and at pressures of 50 bar and 150 bar. The results of the solubility measurements are shown in Table 4.3 while Figures 4.2 (a) and (b) illustrate the interaction between the two factors. The interaction plots again indicate the significant role played by temperature on solubility, while it can be concluded that the effect of pressure on solubility in ethanol-modified subcritical water mixtures remains insignificant. The combined effect of temperature and pressure (i.e. liquid mixture density) on the solvating power of ethanol-modified subcritical water systems, as apparent from Table 4.4, is also insignificant.

Table 4.3: Solubility data of anthracene in subcritical water/ethanol systems at 140 °C and 180 °C and at pressures of 50 bar and 150 bar ($f=0.06$)

Factor: Temperature, T	Factor: Pressure, P	
	P low (50 bar)	P high (150 bar)
T low (140 °C)	4.54×10^{-5}	3.81×10^{-5}
T high (180 °C)	3.29×10^{-4}	3.42×10^{-4}

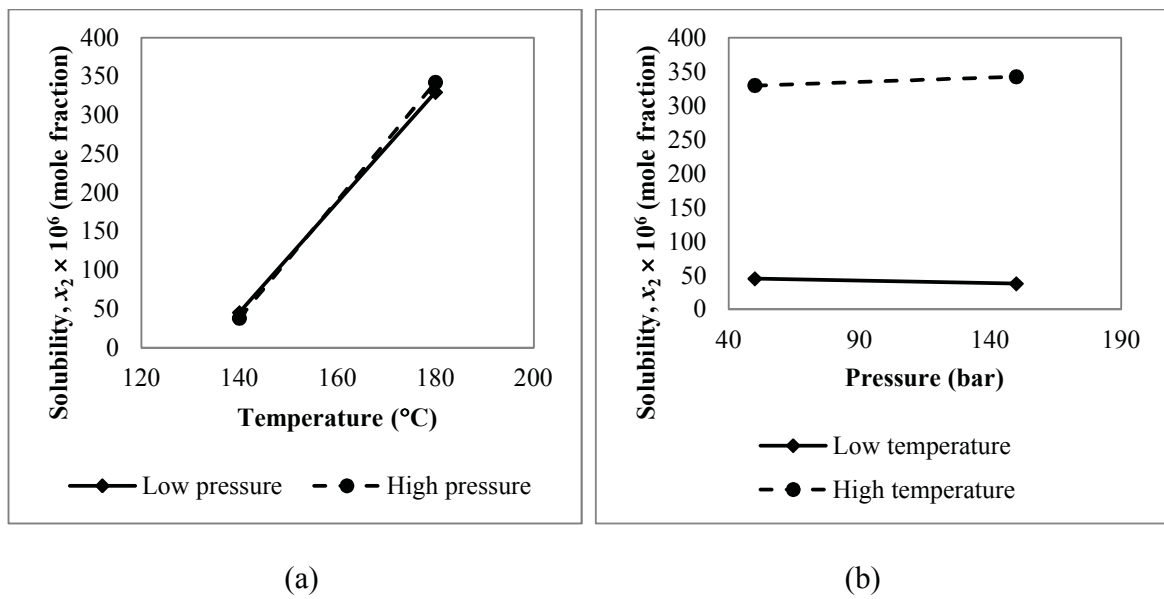


Figure 4.2: Interaction plots: the effects of temperature and pressure on the solubility of anthracene in subcritical water/ethanol system at $f=0.06$

Table 4.4: Main effects that contribute to the solubility of anthracene in subcritical water/ethanol system at 140 °C and 180 °C, and at pressures of 50 bar and 150 bar ($f=0.06$)

Parameter	Main effect	Sum of squares
Temperature	2.94×10^{-4}	8.65×10^{-8}
Pressure	2.85×10^{-6}	8.14×10^{-12}
Combined pressure and temperature	-1.01×10^{-5}	1.02×10^{-10}

A further extension to this study was to investigate the effects of temperature, ethanol mole fractions and the effects from the two factors combined, on the solvating power of subcritical water/ethanol systems. A two-level factorial design, consisting of high and low temperatures of 140 °C and 180 °C, and high and low ethanol fractions at $f = 0.01$ and $f = 0.10$ were used in this study. Table 4.5 shows the solubility of anthracene at these conditions while Figures 4.3 (a) and (b) illustrate the interactions between the two factors (temperature and ethanol mole fraction). While the significant contribution of temperature on increasing the solvating power of subcritical water/ethanol mixtures have been proven, the sums of squares shown in Table 4.6 indicate also the prominent role played by ethanol. In fact, the sums of squares shown in Table 4.6 suggest that ethanol plays a slightly more prominent role than temperature in elevating the solvating power of the modified subcritical water systems. The results from this preliminary investigation match the findings of Curren, M. S. S. and King, J. W. [5] in that the rate of increase in the solubility is higher with the addition of ethanol rather than with an increase in temperature.

Table 4.5: Solubility data of anthracene in subcritical water/ethanol systems at 140 °C and 180 °C and ethanol mole fractions, $f = 0.01$ and $f = 0.10$

Factor: Temperature, T	Factor: Ethanol mole fraction, f	
	$f_{\text{low}} (0.01)$	$f_{\text{high}} (0.10)$
$T_{\text{low}} (140\text{ °C})$	7.03×10^{-6}	2.39×10^{-4}
$T_{\text{high}} (180\text{ °C})$	6.87×10^{-5}	1.74×10^{-3}

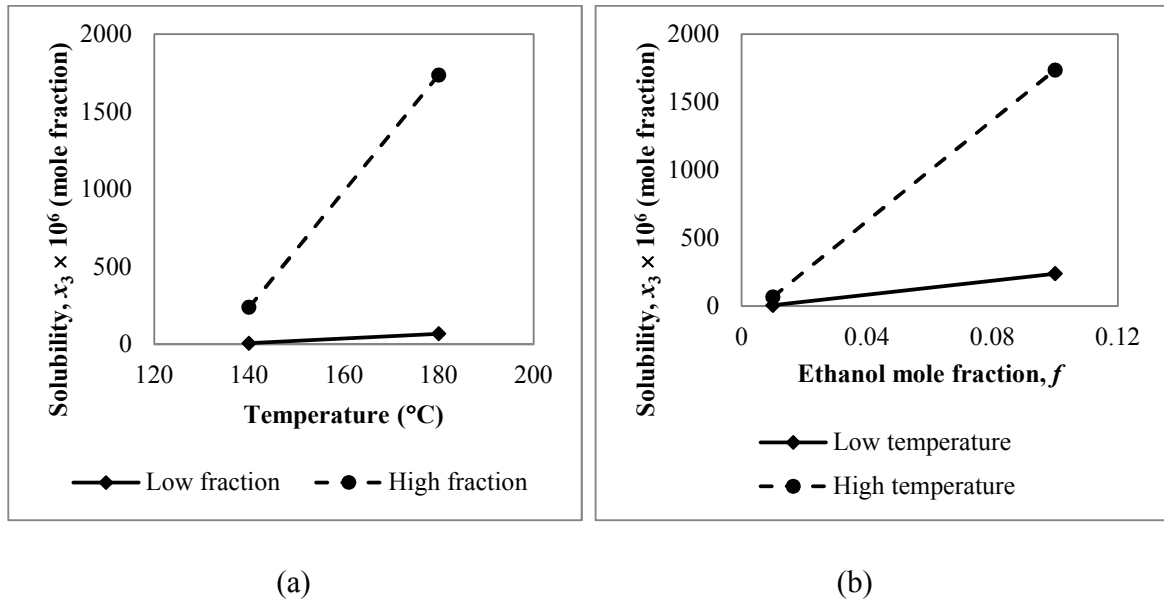


Figure 4.3: Interaction plots: the effects of temperature and ethanol mole fractions on the solubility of anthracene in subcritical water/ethanol system at 50 bar

Table 4.6: Main effects that contribute to the solubility of anthracene in subcritical water/ethanol system at 140 $^{\circ}\text{C}$ and 180 $^{\circ}\text{C}$ and ethanol mole fractions, $f = 0.01$ and $f = 0.10$

Parameter	Main effect	Sum of squares
Temperature	7.79×10^{-4}	6.07×10^{-7}
Ethanol mol fraction	9.50×10^{-4}	9.02×10^{-7}
Combined temperature and ethanol mol fraction	-7.18×10^{-4}	5.15×10^{-7}

4.3.4 The effect of temperature and ethanol mole fraction on the solubility of PAHs in modified subcritical water systems

While solubility measurements were conducted at high and low temperatures of 180 °C and 140 °C in the preliminary study, the temperature range was extended to include 120 °C and 200 °C in the detailed investigation on the effect of temperature and ethanol mole fractions on solubility. Hence, solubility measurements of anthracene and *p*-terphenyl in subcritical water/ethanol system were conducted at 120 °C, 140 °C, 150 °C, 160 °C, 170 °C, 180 °C and 200 °C. Where a *liquid* solute phase was observed at 200 °C (shown in Table 4.2), solubility measurements were not conducted. The solubility data of anthracene and *p*-terphenyl in subcritical water/ethanol systems are shown in Table 4.7. Figures 4.4 - 4.5 illustrate the solubility of anthracene and *p*-terphenyl in modified subcritical water systems with ethanol mole fractions as a function of temperature, while the variation between solubility and temperature as a function of ethanol mole fractions are shown in Figures 4.6 – 4.7. The solubilities of both PAHs were found to increase exponentially with temperature as well as ethanol fractions. Linear plots of natural logarithm of solubility ($\ln x_3$) against temperature and against ethanol fractions were obtained, as shown in Figures 4.8 – 4.11. A 3-dimension plot of $\ln (x_3)$ against temperature and ethanol mole fraction is shown in Figure 4.12 for anthracene and in Figure 4.13 for *p*-terphenyl.

At lower ethanol concentrations, the solubility of both PAHs was observed to increase gradually as temperature was increased from 120 °C to 160 °C, but steepened above 160 °C. The steepening of the solubility curve at 160 °C has been observed in a number of studies [6,9,10]. However, the temperature at which the steepening in solubility was observed decreases as ethanol concentration increases. Both anthracene and *p*-terphenyl demonstrate sharp increases in their solubilities at around 140 °C - 150 °C at ethanol mole fraction, $f = 0.10$. Figures 4.9 and 4.10 also show a steepening in PAHs solubility when solubility was plotted against ethanol mole fraction. The sharp increase in solubility was observed at $f = 0.06$.

Anthracene solubility was found to increase by 19 - 43 fold in modified subcritical water systems as temperature was raised from 120 °C to 180 °C. The solubility of anthracene was found to increase between 25 and 54 folds when ethanol composition was raised from 0.01

mole fraction to 0.10 mole fraction. The effect of adding a co-solvent has greatly enhanced the solubility of anthracene and *p*-terphenyl in subcritical water. In fact, the results obtained in this study show that a small addition of 0.01 to 0.02 mole fractions of ethanol could yield the same increase in the solubility of the PAHs as when temperature was increased by 10 °C. Take for example, the solubility of *p*-terphenyl in subcritical water at 160 °C is 1.96×10^{-6} (mole fraction). The solubility of *p*-terphenyl increased to 3.71×10^{-6} (mole fraction) when temperature was increased to 170 °C. The same increase in the solubility of *p*-terphenyl can also be obtained by adding approximately 0.015 mole of ethanol into the solutions while maintaining the same temperature at 160 °C. Hence, the use of a modifier can easily reduce the need for higher processing temperatures, and subsequently, lowering the temperature at which subcritical water processes such as extraction and micronization can be conducted. It is apparent that both temperature and modifier contribute to the overall increase in the solubility of the two PAHs studied. The results obtained therefore show the flexibility in terms of using temperature, co-solvent or both to enhance the performance of subcritical water processes. However, a cost benefit analysis is required to indicate the better choice, as increasing temperature increases energy cost while a co-solvent has the added cost of extraction/elimination of the co-solvent at process-end.

Table 4.7: Solubility data for ternary water (1) - ethanol (2) – anthracene (3) systems

T (°C)	f_2	x_3	f_2	x_3
120	0.01	$(1.69 \pm 0.04) \times 10^{-6}$	0.04	$(6.43 \pm 0.11) \times 10^{-6}$
140		$(7.03 \pm 0.02) \times 10^{-6}$		$(2.23 \pm 0.04) \times 10^{-5}$
150		$(1.32 \pm 0.03) \times 10^{-5}$		$(3.63 \pm 0.10) \times 10^{-5}$
160		$(2.28 \pm 0.04) \times 10^{-5}$		$(6.25 \pm 0.04) \times 10^{-5}$
170		$(4.32 \pm 0.11) \times 10^{-5}$		$(1.09 \pm 0.01) \times 10^{-4}$
180		$(6.87 \pm 0.29) \times 10^{-5}$		$(2.09 \pm 0.06) \times 10^{-4}$
200		$(2.12 \pm 0.06) \times 10^{-4}$		$(4.91 \pm 0.13) \times 10^{-4}$
120	0.02	$(2.45 \pm 0.12) \times 10^{-6}$	0.06	$(1.53 \pm 0.06) \times 10^{-5}$
140		$(9.72 \pm 0.29) \times 10^{-6}$		$(4.54 \pm 0.19) \times 10^{-5}$
150		$(1.76 \pm 0.06) \times 10^{-5}$		$(7.72 \pm 0.24) \times 10^{-5}$
160		$(3.20 \pm 0.10) \times 10^{-5}$		$(1.19 \pm 0.06) \times 10^{-4}$
170		$(5.85 \pm 0.19) \times 10^{-5}$		$(2.06 \pm 0.09) \times 10^{-4}$
180		$(1.07 \pm 0.03) \times 10^{-4}$		$(3.29 \pm 0.10) \times 10^{-4}$
200		$(2.89 \pm 0.10) \times 10^{-4}$		
120	0.03	$(5.15 \pm 0.08) \times 10^{-6}$	0.10	$(9.09 \pm 0.11) \times 10^{-5}$
140		$(1.67 \pm 0.06) \times 10^{-5}$		$(2.39 \pm 0.05) \times 10^{-4}$
150		$(2.66 \pm 0.07) \times 10^{-5}$		$(4.14 \pm 0.10) \times 10^{-4}$
160		$(4.96 \pm 0.18) \times 10^{-5}$		$(6.52 \pm 0.01) \times 10^{-4}$
170		$(8.13 \pm 0.02) \times 10^{-5}$		$(1.11 \pm 0.00) \times 10^{-3}$
180		$(1.47 \pm 0.07) \times 10^{-4}$		$(1.74 \pm 0.03) \times 10^{-3}$
200		$(3.89 \pm 0.13) \times 10^{-4}$		

Notes:

 f_2 = mole fraction of ethanol in the solvents = moles of ethanol/(moles of ethanol + water)

$$x_1 = (1 - x_3) * (1 - f)$$

$$x_2 = f x_1 / (1 - f)$$

Table 4.8: Solubility data for ternary water (1) - ethanol (2) – *p*-terphenyl (3) systems

T (°C)	f_2	x_3	f_2	x_3
120	0.01	$(2.81 \pm 0.02) \times 10^{-7}$	0.04	$(9.62 \pm 0.41) \times 10^{-7}$
140		$(8.40 \pm 0.17) \times 10^{-7}$		$(3.08 \pm 0.15) \times 10^{-6}$
150		$(1.75 \pm 0.08) \times 10^{-6}$		$(5.47 \pm 0.00) \times 10^{-6}$
160		$(3.15 \pm 0.13) \times 10^{-6}$		$(1.05 \pm 0.04) \times 10^{-5}$
170		$(6.05 \pm 0.02) \times 10^{-6}$		$(2.13 \pm 0.02) \times 10^{-5}$
180		$(1.17 \pm 0.06) \times 10^{-5}$		$(3.34 \pm 0.15) \times 10^{-5}$
200		$(3.76 \pm 0.09) \times 10^{-5}$		
120	0.02	$(4.72 \pm 0.08) \times 10^{-7}$	0.06	$(2.07 \pm 0.05) \times 10^{-6}$
140		$(1.33 \pm 0.01) \times 10^{-6}$		$(6.72 \pm 0.03) \times 10^{-6}$
150		$(2.39 \pm 0.09) \times 10^{-6}$		$(1.25 \pm 0.01) \times 10^{-5}$
160		$(4.77 \pm 0.09) \times 10^{-6}$		$(2.25 \pm 0.09) \times 10^{-5}$
170		$(7.63 \pm 0.20) \times 10^{-6}$		$(4.28 \pm 0.07) \times 10^{-5}$
180		$(1.65 \pm 0.06) \times 10^{-5}$		$(7.29 \pm 0.31) \times 10^{-5}$
120	0.03	$(5.80 \pm 0.09) \times 10^{-7}$	0.10	$(1.34 \pm 0.06) \times 10^{-5}$
140		$(2.28 \pm 0.02) \times 10^{-6}$		$(4.19 \pm 0.12) \times 10^{-5}$
150		$(4.15 \pm 0.04) \times 10^{-6}$		$(6.87 \pm 0.07) \times 10^{-5}$
160		$(7.36 \pm 0.07) \times 10^{-6}$		$(1.33 \pm 0.03) \times 10^{-4}$
170		$(1.35 \pm 0.01) \times 10^{-5}$		$(2.26 \pm 0.03) \times 10^{-4}$
180		$(2.41 \pm 0.08) \times 10^{-5}$		$(3.67 \pm 0.07) \times 10^{-4}$

Notes:

f_2 = mole fraction of ethanol in the solvents = moles of ethanol/(moles of ethanol + water)

$x_1 = (1 - x_3) \cdot (1 - f)$

$x_2 = f x_1 / (1 - f)$

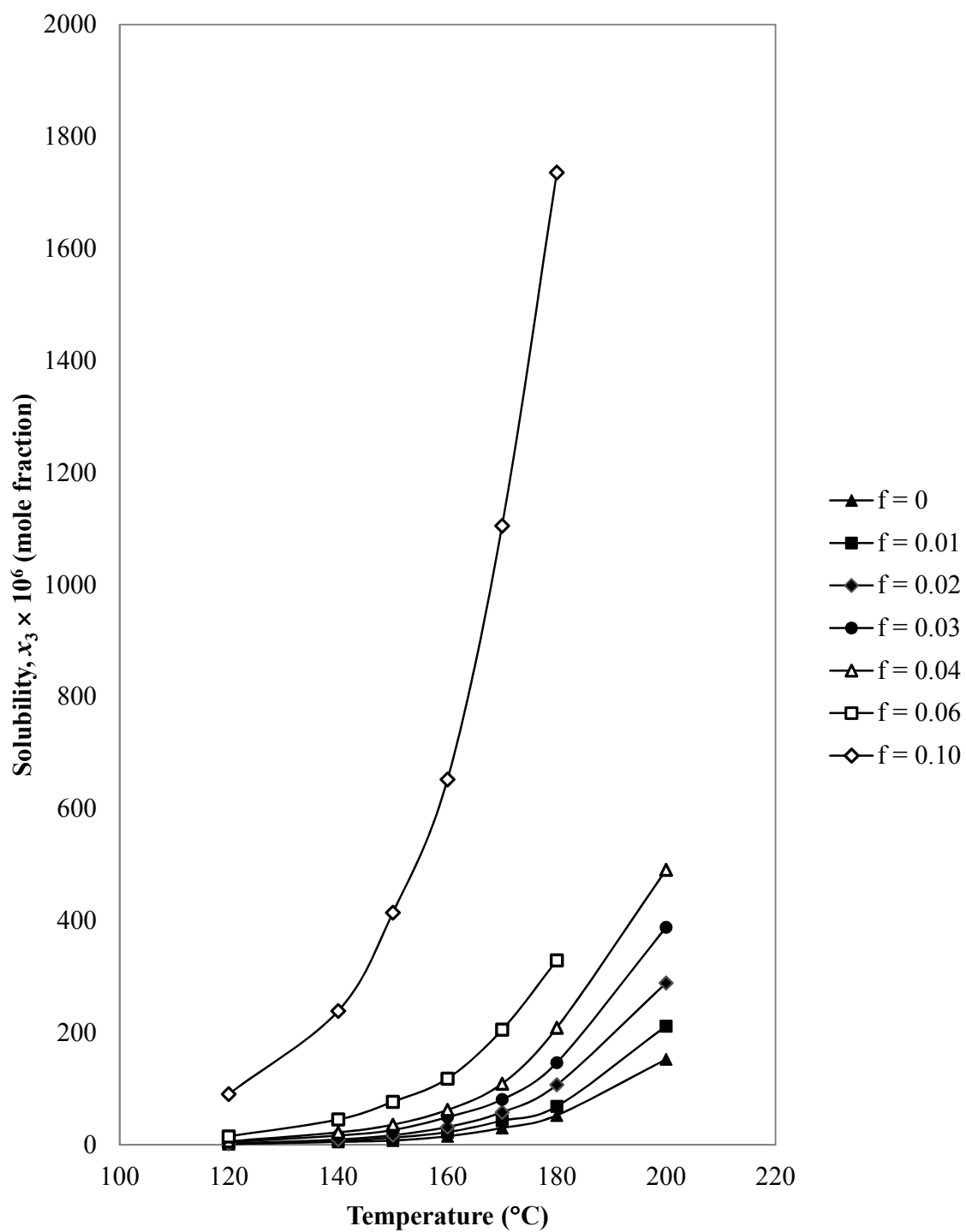


Figure 4.4: Solubility of anthracene as a function of temperature in subcritical water (1) – ethanol (2) – anthracene (3) systems

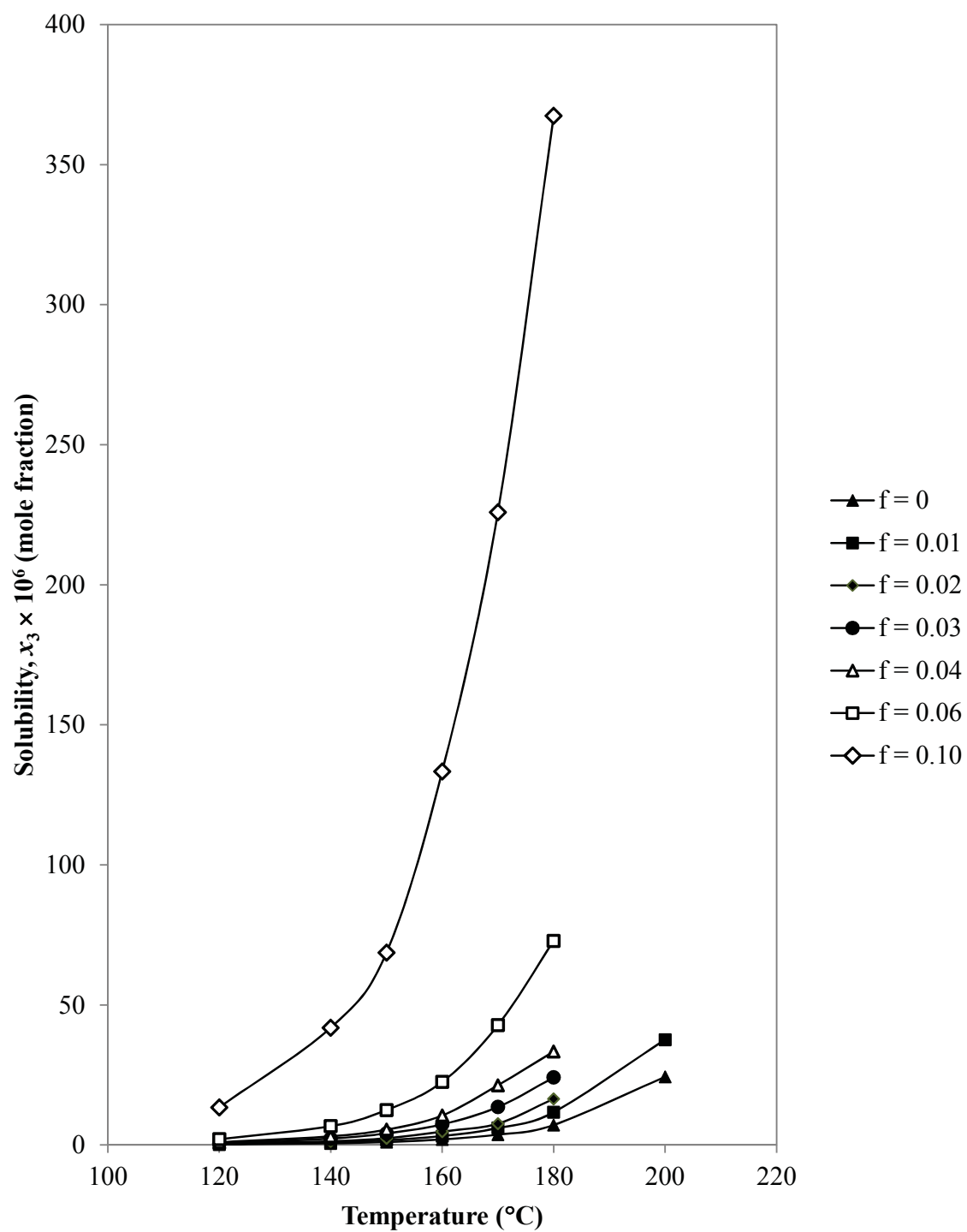


Figure 4.5: Solubility of *p*-terphenyl as a function of temperature in subcritical water (1) – ethanol (2) – *p*-terphenyl (3) systems

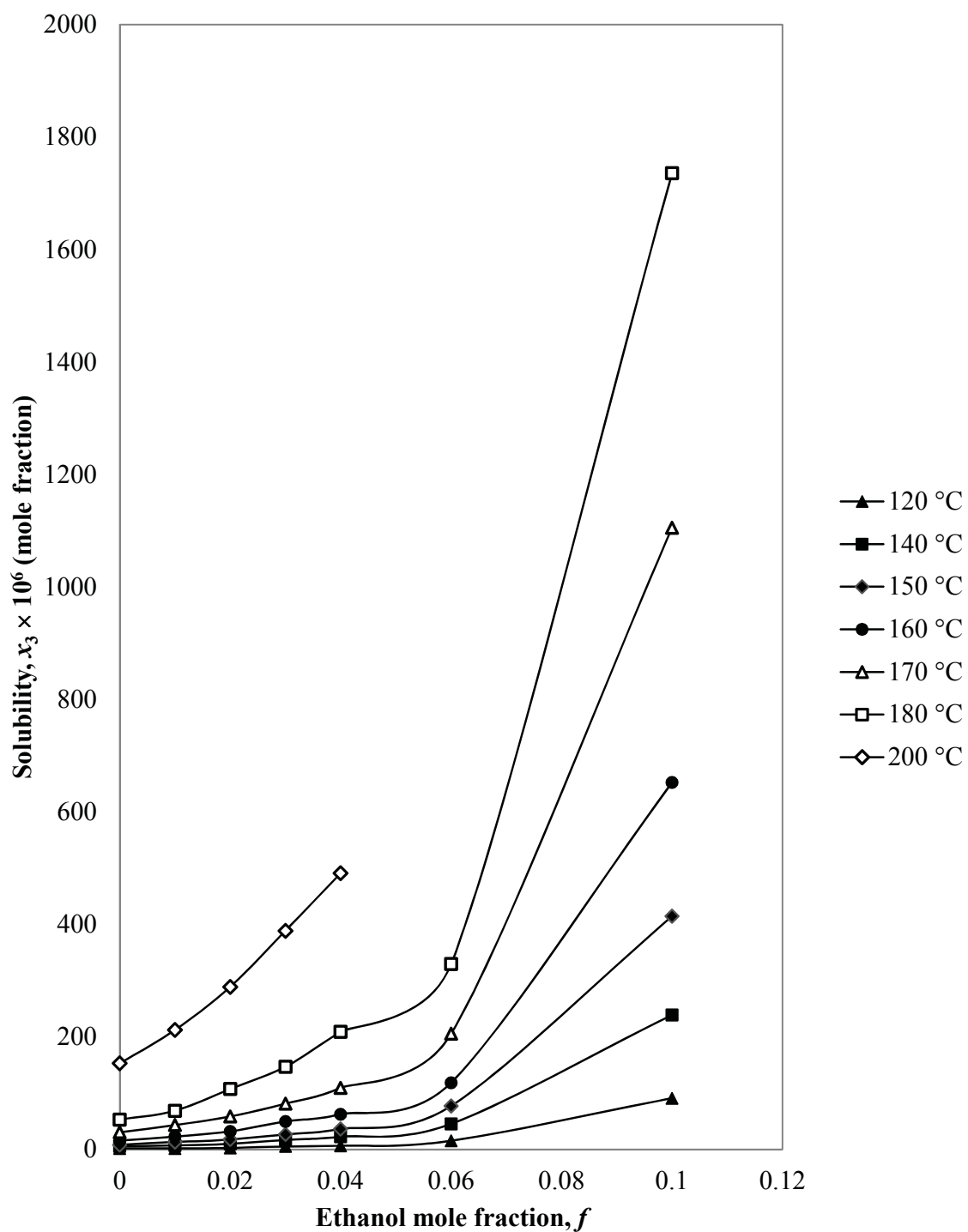


Figure 4.6: Solubility of anthracene as a function of ethanol mole fraction in subcritical water(1) – ethanol (2) – anthracene systems

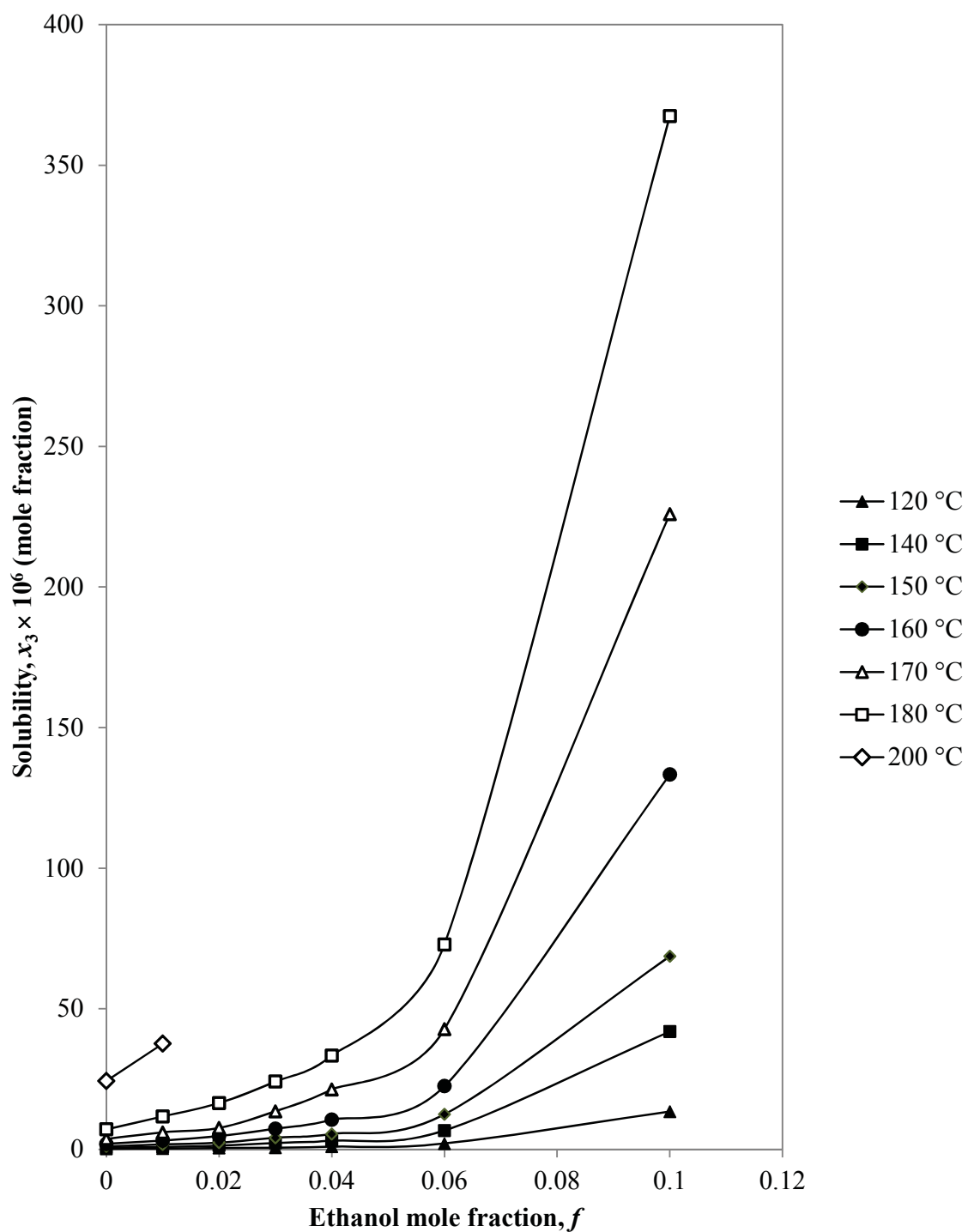


Figure 4.7: Solubility of *p*-terphenyl as a function of ethanol mole fraction in subcritical water
 (1) – ethanol (2) – *p*-terphenyl (3) systems

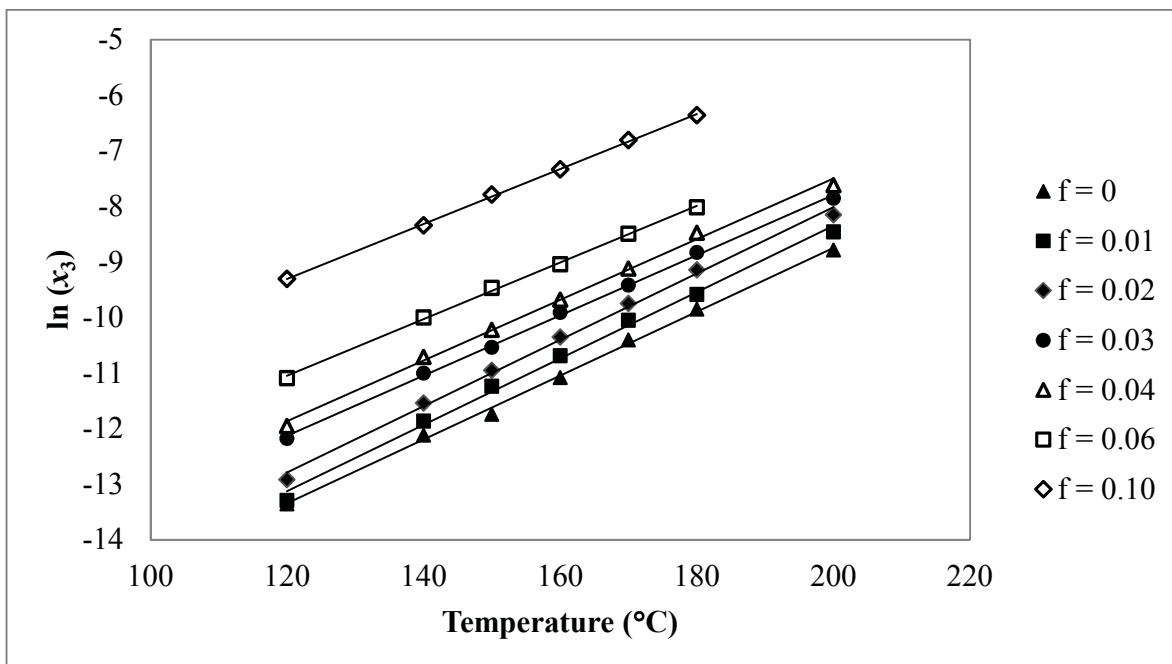


Figure 4.8: Plot of $\ln(x_3)$ versus temperature for anthracene in subcritical water/ethanol

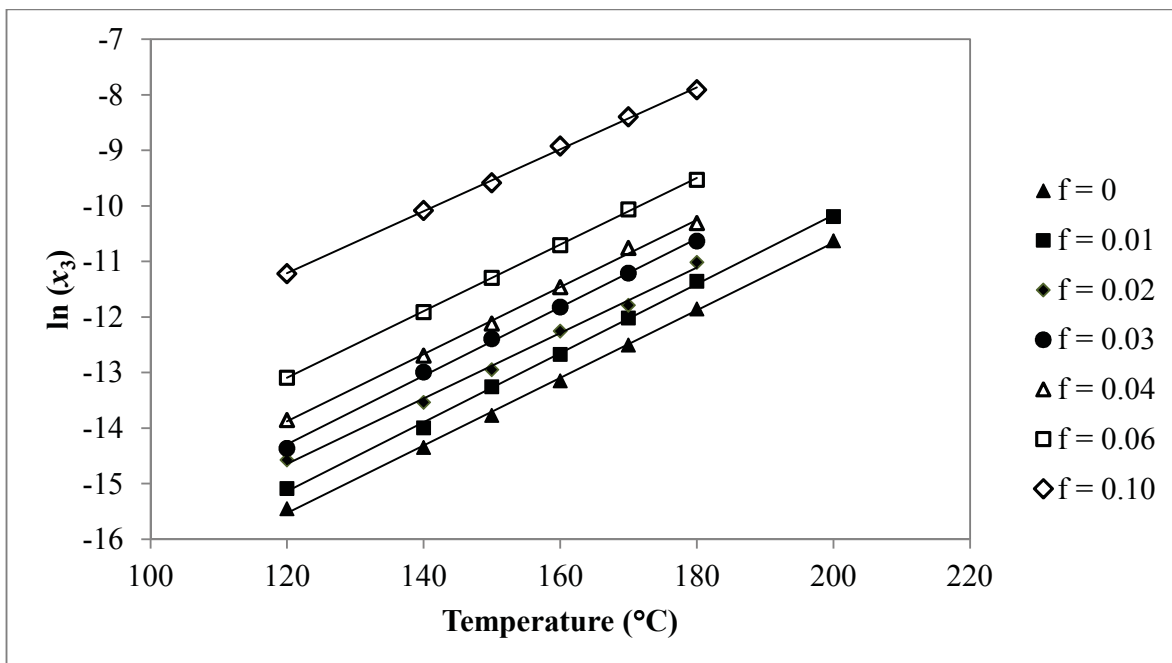


Figure 4.9: Plot of $\ln(x_3)$ versus temperature for *p*-terphenyl in subcritical water/ethanol

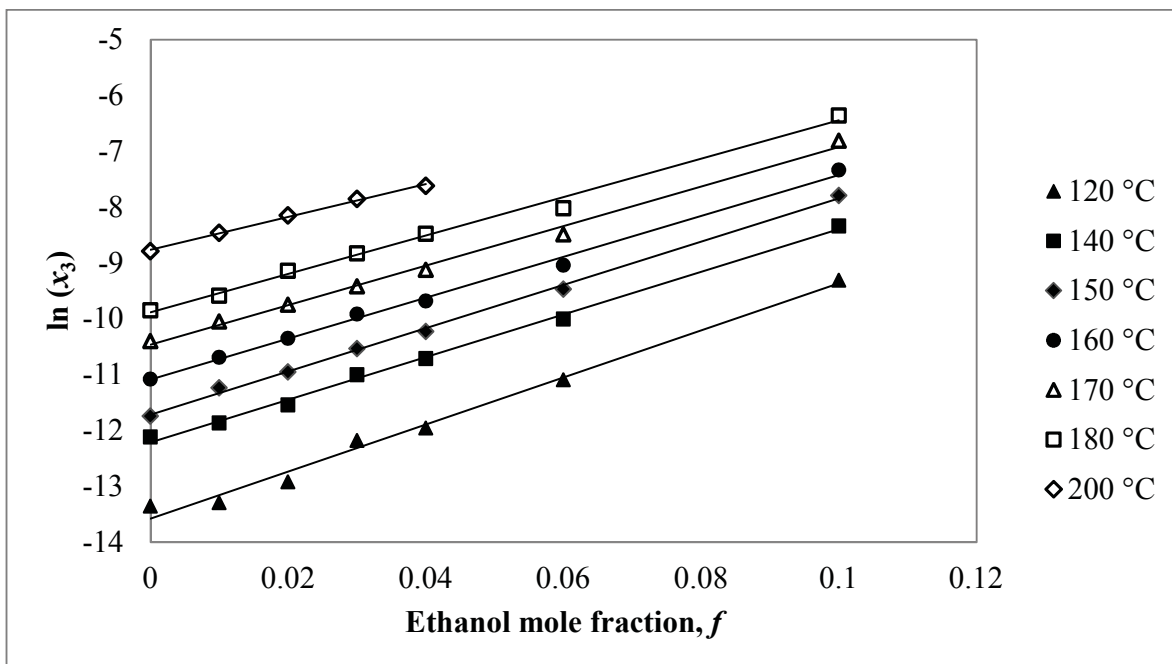


Figure 4.10: Plot of $\ln(x_3)$ versus ethanol mole fraction for anthracene in subcritical water/ethanol

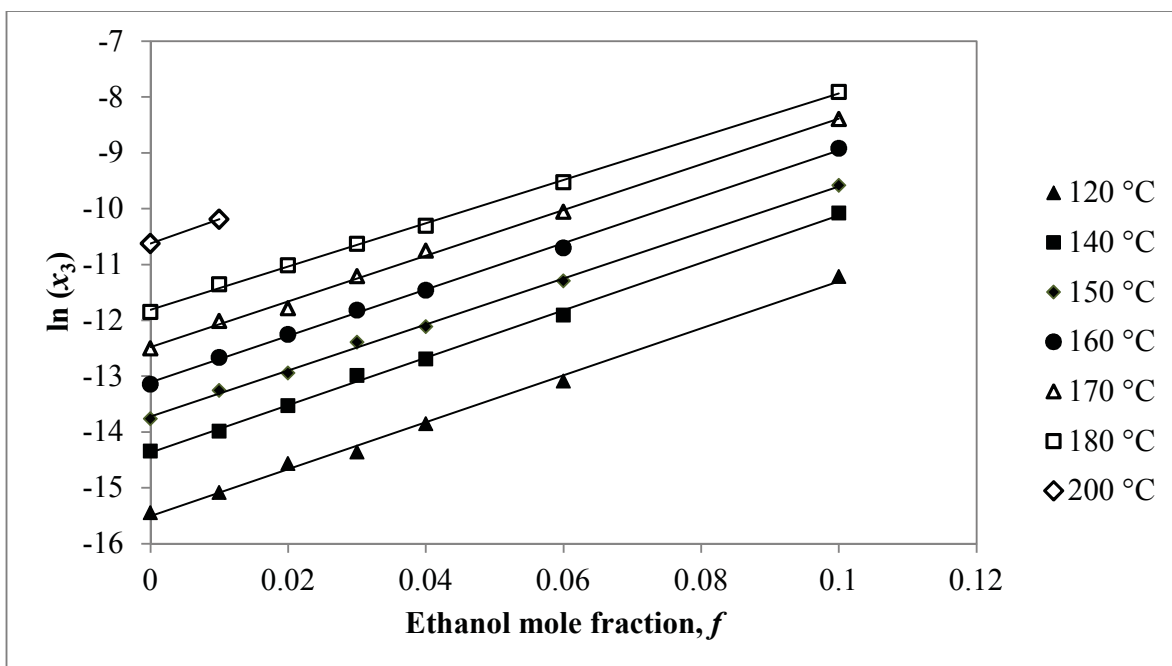


Figure 4.11: Plot of $\ln(x_3)$ versus ethanol mole fraction for *p*-terphenyl in subcritical water/ethanol

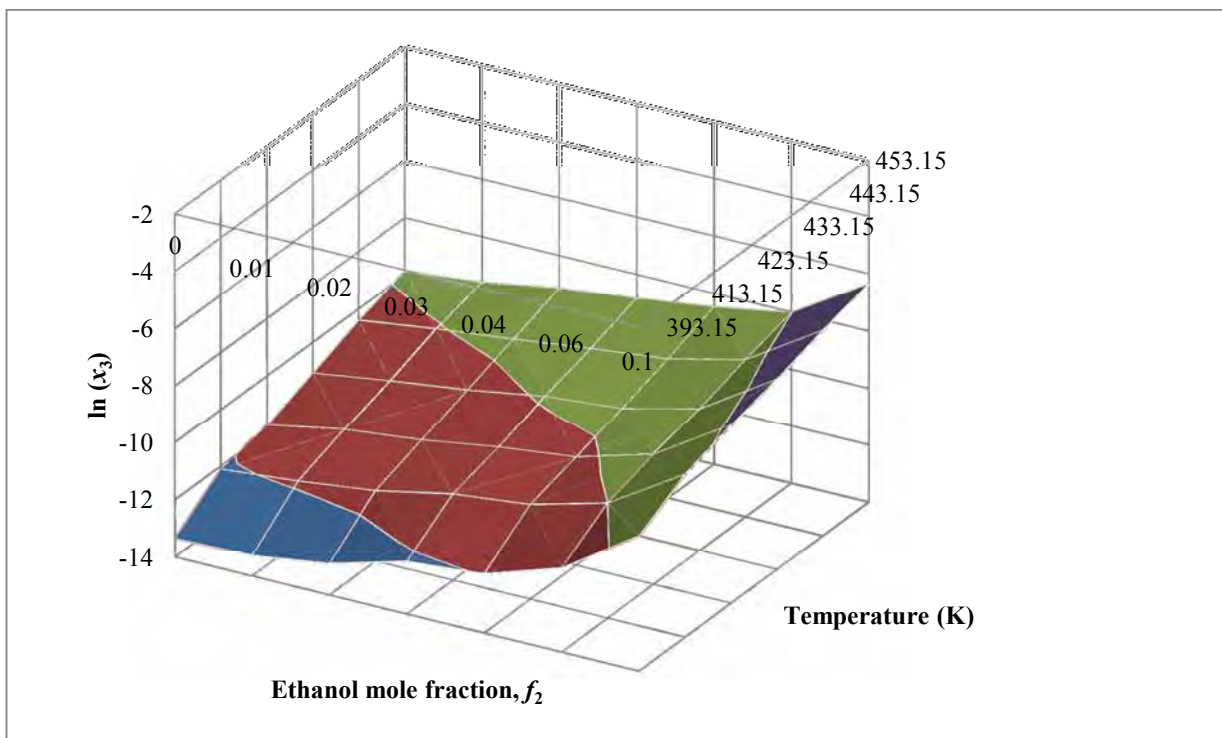


Figure 4.12: Plot of $\ln(x_3)$ against ethanol mole fraction and temperature for anthracene

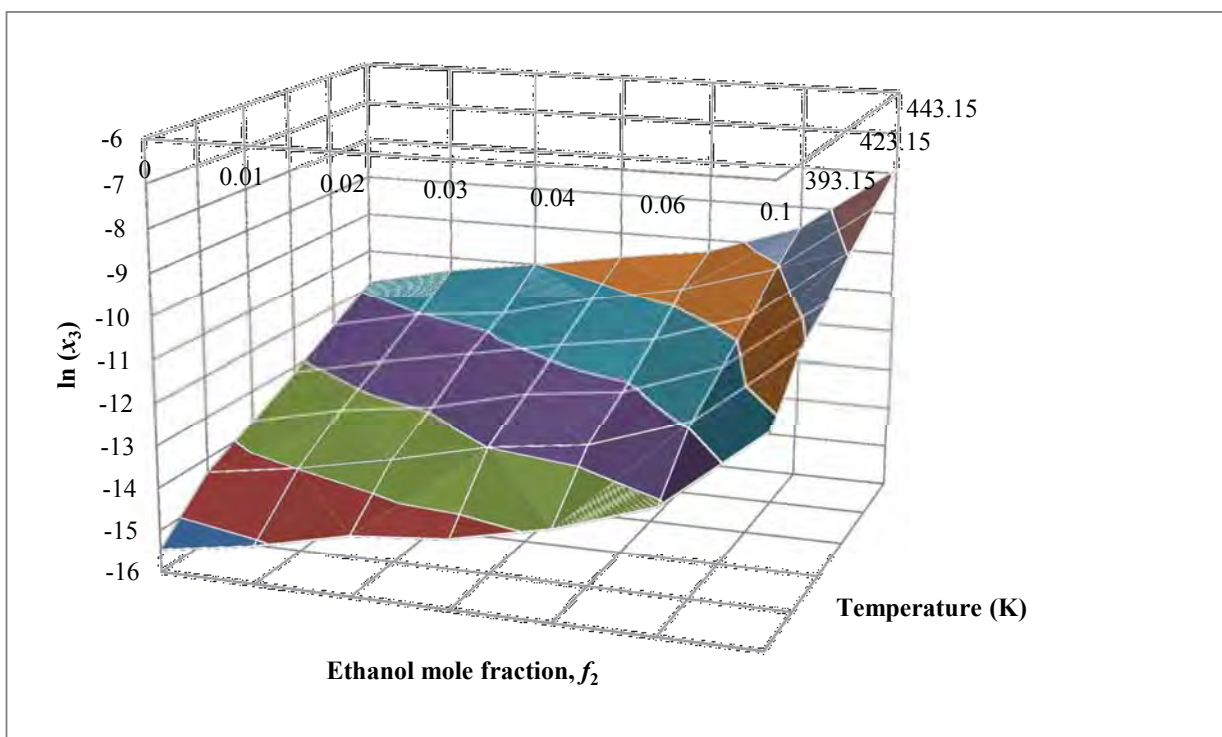


Figure 4.13: Plot of $\ln(x_3)$ against ethanol mole fraction and temperature for *p*-terphenyl

4.4 Solubility measurement of solid PAHs in subcritical ethanol

Solubility study of solid PAHs were also extended to subcritical ethanol system and included in this chapter. The motivation behind the solubility measurements of solid PAHs in subcritical ethanol was, however, purely for thermodynamic modelling rather than practical purposes. The solubilities of PAHs in subcritical ethanol were investigated in order to obtain the binary interaction parameters between PAHs and ethanol for the UNIQUAC model. Hence, solubility measurements were only conducted at selected temperatures at an isobaric condition of 50 bar.

Ethanol is a widely used polar protic solvent due to its low toxicity and high solvating power. Similar to water, the dielectric constant of ethanol decreases with increased temperature, as shown in Figure 4.14. At subcritical conditions, ethanol has been used to extract cotton cellulase, decompose oil palm fruit press fiber through subcritical ethanol liquefaction, and extract lipids from wet microalgae paste of *Nannochloropsis sp.* [11-13]. Subcritical ethanol has also been used to liquefy cornstalks to convert the cornstalk-based biomass into liquid fuel [14]. While a number of studies have been conducted using subcritical ethanol as a processing medium, it is surprising that investigation into the solute-subcritical ethanol behavior cannot be found in the literature. In this study, a static analytical equilibrium method was employed to measure the solubilities of anthracene and *p*-terphenyl in subcritical ethanol at temperatures between 120 °C and 170 °C.

4.4.1 Ethanol VLE and the phase behavior of solutes at subcritical conditions

Saturated vapor pressures of ethanol at various elevated temperatures are shown in Table 4.9. The data from both tables show that 50 bar is sufficient to maintain the liquid state of ethanol at elevated temperatures. The investigation into the phase behavior of the two PAHs in subcritical ethanol was similar to the experimental method described in Chapter 3. Melting point depression was also observed with both compounds behaving as liquids at certain temperatures, as shown in Table 4.10.

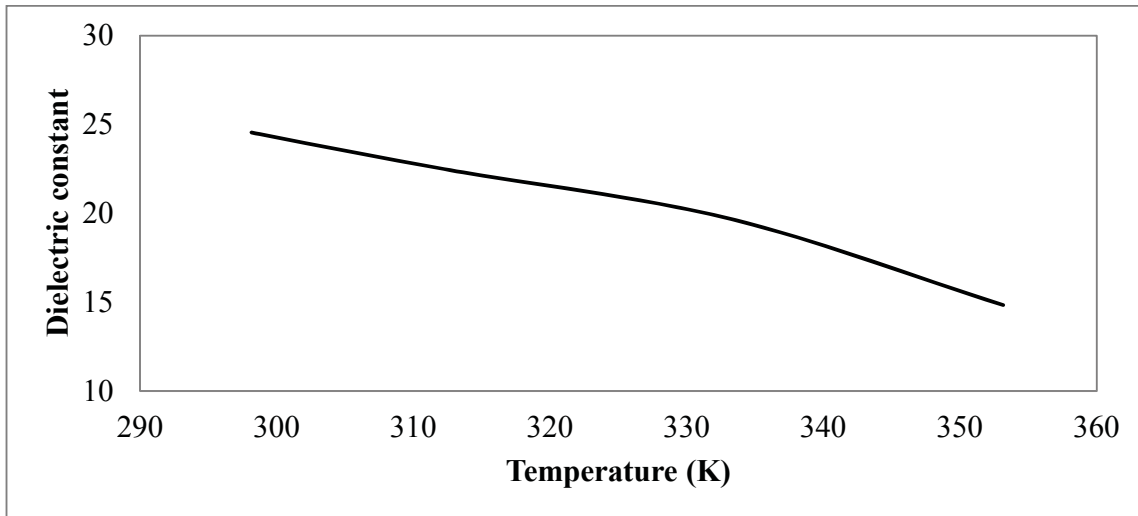


Figure 4.14: The dielectric constant of ethanol at various temperatures, reproduced from [15]

Table 4.9: Saturated pressures of ethanol at various temperatures

Temperature (°C)	Saturated vapor pressure (bar)
120	4.30
140	7.57
150	9.81
160	12.52
170	15.78

Note: Data calculated from:[16] using Antoine equation with $A = 7.68117$, $B = 1332.04$, $C = 199.2$

Table 4.10: Phase behavior of anthracene and *p*-terphenyl in subcritical ethanol at 50 bar and various temperatures

	Temperature (°C)	Phase behavior
Anthracene	120	Solid-liquid
	140	Solid-liquid
	150	Solid-liquid
	160	Solid-liquid
	170	Solid-liquid
	180	Solid-liquid
	200	Liquid-liquid
<i>p</i> -terphenyl	120	Solid-liquid
	140	Solid-liquid
	150	Solid-liquid
	160	Solid-liquid
	170	Solid-liquid
	180	Solid-liquid
	200	Liquid-liquid

4.4.2 Solubility measurement in subcritical ethanol

4.4.2.1 Materials

Anthracene (99 mole %) and *p*-terphenyl (99 mol %) were purchased from Sigma-Aldrich. Both compounds were used as received. Ethanol absolute (99.9%) was purchased from Scharlau Chemie.

4.4.2.2 Apparatus and experimental method

A static equilibrium method was utilized to measure the solubilities of anthracene and *p*-terphenyl in subcritical ethanol. While the experimental method remained the same (as with previous measurements in Chapters 2 and 3), the experimental set-up, and the analysis on the amount of solutes collected were modified to cater to the high solubility of the PAHs in subcritical ethanol, and to reduce the risk of fire hazard arising from the high flammability of ethanol. A schematic diagram of the experimental set-up is shown in Figure 4.15. Among the changes that were made to the rig was the addition of a CO₂ supply line into the GC oven as a fire hazard preventive measure. If leakages were to occur in the rig while the experiment was running, CO₂ as a sweeping gas, would dilute the concentration of oxygen and ethanol vapor in the oven and prevent combustion from occurring. The flow of CO₂ into the oven was controlled by a micro-metering valve. The CO₂ line-end in the oven was coiled to ensure CO₂ attained the temperature of the oven prior to its release. The coiling of the CO₂ line-end also prevented any temperature fluctuations in the oven. The lines external to the oven were also changed to bigger tubes to prevent line-clogging by the solutes. The amount of solutes and ethanol collected were measured gravimetrically.

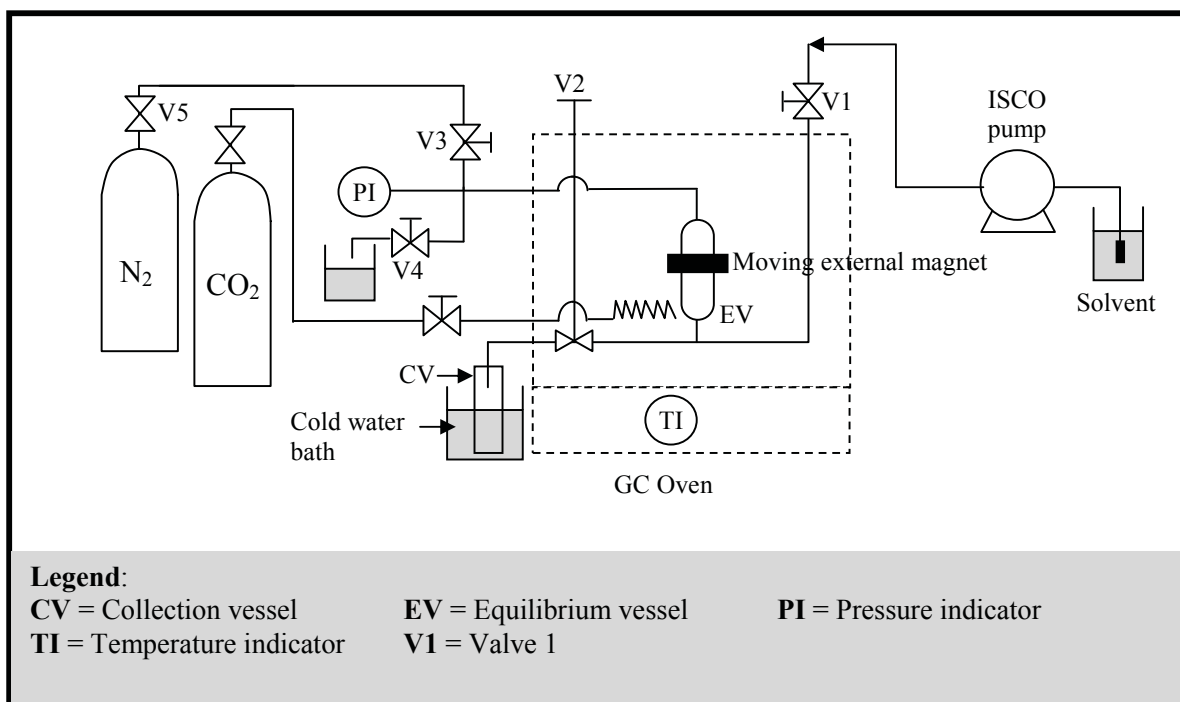


Figure 4.15: Schematic diagram of the solubility apparatus for measurement in subcritical ethanol

4.4.3 The effect of temperature on the solubility of PAHs in subcritical ethanol

Solubility measurements were conducted between 120 °C and 170 °C. Solubility measurements did not proceed above 170 °C due to the limitation in the rig as solutes began to clog the lines external to the oven. The pressure of the system was kept constant at 50 bar. The solubility data of pure anthracene and *p*-terphenyl in subcritical ethanol were found to increase exponentially with temperature, and are shown in Table 4.11 and Figure 4.16. The rate with which the solubility of *p*-terphenyl increases with temperature is found to be higher than for anthracene. The probable cause for the increase is the higher rate of increase in the sublimation pressure of *p*-terphenyl. Further discussion on this subject is given in Chapter 5.

Table 4.11: Solubility data for binary subcritical ethanol (1) – anthracene (2) and subcritical ethanol (1) – *p*-terphenyl (2)

T (°C)	anthracene x_2	<i>p</i> -terphenyl x_2
120	$(1.64 \pm 0.05) \times 10^{-2}$	$(6.55 \pm 0.13) \times 10^{-3}$
140	$(2.79 \pm 0.13) \times 10^{-2}$	$(1.51 \pm 0.05) \times 10^{-2}$
150	$(3.20 \pm 0.16) \times 10^{-2}$	$(2.50 \pm 0.03) \times 10^{-2}$
160	$(4.36 \pm 0.19) \times 10^{-2}$	$(4.36 \pm 0.06) \times 10^{-2}$
170	$(6.82 \pm 0.18) \times 10^{-2}$	$(9.54 \pm 0.20) \times 10^{-2}$

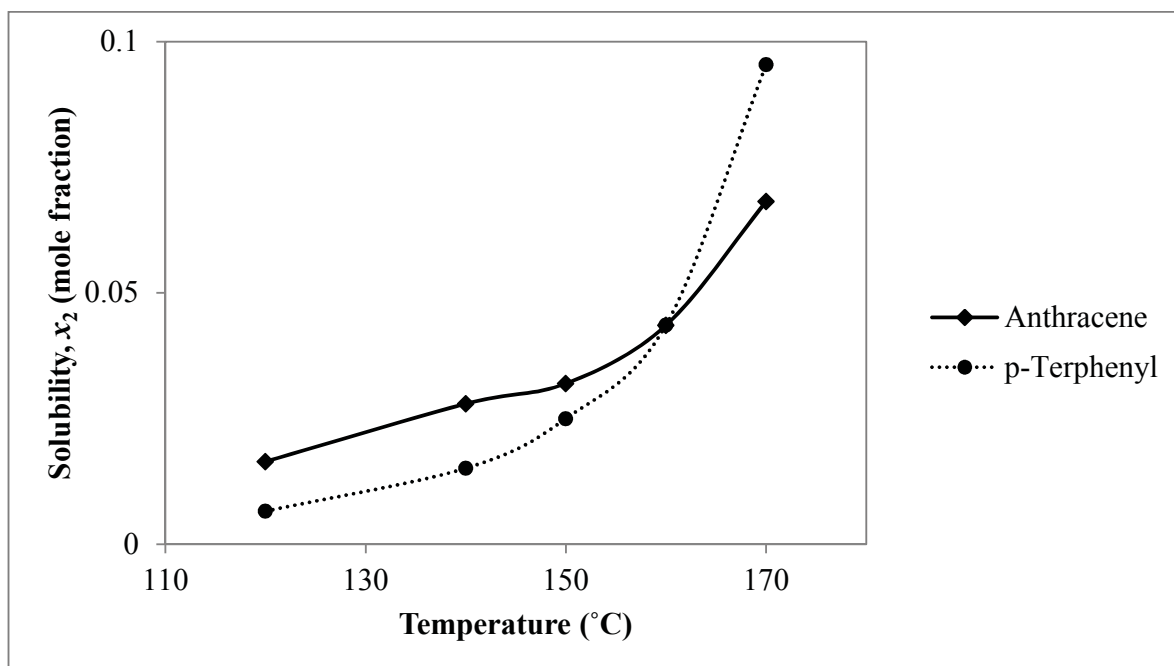


Figure 4.16: Solubility data of anthracene and *p*-terphenyl in subcritical ethanol at 50 bar and various temperatures

4.5 Conclusion

The solubilities of anthracene and *p*-terphenyl in modified subcritical water systems have been found to increase exponentially with temperature, as well as with ethanol concentration. Sharp increases in solubility were observed at 140 °C – 160 °C, and at $f \geq 0.06$. In a modified subcritical water system, temperature and the composition of a co-solvent are significant contributors to solubility. The effect on solubility from pressure in the 50 - 150 bar range and the combined effect of pressure and temperature in a modified subcritical water system are negligible. The solubilities of anthracene and *p*-terphenyl in subcritical ethanol are shown in this study to increase exponentially with temperature although anthracene increases at a slower rate than *p*-terphenyl

4.6 Bibliography

- [1] Albright PS, Gosting LJ. Dielectric constants of the methanol-water system from 5 to 55°C. *Journal of the American Chemical Society* 1946;68 (6):1061-3.
- [2] Field JA, Reed RL. Subcritical (hot) water/ethanol extraction of nonylphenol polyethoxy carboxylates from industrial and municipal sludges. *Environmental Science & Technology* 1999;33 (16):2782-7.
- [3] Curren MSS, King JW. Ethanol-modified subcritical water extraction combined with solid-phase microextraction for determining atrazine in beef kidney. *Journal of Agricultural and Food Chemistry* 2001;49 (5):2175-80.
- [4] Carr AG, Mammucari R, Foster NR. Particle formation of budesonide from alcohol-modified subcritical water solutions. *International Journal of Pharmaceutics* 2011;405 (1-2):169-80.
- [5] Curren MSS, King JW. Solubility of triazine pesticides in pure and modified subcritical water. *Analytical Chemistry* 2001;73 (4):740-5.
- [6] Carr AG, Branch A, Mammucari R, Foster NR. The solubility and solubility modelling of budesonide in pure and modified subcritical water solutions. *The Journal of Supercritical Fluids* 2010;55 (1):37-42.
- [7] Zhou B, Cai W, Zou L. Thermodynamic functions for transfer of anthracene from water to (water + alcohol) mixtures at 298.15 K. *Journal of Chemical & Engineering Data* 2003;48 (3):742-5.
- [8] Barr-David F, Dodge BF. Vapor-liquid equilibrium at high pressures. The systems ethanol-water and 2-propanol-water. *Journal of Chemical & Engineering Data* 1959;4 (2):107-21.
- [9] Bohon RL, Claussen WF. The solubility of aromatic hydrocarbons in water 1. *Journal of the American Chemical Society* 1951;73 (4):1571-8.
- [10] Shinoda K. "Iceberg" formation and solubility. *The Journal of Physical Chemistry* 1977;81 (13):1300-2.
- [11] Chen M, Chen X, Liu T, Zhang W. Subcritical ethanol extraction of lipid from wet microalgae paste of *nannochloropsis* sp. *Journal of Biobased Materials and Bioenergy*;5 (3):385-9.
- [12] Xueren Q, Jian L. Extraction of cellulose with subcritical and supercritical ethanol. *Journal of Forestry Research* 1999;10 (4):195-8.
- [13] Mazaheri H, Lee KT, Bhatia S, Mohamed AR. Sub/supercritical liquefaction of oil palm fruit press fiber for the production of bio-oil: Effect of solvents. *Bioresource Technology* 2010;101 (19):7641-7.
- [14] Liu H-M, Xie X-A, Feng B, Sun R-C. Effect of catalysts on 5-lump distribution of cornstalk liquefaction in subcritical ethanol. *BioResource* 2011;6 (3):2592-604.
- [15] Dannhauser W, Bahe LW. Dielectric constant of hydrogen bonded liquids. III. superheated alcohols. *The Journal of Chemical Physics* 1964;40 (10):3058-66.
- [16] GmbH DDBSaST. Saturated vapor pressure: calculation by Antoine equation. 2010.

5 Thermodynamic Modelling

5.1 Introduction

Classical chemical engineering thermodynamic models can generally be categorized into three types, with the models being based on (a) the excess Gibbs free energy or activity coefficient, (b) equations of state, and (c) empirical methods. A number of thermodynamic models have been utilized to calculate the solubility of organic compounds in subcritical water. Solubility data have been correlated empirically with temperature in the simplistic form of $(\partial \ln x_2 / \partial T)$ where the relative increase in solubility of compounds with temperature can be compared [1]. An approximation model was also developed in which solubility was estimated from values at ambient temperature [2]. The equation for the approximation is shown in Equation (5.1):

$$\ln x_2(T) = \left(\frac{T_0}{T}\right) \ln x_2(T_0) \quad (5.1)$$

where $x_2(T)$ is the mole fraction of solubility at any given temperature while $x_2(T_0)$ is the solubility at ambient temperature. Equation (5.1) is based on the premise that the Gibbs function for the solution does not change over the temperature range considered as the enthalpies of solution for the solutes investigated do not change greatly with temperature, and are greater than their entropy of contribution [2]. Further extensions were made to Equation (5.1) through the addition of a cubic equation to the base of Equation (5.1) [2,3], as given by Equations (5.2) and (5.3).

$$\ln x_2(T) = \left(\frac{T_0}{T}\right) \ln x_2(T_0) + 15 \left(\frac{T_0}{T} - 1\right)^3 \quad (5.2)$$

$$\ln x_2(T) = \left(\frac{T_0}{T}\right) \ln x_2(T_0) + 2 \left(\frac{T-T_0}{T_0} - 1\right)^3 \quad (5.3)$$

While Equations (5.1) to (5.3) could provide moderate estimates of solubility data, the fact that each equation works better at different temperature ranges indicate the difficulty in generalizing these equations for application to a wide range of compounds and temperatures.

In a liquid mixture, calculations of activity coefficients are generally used to predict solubility, with the binary-pair interactions and the group contribution methods frequently used. The most commonly used binary interaction methods are the Universal Quasi-Chemical equations [UNIQUAC] [4] and the Non-random two liquid model [NRTL], while the most widely used group contribution method is the Universal Functional Activity Coefficient method [UNIFAC] [5]. The advantage of using the UNIQUAC method compared with the NRTL is the requirement of *two* adjustable parameters per binary, whereas the NRTL requires a *third* parameter that accounts for non-randomness. Andersson and Prausnitz [6] further argued that the accuracy of experimental data is rarely high, and of sufficient quality and quantity to justify more than two binary parameters. A further advantage in using the UNIQUAC model is the ability to extend the application of the interaction parameters from binary systems to ternary systems; allowing for an estimate of phase equilibrium data for ternary systems. The drawback of the UNIQUAC model was removed by the group contribution approach as the interaction parameters are assigned to functional groups rather than compounds. Thus, the activity coefficients of a mixture consisting of multiple components can be calculated by relatively few functional groups.

The UNIQUAC functional group activity coefficients model (UNIFAC) is the most well-known group contribution method and has been used to calculate vapour-liquid equilibria (VLE), liquid-liquid equilibria (LLE), solid-liquid equilibria (SLE) and to determine the activities in polymer solutions [7]. The UNIFAC-based model has been used to calculate the solubility of various organic and inorganic systems [8,9]; the advantage being its extensive database that can be applied to multi-component mixtures. The UNIFAC model proposed in 1975, also known as the original UNIFAC (O-UNIFAC) model, was found to be inadequate in terms of its calculation of the activity coefficients of solutions at infinite dilutions and in its lack of temperature dependence for the excess Gibbs energy. Various researchers have shown that the calculations for the activity coefficients at infinite dilution are unsatisfactory [7,10]. The O-UNIFAC also falls short in its predictability capabilities for the enthalpies of mixing. Hence, the O-UNIFAC went through a series of revisions and extensions, and has since evolved into what is now known as the M-UNIFAC (modified UNIFAC) model [7,11-13]. The primary changes made to the M-UNIFAC method was inclusion of the temperature dependence of the activity coefficients; reflecting real behavior in multi-component systems. In addition, the

combinatorial part was changed empirically to account for compounds very different in size. One of the drawbacks of using the UNIFAC models is that not all group parameters for compounds are available. When group parameters are unavailable, data have to be taken from structurally similar substances, reducing the reliability of solubility estimations.

Since their introduction, a number of modifications have also been applied to the UNIFAC-based models, which include the addition of an association term to the UNIFAC-based models. A number of the association terms included in the UNIFAC models take into account the self- and cross-association in mixtures, and are based upon the Wertheim's perturbation theory. The capabilities of the different UNIFAC-based models for the prediction of solubilities of PAHs in subcritical water were studied by Fornari et al. [8]. The investigation concluded with the findings that the M-UNIFAC model, incorporating temperature dependent aromatic-water interaction parameters, provided the best prediction and representation of solubility as a function of temperature for a number of PAHs in subcritical water. The A-UNIFAC model (association term included) performed poorly in comparison to both the M- and O-UNIFAC models; the reason being the non-dependencies of the association energy on temperature. One major consideration in the use of the UNIQUAC and UNIFAC models was that these models were conceived on the basis of low pressure data. Hence, there is an approximation when these models are applied at high pressures. However, as established in previous chapters, the effects of pressure on solubility in subcritical water and ethanol-modified water systems are insignificant. Hence, the use of the UNIQUAC and UNIFAC models for analysis of these systems is still valid. The thermodynamic models are given in detail in the following sections.

5.2 Thermodynamic framework

When a solid solute is in equilibrium with its liquid phase in a mixture, the equi-fugacity equation is given by:

$$\hat{f}_2^S = \hat{f}_2^L \quad (5.4)$$

where \hat{f}_2^S is the fugacity of the solid solute and \hat{f}_2^L is the fugacity of the solute in a liquid solution. The solvent is assumed not to dissolve into the solid phase, and thus, if the solid phase is a pure compound, then f_2^S is the fugacity of the pure solid solute where

$$\hat{f}_2^S = f_2^S \quad (5.5)$$

In the liquid phase, the fugacity of the solute is related to its activity coefficient given by:

$$\hat{f}_2^L = \gamma_2 x_2 f_2^L \quad (5.6)$$

where x_2 is the mole fraction of the solute in the liquid solution, γ_2 is the activity coefficient and f_2^L is the fugacity of pure liquid of the solute at system temperature. In the system considered in this study, subcooled liquid is the best state to represent the fugacity of the pure component in the reference state. Therefore, equating Equations (5.5) and (5.6),

$$f_2^S = \gamma_2 x_2 f_2^L \quad (5.7)$$

$$\frac{f_2^S}{f_2^L} = \gamma_2 x_2 \quad (5.8)$$

The ratio of the fugacities in Equation (5.8) has been discussed elsewhere [14] and can be written in the form of:

$$\ln\left(\frac{f_2^S}{f_2^L}\right) = -\frac{\Delta H_f}{RT_{m2}}\left(\frac{T_{m2}}{T} - 1\right) + \frac{\Delta C_{P2}}{R}\left(\frac{T_{m2}}{T} - 1\right) + \frac{\Delta C_{P2}}{R} \ln\left(\frac{T}{T_{m2}}\right) - \int_{P_{sat}}^P \frac{V_2^L - V_2^S}{RT} dP \quad (5.9)$$

where ΔH_f is the enthalpy of fusion, R is the gas constant, T_m is the melting temperature of pure substance 2 and T is the temperature of the system. Consequently, the solubility of a solute in equilibrium with a liquid mixture can be calculated by equating Equations (5.8) and (5.9) and expressed through Equation (5.10) while the activity coefficient was obtained through the UNIQUAC and UNIFAC models.

$$\ln(x_2) = -\frac{\Delta H_f}{RT_{m2}}\left(\frac{T_{m2}}{T} - 1\right) + \frac{\Delta C_{P2}}{R}\left(\frac{T_{m2}}{T} - 1\right) + \frac{\Delta C_{P2}}{R}\ln\left(\frac{T}{T_{m2}}\right) - \int_{P_{sat}}^P \frac{V_2^L - V_2^S}{RT}dP - \ln \gamma_2 \quad (5.10)$$

ΔH_f is the enthalpy of fusion, R is the gas constant, T_m is the melting temperature of pure substance 2, γ_2 is the activity coefficient of pure substance 2, T is the temperature of the system, and ΔC_{P2} is the difference between the heat capacity of the pure liquid and the solid solute. V_2^L and V_2^S are the molar volumes of pure solid solute and subcooled liquid solute respectively.

The fourth term on the right hand side of Equation (5.10) takes into consideration the added effect of pressure on the fugacity of the solute, and is only significant at very high pressures [8]. The second and third term on the right hand side of Equation (5.10) are generally assumed to cancel out each other when the temperature of the mixture is near to the solute melting temperature [8], or is generally considered to be insignificant compared with the first term [15]. Hence, Equation (5.10) is reduced to Equation (5.11) from which the activity coefficient can be estimated.

$$\ln(x_2) = -\frac{\Delta H_f}{RT_{m2}}\left(\frac{T_{m2}}{T} - 1\right) - \ln \gamma_2 \quad (5.11)$$

5.2.1 The UNIQUAC Model

Fundamental to the UNIQUAC method is the calculation of the activity coefficient based on two separate parts: the combinatorial part that contributes to the activity coefficient of a molecule due to the differences in the molecular size and shape, and the residual contribution due to molecular interactions. In the residual part, energy interactions, functional group sizes and interaction surface areas are introduced from independently obtained pure component molecular structure data. The UNIQUAC model is primarily used to represent vapour-liquid and liquid-liquid equilibria (VLE and LLE) of multi-component mixtures at pressures far from the critical pressure. In this work, where the solubility data were measured at 50 bar, the UNIQUAC model was chosen, supported by the negligible effect of pressure on solid solubility shown in Chapters 3 and 4. The activity coefficient of a molecular component in a multi-component mixture is given by:

$$\ln \gamma_i = \ln \gamma_i^C + \ln \gamma_i^R \quad (5.12)$$

where γ_i is the activity coefficient of a component in a mixture, γ_i^C is the combinatorial part of the activity coefficient while γ_i^R is the residual part of the activity coefficient. The combinatorial part of the activity coefficient is expressed as:

$$\gamma_i^C = \ln \frac{\Phi_i}{x_i} + \frac{z}{2} q_i \ln \frac{\theta_i}{\Phi_i} + l_i - \frac{\Phi_i}{x_i} \sum_j x_j l_j \quad (5.13)$$

while the residual part is expressed as:

$$\ln \gamma_i^R = q_i \left[1 - \ln \left(\sum_j \theta_j \tau_{ji} \right) - \sum_j \frac{\theta_j \tau_{ij}}{\sum_k \theta_k \tau_{kj}} \right] \quad (5.14)$$

where

$$l_i = \frac{z}{2} (r_i - q_i) - (r_i - 1) \quad (5.15)$$

$$\theta_i = \frac{q_i x_i}{\sum_j q_j x_j} \quad (5.16)$$

$$\Phi_i = \frac{r_i x_i}{\sum_j r_j x_j} \quad (5.17)$$

$$\tau_{ji} = \exp \left(-\frac{u_{ji} - u_{ii}}{RT} \right) = \exp \left(-\frac{a_{ji}}{T} \right) \quad (5.18)$$

$$r_i = \sum v_k^{(i)} R_k \quad (5.19)$$

$$q_i = \sum v_k^{(i)} Q_k \quad (5.20)$$

x_i is the mole fraction of component i , θ_i is the area fraction while Φ_i is the segment/volume fraction for component i . Parameters r_i and q_i are calculated from the van der Waals volumes and surface areas whereas z is the coordination number, usually associated with the number 10. Parameters τ_{ji} and τ_{ij} are the two adjustable binary parameters obtained from experimental data.

5.2.2 The O-UNIFAC model

The O-UNIFAC model [5] was developed from the UNIQUAC model where the combinatorial part of the activity coefficient was used directly from the UNIQUAC model. The residual part of the activity coefficient is given by:

$$\ln \gamma_i^R = \sum_k v_k^{(i)} \left[\ln \Gamma_k - \ln \Gamma_k^{(i)} \right] \quad (5.21)$$

where Γ_k is the group residual activity coefficient while $\Gamma_k^{(i)}$ is the group residual activity coefficient in a solution containing only molecule i . Γ_k and $\Gamma_k^{(i)}$ can be calculated from

$$\ln \Gamma_k = Q_k \left[1 - \ln \left(\sum_m \Theta_m \Psi_{mk} \right) - \sum_m \frac{\Theta_m \Psi_{km}}{\sum_n \Theta_n \Psi_{nm}} \right] \quad (5.22)$$

Θ_m is the group area fraction and X_m is the group mole fraction given by

$$\Theta_m = \frac{Q_m X_m}{\sum_n Q_n X_n} \quad (5.23)$$

$$X_m = \frac{\sum_j v_m^{(j)} x_j}{\sum_j \sum_n v_n^{(j)} x_j} \quad (5.24)$$

Ψ_{nm} is the UNIFAC group interaction parameters given by equation:

$$\Psi_{nm} = \exp \left(-\frac{a_{nm}}{T} \right) \quad (5.25)$$

where a_{nm} is the UNIFAC group interaction parameters between groups n and m .

5.2.3 M-UNIFAC model

The Modified UNIFAC model semi-empirically estimates the activity coefficient through the sum of a combinatorial and a residual part given by Equation (5.12). The combinatorial part was originally derived from the Flory-Huggins equation, but has since been changed in an empirical way to deal with compounds of very different sizes. The combinatorial activity coefficient is given by:

$$\ln \gamma_i^C = 1 - V'_i + \ln V'_i - 5q_i \left[1 - \frac{V_i}{F_i} + \ln \left(\frac{V_i}{F_i} \right) \right] \quad (5.26)$$

Parameter V'_i is calculated from the relative van der Waals volumes R_k of different groups where:

$$V'_i = \frac{r_i^{3/4}}{\sum_j x_j r_j^{3/4}} \quad (5.27)$$

Parameters r_i and q_i are the sum of the group volume, R_k and group area, Q_k parameters, given by:

$$r_i = \sum v_k^{(i)} R_k \quad (5.28)$$

$$q_i = \sum v_k^{(i)} Q_k \quad (5.29)$$

where $v_k^{(i)}$ is the number of type k groups in molecule i , and is always an integer. R_k and Q_k are obtained from the van der Waals group volume and surface areas. V_i is the auxiliary property (volume fraction/mole fraction) for component i given by equation

$$V_i = \frac{r_i}{\sum_j x_j r_j} \quad (5.30)$$

while F_i is the auxiliary property (surface fraction/mole fraction) for component i given by

$$F_i = \frac{q_i}{\sum_j x_j q_j} \quad (5.31)$$

The residual section of the activity coefficient is given by

$$\ln \gamma_i^R = \sum_k v_k^{(i)} \left(\ln \Gamma_k - \ln \Gamma_k^{(i)} \right) \quad (5.32)$$

where

$$\ln \Gamma_k = Q_k \left[1 - \ln \left(\sum_m \theta_m \Psi_{mk} \right) - \sum_m \frac{\theta_m \Psi_{km}}{\sum_n \theta_n \Psi_{nm}} \right] \quad (5.33)$$

$\ln \Gamma_k$ is the group residual activity coefficient while $\Gamma_k^{(i)}$ is the residual activity coefficient of group k in a reference solution containing only molecules of type i . θ_m is the group area fraction and X_m is the group mole fraction given by:

$$\theta_m = \frac{Q_m X_m}{\sum_n Q_n X_n} \quad (5.34)$$

$$X_m = \frac{\sum_j v_m^{(j)} x_j}{\sum_j \sum_n v_n^{(j)} x_j} \quad (5.35)$$

Ψ_{nm} is the UNIFAC group interaction parameters given by equation:

$$\Psi_{nm} = \exp \left(-\frac{a_{nm} + b_{nm}T + c_{nm}T^2}{T} \right) \quad (5.36)$$

where a_{nm} , b_{nm} and c_{nm} are UNIFAC group interaction parameters between groups n and m .

In this study, the UNIQUAC, O-UNIFAC and M-UNIFAC methods were used to calculate the solubilities of anthracene and *p*-terphenyl in various binary and ternary subcritical solvent systems. The combinatorial and residual contributions of these three methods were compared and results are discussed in the following sections.

5.3 Results and Discussion

5.3.1 Empirical model: Variation of solubility with temperature

The solubilities of anthracene and *p*-terphenyl in subcritical water, subcritical ethanol and modified-subcritical water have been shown in previous chapters to increase exponentially with temperature. Plots of natural logarithm of solubilities [$\ln (x_2)$] of anthracene and *p*-terphenyl as a function of temperature yield near linear relationship, as shown in Figures 5.1 - 5.4. A simple empirical equation, Equation (5.37), can be used to describe the solubility behavior of anthracene and *p*-terphenyl given by

$$\ln x_{\text{solute}} = mT + c \quad (5.37)$$

where x_{solute} is the solubility of the solute, T is the absolute temperature, while m and c are constants. The values of m and c are given together with the correlation coefficients, in Table 5.1.

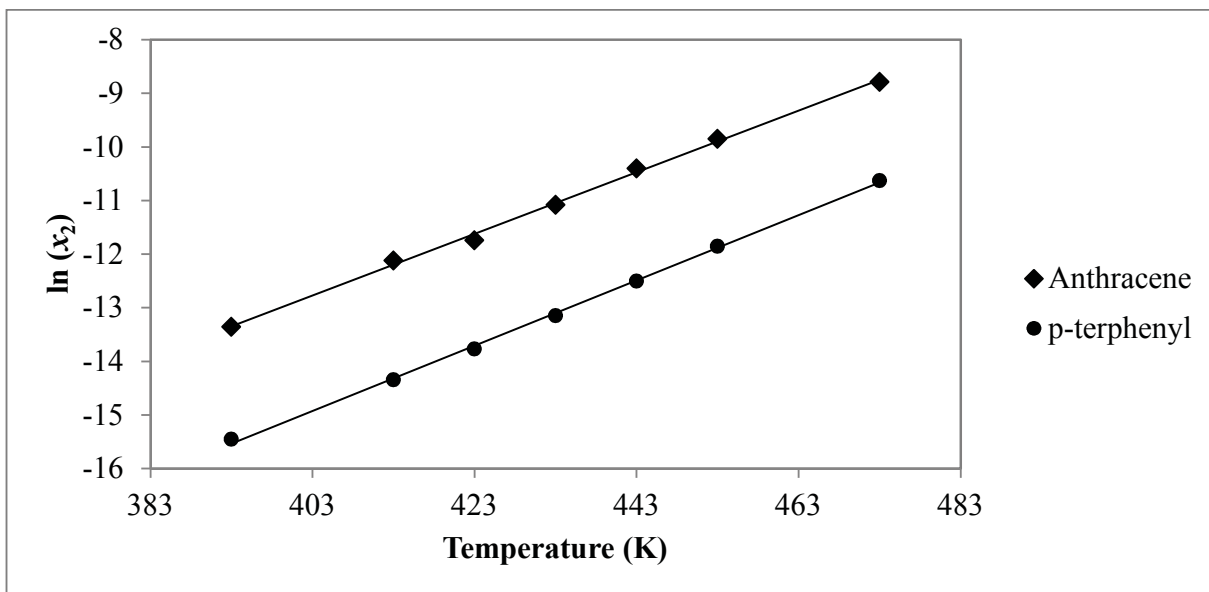


Figure 5.1: $\ln(x_2)$ as a function of temperature for subcritical water (1) – anthracene (2) and subcritical water (1) – *p*-terphenyl (2) systems

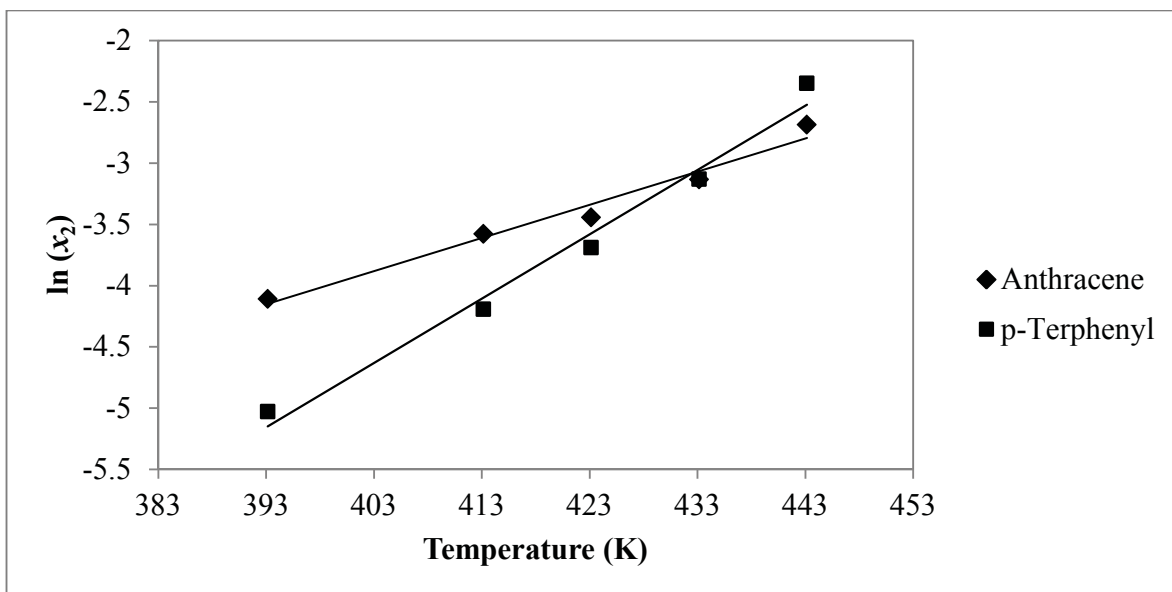


Figure 5.2: $\ln(x_2)$ as a function of temperature for subcritical ethanol (1) – anthracene (2) and subcritical ethanol (1) – *p*-terphenyl (2) systems

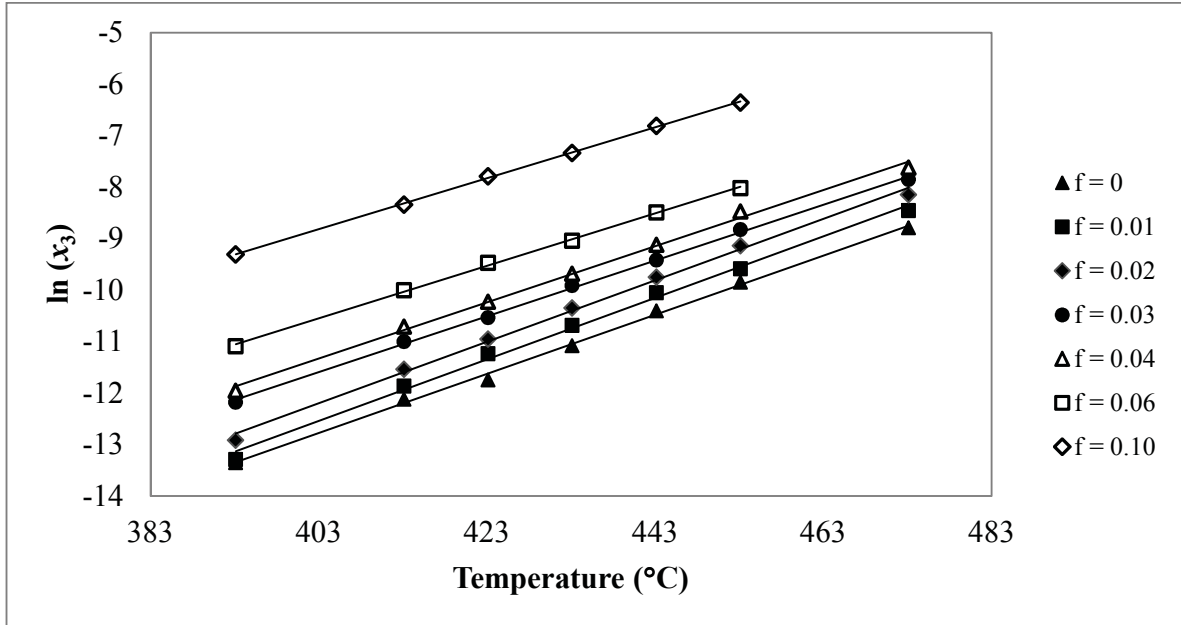


Figure 5.3: $\ln(x_3)$ as a function of temperature for subcritical water (1) – ethanol (2) – anthracene (3) system [f = moles of ethanol / moles of ethanol + water]

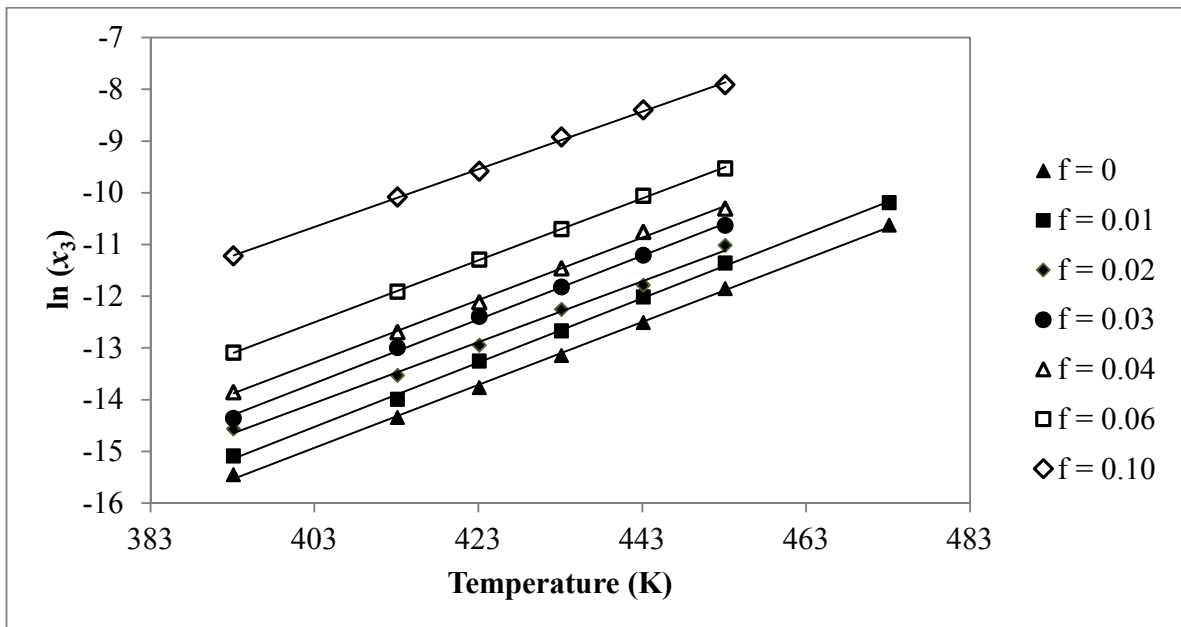


Figure 5.4: $\ln(x_3)$ as a function of temperature for subcritical water (1) – ethanol (2) – *p*-terphenyl (3) system [f = moles of ethanol / moles of ethanol + water]

Table 5.1: Parameters m and c derived from Equation (5.37) for anthracene and p -terphenyl in various subcritical solvent systems

Solvent(s)	Compound	m	c	correlation coefficient, r
Water	Anthracene	0.0575	-35.938	0.9989
	p -terphenyl	0.0609	-39.450	0.9994
Ethanol	Anthracene	0.0217	-14.797	0.9863
	p -terphenyl	0.0525	-25.787	0.9991
Water-ethanol $f = 0.01$	Anthracene	0.0597	-36.602	0.9978
	p -terphenyl	0.0621	-39.569	0.9995
Water-ethanol $f = 0.02$	Anthracene	0.0597	-36.257	0.9983
	p -terphenyl	0.0589	-37.785	0.9980
Water-ethanol $f = 0.03$	Anthracene	0.0542	-33.423	0.9984
	p -terphenyl	0.0617	-38.562	0.9992
Water-ethanol $f = 0.04$	Anthracene	0.0546	-33.423	0.9994
	p -terphenyl	0.0604	-37.613	0.9990
Water-ethanol $f = 0.06$	Anthracene	0.0510	-31.092	0.9994
	p -terphenyl	0.0599	-36.636	0.9998
Water-ethanol $f = 0.10$	Anthracene	0.0495	-28.752	0.9997
	p -terphenyl	0.0557	-33.109	0.9993

The $\ln x_{\text{solute}} = mT + c$ model is the simplest representation of the solubilities of anthracene and p -terphenyl at various temperatures. It is noteworthy that the rate with which solubility increases with temperature in subcritical water is higher for p -terphenyl than for anthracene, as observed in the higher m value. The possible explanation for this behavior is the lower rate of increase in the sublimation pressure of anthracene with temperature. The sublimation pressure ratio of anthracene relative to p -terphenyl is shown in Figure 5.5, of which the sublimation pressure ratio decreases with rising temperature. Similar observations can be made for the ethanol and ethanol-modified systems in which the rates of increase for anthracene are lower. It is of interest to note that the rate with which the solubility of p -terphenyl increases with temperature in subcritical *ethanol* is higher than in subcritical water, while anthracene has a lower rate in subcritical ethanol than in water. However, in the water-ethanol solvent systems,

the rate with which the solubilities of *p*-terphenyl and anthracene increase with temperature is lowered with higher ethanol concentration. The linear plots obtained from Equation 5.37 allowed for an easy prediction/extrapolation of anthracene solubility to higher temperatures, although the simplicity of the empirical model limits its ability to forecast solubility to the temperature range investigated in this study.

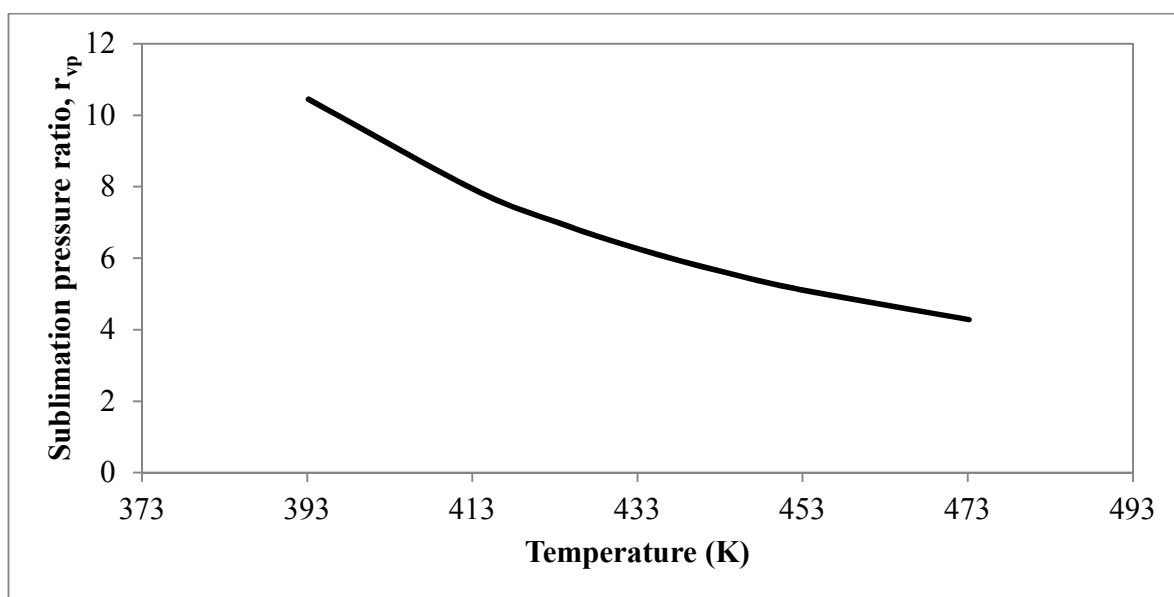


Figure 5.5: Sublimation pressure ratio of anthracene relative to *p*-terphenyl with data reproduced from [16] [r_{vp} = sublimation pressure of anthracene / sublimation pressure of *p*-terphenyl]

5.3.2 Correlation via the UNIQUAC model

The UNIQUAC method was applied to all solute-solvent systems investigated in this thesis. The UNIQUAC-based parameters employed in the calculation of PAHs solubility are shown in Table 5.2. Group volume parameter (R_k) and surface area parameter (Q_k) values are taken from an updated O-UNIFAC group specifications data since the combinatorial part of the activity coefficient ($\ln \gamma_i^C$) in the O-UNIFAC model was taken directly from the UNIQUAC model.

Table 5.2: Parameters used in the UNIQUAC and O-UNIFAC models (values obtained from [15])

Compound	Group	Group volume parameter (R_k)	Surface area parameter (Q_k)
anthracene/ <i>p</i> -terphenyl	ACH (9)	0.5313	0.400
	AC (10)	0.3652	0.120
water	H ₂ O (7)	0.9200	1.400
ethanol	CH ₃ (1)	0.9011	0.848
	CH ₂ (2)	0.6744	0.540
	OH (14)	1.0000	1.200

The energy interaction parameters, u_{ij} and u_{ji} were obtained from binary systems, and these values were extended to ternary systems. For the PAH-ethanol and PAH-water systems, the u_{ij} and u_{ji} parameters were calculated directly from the experimental data collected in this thesis while the u_{ij} and u_{ji} values for the water-ethanol system were obtained from the DECHEMA series [17]. The binary interaction parameters for the water-ethanol systems were chosen from a VLE system that best describes the temperature range of this investigation. The use of VLE parameters in this analysis is perhaps a cause for concern since it is not the same as experimental conditions. However, it has been ascertained that activity coefficients for SLE can often be estimated from VLE data at higher temperatures [18]. Moreover, the VLE effect in the modelling of the ternary systems were found to be negligible as the variations to the solubility data calculated with different VLE-related u_{ij} and u_{ji} values were less than 2%. The main

contributions to the calculated solubility data in the ternary systems were due to the interaction parameters that came from the PAH-ethanol and PAH-water interactions.

In the calculation of the energy interaction parameters, a Generalized Reduced Gradient [19] algorithm was used. Initially, u_{ij} was correlated to a single parameter, given by $\frac{u_{ji}-u_{ii}}{R} = a_{ij}$. In the calculation of the a_{ij} variable, an objective function approach, coupled with a sensitivity analysis, was employed since the existence of local minima creates convergences that are dependent on the initial value. The objective function (OF) used is given by Equation (5.38). The results of the sensitivity analysis for each binary component are shown in Figures 5.6-5.9 and Table 5.3.

$$\text{OF} = \sum_{i=1}^N (\ln \gamma_i^{\text{exp}} - \ln \gamma_i^{\text{cal}})^2 / N \quad (5.38)$$

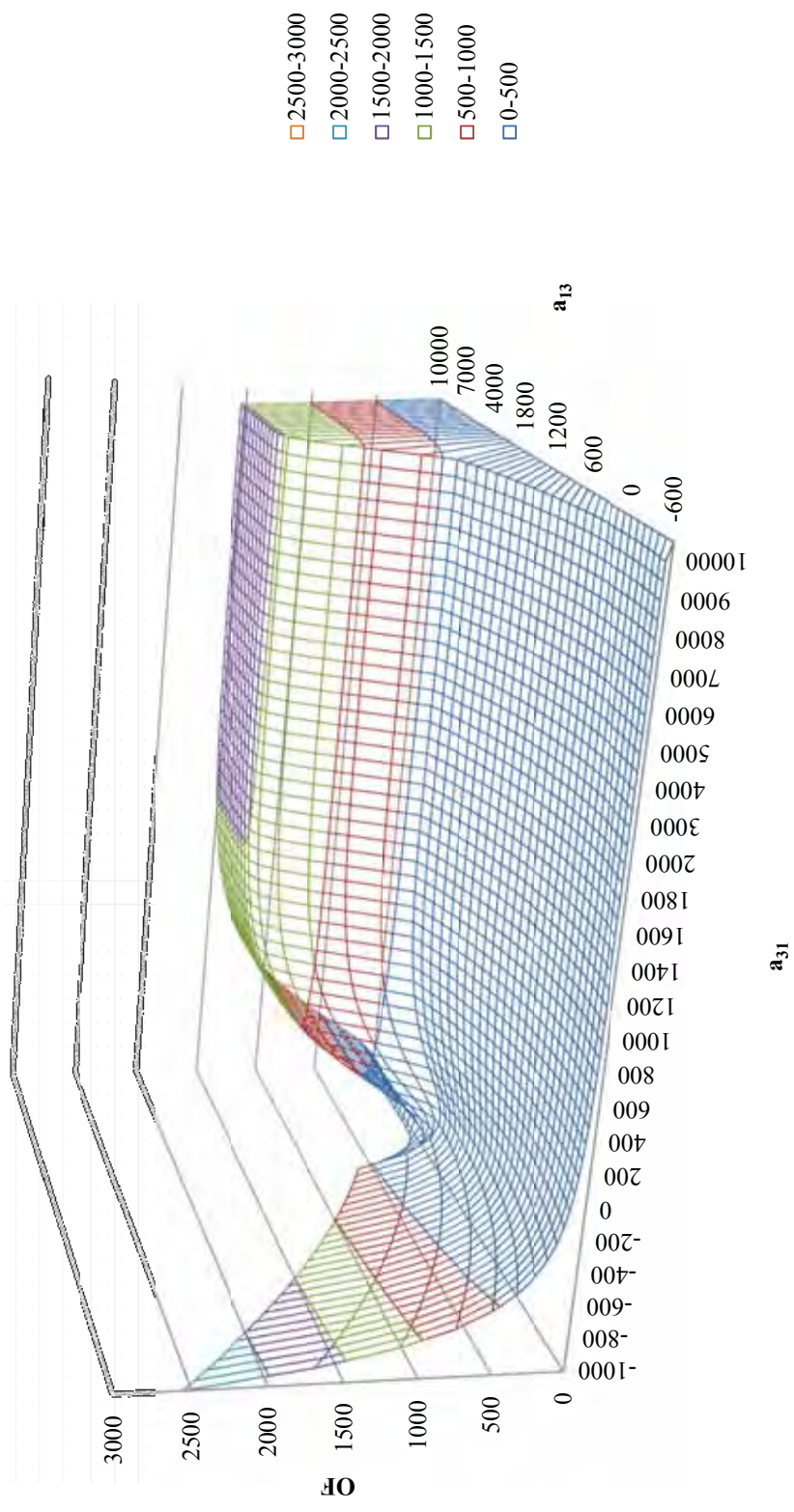


Figure 5.6: Sensitivity analysis conducted on subcritical water (1) - anthracene (3) system to obtain global minima [$a_{ji} = (u_{ji} - u_i)/R$]

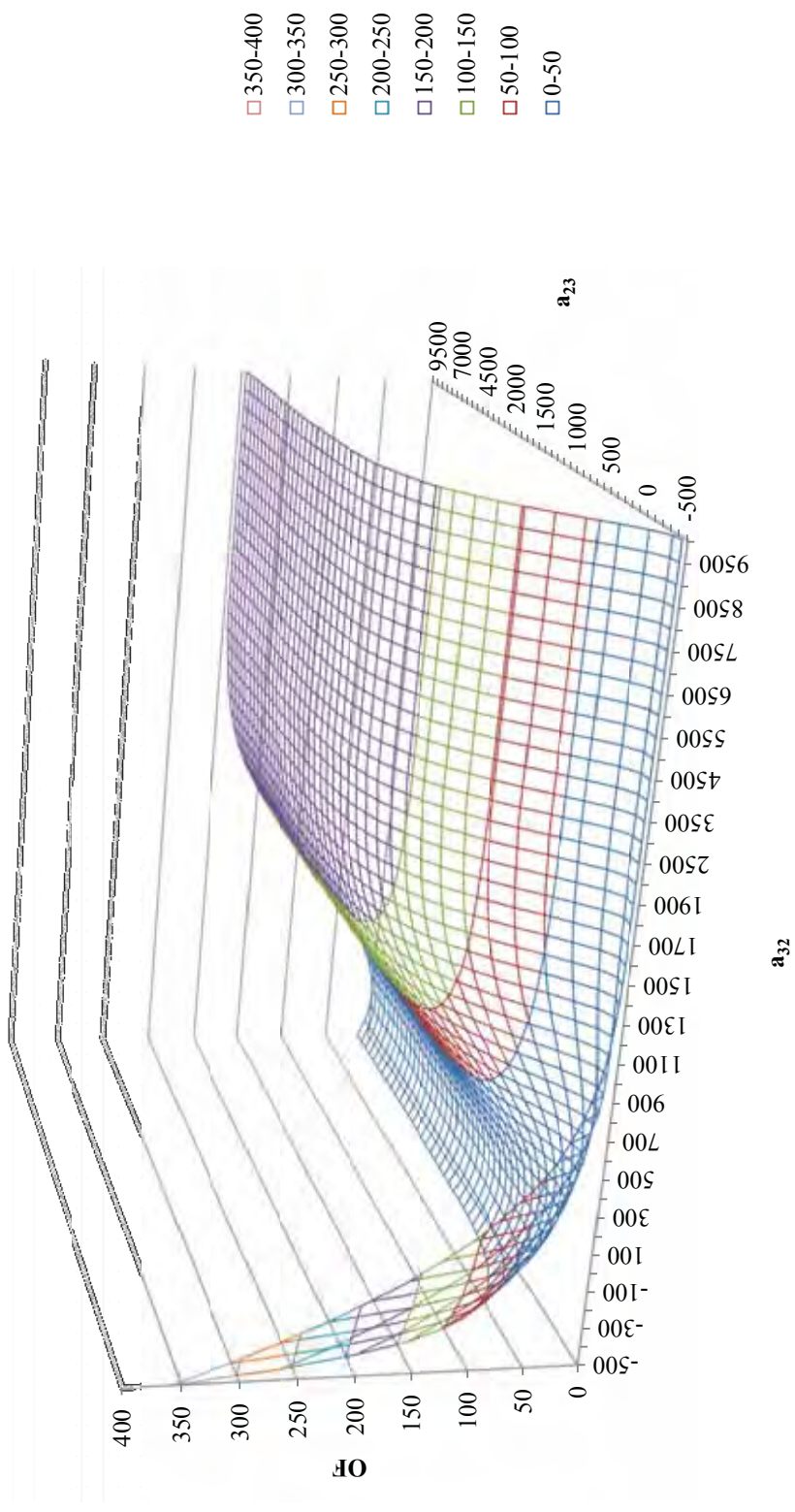


Figure 5.7: Sensitivity analysis conducted on subcritical ethanol (2) - anthracene (3) system to obtain global minima [$a_{ji} = (u_{ji} - u_{ii})/R$]

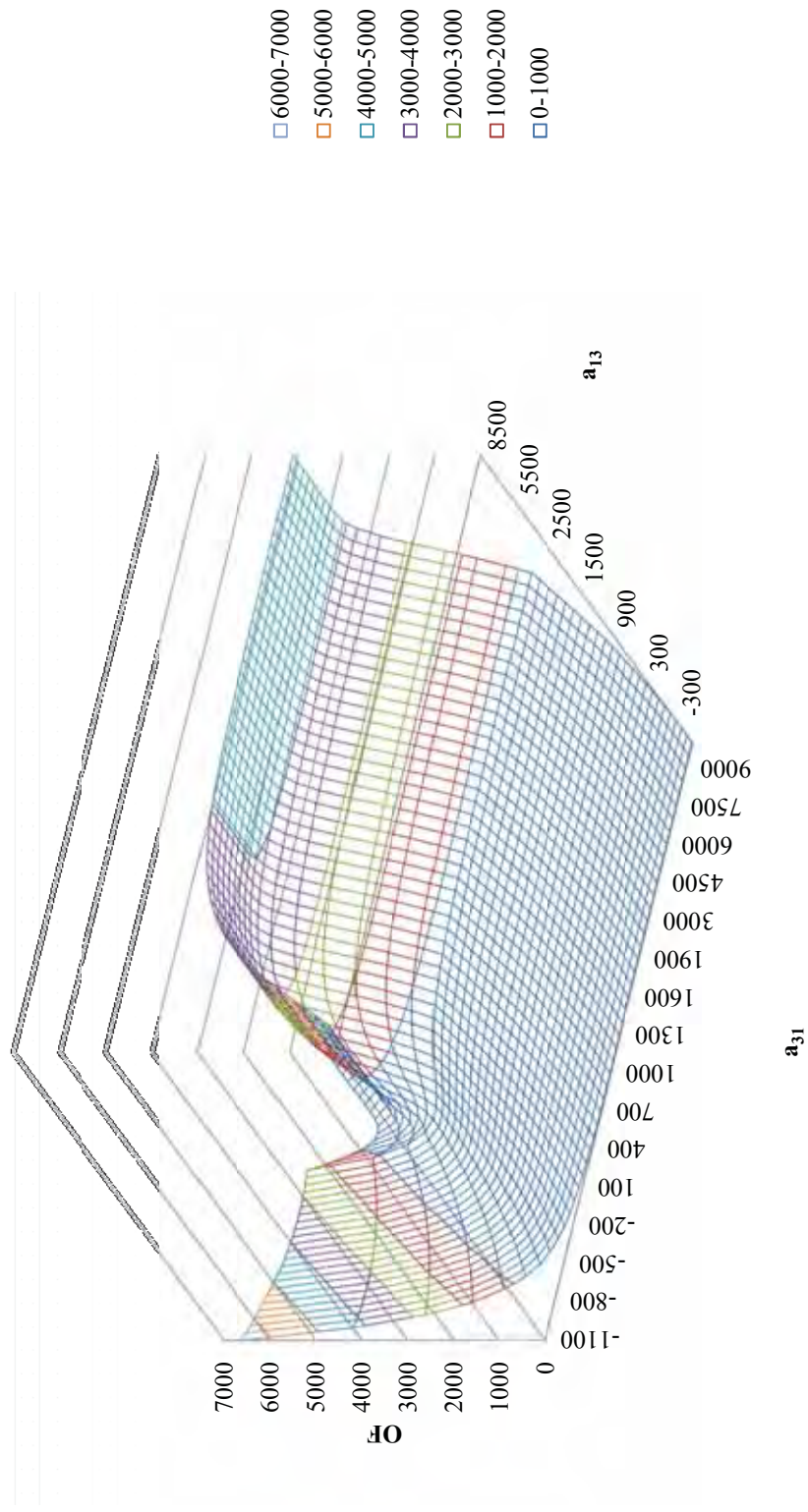


Figure 5.8: Sensitivity analysis conducted on subcritical water (1) - *p*-terphenyl (3) system to obtain global minima [$a_{ji} = (u_{ji} - u_{ii})/R$]

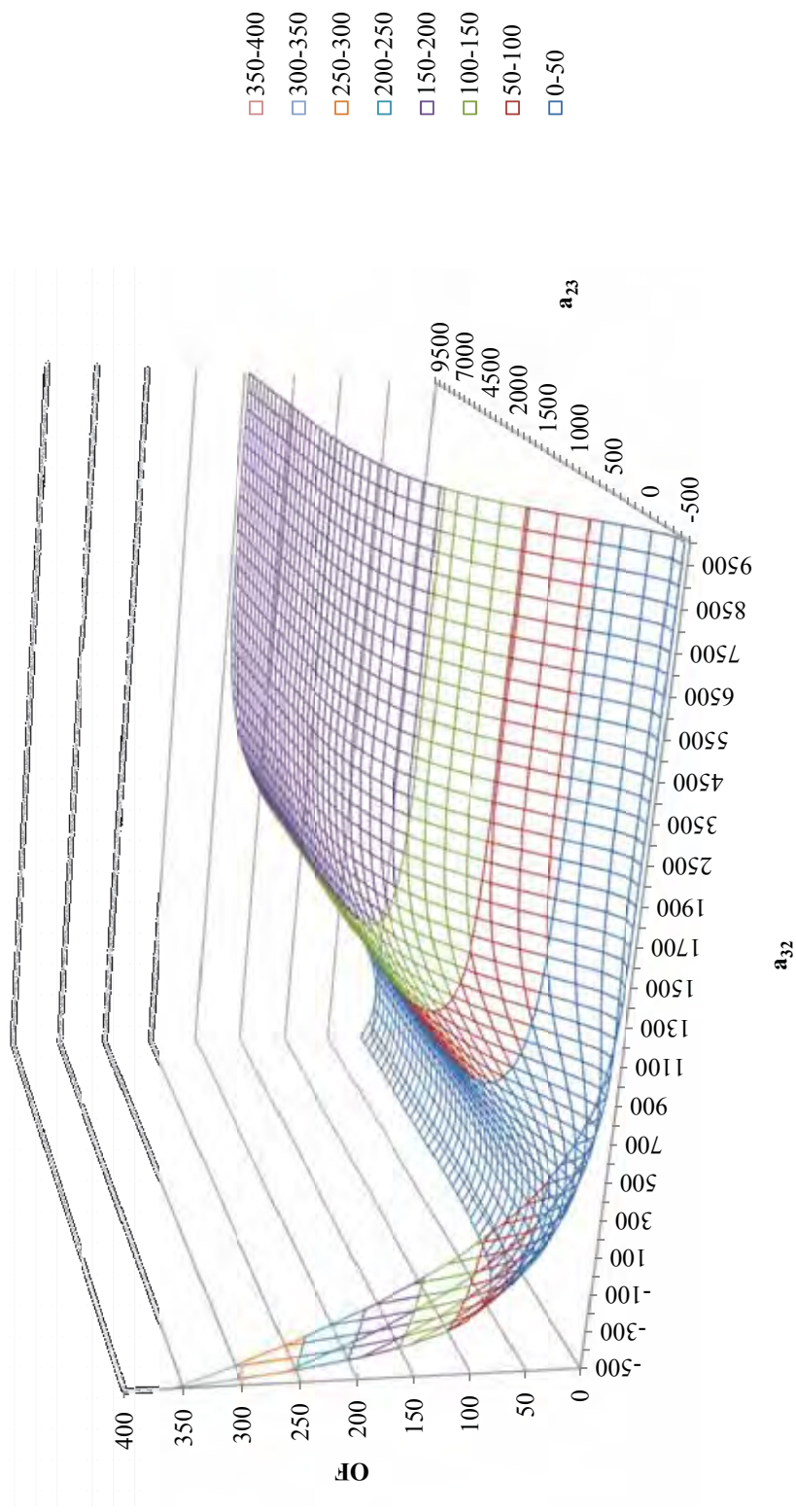


Figure 5.9: Sensitivity analysis conducted on subcritical ethanol (2) - *p*-terphenyl (3) system to obtain global minima [$a_{ji} = (u_{ji} - u_{ii})/R$]

Table 5.3: Values of a_{ij} for water (1) - ethanol (2) - PAH (3) systems obtained with $z = 10$ and $(u_{ji} - u_{ii})/R = a_{ji}$

	Anthracene	<i>p</i> -Terphenyl
a_{12}	368.6547	368.6547
a_{21}	-102.5521	-102.5521
a_{13}	389.2981	394.1085
a_{31}	-2.5598	-0.5681
a_{23}	-97.7478	225.6717
a_{32}	420.0203	-35.6459

When the single variable, a_{ij} was used, the resulting solubility and activity coefficients calculated from the UNIQUAC model was found to be a good fit for PAH-ethanol system, as observed in Figures 5.10 – 5.11. However, the UNIQUAC model, while yielding reasonable average absolute standard deviations for PAH-water systems, could not provide a fitting trend that reflects the rate of increase in PAHs solubility (Figures 5.12 – 5.13). Above 170 °C, the calculated values deviate substantially from experimental values. The deviations observed show that the parameter τ_{ji} given by $\tau_{ji} = \exp\left(-\frac{u_{ji}-u_{ii}}{RT}\right) = \exp\left(-\frac{a_{ji}}{T}\right)$ is not sufficiently represented by the a_{ji} variable. Indeed, a number of literature studies [20-22] have used a quadratic temperature function to better reflect the τ_{ji} relationship with temperature. Hence, when the fitted energy parameters, a_{ji} were extended to ternary systems consisting of PAH-water-ethanol, deviations that mirror the trend in the PAH-water systems were observed, as shown in Figures 5.14 – 5.17. It is also of interest to note that as the fraction of ethanol increased in the PAH-water-ethanol systems, deviations from experimental data also increased. Therefore, a quadratic temperature function was used in this study, giving rise to

$$\tau_{ji} = \exp\left(-\frac{u_{ji}-u_{ii}}{RT}\right) = \exp\left(-\frac{a_{ij}+b_{ij}T+c_{ij}T^2}{T}\right) \quad (5.39)$$

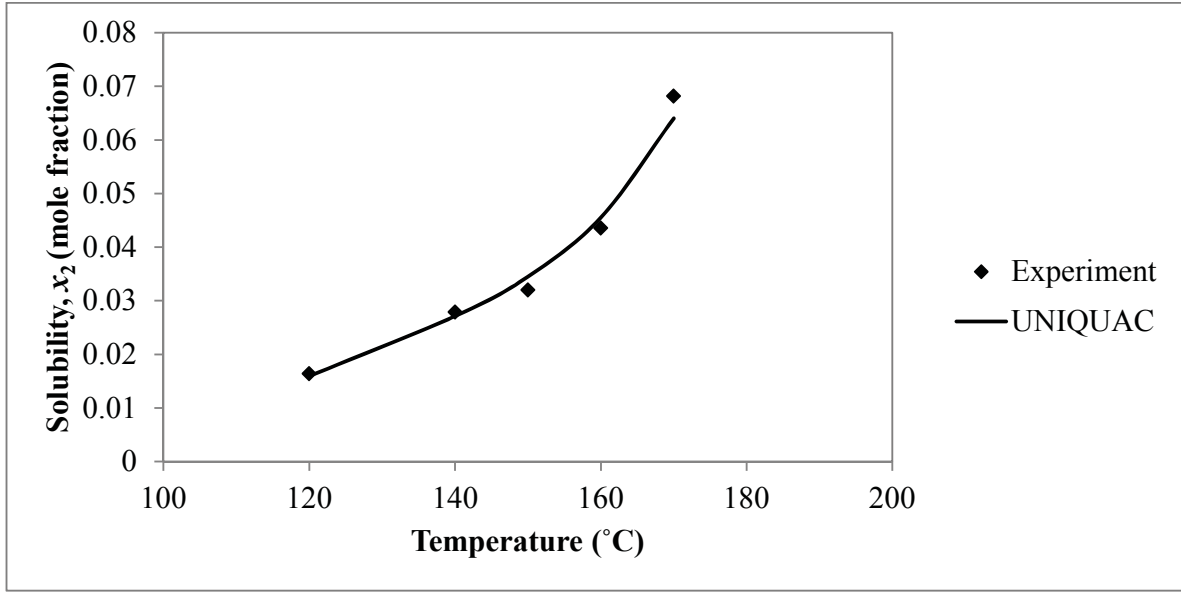


Figure 5.10: Experimental and UNIQUAC calculated solubility at various temperatures in ethanol (1) – anthracene (2) system with $(u_{ji} - u_{ii})/R = a_{ji}$

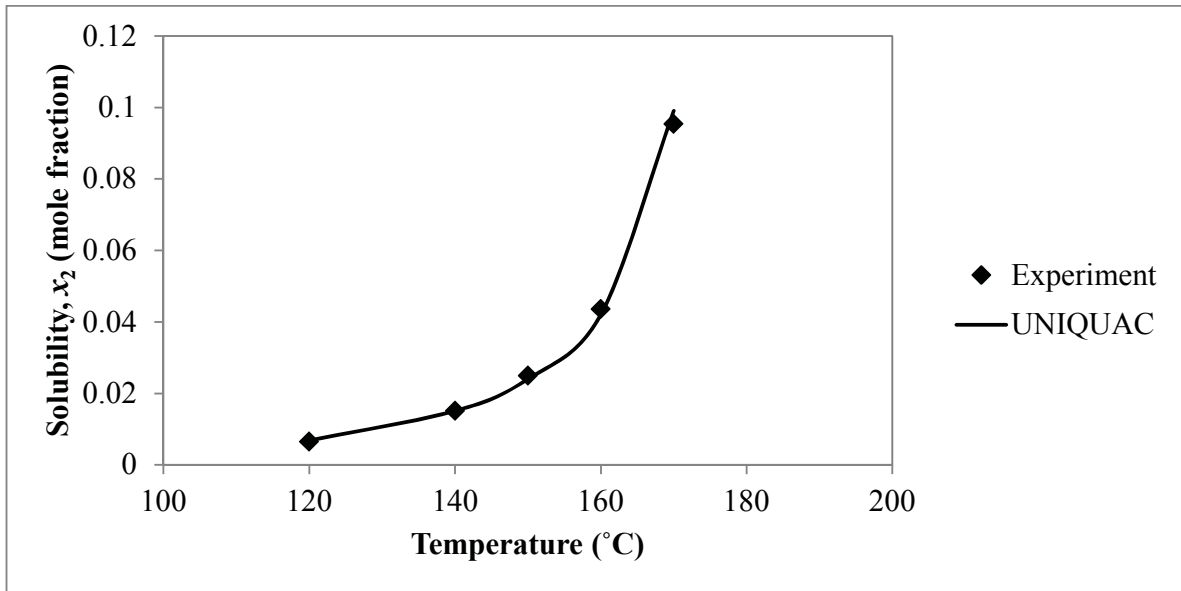


Figure 5.11: Experimental and UNIQUAC calculated solubility at various temperatures in ethanol (1) – *p*-terphenyl (2) system with $(u_{ji} - u_{ii})/R = a_{ji}$

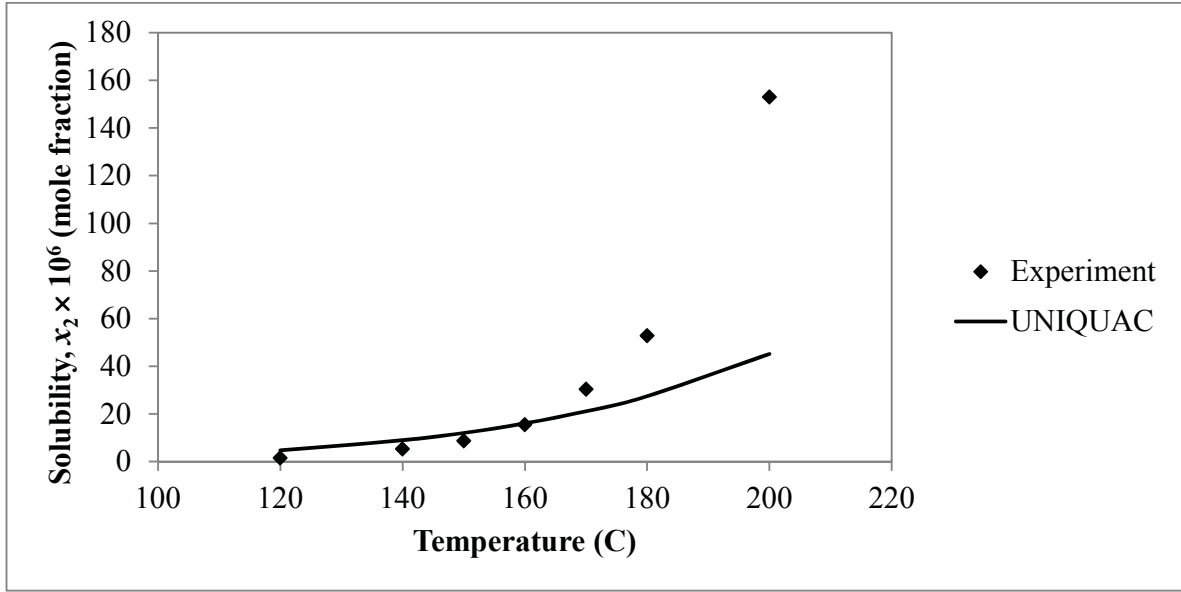


Figure 5.12: Experimental and UNIQUAC calculated solubility at various temperatures in water
(1) – anthracene (2) system with $(u_{ji} - u_{ii})/R = a_{ji}$

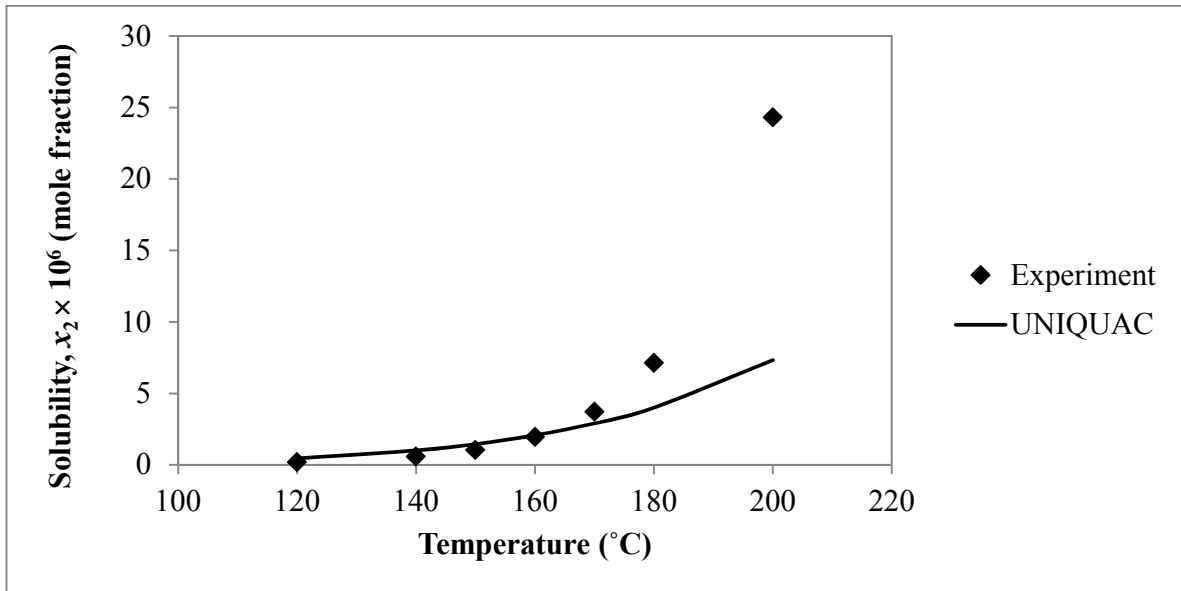


Figure 5.13: Experimental and UNIQUAC calculated solubility at various temperatures in water
(1) – *p*-terphenyl (2) system with $(u_{ji} - u_{ii})/R = a_{ji}$

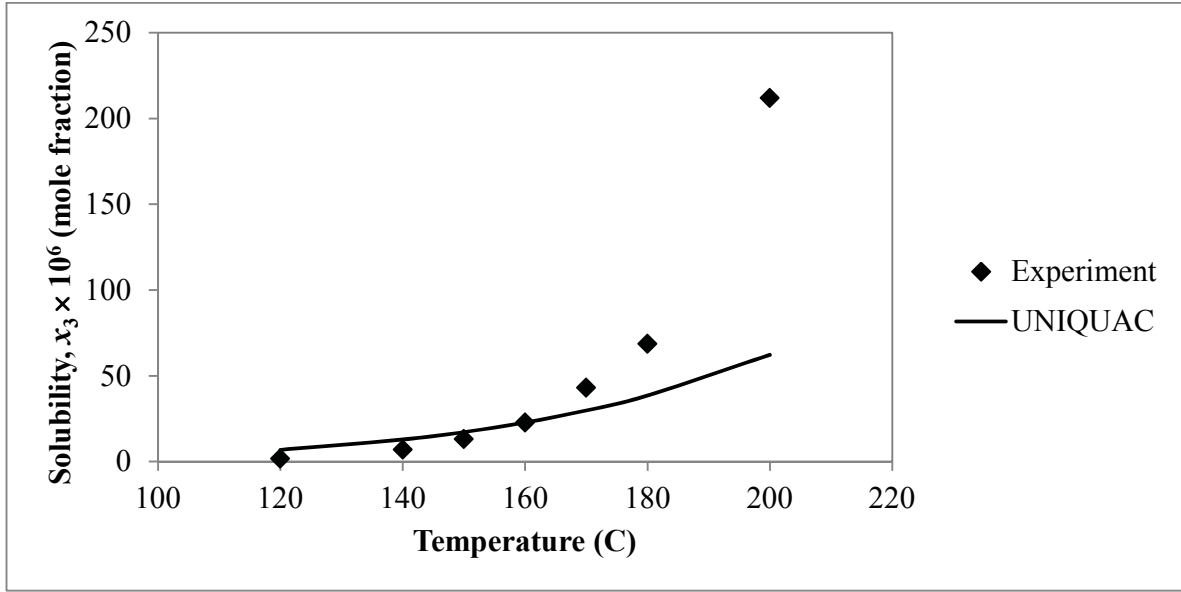


Figure 5.14: Experimental and UNIQUAC calculated solubility at various temperatures with $(u_{ji} - u_{ii})/R = a_{ji}$ in water (1) – ethanol (2) – anthracene (3) system, $f = 0.01$

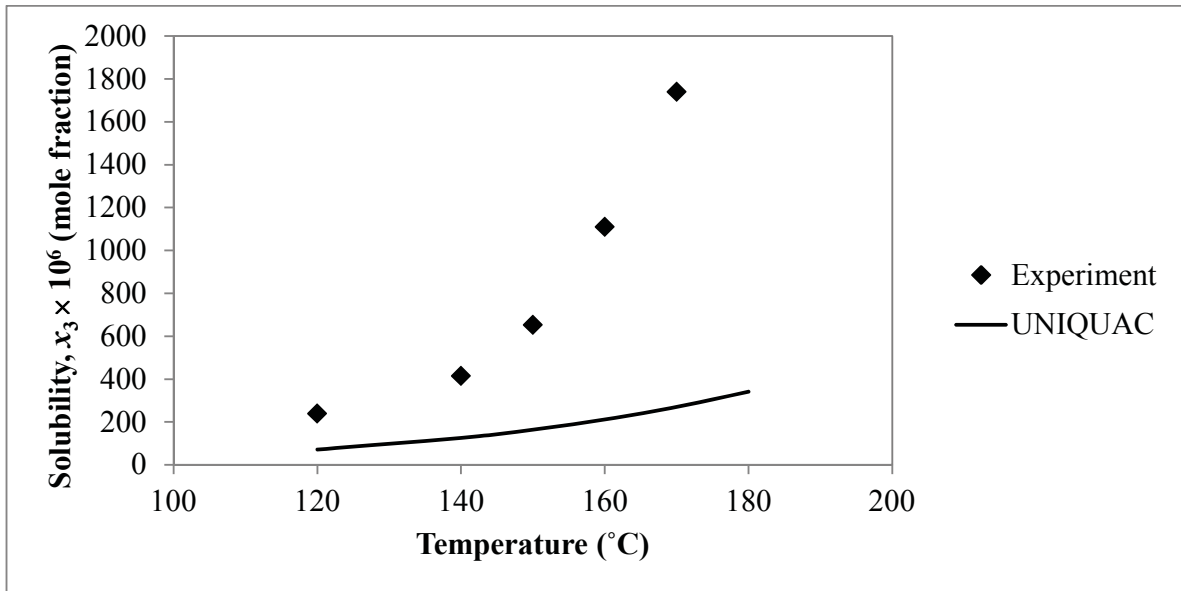


Figure 5.15: Experimental and UNIQUAC calculated solubility at various temperatures with $(u_{ji} - u_{ii})/R = a_{ji}$ in water (1) – ethanol (2) – anthracene (3) system, $f = 0.10$

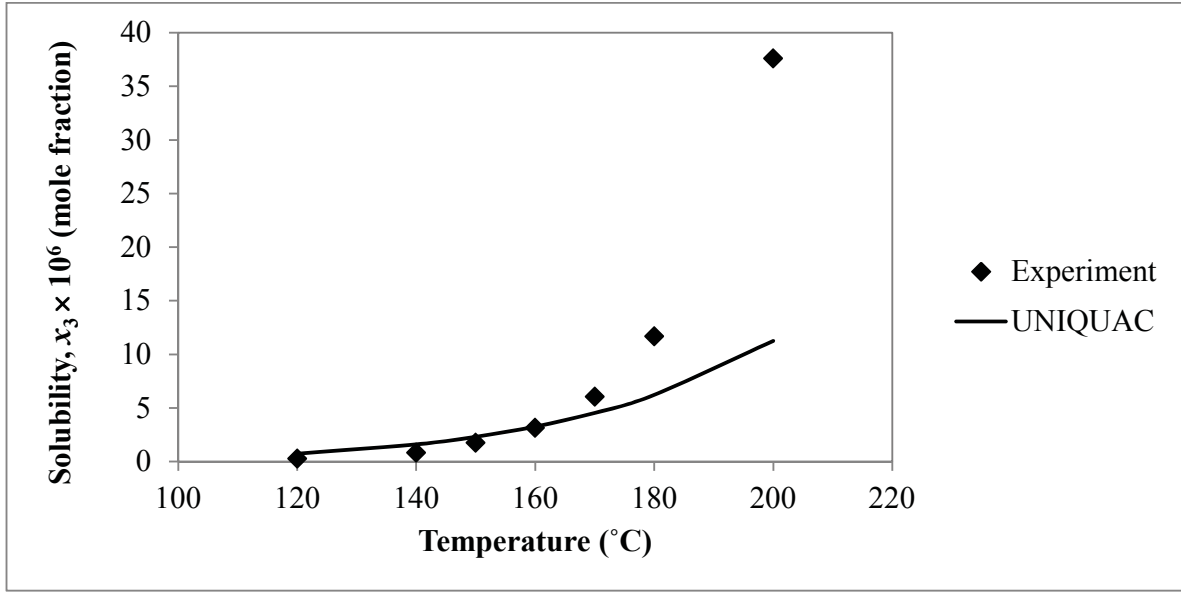


Figure 5.16: Experimental and UNIQUAC calculated solubility at various temperatures with $(u_{ji} - u_{ii})/R = a_{ji}$ in water (1) – ethanol (2) – *p*-terphenyl (3) system, $f = 0.01$

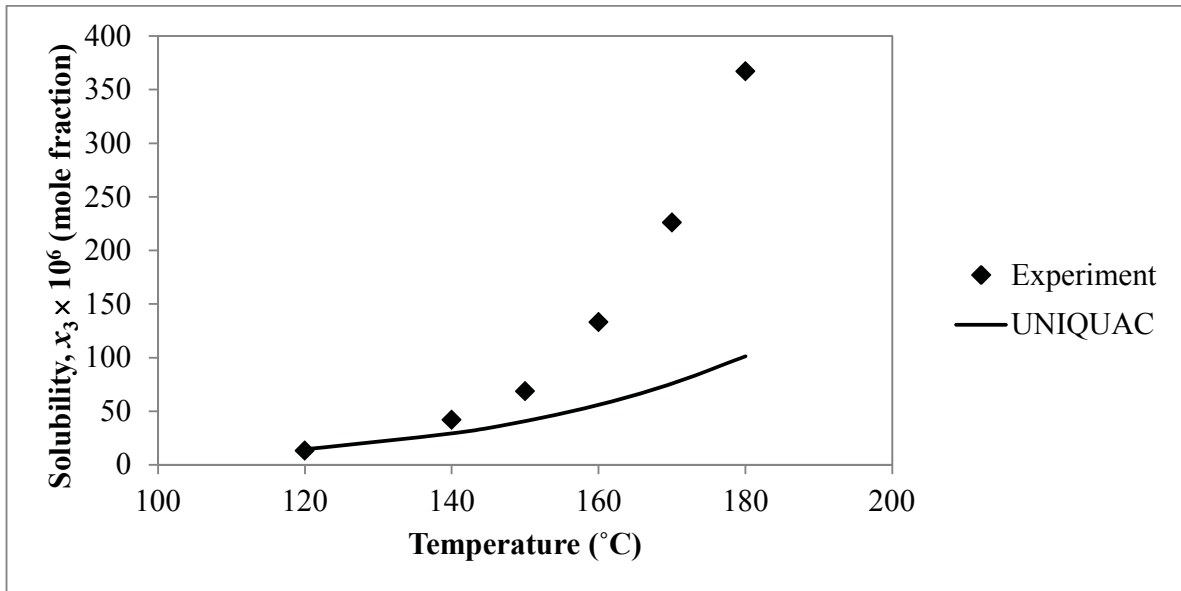


Figure 5.17: Experimental and UNIQUAC calculated solubility at various temperatures with $(u_{ji} - u_{ii})/R = a_{ji}$ in water (1) – ethanol (2) – *p*-terphenyl (3) system, $f = 0.10$

The a_{ij} , b_{ij} and c_{ij} values used in the quadratic temperature functions are shown in Table 5.4. The UNIQUAC model calculated solubility of anthracene and *p*-terphenyl in the various subcritical solvent systems investigated and their corresponding activity coefficients were compared with experimental values and are shown in Tables 5.5 – 5.12. Figures 5.18 – 5.25 show the experimental and calculated solubility of anthracene and *p*-terphenyl in subcritical water, subcritical ethanol and ethanol-modified subcritical water at $f = 0.01$ and $f = 0.10$. The UNIQUAC calculated values in combination with the quadratic temperature function can be seen to better reflect the solubility trends observed in the systems measured in this study.

The experimental activity coefficients were calculated from the truncated version of Equation (5.10), given by Equation (5.11). Both equations are reproduced in this section for easy reference.

$$\ln(x_2) = -\frac{\Delta H_f}{RT_{m2}}\left(\frac{T_{m2}}{T} - 1\right) + \frac{\Delta C_{P2}}{R}\left(\frac{T_{m2}}{T} - 1\right) + \frac{\Delta C_{P2}}{R}\ln\left(\frac{T}{T_{m2}}\right) - \int_{P_{sat}}^P \frac{V_2^L - V_2^S}{RT}dP - \ln \gamma_2 \quad (5.10)$$

$$\ln(x_2) = -\frac{\Delta H_f}{RT_{m2}}\left(\frac{T_{m2}}{T} - 1\right) - \ln \gamma_2 \quad (5.11)$$

A closer examination of Equation (5.10) found that the assumptions with regard to the cancellations between the second and the third term cannot be used, particularly when temperature is more than 100 °C below the melting point of the solid solute. Calculations of solubility/activity coefficient values found that the difference between the truncated version [Equation (5.11)] and Equation (5.10) was 0.06 % at 200 °C, 5 % at 140 C, and 10 % at 120 °C. It is expected that the further the temperature of the system is from the melting point of the solute, the bigger the difference is between the values calculated by the two equations. The truncated version was used in this study as the differences in the values obtained were considered to be small within the range of temperature investigated. However, had the temperatures investigated been more that 100 °C below the melting temperatures of the PAHs, Equation (5.10) would have to be employed.

The ability of the UNIQUAC model to calculate PAHs solubility in the ethanol-modified systems was found to deviate further from experimental values as the fraction of ethanol increases. However, the average standard deviations of the UNIQUAC calculated values were well within 7% of experimental values. The deviations between UNIQUAC calculated and

experimental data are shown in Figures 5.26 – 5.27 given by a plot of $\ln(x^{\text{cal}})$ versus $\ln(x^{\text{exp}})$. The predictive ability of a thermodynamic model is considered more accurate if the plotted data points are located nearer to the best fit line. Hence, it can be concluded that the UNIQUAC model can predict very well the solubilities of the ternary systems containing ethanol. Diagrams comparing the experimental and UNIQUAC calculated solubilities for all compounds and at all conditions are shown in later sections together for comparisons with other thermodynamic models.

Table 5.4: The a_{ij} , b_{ij} , and c_{ij} values in water (1) - ethanol (2) - PAH (3) systems obtained with $z = 10$ and $[(u_{ji} - u_{ii})/R = a_{ij} + b_{ij}T + c_{ij}T^2]$

	Anthracene	<i>p</i> -Terphenyl
a_{12}	368.6547	368.6547
a_{21}	-102.5521	-102.5521
a_{13}	389.2981	394.1085
a_{31}	-2.5598	-0.5681
a_{23}	-97.7478	225.6717
a_{32}	420.0203	-35.6459
b_{12}	0	0
b_{21}	0	0
b_{13}	1.4879	1.2796
b_{31}	0.8981	0.5100
b_{23}	0.3158	0.5530
b_{32}	-0.3389	-0.2773
c_{12}	0	0
c_{21}	0	0
c_{13}	-0.0025	-0.0026
c_{31}	-0.0028	-0.0015
c_{23}	-0.0012	-0.0018
c_{32}	0.0023	0.0012

Table 5.5: Experimental and UNIQUAC calculated solubility data and the corresponding activity coefficients for binary water (1) - anthracene (2) system

T (°C)	x_2^{exp}	x_2^{UNIQUAC}	γ_2^{exp}	$\gamma_2^{\text{UNIQUAC}}$	ASD (%)
120	$(1.59 \pm 0.04) \times 10^{-6}$	1.57×10^{-6}	1.09×10^5	1.11×10^5	0.11
140	$(5.34 \pm 0.09) \times 10^{-6}$	5.18×10^{-6}	4.98×10^4	5.13×10^4	0.24
150	$(8.75 \pm 0.24) \times 10^{-6}$	9.29×10^{-6}	3.71×10^4	3.50×10^4	0.51
160	$(1.55 \pm 0.03) \times 10^{-5}$	1.65×10^{-5}	2.53×10^4	2.38×10^4	0.56
170	$(3.04 \pm 0.16) \times 10^{-5}$	2.91×10^{-5}	1.55×10^4	1.62×10^4	0.42
180	$(5.29 \pm 0.10) \times 10^{-5}$	5.10×10^{-5}	1.06×10^4	1.10×10^4	0.36
200	$(1.53 \pm 0.01) \times 10^{-4}$	1.55×10^{-4}	5.07×10^3	5.00×10^3	0.16
Average					0.34

Note: $\text{ASD}(\%) = \left| \frac{\ln(x_2^{\text{exp}}) - \ln(x_2^{\text{calc}})}{\ln(x_2^{\text{exp}})} \right| \times 100$

Table 5.6: Experimental and UNIQUAC calculated solubility data and the corresponding activity coefficients for binary water (1) - *p*-terphenyl (2) system

T (°C)	x_2^{exp}	x_2^{UNIQUAC}	γ_2^{exp}	$\gamma_2^{\text{UNIQUAC}}$	ASD (%)
120	$(1.95 \pm 0.08) \times 10^{-7}$	1.64×10^{-7}	7.28×10^5	8.65×10^5	1.11
140	$(5.90 \pm 0.05) \times 10^{-7}$	6.12×10^{-7}	3.96×10^5	3.82×10^5	0.25
150	$(1.05 \pm 0.03) \times 10^{-6}$	1.15×10^{-6}	2.81×10^5	2.56×10^5	0.66
160	$(1.96 \pm 0.06) \times 10^{-6}$	2.13×10^{-6}	1.88×10^5	1.73×10^5	0.64
170	$(3.71 \pm 0.12) \times 10^{-6}$	3.89×10^{-6}	1.22×10^5	1.17×10^5	0.39
180	$(7.14 \pm 0.24) \times 10^{-6}$	7.02×10^{-6}	7.78×10^4	7.91×10^4	0.14
200	$(2.43 \pm 0.03) \times 10^{-5}$	2.21×10^{-5}	3.34×10^4	3.67×10^4	0.90
Average					0.58

Table 5.7: Experimental and UNIQUAC calculated solubility data and the corresponding activity coefficients for binary ethanol (1) - anthracene (2) system

T (°C)	x_2^{exp}	x_2^{UNIQUAC}	γ_2^{exp}	$\gamma_2^{\text{UNIQUAC}}$	ASD (%)
120	$(1.64 \pm 0.05) \times 10^{-2}$	1.58×10^{-2}	10.56	10.98	0.94
140	$(2.79 \pm 0.13) \times 10^{-2}$	2.72×10^{-2}	9.54	9.77	0.69
150	$(3.20 \pm 0.16) \times 10^{-2}$	3.49×10^{-2}	10.15	9.32	2.49
160	$(4.36 \pm 0.19) \times 10^{-2}$	4.59×10^{-2}	9.01	8.56	1.62
170	$(6.82 \pm 0.18) \times 10^{-2}$	6.33×10^{-2}	6.91	7.44	2.77
Average					1.70

Table 5.8: Experimental and UNIQUAC calculated solubility data and the corresponding activity coefficients for binary ethanol (1) - *p*-terphenyl (2) system

T (°C)	x_2^{exp}	x_2^{UNIQUAC}	γ_2^{exp}	$\gamma_2^{\text{UNIQUAC}}$	ASD (%)
120	$(6.55 \pm 0.13) \times 10^{-3}$	6.48×10^{-3}	21.67	21.91	0.22
140	$(1.51 \pm 0.05) \times 10^{-2}$	1.54×10^{-2}	15.48	15.15	0.51
150	$(2.50 \pm 0.03) \times 10^{-2}$	2.49×10^{-2}	11.79	11.82	0.07
160	$(4.36 \pm 0.06) \times 10^{-2}$	4.33×10^{-2}	8.43	8.50	0.25
170	$(9.54 \pm 0.20) \times 10^{-2}$	9.60×10^{-2}	4.76	4.73	0.26
Average					0.26

Table 5.9: Experimental and UNIQUAC calculated solubility data and the corresponding activity coefficients for ternary water (1) – ethanol (2) – anthracene (3) systems [$f = 0.01-0.03$]

T (°C)	f_2	x_3^{exp}	x_3^{UNIQUAC}	γ_3^{exp}	$\gamma_3^{\text{UNIQUAC}}$	ASD (%)
120	0.01	$(1.69 \pm 0.04) \times 10^{-6}$	2.72×10^{-6}	1.02×10^5	6.36×10^4	3.59
140		$(7.03 \pm 0.02) \times 10^{-6}$	8.60×10^{-6}	3.78×10^4	3.09×10^4	1.70
150		$(1.32 \pm 0.03) \times 10^{-5}$	1.51×10^{-5}	2.46×10^4	2.15×10^4	1.19
160		$(2.28 \pm 0.04) \times 10^{-5}$	2.63×10^{-5}	1.72×10^4	1.50×10^4	1.33
170		$(4.32 \pm 0.11) \times 10^{-5}$	4.55×10^{-5}	1.09×10^4	1.04×10^4	0.51
180		$(6.87 \pm 0.29) \times 10^{-5}$	7.83×10^{-5}	8.16×10^3	7.16×10^3	1.37
200		$(2.12 \pm 0.06) \times 10^{-4}$	2.31×10^{-4}	3.66×10^3	3.36×10^3	1.01
Average						1.53
120	0.02	$(2.45 \pm 0.12) \times 10^{-6}$	4.49×10^{-6}	7.07×10^4	3.85×10^4	4.70
140		$(9.72 \pm 0.29) \times 10^{-6}$	1.36×10^{-5}	2.74×10^4	1.95×10^4	2.94
150		$(1.76 \pm 0.06) \times 10^{-5}$	2.35×10^{-5}	1.85×10^4	1.38×10^4	2.64
160		$(3.20 \pm 0.10) \times 10^{-5}$	4.02×10^{-5}	1.23×10^4	9.77×10^3	2.21
170		$(5.85 \pm 0.19) \times 10^{-5}$	6.85×10^{-5}	8.05×10^3	6.88×10^3	1.62
180		$(1.07 \pm 0.03) \times 10^{-4}$	1.16×10^{-4}	5.24×10^3	4.82×10^3	0.90
200		$(2.89 \pm 0.10) \times 10^{-4}$	3.34×10^{-4}	2.69×10^3	2.32×10^3	1.77
Average						2.40
120	0.03	$(5.15 \pm 0.08) \times 10^{-6}$	7.09×10^{-6}	3.36×10^4	2.44×10^4	2.63
140		$(1.67 \pm 0.06) \times 10^{-5}$	2.08×10^{-5}	1.59×10^4	1.28×10^4	2.01
150		$(2.66 \pm 0.07) \times 10^{-5}$	3.53×10^{-5}	1.22×10^4	9.20×10^3	2.69
160		$(4.96 \pm 0.18) \times 10^{-5}$	5.95×10^{-5}	7.92×10^3	6.60×10^3	1.84
170		$(8.13 \pm 0.02) \times 10^{-5}$	9.99×10^{-5}	5.80×10^3	4.72×10^3	2.19
180		$(1.47 \pm 0.07) \times 10^{-4}$	1.67×10^{-4}	3.81×10^3	3.35×10^3	1.46
200		$(3.89 \pm 0.13) \times 10^{-4}$	4.70×10^{-4}	2.00×10^3	1.65×10^3	2.41
Average						2.18

Table 5.10: Experimental and UNIQUAC calculated solubility data and the corresponding activity coefficients for ternary water (1) – ethanol (2) – anthracene (3) systems [$f = 0.04$ - 0.06]

T (°C)	f_2	x_3^{exp}	x_3^{UNIQUAC}	γ_3^{exp}	$\gamma_3^{\text{UNIQUAC}}$	ASD (%)
120	0.04	$(6.43 \pm 0.11) \times 10^{-6}$	1.08×10^{-5}	2.69×10^4	2.69×10^4	4.32
140		$(2.23 \pm 0.04) \times 10^{-5}$	3.07×10^{-5}	1.19×10^4	1.19×10^4	2.99
150		$(3.63 \pm 0.10) \times 10^{-5}$	5.14×10^{-5}	8.95×10^3	8.95×10^3	3.40
160		$(6.25 \pm 0.04) \times 10^{-5}$	8.54×10^{-5}	6.29×10^3	6.29×10^3	3.23
170		$(1.09 \pm 0.01) \times 10^{-4}$	1.42×10^{-4}	4.32×10^3	4.32×10^3	2.87
180		$(2.09 \pm 0.06) \times 10^{-4}$	2.35×10^{-4}	2.68×10^3	2.68×10^3	1.36
200		$(4.91 \pm 0.13) \times 10^{-4}$	6.47×10^{-4}	1.58×10^3	1.58×10^3	3.63
Average						3.12
120	0.06	$(1.53 \pm 0.06) \times 10^{-5}$	2.26×10^{-5}	1.13×10^4	7.65×10^3	3.53
140		$(4.54 \pm 0.19) \times 10^{-5}$	6.14×10^{-5}	5.86×10^3	4.33×10^3	3.02
150		$(7.72 \pm 0.24) \times 10^{-5}$	1.00×10^{-4}	4.21×10^3	3.24×10^3	2.76
160		$(1.19 \pm 0.06) \times 10^{-4}$	1.63×10^{-4}	3.30×10^3	2.41×10^3	3.50
170		$(2.06 \pm 0.09) \times 10^{-4}$	2.65×10^{-4}	2.29×10^3	1.78×10^3	2.98
180		$(3.29 \pm 0.10) \times 10^{-4}$	4.31×10^{-4}	1.70×10^3	1.30×10^3	3.37
Average						3.19
120	0.10	$(9.09 \pm 0.11) \times 10^{-5}$	7.47×10^{-5}	1.90×10^3	2.32×10^3	2.11
140		$(2.39 \pm 0.05) \times 10^{-4}$	1.89×10^{-4}	1.41×10^3	1.41×10^3	2.84
150		$(4.14 \pm 0.10) \times 10^{-4}$	2.98×10^{-4}	7.84×10^2	1.09×10^3	4.22
160		$(6.52 \pm 0.01) \times 10^{-4}$	4.70×10^{-4}	6.03×10^2	8.35×10^2	4.45
170		$(1.11 \pm 0.00) \times 10^{-3}$	7.43×10^{-4}	4.24×10^2	6.34×10^2	5.89
180		$(1.74 \pm 0.03) \times 10^{-3}$	1.18×10^{-3}	3.22×10^2	4.74×10^2	6.09
Average						4.27

Table 5.11: Experimental and UNIQUAC calculated solubility data and the corresponding activity coefficients for ternary water (1) – ethanol (2) – *p*-terphenyl (3) systems [$f = 0.01$ - 0.03]

T (°C)	f_2	x_3^{exp}	x_3^{UNIQUAC}	γ_3^{exp}	$\gamma_3^{\text{UNIQUAC}}$	ASD (%)
120	0.01	$(2.81 \pm 0.02) \times 10^{-7}$	2.75×10^{-7}	5.05×10^5	5.16×10^5	0.86
140		$(8.40 \pm 0.17) \times 10^{-7}$	9.95×10^{-7}	2.78×10^5	2.35×10^5	6.71
150		$(1.75 \pm 0.08) \times 10^{-6}$	1.85×10^{-6}	1.68×10^5	1.60×10^5	2.19
160		$(3.15 \pm 0.13) \times 10^{-6}$	3.38×10^{-6}	1.17×10^5	1.09×10^5	2.88
170		$(6.05 \pm 0.02) \times 10^{-6}$	6.10×10^{-6}	7.51×10^4	7.44×10^4	0.07
180		$(1.17 \pm 0.06) \times 10^{-5}$	1.09×10^{-5}	4.75×10^4	5.11×10^4	0.64
200		$(3.76 \pm 0.09) \times 10^{-5}$	3.35×10^{-5}	2.16×10^4	2.42×10^4	1.13
Average						2.07
120	0.02	$(4.72 \pm 0.08) \times 10^{-7}$	3.41×10^{-7}	3.01×10^5	4.16×10^5	2.23
140		$(1.33 \pm 0.01) \times 10^{-6}$	9.46×10^{-7}	1.76×10^5	2.47×10^5	2.52
150		$(2.39 \pm 0.09) \times 10^{-6}$	1.54×10^{-6}	1.23×10^5	1.91×10^5	3.39
160		$(4.77 \pm 0.09) \times 10^{-6}$	2.48×10^{-6}	7.71×10^4	1.48×10^5	5.34
170		$(7.63 \pm 0.20) \times 10^{-6}$	3.94×10^{-6}	5.95×10^4	1.15×10^5	5.61
180		$(1.65 \pm 0.06) \times 10^{-5}$	6.20×10^{-6}	3.37×10^4	8.97×10^4	8.89
Average						4.66
120	0.03	$(5.80 \pm 0.09) \times 10^{-7}$	7.00×10^{-7}	2.45×10^5	2.03×10^5	1.31
140		$(2.28 \pm 0.02) \times 10^{-6}$	2.41×10^{-6}	1.03×10^5	9.69×10^4	0.44
150		$(4.15 \pm 0.04) \times 10^{-6}$	4.38×10^{-6}	7.10×10^4	6.73×10^4	0.43
160		$(7.36 \pm 0.07) \times 10^{-6}$	7.83×10^{-6}	5.00×10^4	4.69×10^4	0.53
170		$(1.35 \pm 0.01) \times 10^{-5}$	1.38×10^{-5}	3.36×10^4	3.28×10^4	0.23
180		$(2.41 \pm 0.08) \times 10^{-5}$	2.42×10^{-5}	2.31×10^4	2.30×10^4	0.04
Average						0.50

Table 5.12: Experimental and UNIQUAC calculated solubility data and the corresponding activity coefficients for ternary water (1) – ethanol (2) – *p*-terphenyl (3) systems [$f = 0.04$ -0.06]

T (°C)	f_2	x_3^{exp}	x_3^{UNIQUAC}	γ_3^{exp}	$\gamma_3^{\text{UNIQUAC}}$	ASD (%)
120	0.04	$(9.62 \pm 0.41) \times 10^{-7}$	1.07×10^{-6}	1.48×10^5	1.32×10^5	0.78
140		$(3.08 \pm 0.15) \times 10^{-6}$	3.61×10^{-6}	7.59×10^4	6.47×10^4	1.26
150		$(5.47 \pm 0.00) \times 10^{-6}$	6.49×10^{-6}	5.39×10^4	4.54×10^4	1.41
160		$(1.05 \pm 0.04) \times 10^{-5}$	1.15×10^{-5}	3.50×10^4	3.20×10^4	0.79
170		$(2.13 \pm 0.02) \times 10^{-5}$	2.01×10^{-5}	2.13×10^4	2.26×10^4	0.53
180		$(3.34 \pm 0.15) \times 10^{-5}$	3.49×10^{-5}	1.66×10^4	1.59×10^4	0.42
Average						0.86
120	0.06	$(2.07 \pm 0.05) \times 10^{-6}$	2.33×10^{-6}	6.86×10^4	6.09×10^4	0.90
140		$(6.72 \pm 0.03) \times 10^{-6}$	7.55×10^{-6}	3.48×10^4	3.09×10^4	0.98
150		$(1.25 \pm 0.01) \times 10^{-5}$	1.33×10^{-5}	2.36×10^4	2.21×10^4	0.56
160		$(2.25 \pm 0.09) \times 10^{-5}$	2.32×10^{-5}	1.63×10^4	1.59×10^4	0.28
170		$(4.28 \pm 0.07) \times 10^{-5}$	4.00×10^{-5}	1.06×10^4	1.14×10^4	0.68
180		$(7.29 \pm 0.31) \times 10^{-5}$	6.82×10^{-5}	7.62×10^3	8.15×10^3	0.70
Average						0.69
120	0.10	$(1.34 \pm 0.06) \times 10^{-5}$	8.61×10^{-6}	1.06×10^4	1.65×10^4	3.95
140		$(4.19 \pm 0.12) \times 10^{-5}$	2.62×10^{-5}	5.58×10^3	8.91×10^3	4.64
150		$(6.87 \pm 0.07) \times 10^{-5}$	4.50×10^{-5}	4.29×10^3	6.56×10^3	4.42
160		$(1.33 \pm 0.03) \times 10^{-4}$	7.62×10^{-5}	2.76×10^3	4.83×10^3	6.24
170		$(2.26 \pm 0.03) \times 10^{-4}$	1.28×10^{-4}	2.01×10^3	3.55×10^3	6.77
180		$(3.67 \pm 0.07) \times 10^{-4}$	2.13×10^{-4}	1.51×10^3	2.60×10^3	6.85
Average						5.48

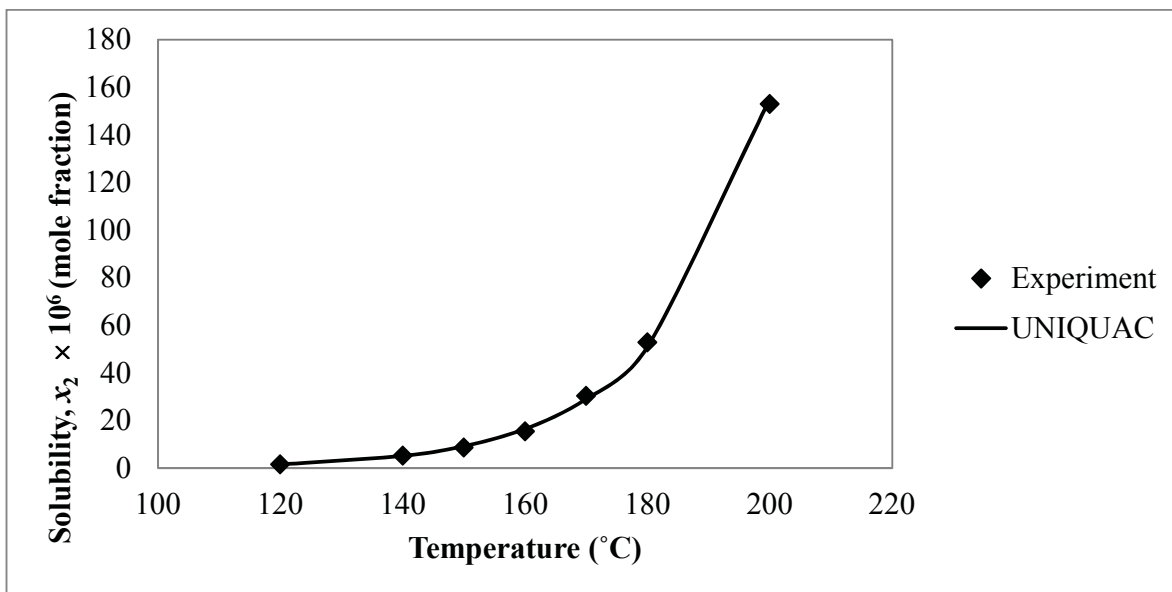


Figure 5.18: Experimental and UNIQUAC calculated solubility as a function of temperature in subcritical water (1) – anthracene (2) system

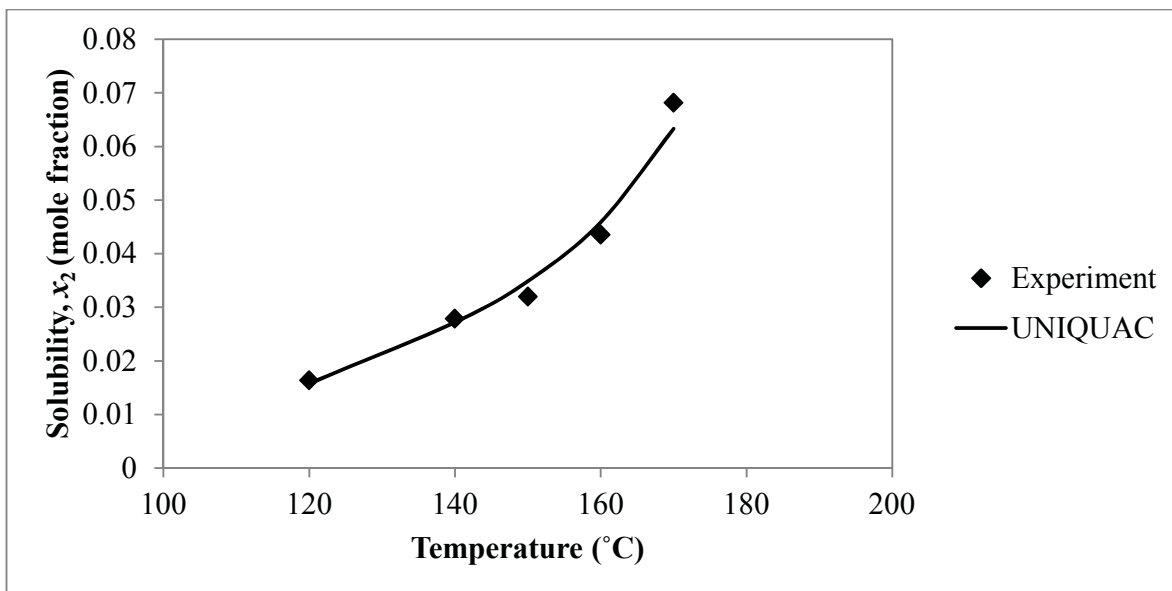


Figure 5.19: Experimental and UNIQUAC calculated solubility as a function of temperature in subcritical ethanol (1) – anthracene (2) system

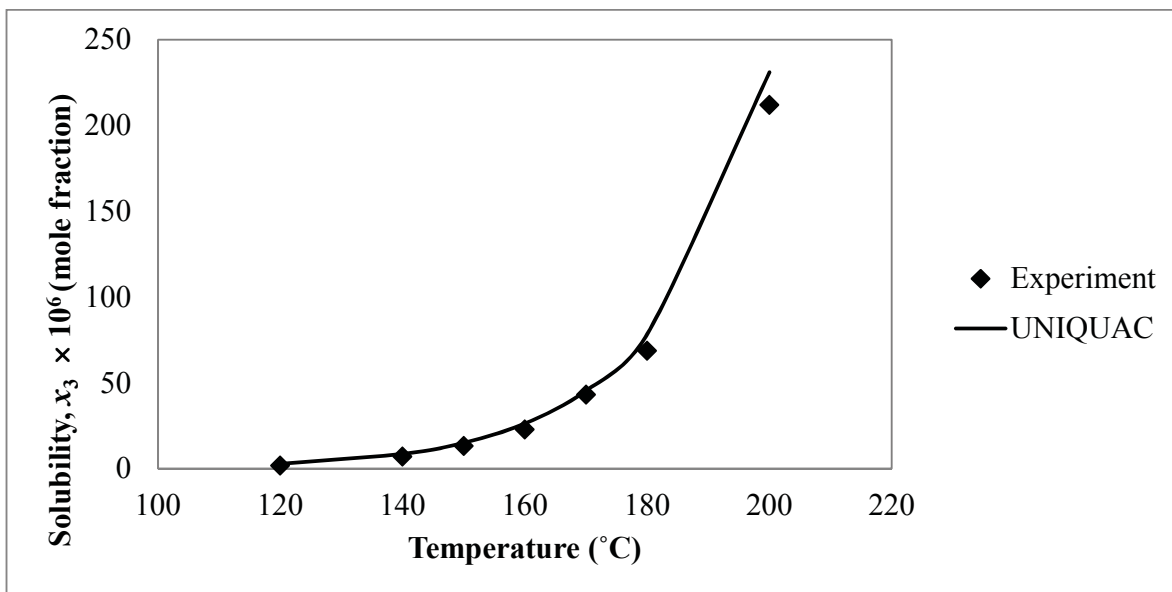


Figure 5.20: Experimental and UNIQUAC calculated solubility as a function of temperature in subcritical water (1) – ethanol (2) – anthracene (3) system, $f = 0.01$

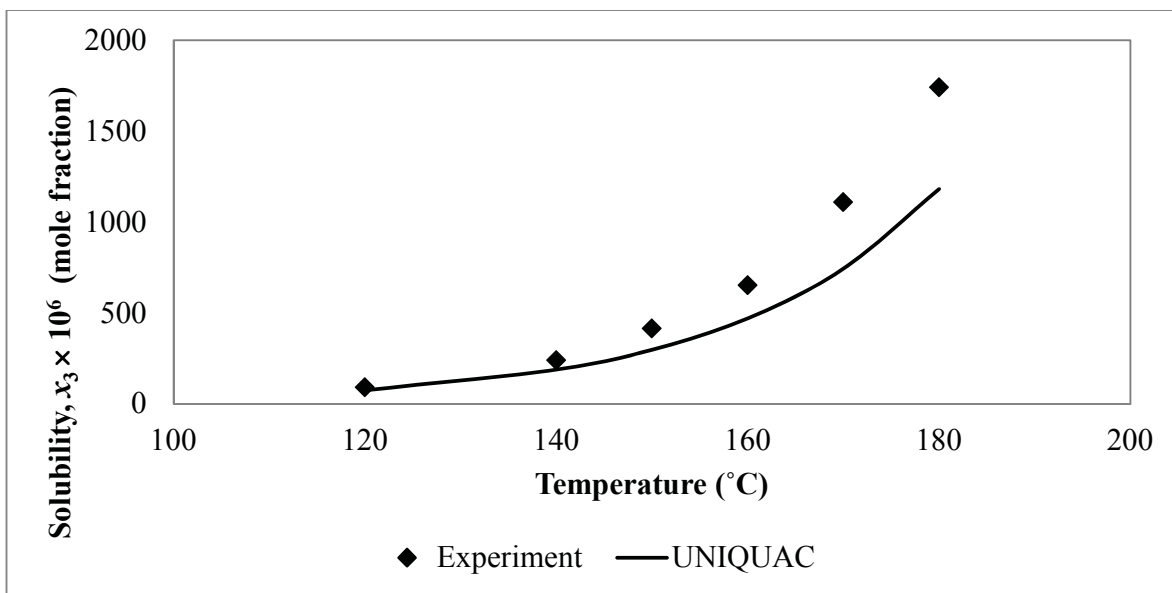


Figure 5.21: Experimental and UNIQUAC calculated solubility as a function of temperature in subcritical water (1) – ethanol (2) – anthracene (3) system, $f = 0.10$

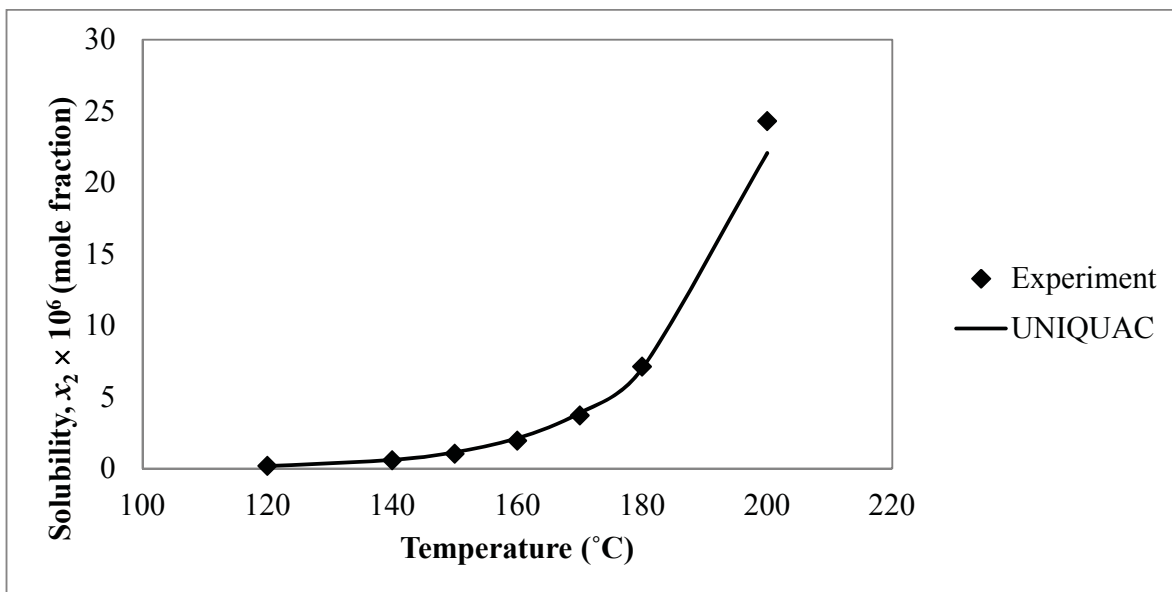


Figure 5.22: Experimental and UNIQUAC calculated solubility as a function of temperature in subcritical water (1) – *p*-terphenyl (2) system

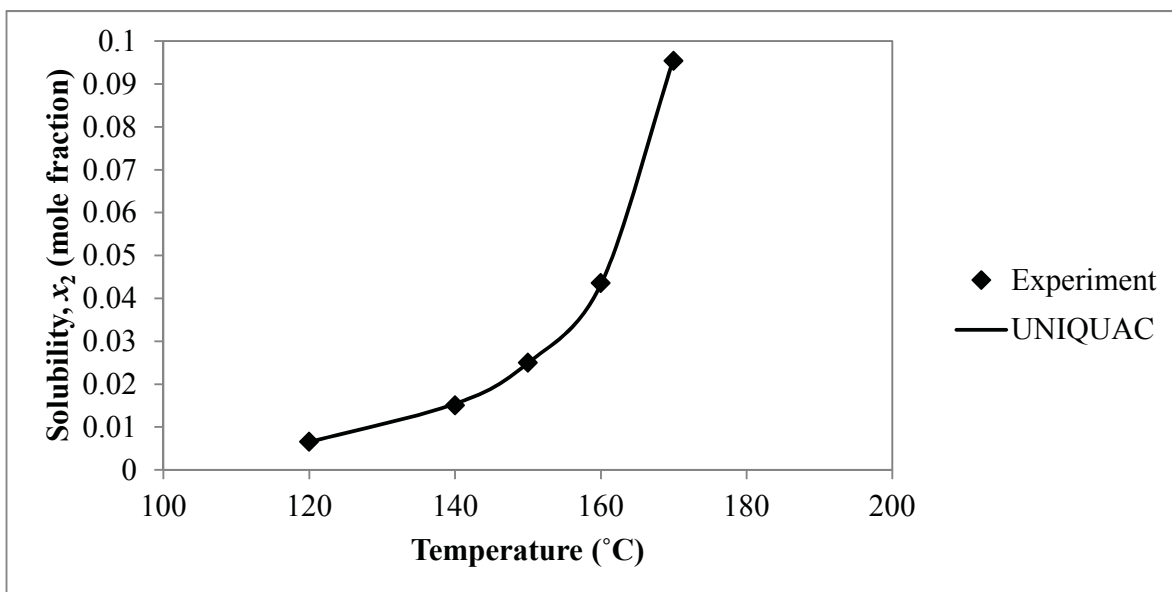


Figure 5.23: Experimental and UNIQUAC calculated solubility as a function of temperature in subcritical ethanol (1) – *p*-terphenyl (2) system

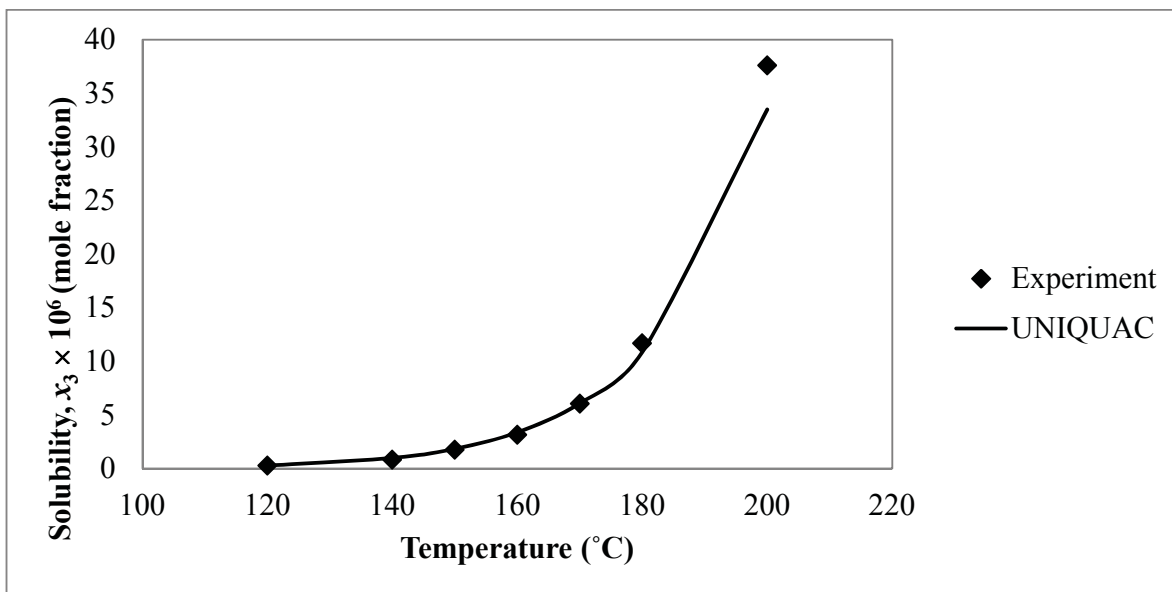


Figure 5.24: Experimental and UNIQUAC calculated solubility as a function of temperature in subcritical water (1) – ethanol (2) – *p*-terphenyl (3) system, $f = 0.01$

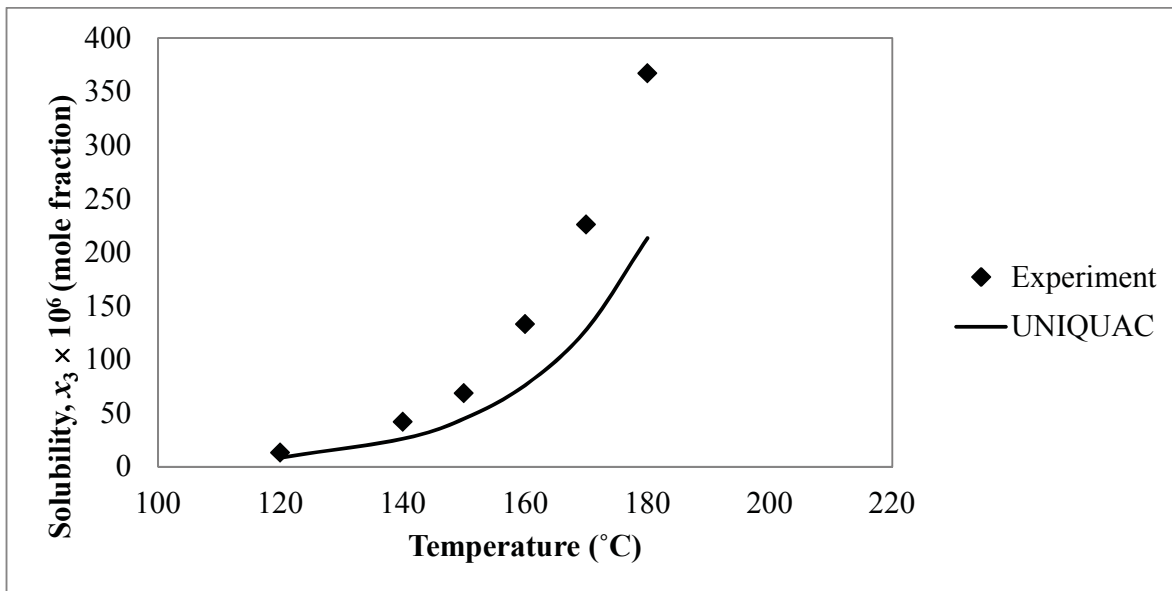


Figure 5.25: Experimental and UNIQUAC calculated solubility as a function of temperature in subcritical water (1) – ethanol (2) – *p*-terphenyl (3) system, $f = 0.10$

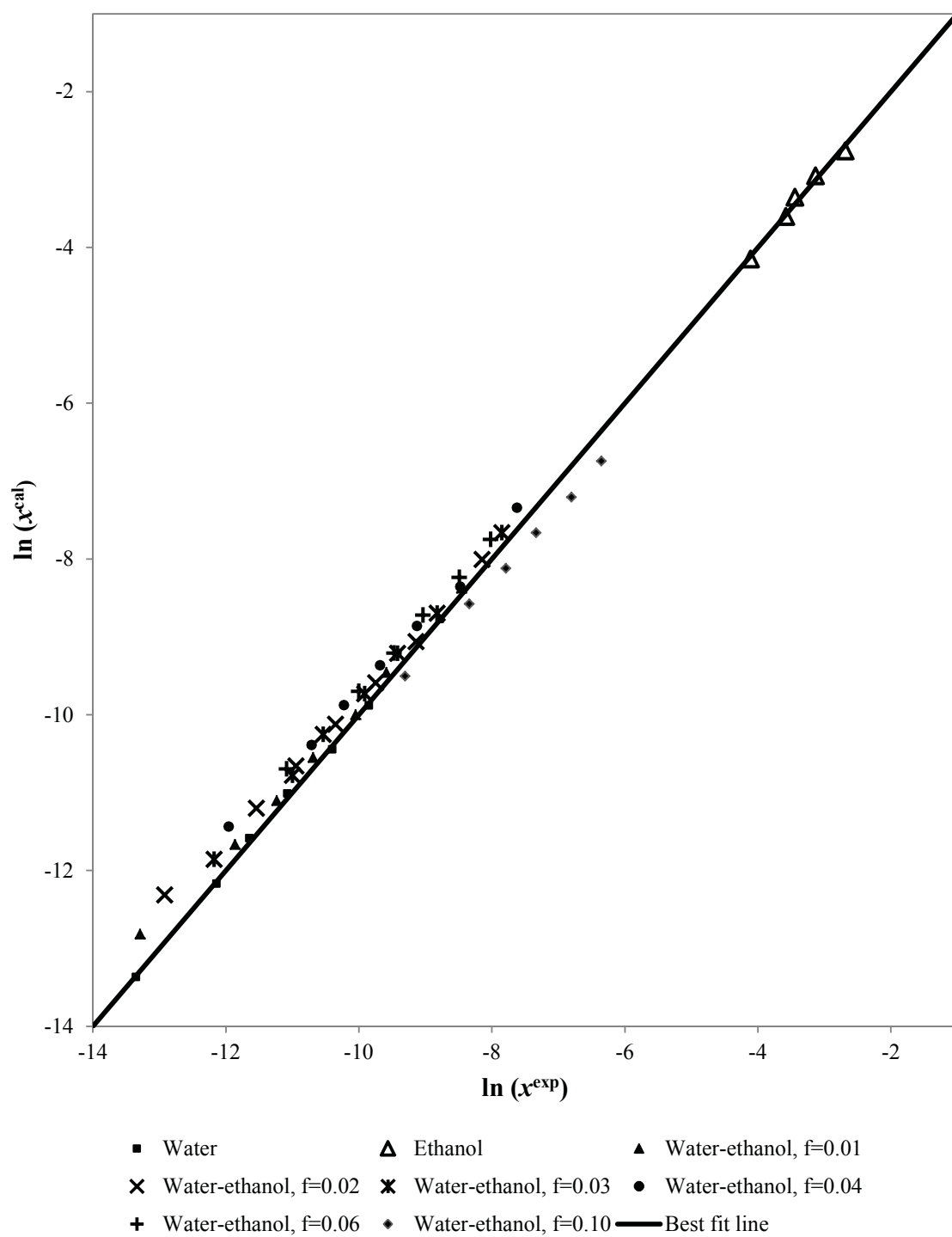


Figure 5.26: Deviation between UNIQUAC calculated and experimental solubility data: anthracene in subcritical water, subcritical ethanol and ethanol-modified subcritical water

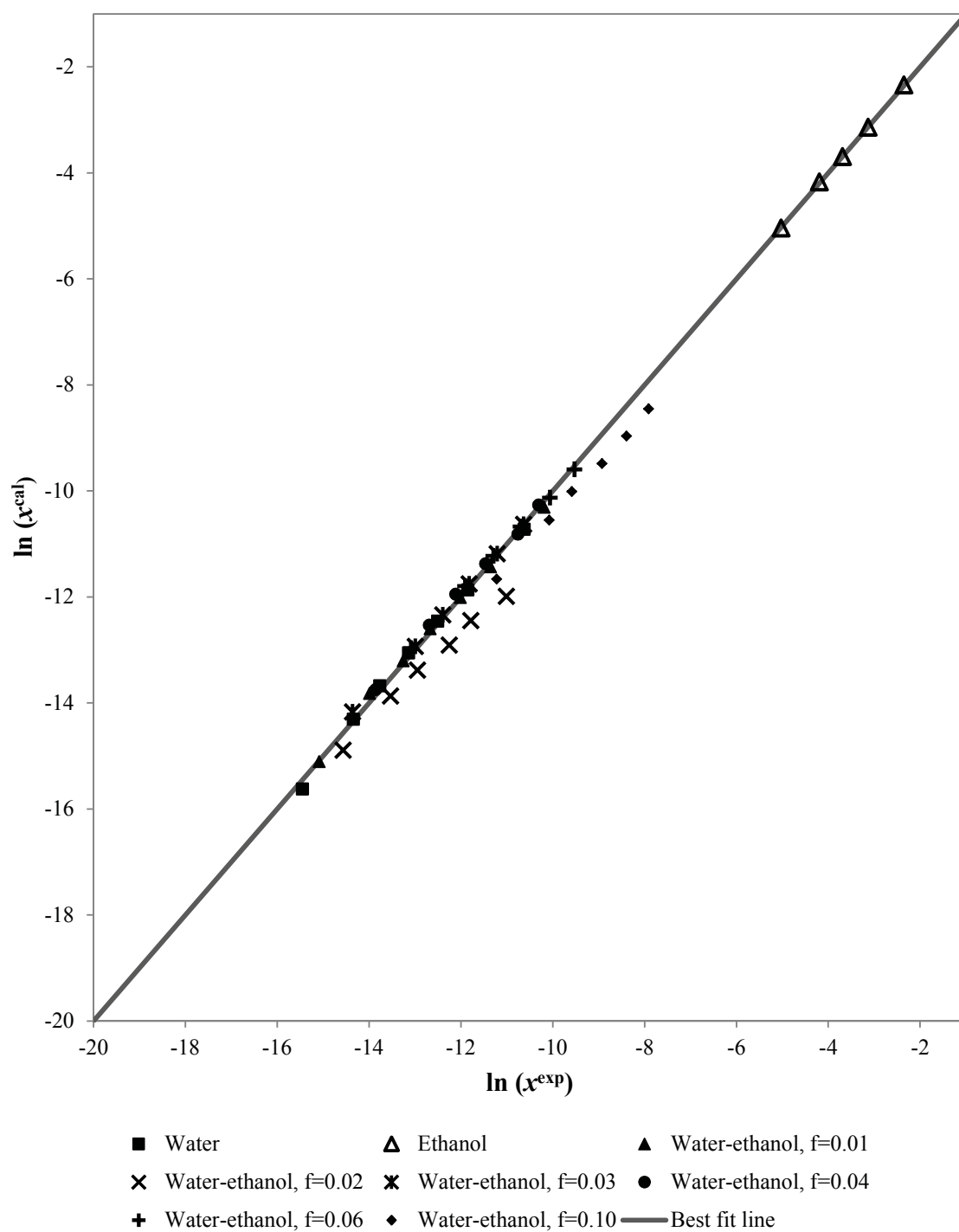


Figure 5.27: Deviation between UNIQUAC calculated and experimental data: *p*-terphenyl in subcritical water, subcritical ethanol and ethanol-modified subcritical water

*Estimating the τ_{ij} for anthracene-*p*-terphenyl*

The UNIQUAC calculation was extended to the water (1) – anthracene (2) – *p*-terphenyl (3) system to obtain the binary interaction parameters between anthracene and *p*-terphenyl. The results obtained point towards temperature *independent* binary interaction parameters for anthracene and *p*-terphenyl. The values obtained for a_{23} and a_{32} are -1000.03 and -1000.05 respectively. The calculated solubility values obtained via the UNIQUAC model are shown in Figure 5.28 and Table 5.13 while the corresponding activity coefficients are shown in Table 5.14.

Table 5.13: Experimental and UNIQUAC calculated solubility data and the absolute standard deviations for ternary water (1) - anthracene (2) - *p*-terphenyl (3) system with $a_{23} = -1000.03$ and $a_{32} = -1000.05$

T (°C)	x_2^{UNIQUAC}	x_3^{UNIQUAC}	ASD (%)
120	1.57×10^{-6}	1.64×10^{-7}	0.00
140	5.18×10^{-6}	6.12×10^{-7}	1.28
150	9.29×10^{-6}	1.15×10^{-6}	1.56
160	1.65×10^{-5}	2.13×10^{-6}	1.51
170	2.91×10^{-5}	3.90×10^{-6}	1.97
Average			1.27

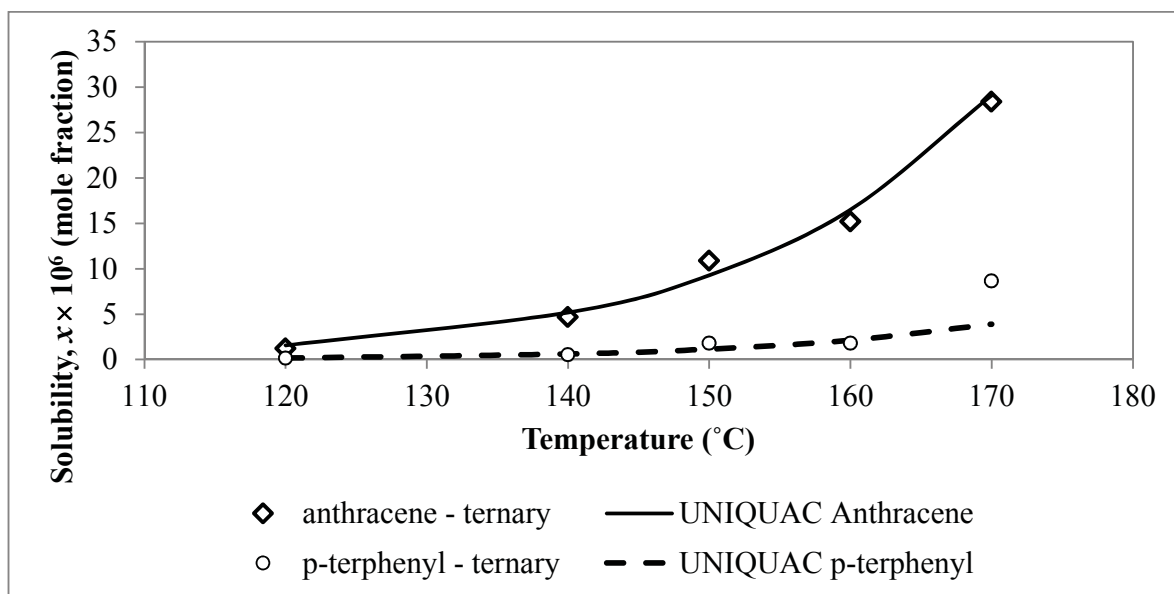


Figure 5.28: Experimental and UNIQUAC calculated solubility as a function of temperature in subcritical water (1) – anthracene (2) – *p*-terphenyl (3) system

Table 5.14: Experimental and UNIQUAC calculated activity coefficients for ternary water (1) - anthracene (2) - *p*-terphenyl (3) system

T (°C)	γ_2^{exp}	γ_3^{exp}	$\gamma_2^{\text{UNIQUAC}}$	$\gamma_3^{\text{UNIQUAC}}$
120	1.11×10^5	8.64×10^5	1.11×10^5	8.64×10^5
140	5.13×10^4	3.82×10^5	5.13×10^4	3.82×10^5
150	3.50×10^4	2.56×10^5	3.50×10^4	2.56×10^5
160	2.38×10^4	1.72×10^5	2.38×10^4	1.72×10^5
170	1.62×10^4	1.16×10^5	1.62×10^4	1.16×10^5

5.3.3 Correlation via the O-UNIFAC model

The surface area and volume parameters used in the O-UNIFAC model are shown in Table 5.2 while the group interaction parameters are taken from Poling et al. [15]. The activity coefficient and the resultant solubility values for all systems investigated in this study are shown in Tables 5.15 - 5.22. Figures 5.29 - 5.36 show the experimental and O-UNIFAC calculated solubility of anthracene and *p*-terphenyl as a function of temperature in subcritical water, ethanol and various ethanol-modified systems. The O-UNIFAC is found to predict fairly inaccurately the solubilities of both PAHs in all systems containing water, particularly at higher temperatures. The high deviations between experimental and O-UNIFAC calculated data are evident in Figures 5.38 - 5.39. The O-UNIFAC model clearly could not account for the dramatic increase in solubility at temperatures above 150 °C. While the O-UNIFAC model could provide a fitting trend that reflects the solubilities of PAHs in subcritical ethanol, the deviations from experimental values are very high in that the majority of the calculated values did not fall within the same order of magnitude as experimental values.

Table 5.15: O-UNIFAC calculated solubility data (mole fraction), the corresponding activity coefficients and the absolute standard deviations (ASD) from experimental data in subcritical water (1) – anthracene (2) system

T (°C)	$x_2^{\text{O-UNIFAC}}$	$\gamma_2^{\text{O-UNIFAC}}$	ASD (%)
120	1.10×10^{-7}	1.57×10^6	20.0
140	2.18×10^{-7}	1.22×10^6	26.3
150	3.00×10^{-7}	1.08×10^6	29.0
160	4.08×10^{-7}	9.64×10^5	32.9
170	5.46×10^{-7}	8.62×10^5	38.6
180	7.24×10^{-7}	7.74×10^5	43.6
200	1.23×10^{-6}	6.31×10^5	54.9
Average			35.0

Table 5.16: O-UNIFAC calculated solubility data (mole fraction), the corresponding activity coefficients and the absolute standard deviations (ASD) from experimental data in subcritical water (1) – *p*-terphenyl (2) system

T (°C)	$x_2^{\text{O-UNIFAC}}$	$\gamma_2^{\text{O-UNIFAC}}$	ASD (%)
120	3.11×10^{-9}	4.56×10^7	26.8
140	7.23×10^{-9}	3.23×10^7	30.7
150	1.72×10^{-8}	2.75×10^7	33.3
160	1.56×10^{-8}	2.35×10^7	36.8
170	2.25×10^{-8}	2.02×10^7	40.8
180	3.18×10^{-8}	1.75×10^7	45.7
200	6.13×10^{-8}	1.32×10^7	56.3
Average			38.6

Table 5.17: O-UNIFAC calculated solubility data (mole fraction), the corresponding activity coefficients and the absolute standard deviations (ASD) from experimental data in subcritical ethanol (1) – anthracene (2) system

T (°C)	$x_2^{\text{O-UNIFAC}}$	$\gamma_2^{\text{O-UNIFAC}}$	ASD (%)
120	2.28×10^{-2}	7.61	7.97
140	4.27×10^{-2}	6.23	11.9
150	5.97×10^{-2}	5.44	18.1
160	8.62×10^{-2}	4.56	21.8
170	1.34×10^{-1}	3.52	25.1
Average			17.0

Table 5.18: O-UNIFAC calculated solubility data (mole fraction), the corresponding activity coefficients and the absolute standard deviations (ASD) from experimental data in subcritical ethanol (1) – *p*-terphenyl (2) system

T (°C)	$x_2^{\text{O-UNIFAC}}$	$\gamma_2^{\text{O-UNIFAC}}$	ASD (%)
120	1.61×10^{-2}	8.82	17.9
140	3.43×10^{-2}	6.81	19.6
150	5.23×10^{-2}	5.64	20.0
160	8.59×10^{-2}	4.28	21.7
170	1.73×10^{-1}	2.63	25.2
Average			20.9

Table 5.19: O-UNIFAC calculated solubility data (mole fraction), the corresponding activity coefficients and the absolute standard deviations (ASD) from experimental data in subcritical water (1) – ethanol (2) – anthracene (3) system [$f = 0.01 - 0.03$]

T (°C)	f_2	$x_3^{\text{O-UNIFAC}}$	$\gamma_3^{\text{O-UNIFAC}}$	ASD (%)
120	0.01	3.67×10^{-7}	4.72×10^5	11.5
140		7.66×10^{-7}	3.47×10^5	18.7
150		1.08×10^{-6}	3.00×10^5	22.3
160		1.50×10^{-6}	2.61×10^5	25.4
170		2.06×10^{-6}	2.28×10^5	30.3
180		2.80×10^{-6}	2.00×10^5	33.4
200		4.97×10^{-6}	1.56×10^5	44.4
Average				26.6
120	0.02	5.49×10^{-7}	3.16×10^5	11.6
140		1.13×10^{-6}	2.35×10^5	18.6
150		1.59×10^{-6}	2.05×10^5	22.0
160		2.20×10^{-6}	1.79×10^5	25.9
170		3.00×10^{-6}	1.57×10^5	30.5
180		4.05×10^{-6}	1.38×10^5	35.8
200		7.14×10^{-6}	1.09×10^5	45.4
Average				27.1
120	0.03	8.05×10^{-7}	2.15×10^5	15.2
140		1.64×10^{-6}	1.62×10^5	21.1
150		2.29×10^{-6}	1.42×10^5	23.3
160		3.16×10^{-6}	1.24×10^5	27.8
170		4.29×10^{-6}	1.10×10^5	31.2
180		5.77×10^{-6}	9.72×10^4	36.7
200		1.01×10^{-5}	7.70×10^4	46.5
Average				28.8

Table 5.20: O-UNIFAC calculated solubility data (mole fraction), the corresponding activity coefficients and the absolute standard deviations (ASD) from experimental data in subcritical water (1) – ethanol (2) – anthracene (3) system [$f = 0.04 - 0.10$]

T (°C)	f_2	$x_3^{\text{O-UNIFAC}}$	$\gamma_3^{\text{O-UNIFAC}}$	ASD (%)
120	0.04	1.16×10^{-6}	1.49×10^5	14.3
140		2.34×10^{-6}	1.14×10^4	21.1
150		3.25×10^{-6}	9.99×10^4	23.6
160		4.46×10^{-6}	8.81×10^4	27.3
170		6.04×10^{-6}	7.80×10^4	31.7
180		8.08×10^{-6}	6.93×10^4	38.4
200		1.40×10^{-5}	5.53×10^4	46.7
Average				29.0
120	0.06	2.29×10^{-6}	7.56×10^4	17.1
140		4.53×10^{-6}	5.87×10^4	23.0
150		6.25×10^{-6}	5.20×10^4	26.6
160		8.50×10^{-6}	4.62×10^4	29.2
170		1.14×10^{-5}	4.12×10^4	34.1
180		1.52×10^{-5}	3.69×10^4	38.4
Average				28.1
120	0.10	7.54×10^{-6}	2.30×10^4	26.8
140		1.45×10^{-5}	1.84×10^4	33.6
150		1.97×10^{-5}	1.65×10^4	39.1
160		2.65×10^{-5}	1.48×10^4	43.7
170		3.52×10^{-5}	1.34×10^4	50.8
180		4.62×10^{-5}	1.21×10^4	57.1
Average				41.8

Table 5.21: O-UNIFAC calculated solubility data (mole fraction), the corresponding activity coefficients and the absolute standard deviations (ASD) from experimental data in subcritical water (1) – ethanol (2) – *p*-terphenyl (3) system [$f = 0.01 - 0.03$]

T (°C)	f_2	$x_3^{\text{O-UNIFAC}}$	$\gamma_3^{\text{O-UNIFAC}}$	ASD (%)
120	0.01	1.36×10^{-8}	1.04×10^7	20.1
140		3.34×10^{-8}	6.99×10^6	23.0
150		5.10×10^{-8}	5.78×10^6	26.7
160		7.63×10^{-8}	4.82×10^6	29.4
170		1.12×10^{-7}	4.04×10^6	33.2
180		1.63×10^{-7}	3.40×10^6	37.6
200		3.30×10^{-7}	2.46×10^6	46.5
Average				30.9
120	0.02	2.27×10^{-8}	6.25×10^6	20.8
140		5.49×10^{-8}	4.26×10^6	23.6
150		8.31×10^{-8}	3.55×10^6	26.0
160		1.24×10^{-7}	2.97×10^6	29.8
170		1.81×10^{-7}	2.51×10^6	31.7
180		2.61×10^{-7}	2.13×10^6	27.6
Average				28.3
120	0.03	3.69×10^{-8}	3.84×10^6	19.2
140		8.81×10^{-8}	2.65×10^6	25.0
150		1.33×10^{-7}	2.22×10^6	27.8
160		1.96×10^{-7}	1.88×10^6	30.7
170		2.85×10^{-7}	1.59×10^6	34.4
180		4.10×10^{-7}	1.36×10^6	38.3
Average				29.2

Table 5.22: O-UNIFAC calculated solubility data (mole fractions), the corresponding activity coefficients and the absolute standard deviations (ASD) from experimental data in subcritical water (1) – ethanol (2) – *p*-terphenyl (3) system [$f = 0.04 - 0.10$]

T (°C)	f_2	$x_3^{\text{O-UNIFAC}}$	$\gamma_3^{\text{O-UNIFAC}}$	ASD (%)
120	0.04	5.88×10^{-8}	2.42×10^6	20.2
140		1.38×10^{-7}	1.69×10^6	24.5
150		2.07×10^{-7}	1.43×10^6	27.0
160		3.04×10^{-7}	1.21×10^6	30.9
170		4.40×10^{-7}	1.03×10^6	36.1
180		6.29×10^{-7}	8.84×10^5	38.5
Average				29.5
120	0.06	1.40×10^{-7}	1.02×10^6	20.6
140		3.21×10^{-7}	7.28×10^5	25.5
150		4.74×10^{-7}	6.21×10^5	29.0
160		6.91×10^{-7}	5.32×10^5	32.6
170		9.91×10^{-7}	4.58×10^5	37.4
180		1.40×10^{-6}	3.96×10^5	41.5
Average				31.1
120	0.10	6.35×10^{-7}	2.24×10^5	27.2
140		1.40×10^{-6}	1.67×10^5	33.7
150		2.04×10^{-6}	1.45×10^5	36.7
160		2.92×10^{-6}	1.26×10^5	42.8
170		4.12×10^{-6}	1.10×10^5	47.7
180		5.74×10^{-6}	9.68×10^4	52.6
Average				40.1

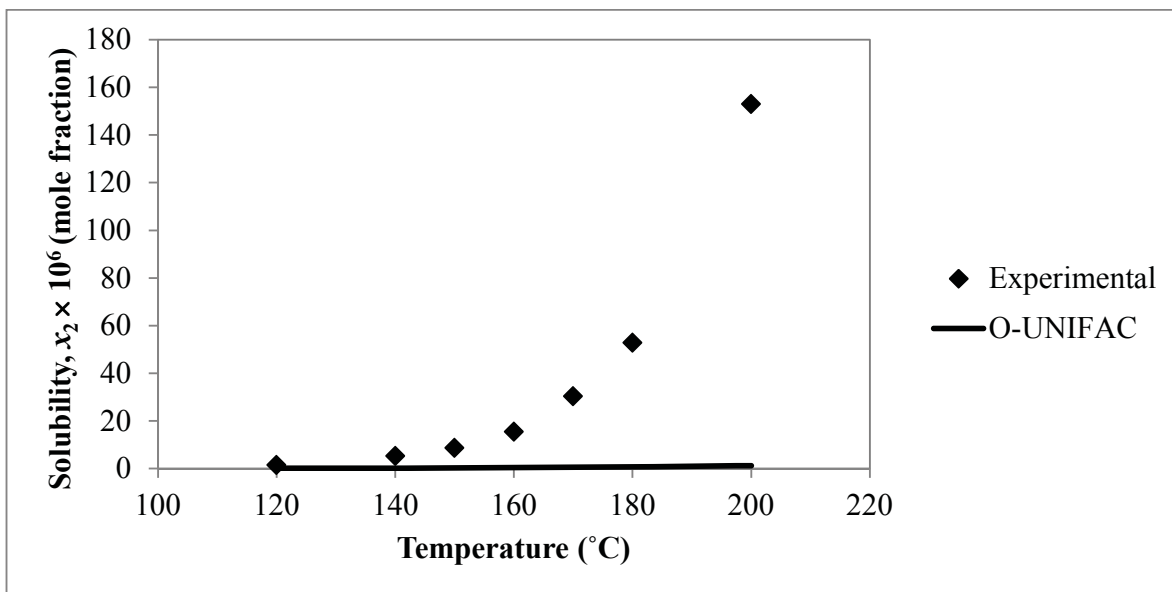


Figure 5.29: Experimental and O-UNIFAC calculated solubility as a function of temperature in subcritical water (1) – anthracene (2) system

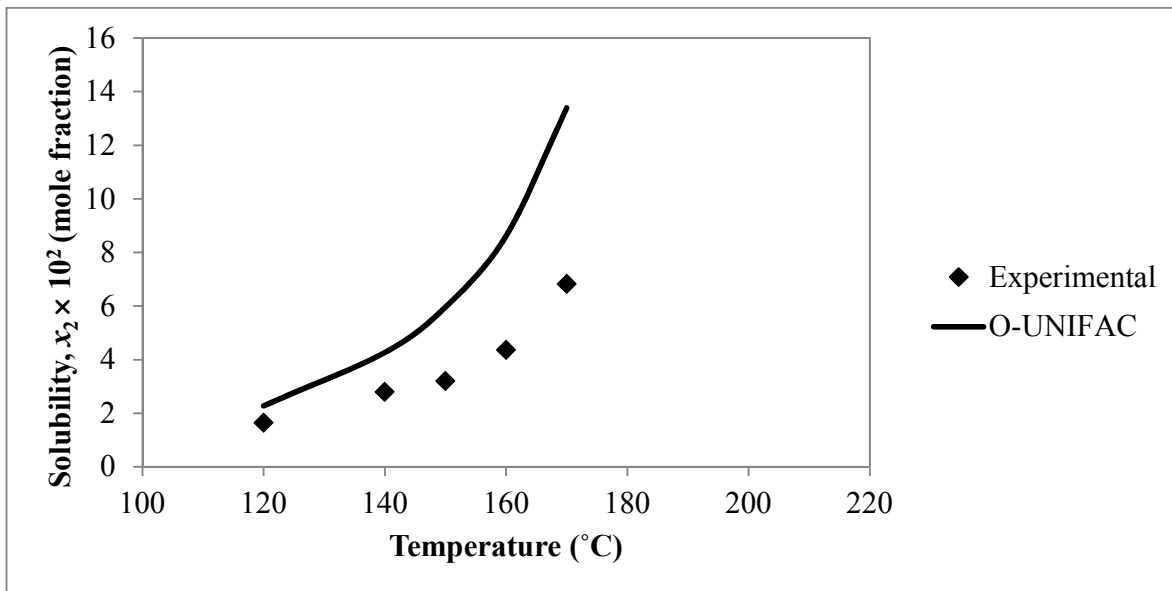


Figure 5.30: Experimental and O-UNIFAC calculated solubility as a function of temperature in subcritical ethanol (1) – anthracene (2) system

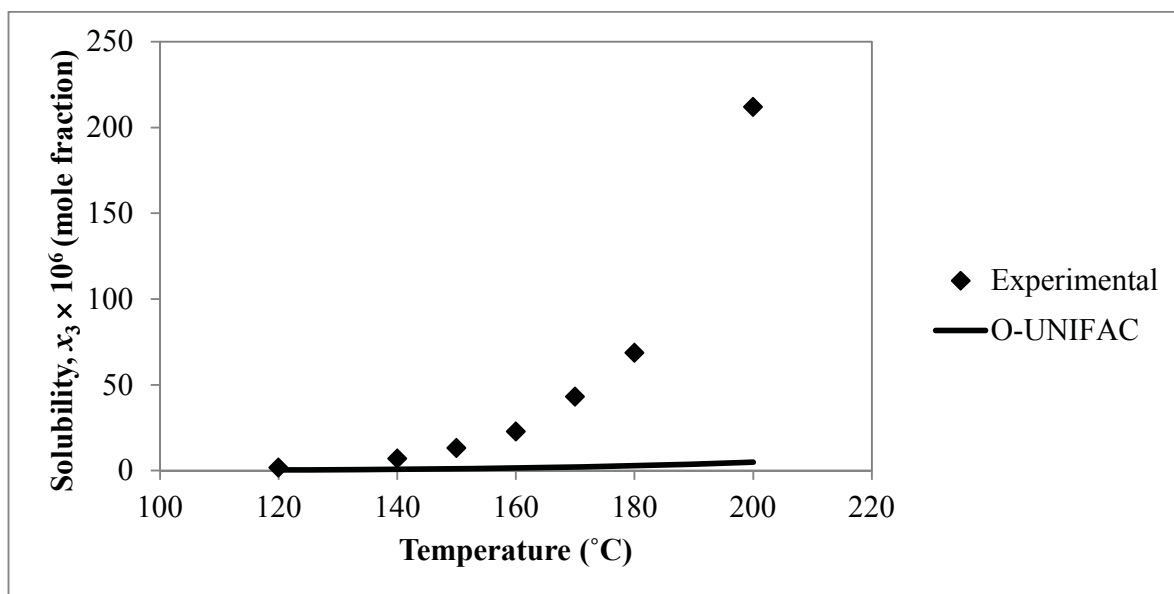


Figure 5.31: Experimental and O-UNIFAC calculated solubility as a function of temperature in subcritical water (1) – ethanol (2) – anthracene (3) system, $f = 0.01$

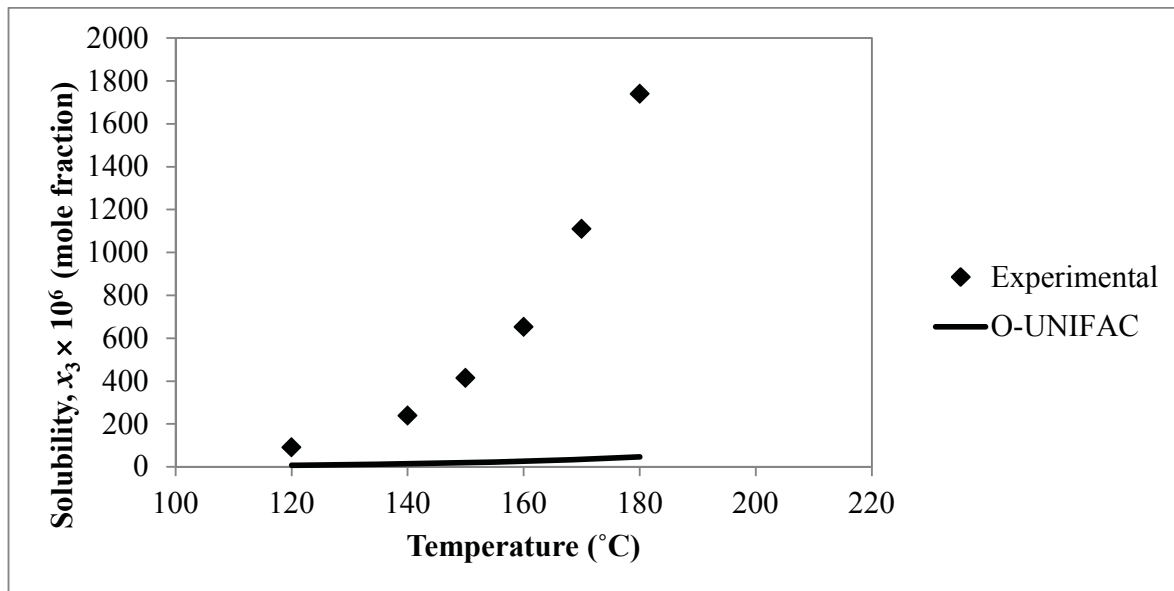


Figure 5.32: Experimental and O-UNIFAC calculated solubility as a function of temperature in subcritical water (1) – ethanol (2) – anthracene (3) system, $f = 0.10$

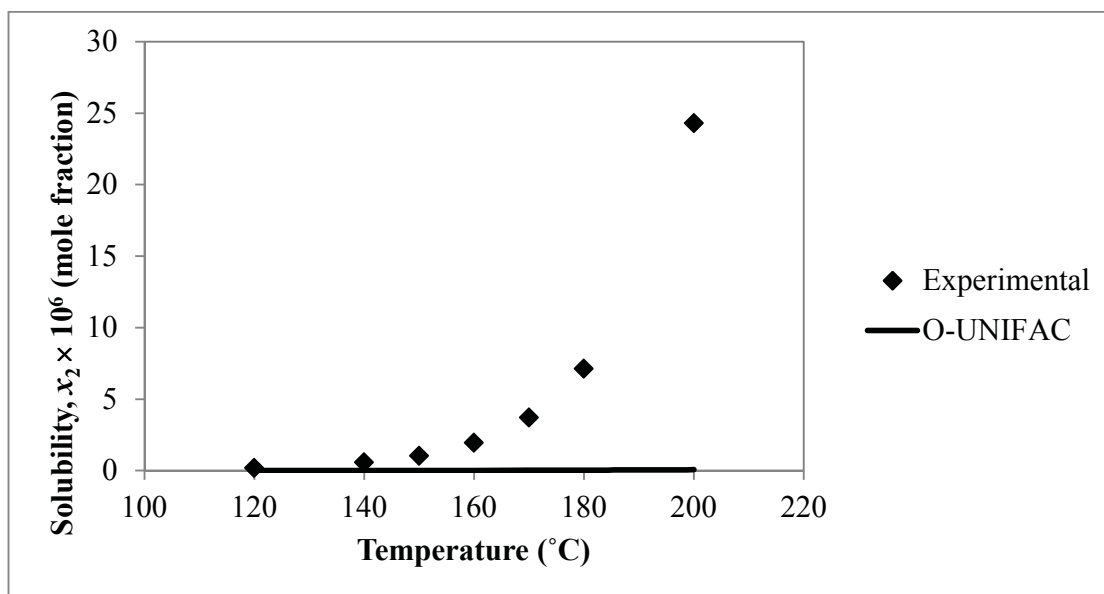


Figure 5.33: Experimental and O-UNIFAC calculated solubility as a function of temperature in subcritical water (1) – *p*-terphenyl (2) system

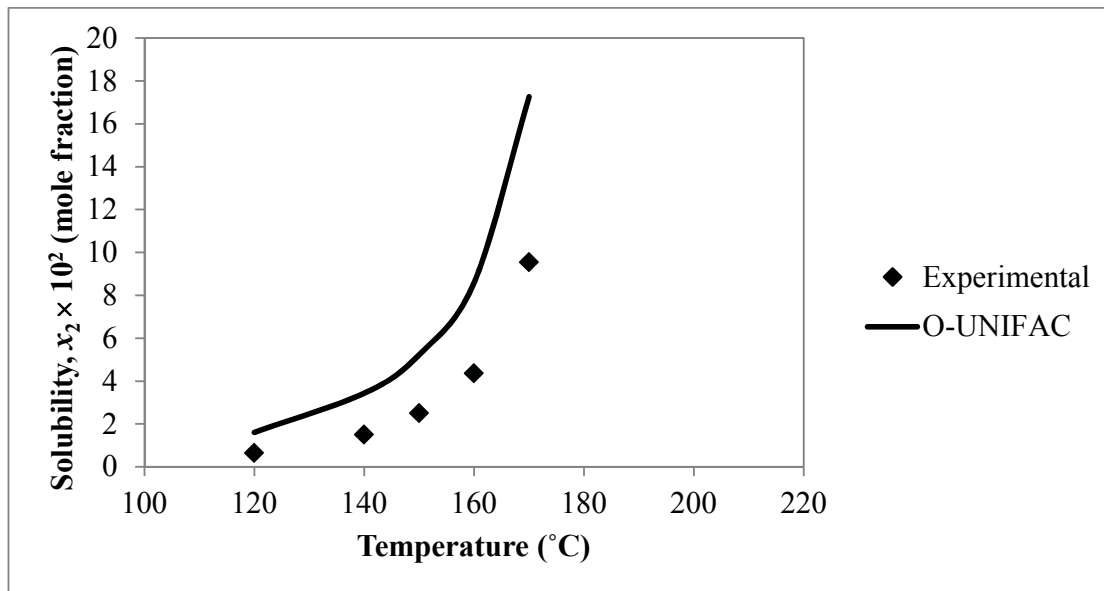


Figure 5.34: Experimental and O-UNIFAC calculated solubility as a function of temperature in subcritical ethanol (1) – *p*-terphenyl (2) system

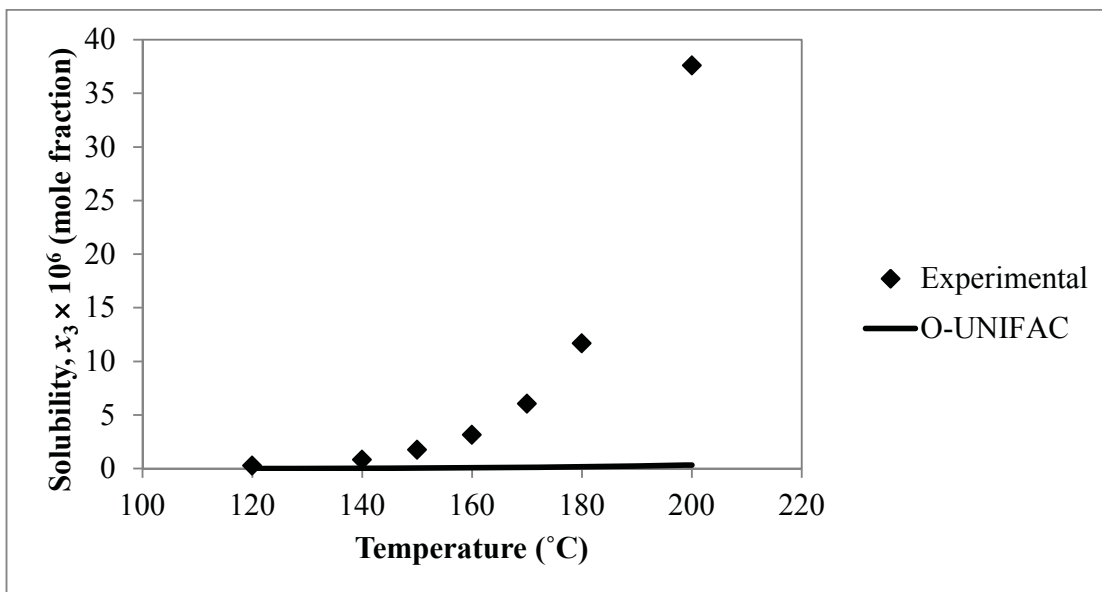


Figure 5.35: Experimental and O-UNIFAC calculated solubility as a function of temperature in subcritical water (1) – ethanol (2) – *p*-terphenyl (3) system, $f = 0.01$

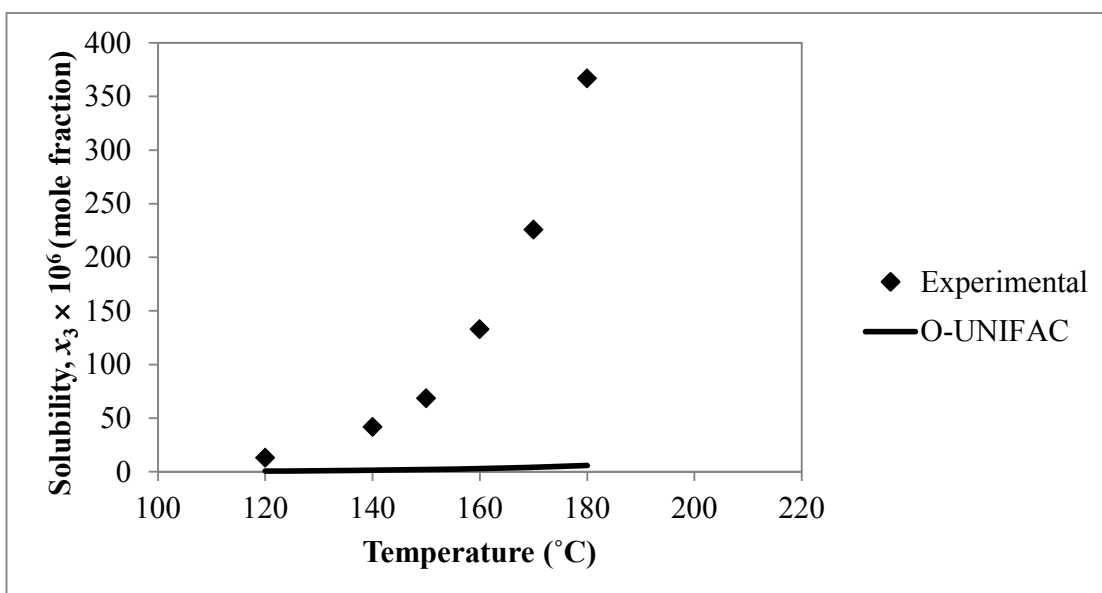


Figure 5.36: Experimental and O-UNIFAC calculated solubility as a function of temperature in subcritical water (1) – ethanol (2) – *p*-terphenyl (3) system, $f = 0.10$

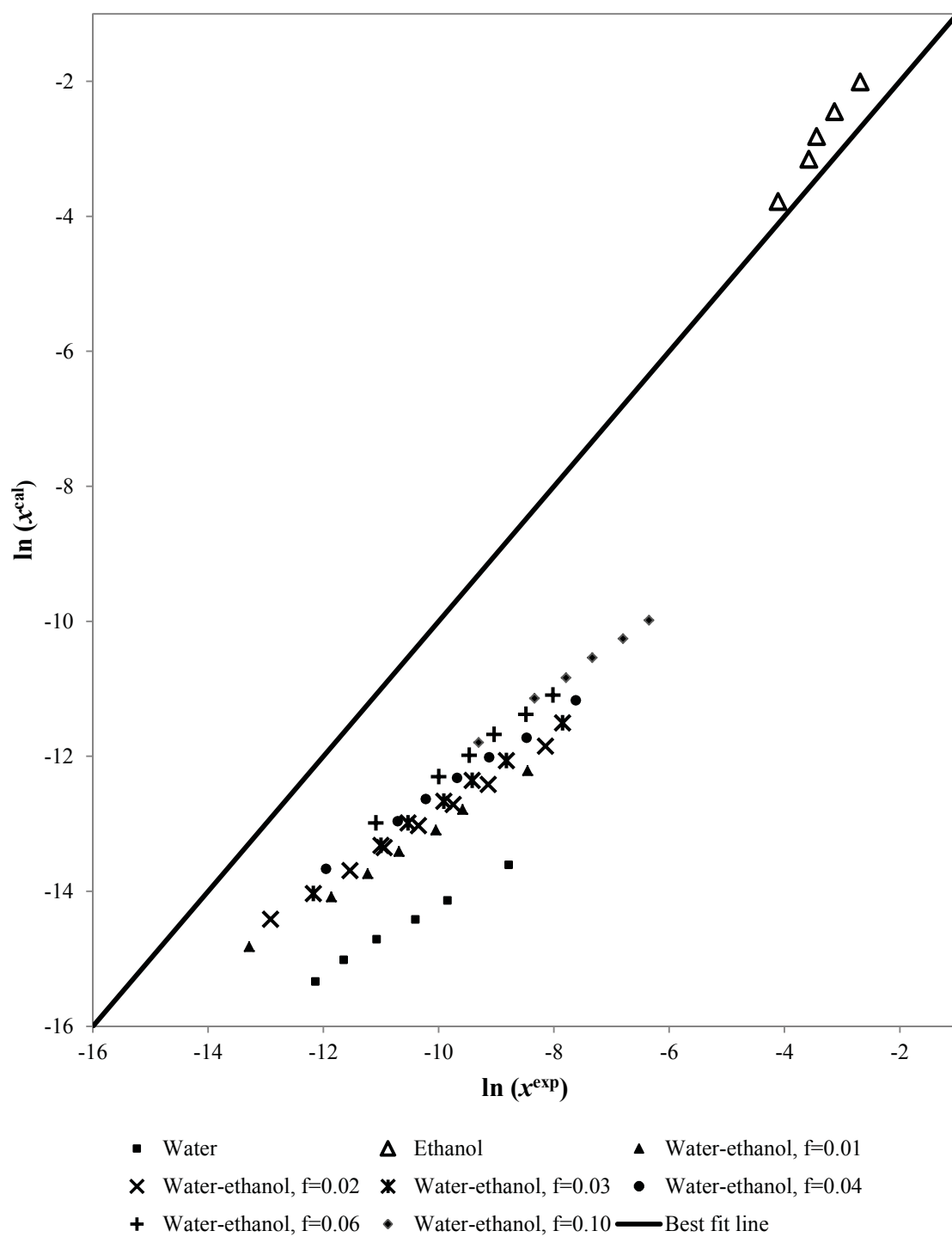


Figure 5.37: Deviation between O-UNIFAC calculated and experimental solubility data: anthracene in subcritical water, subcritical ethanol and ethanol-modified subcritical water

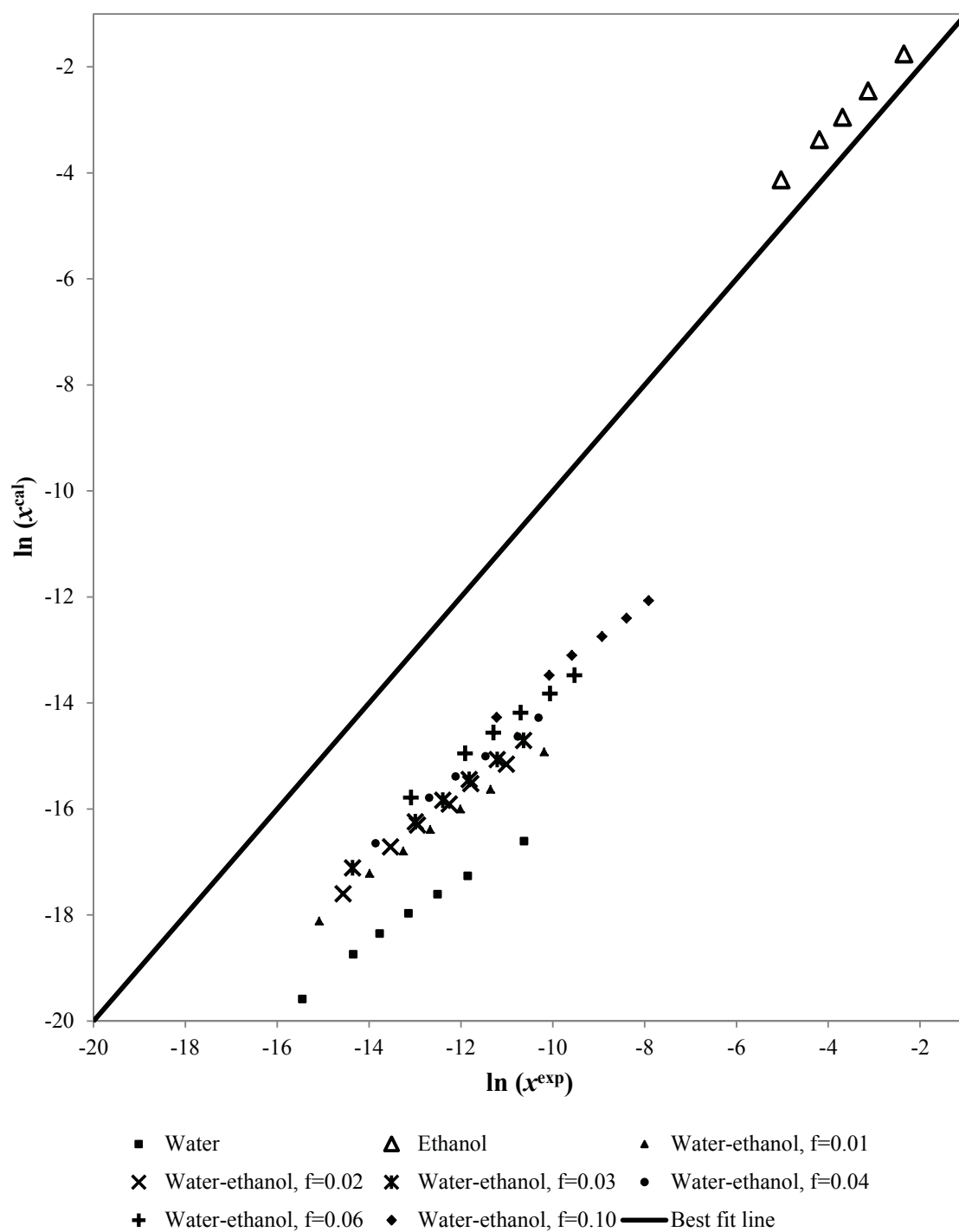


Figure 5.38: Deviation between O-UNIFAC calculated and experimental solubility data: *p*-terphenyl in subcritical water, subcritical ethanol and ethanol-modified subcritical water

As the O-UNIFAC model was found to perform poorly in water containing binary and ternary subcritical systems, similar results were expected for the ternary water–anthracene–*p*-terphenyl system. The O-UNIFAC calculated solubility values are shown in Table 5.23 and Figure 5.39 while the absolute standard deviations obtained are given in Table 5.24.

Table 5.23: The calculated solubility values and activity coefficients obtained from the O-UNIFAC model for water (1) – anthracene (2) – *p*-terphenyl (3) system at various temperatures

T (°C)	$x_2^{\text{O-UNIFAC}}$	$\gamma_2^{\text{O-UNIFAC}}$	$x_3^{\text{O-UNIFAC}}$	$\gamma_3^{\text{O-UNIFAC}}$
120	2.40×10^{-7}	7.21×10^5	7.94×10^{-9}	1.79×10^7
140	5.08×10^{-7}	5.23×10^5	1.99×10^{-8}	1.18×10^7
150	7.22×10^{-7}	4.5×10^5	3.05×10^{-8}	9.67×10^6
160	1.01×10^{-6}	3.89×10^5	4.60×10^{-8}	8.00×10^6
170	1.39×10^{-6}	3.38×10^5	6.82×10^{-8}	6.66×10^6

Table 5.24: Absolute standard deviation (ASD) obtained with the O-UNIFAC model for water (1) – anthracene (2) – *p*-terphenyl (3) system

Temperature (°C)	Anthracene	<i>p</i> -Terphenyl
	ASD(%)	ASD (%)
120	16.8	10.7
140	18.8	15.3
150	23.7	19.2
160	21.8	19.4
170	29.1	22.4
AASD (%)	22.1	17.4

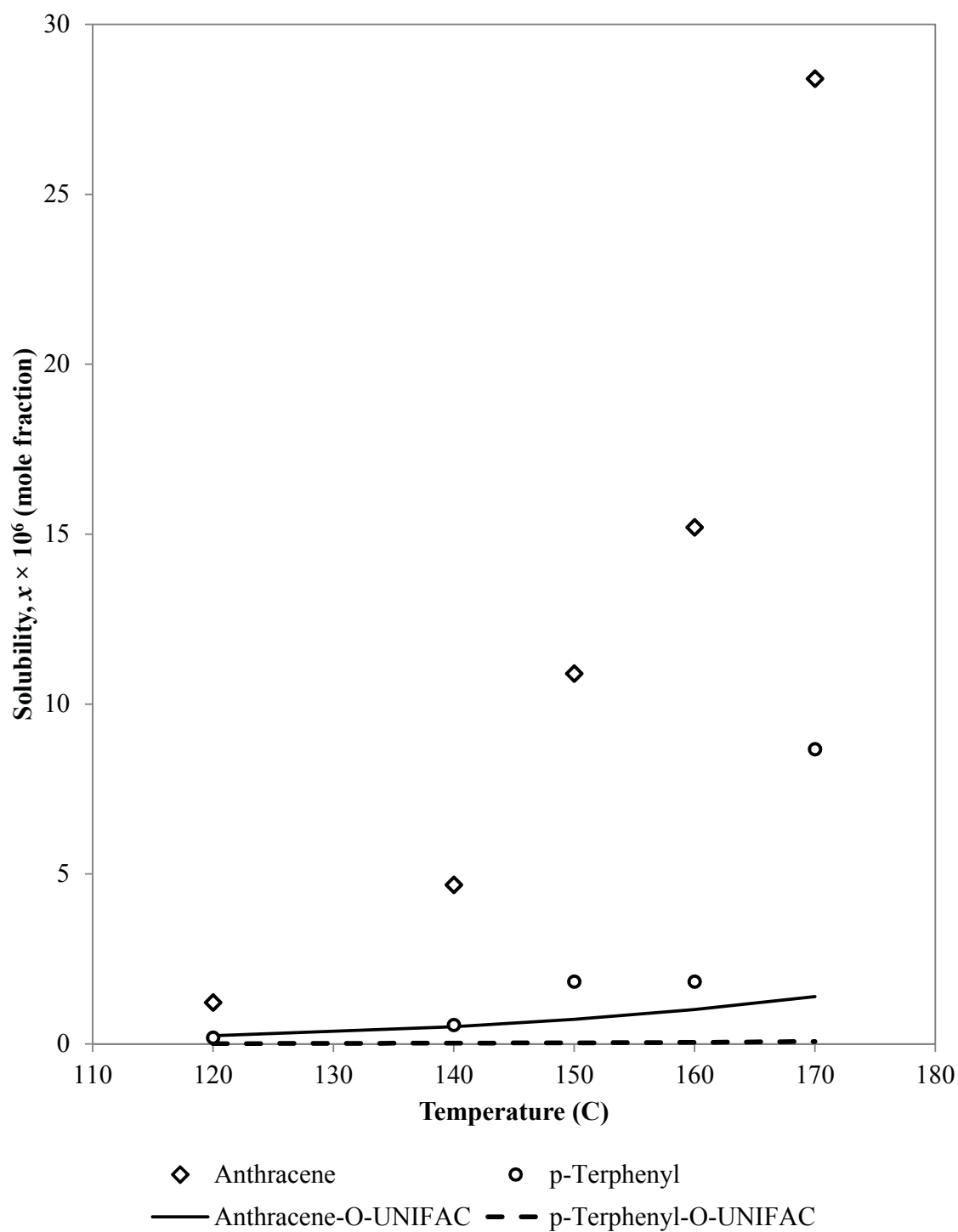


Figure 5.39: O-UNIFAC calculated and experimental solubility values as a function of temperature in ternary system consisting of anthracene, *p*-terphenyl and subcritical water

5.3.4 Correlation via the M-UNIFAC model

The surface, volume and interaction parameters used in this section of the study were obtained from Gmehling et al. [11]. The physical properties used in this study are shown in Table 5.25. The solubility values and the corresponding activity coefficients of anthracene and *p*-terphenyl predicted from the M-UNIFAC model are shown in Tables 5.26 - 5.33. The M-UNIFAC model was also found to perform poorly, particularly in water-containing systems, at temperatures above 150 °C. Similar to its predecessor, the solubility data calculated from the M-UNIFAC model was not in the same order of magnitude as experimental data. In fact, the margin of error between the two UNIFAC models was almost similar. The M-UNIFAC model generally performed better than the O-UNIFAC model in binary subcritical ethanol and subcritical water systems. However, in ternary systems containing ethanol, both models performed poorly, particularly as the concentration of ethanol increased. Fornari et al. [8] found that the quality and predictive power of the UNIFAC models degrade for compounds with low solubility as solutes with low solubility tend to have higher molecular weight, size and melting temperature. In contrast, the M-UNIFAC model is based on regressing VLE and excess enthalpy data of mixtures containing only low molecular weight aromatic compounds; the consequence of which can be seen in this study.

Table 5.25: Physical properties of anthracene and *p*-terphenyl used in this study

	Anthracene	<i>p</i> -Terphenyl
Molecular formula	C ₁₄ H ₁₀	C ₆ H ₅ C ₆ H ₄ C ₆ H ₅
Molecular weight	178.23	230.30
Melting point	490 K	485 K
Enthalpy of fusion, ΔH_m	29000 J/mol	33700 J/mol
Subgroups used in M-UNIFAC	ACH, AC, H ₂ O	ACH, AC, H ₂ O

Table 5.26: M-UNIFAC calculated solubility data (mole fraction), the corresponding activity coefficients and the absolute standard deviations (ASD) from experimental data in subcritical water (1) – anthracene (2) system

T (°C)	$x_2^{\text{M-UNIFAC}}$	$\gamma_2^{\text{M-UNIFAC}}$	ASD (%)
120	3.33×10^{-7}	5.20×10^5	11.7
140	9.40×10^{-7}	2.83×10^5	14.3
150	1.54×10^{-6}	2.10×10^5	14.9
160	2.50×10^{-6}	1.57×10^5	16.5
170	3.99×10^{-6}	1.18×10^5	19.5
180	6.28×10^{-6}	8.92×10^4	21.6
200	1.51×10^{-5}	5.15×10^4	26.4
Average			17.9

Table 5.27: M-UNIFAC calculated solubility data (mole fraction), the corresponding activity coefficients and the absolute standard deviations (ASD) from experimental data in subcritical water (1) – *p*-terphenyl (2) system

T (°C)	$x_2^{\text{M-UNIFAC}}$	$\gamma_2^{\text{M-UNIFAC}}$	ASD (%)
120	6.53×10^{-9}	2.17×10^7	22.0
140	2.42×10^{-8}	9.65×10^6	22.3
150	4.53×10^{-8}	6.50×10^6	22.8
160	8.34×10^{-8}	4.41×10^6	24.0
170	1.51×10^{-7}	3.01×10^6	25.6
180	2.68×10^{-7}	2.07×10^6	27.7
200	8.14×10^{-7}	9.96×10^5	32.0
Average			25.2

Table 5.28: M-UNIFAC calculated solubility data (mole fraction), the corresponding activity coefficients and the absolute standard deviations (ASD) from experimental data in subcritical ethanol (1) – anthracene (2) system

T (°C)	$x_2^{\text{M-UNIFAC}}$	$\gamma_2^{\text{M-UNIFAC}}$	ASD (%)
120	6.13×10^{-3}	11.2	24.0
140	1.32×10^{-2}	8.71	21.0
150	1.93×10^{-2}	7.46	14.6
160	2.90×10^{-2}	6.12	13.0
170	4.70×10^{-2}	4.49	13.8
Average			17.3

Table 5.29: M-UNIFAC calculated solubility data (mole fraction), the corresponding activity coefficients and the absolute standard deviations (ASD) from experimental data in subcritical ethanol (1) – *p*-terphenyl (2) system

T (°C)	$x_2^{\text{M-UNIFAC}}$	$\gamma_2^{\text{M-UNIFAC}}$	ASD (%)
120	1.54×10^{-2}	23.2	17.0
140	3.05×10^{-2}	17.7	16.8
150	4.35×10^{-2}	15.3	15.0
160	6.42×10^{-2}	12.7	12.3
170	1.05×10^{-1}	9.65	4.08
Average			13.1

Table 5.30: M-UNIFAC calculated solubility data (mole fraction), the corresponding activity coefficients and the absolute standard deviations (ASD) from experimental data in subcritical water (1) – ethanol (2) – anthracene (3) system [$f=0.01-0.03$]

T (°C)	f_2	$x_3^{\text{M-UNIFAC}}$	$\gamma_3^{\text{M-UNIFAC}}$	ASD (%)
120	0.01	4.67×10^{-7}	3.71×10^5	9.68
140		1.31×10^{-6}	2.03×10^5	14.1
150		2.15×10^{-6}	1.51×10^5	16.2
160		3.47×10^{-6}	1.13×10^5	17.6
170		5.53×10^{-6}	8.52×10^4	20.5
180		8.69×10^{-6}	6.45×10^4	21.6
200		2.07×10^{-5}	3.74×10^4	27.5
Average				18.2
120	0.02	6.44×10^{-7}	2.69×10^5	10.3
140		1.80×10^{-6}	1.47×10^5	14.6
150		2.95×10^{-6}	1.10×10^5	16.3
160		4.74×10^{-6}	8.29×10^4	18.5
170		7.53×10^{-6}	6.26×10^4	21.0
180		1.18×10^{-5}	4.75×10^4	24.1
200		2.80×10^{-5}	2.78×10^4	28.6
Average				19.1
120	0.03	8.76×10^{-7}	1.98×10^5	14.6
140		2.44×10^{-6}	1.09×10^5	17.5
150		3.97×10^{-6}	8.18×10^4	18.1
160		6.37×10^{-6}	6.17×10^4	20.7
170		1.01×10^{-5}	4.68×10^4	22.2
180		1.57×10^{-5}	3.56×10^4	25.3
200		3.70×10^{-5}	2.10×10^4	30.0
Average				21.2

Table 5.31: M-UNIFAC calculated solubility data (mole fraction), the corresponding activity coefficients and the absolute standard deviations (ASD) from experimental data in subcritical water (1) – ethanol (2) – anthracene (3) system [$f = 0.04 - 0.10$]

T (°C)	f_2	$x_3^{\text{M-UNIFAC}}$	$\gamma_3^{\text{M-UNIFAC}}$	ASD (%)
120	0.04	1.18×10^{-6}	1.47×10^5	14.2
140		3.25×10^{-6}	8.18×10^4	18.0
150		5.28×10^{-6}	6.16×10^4	18.9
160		8.43×10^{-6}	4.66×10^4	20.7
170		1.33×10^{-5}	3.55×10^4	23.1
180		2.06×10^{-5}	2.71×10^4	27.3
200		4.81×10^{-5}	1.61×10^4	30.5
Average				21.8
120	0.06	2.04×10^{-6}	8.50×10^4	18.2
140		5.56×10^{-6}	4.78×10^4	21.0
150		8.95×10^{-6}	3.63×10^4	22.8
160		1.42×10^{-5}	2.77×10^4	23.5
170		2.22×10^{-5}	2.13×10^4	26.3
180		3.41×10^{-5}	1.64×10^4	28.5
Average				23.3
120	0.10	5.40×10^{-6}	3.21×10^4	30.3
140		1.43×10^{-5}	1.86×10^4	33.8
150		2.26×10^{-5}	1.44×10^4	37.3
160		3.52×10^{-5}	1.12×10^4	39.8
170		5.39×10^{-5}	8.74×10^3	44.5
180		8.14×10^{-5}	6.89×10^3	48.2
Average				39.0

Table 5.32: M-UNIFAC calculated solubility data (mole fraction), the corresponding activity coefficients and the absolute standard deviations (ASD) from experimental data in subcritical water (1) – ethanol (2) – *p*-terphenyl (3) system [$f = 0.01 - 0.03$]

T (°C)	f_2	$x_3^{\text{M-UNIFAC}}$	$\gamma_3^{\text{M-UNIFAC}}$	ASD (%)
120	0.01	1.02×10^{-8}	1.39×10^7	22.0
140		3.76×10^{-8}	6.22×10^6	22.2
150		7.01×10^{-8}	4.20×10^6	24.3
160		1.29×10^{-7}	2.86×10^6	25.3
170		2.32×10^{-7}	1.96×10^6	27.2
180		4.11×10^{-7}	1.35×10^6	29.5
200		1.24×10^{-6}	6.55×10^5	33.5
Average				26.3
120	0.02	1.55×10^{-8}	9.13×10^6	23.4
140		5.70×10^{-8}	4.10×10^6	23.3
150		1.06×10^{-7}	2.78×10^6	24.1
160		1.94×10^{-7}	1.90×10^6	26.2
170		3.47×10^{-7}	1.31×10^6	26.2
180		6.14×10^{-7}	9.06×10^5	29.9
Average				25.5
120	0.03	2.33×10^{-8}	6.10×10^6	22.4
140		8.47×10^{-8}	2.76×10^6	25.4
150		1.57×10^{-7}	1.88×10^6	26.4
160		2.85×10^{-7}	1.29×10^6	27.5
170		5.09×10^{-7}	8.92×10^5	29.2
180		8.95×10^{-7}	6.21×10^5	31.0
Average				27.0

Table 5.33: M-UNIFAC calculated solubility data (mole fraction), the corresponding activity coefficients and the absolute standard deviations (ASD) from experimental data in subcritical water (1) – ethanol (2) – *p*-terphenyl (3) system [$f = 0.04 - 0.10$]

T (°C)	f_2	$x_3^{\text{M-UNIFAC}}$	$\gamma_3^{\text{M-UNIFAC}}$	ASD (%)
120	0.04	3.42×10^{-8}	4.15×10^6	24.1
140		1.24×10^{-7}	1.89×10^6	25.3
150		2.28×10^{-7}	1.29×10^6	26.2
160		4.12×10^{-7}	8.93×10^5	28.3
170		7.31×10^{-7}	6.21×10^5	31.4
180		1.28×10^{-6}	4.35×10^5	31.7
Average				27.8
120	0.06	7.04×10^{-8}	2.02×10^6	25.8
140		2.50×10^{-7}	9.37×10^5	27.7
150		4.55×10^{-7}	6.48×10^5	29.4
160		8.14×10^{-7}	4.52×10^5	31.0
170		1.43×10^{-6}	3.18×10^5	33.8
180		2.46×10^{-6}	2.26×10^5	35.6
Average				30.5
120	0.10	2.52×10^{-7}	5.63×10^5	35.4
140		8.57×10^{-7}	2.73×10^5	38.6
150		1.53×10^{-6}	1.93×10^5	39.7
160		2.66×10^{-6}	1.38×10^5	43.8
170		4.55×10^{-6}	9.98×10^4	46.5
180		7.63×10^{-6}	7.28×10^4	49.0
Average				42.2

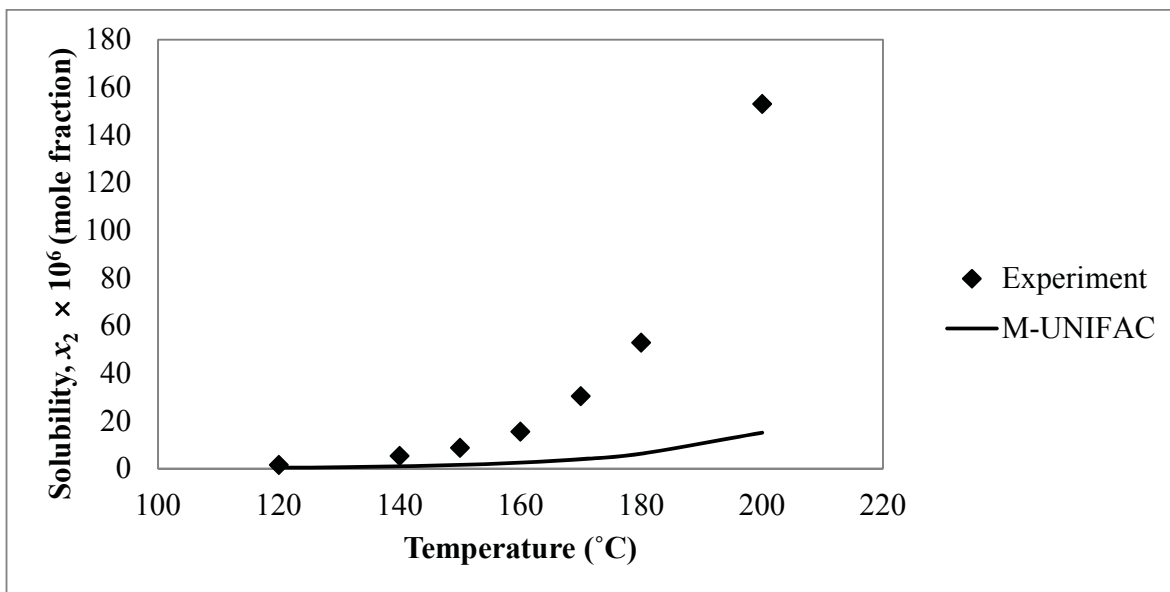


Figure 5.40: Experimental and M-UNIFAC calculated solubility as a function of temperature in subcritical water (1) – anthracene (2) system

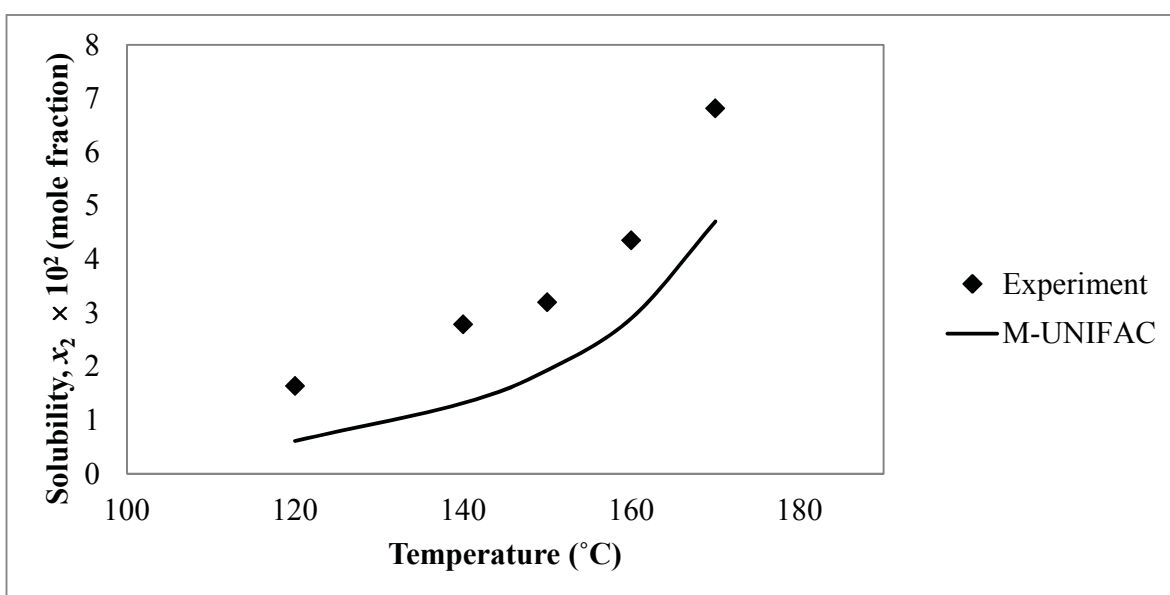


Figure 5.41: Experimental and M-UNIFAC calculated solubility as a function of temperature in subcritical ethanol (1) – anthracene (2) system

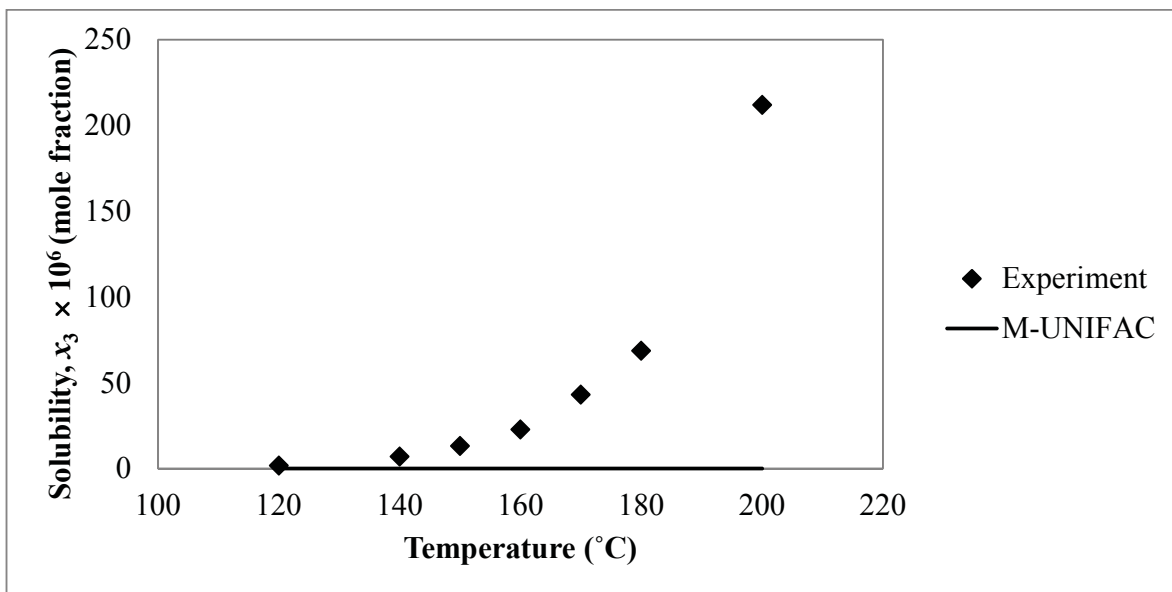


Figure 5.42: Experimental and M-UNIFAC calculated solubility as a function of temperature in subcritical water (1) – ethanol (2) – anthracene (3) system, $f = 0.01$

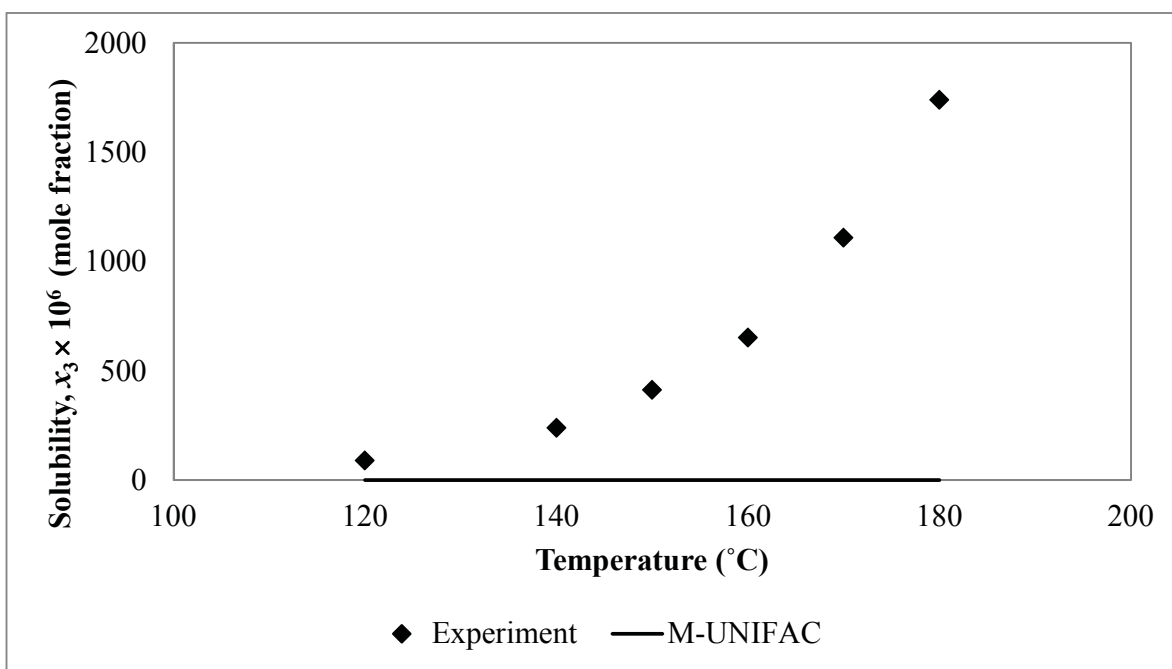


Figure 5.43: Experimental and M-UNIFAC calculated solubility as a function of temperature in subcritical water (1) – ethanol (2) – anthracene (3) system, $f = 0.10$

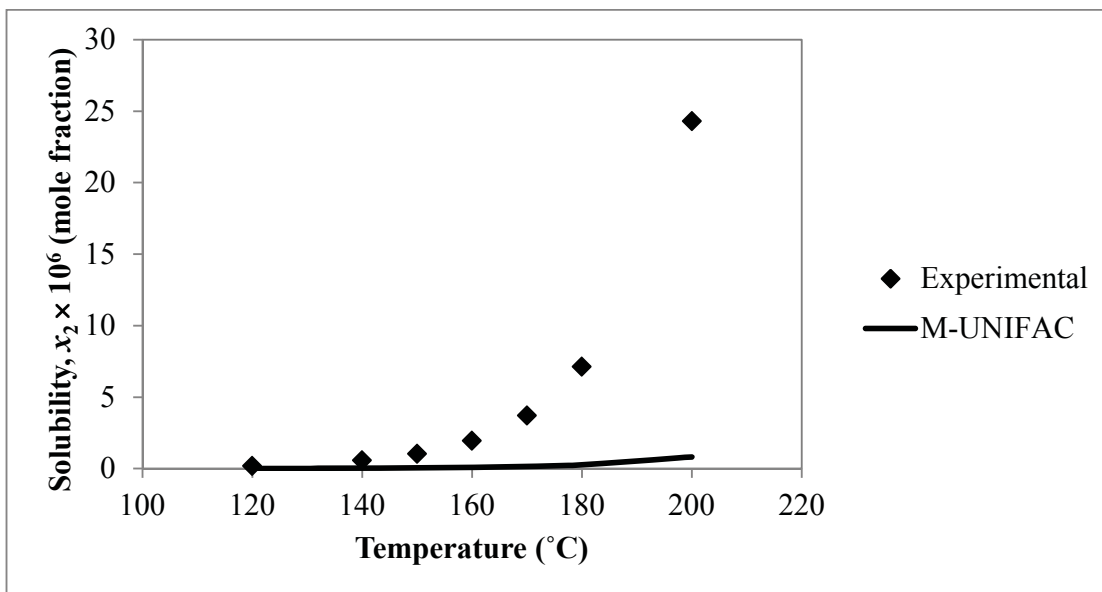


Figure 5.44: Experimental and M-UNIFAC calculated solubility as a function of temperature in subcritical water (1) – *p*-terphenyl (2) system

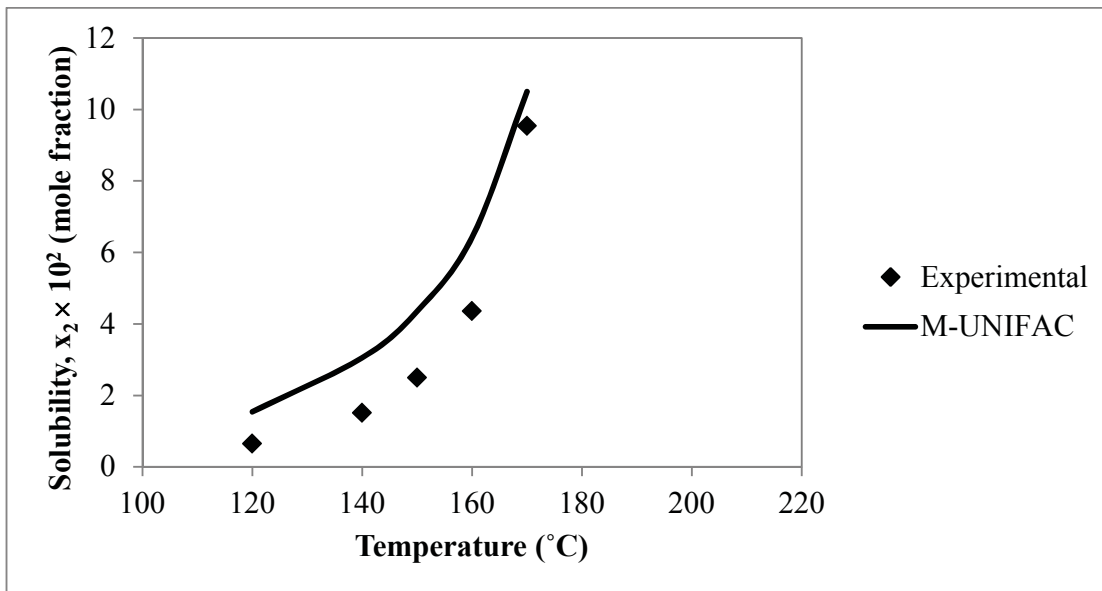


Figure 5.45: Experimental and M-UNIFAC calculated solubility as a function of temperature in subcritical ethanol (1) – *p*-terphenyl (2) system

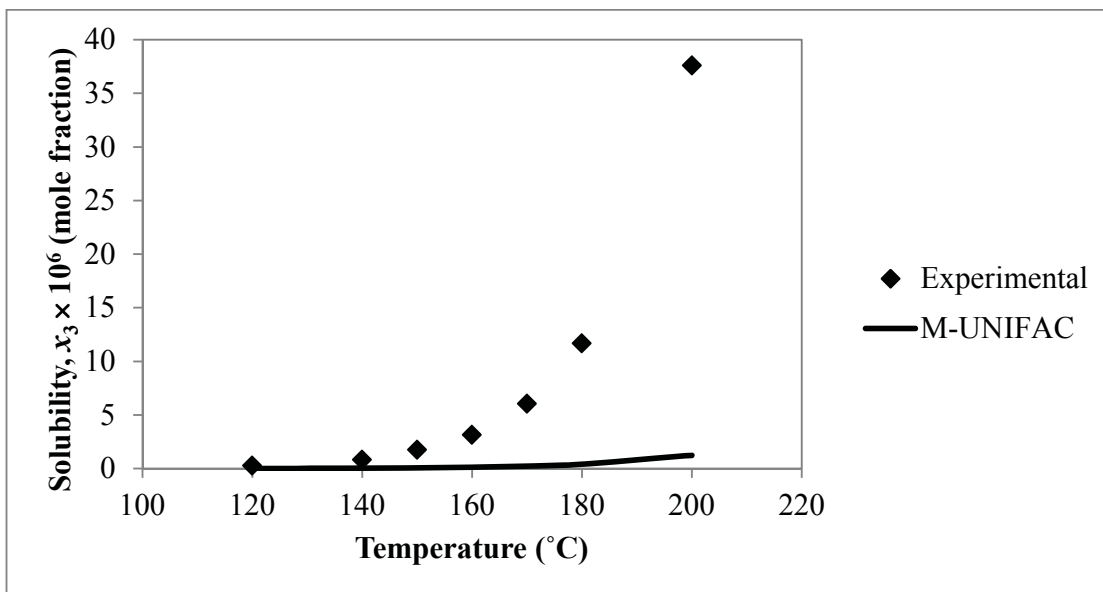


Figure 5.46: Experimental and M-UNIFAC calculated solubility as a function of temperature in subcritical water (1) – ethanol (2) – *p*-terphenyl (3) system, $f = 0.01$

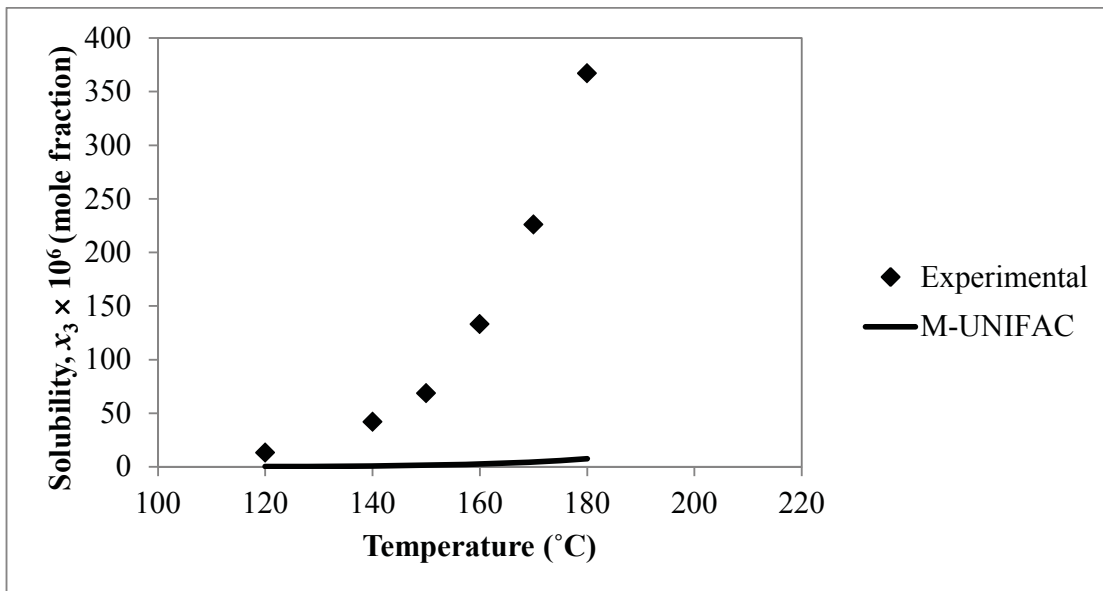


Figure 5.47: Experimental and M-UNIFAC calculated solubility as a function of temperature in subcritical water (1) – ethanol (2) – *p*-terphenyl (3) system, $f = 0.10$

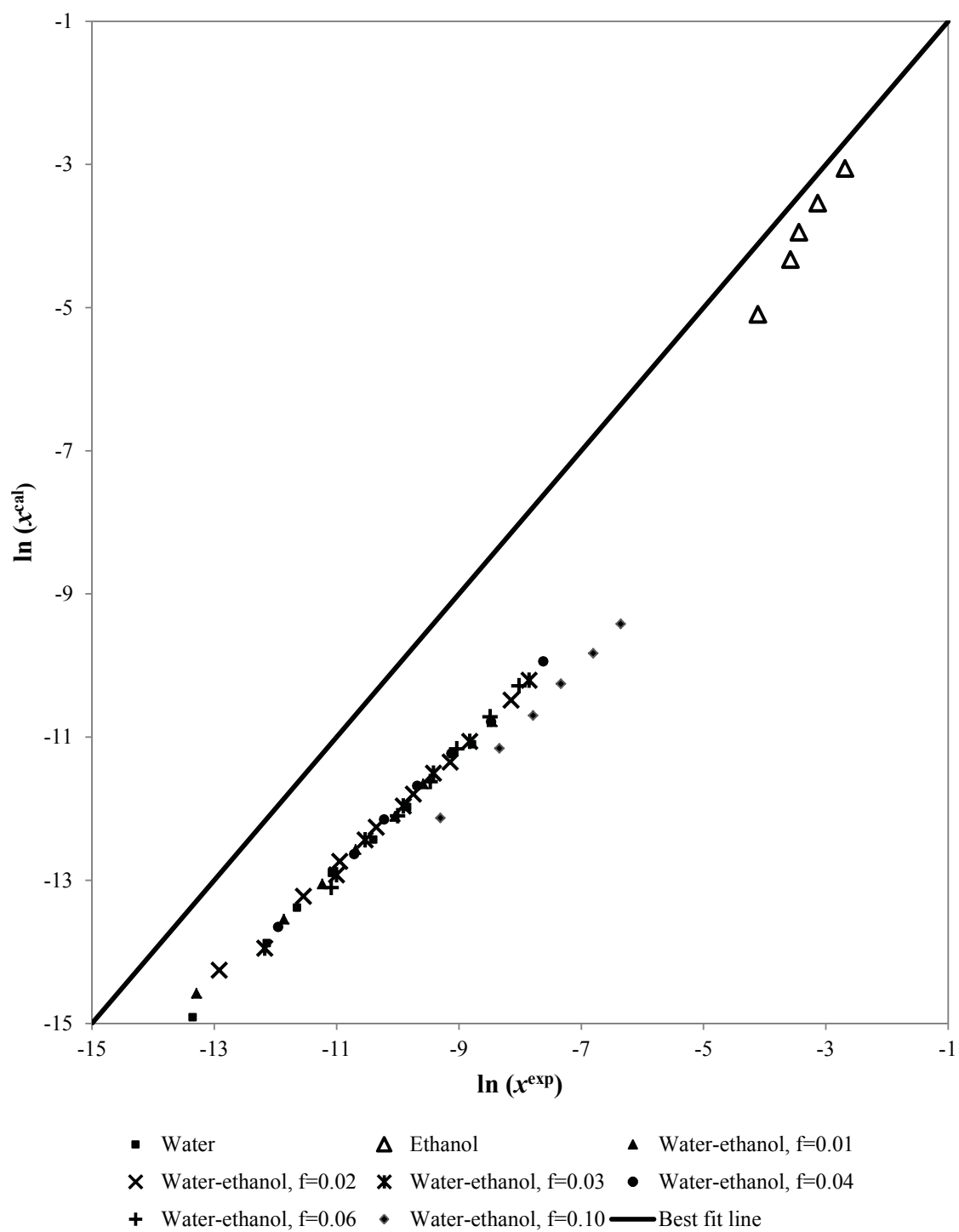


Figure 5.48: Deviation between M-UNIFAC calculated and experimental values: anthracene in subcritical water, subcritical ethanol and ethanol-modified subcritical water

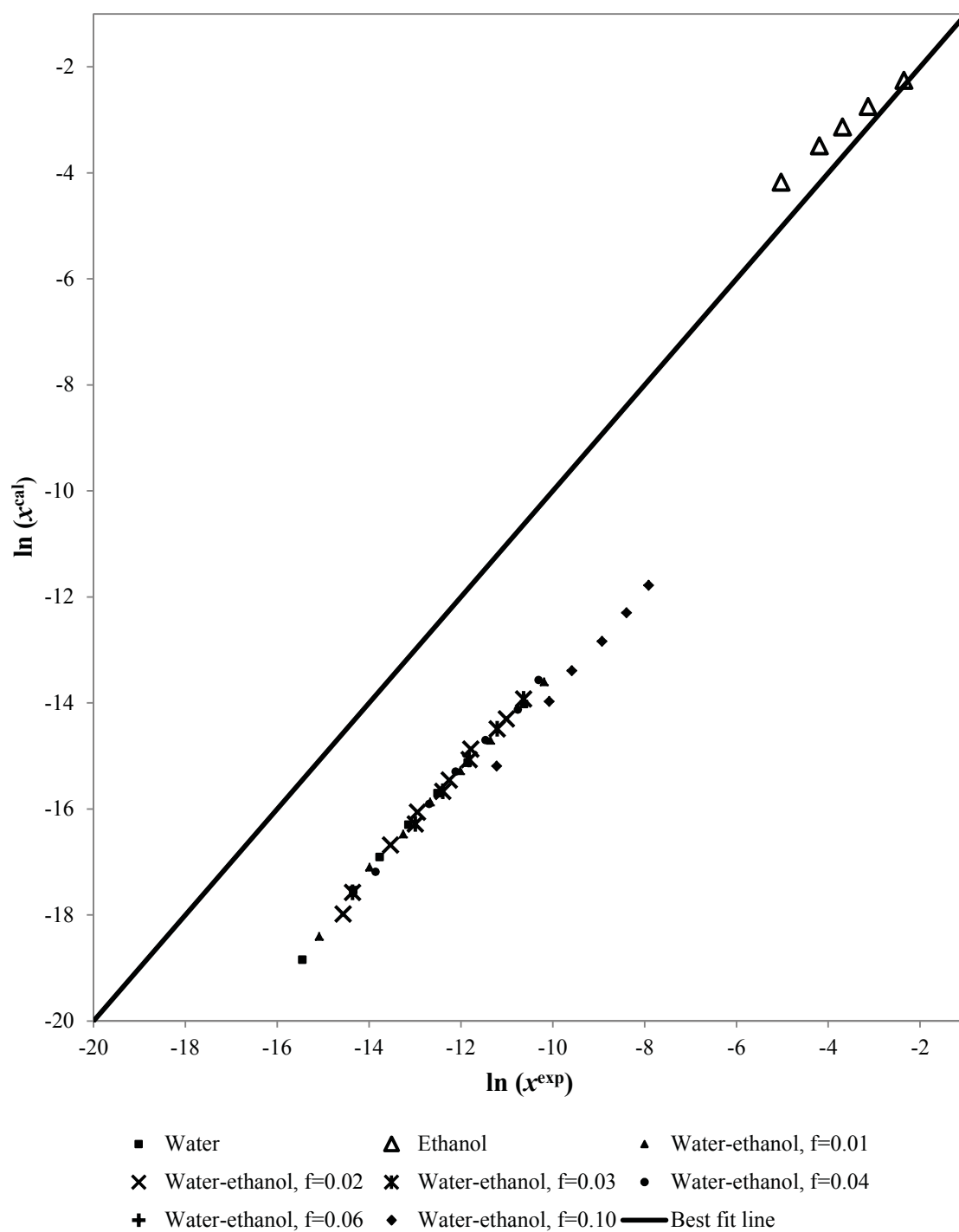


Figure 5.49: Deviation between M-UNIFAC calculated and experimental values: *p*-terphenyl in subcritical water, subcritical ethanol and ethanol-modified subcritical water

The M-UNIFAC has been used to predict the solubilities of anthracene and *p*-terphenyl in the ternary mixtures with poor results. The solubility values and the activity coefficients calculated from the M-UNIFAC model are given in Table 5.34 while the absolute standard deviations obtained are given in Table 5.35. Comparisons between the experimental and the M-UNIFAC calculated solubilities for both anthracene and *p*-terphenyl are shown in Figure 5.50. Similarities were observed for the predictive power of the M-UNIFAC model in the ternary and binary systems, in that, the M-UNIFAC model becomes less accurate as temperature increases.

Table 5.34: The calculated solubility values and activity coefficients obtained from the M-UNIFAC model for water (1) – anthracene (2) – *p*-terphenyl (3) system at various temperatures

T (°C)	$x_2^{\text{M-UNIFAC}}$	$\gamma_2^{\text{M-UNIFAC}}$	$x_3^{\text{M-UNIFAC}}$	$\gamma_3^{\text{M-UNIFAC}}$
120	3.33×10^{-7}	5.20×10^5	6.53×10^{-9}	2.17×10^7
140	9.40×10^{-7}	6.20×10^4	2.42×10^{-8}	2.49×10^6
150	1.54×10^{-6}	4.61×10^4	4.53×10^{-8}	1.68×10^6
160	2.50×10^{-6}	3.45×10^4	8.34×10^{-8}	1.14×10^6
170	3.99×10^{-6}	2.59×10^4	1.51×10^{-7}	7.77×10^5

Table 5.35: Absolute standard deviation (ASD) obtained with the M-UNIFAC model for water (1) – anthracene (2) – *p*-terphenyl (3) system

Temperature	Anthracene	<i>p</i> -Terphenyl
(°C)	ASD (%)	ASD(%)
120	8.7	17.7
140	11.6	17.9
150	14.6	21.9
160	14.0	19.0
170	15.8	25.8
Average	12.9	20.4

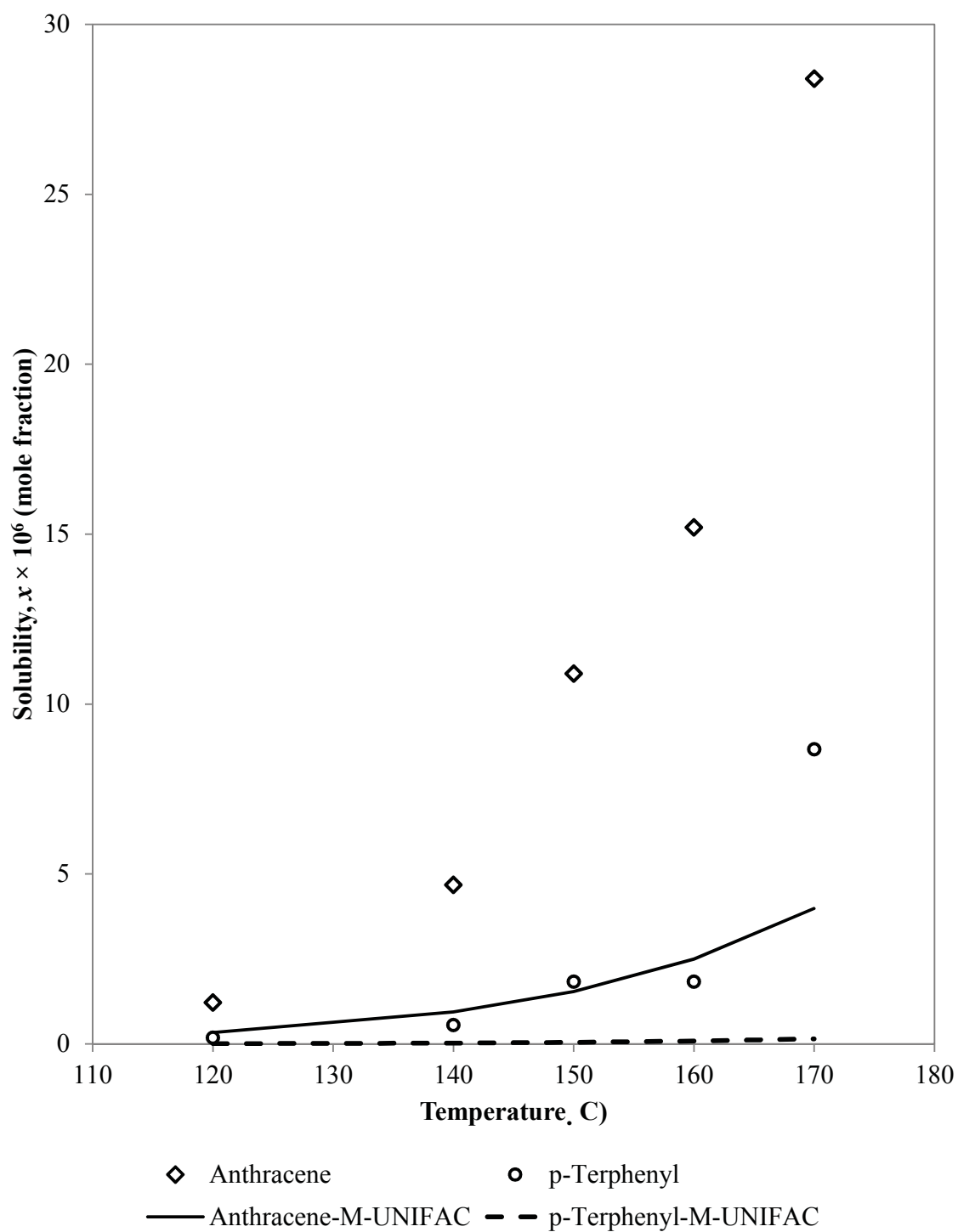


Figure 5.50: Comparisons between the M-UNIFAC calculated and experimental solubility values in ternary water (1) – anthracene (2) – *p*-terphenyl (3) system

5.3.5 Comparing the UNIQUAC, O-UNIFAC and M-UNIFAC models

The solubilities of PAHs in various subcritical systems investigated in this study are shown together with UNIQUAC, O-UNIFAC and M-UNIFAC calculated data in Figures 5.51 - 5.68. The UNIQUAC model was found to provide the best representation of solubility since the binary interaction parameters per binary compounds were matched with experimental data. The extension of the UNIQUAC model to ternary systems also yielded good results. Both O-UNIFAC and M-UNIFAC models performed poorly in both the binary and ternary systems, yielding average absolute standard deviations between 13% and 42%. In water-based solvent systems, both UNIFAC models rarely fall within the same order of magnitude as experimental data, and failed to account for the dramatic rise in solubility with temperature. All three models showed higher deviations from experimental data as ethanol mole fraction increased. Comparisons of their activity coefficients are shown in Figures 5.69 - 5.76.

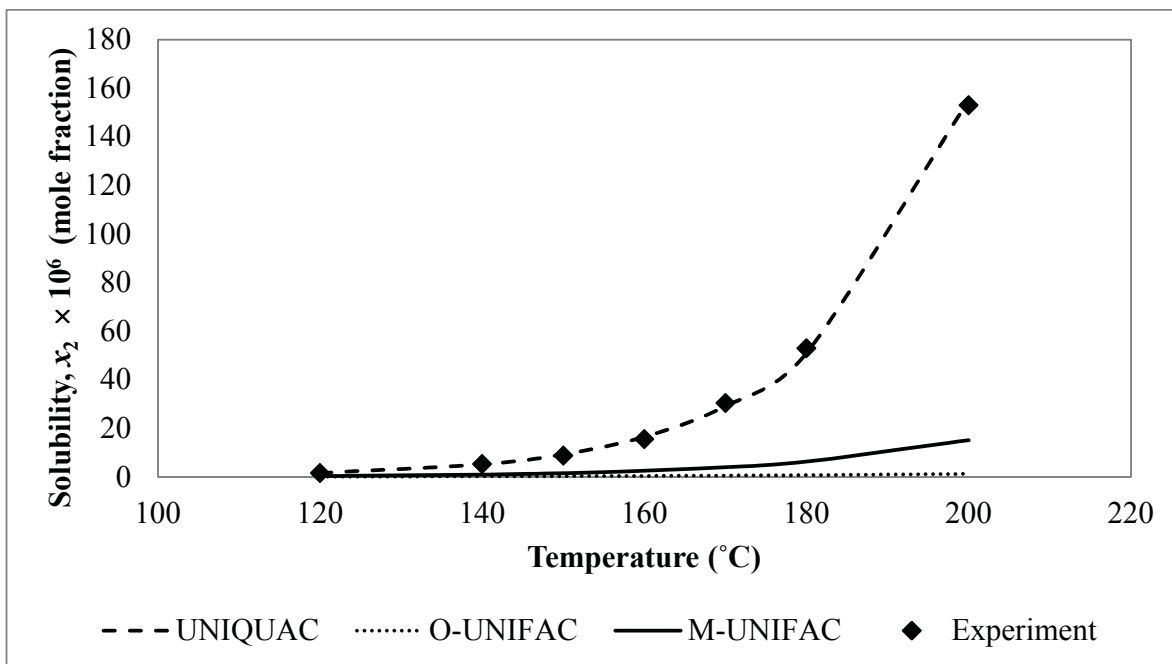


Figure 5.51: Anthracene solubility in subcritical water calculated from various models and in comparison with experimental data

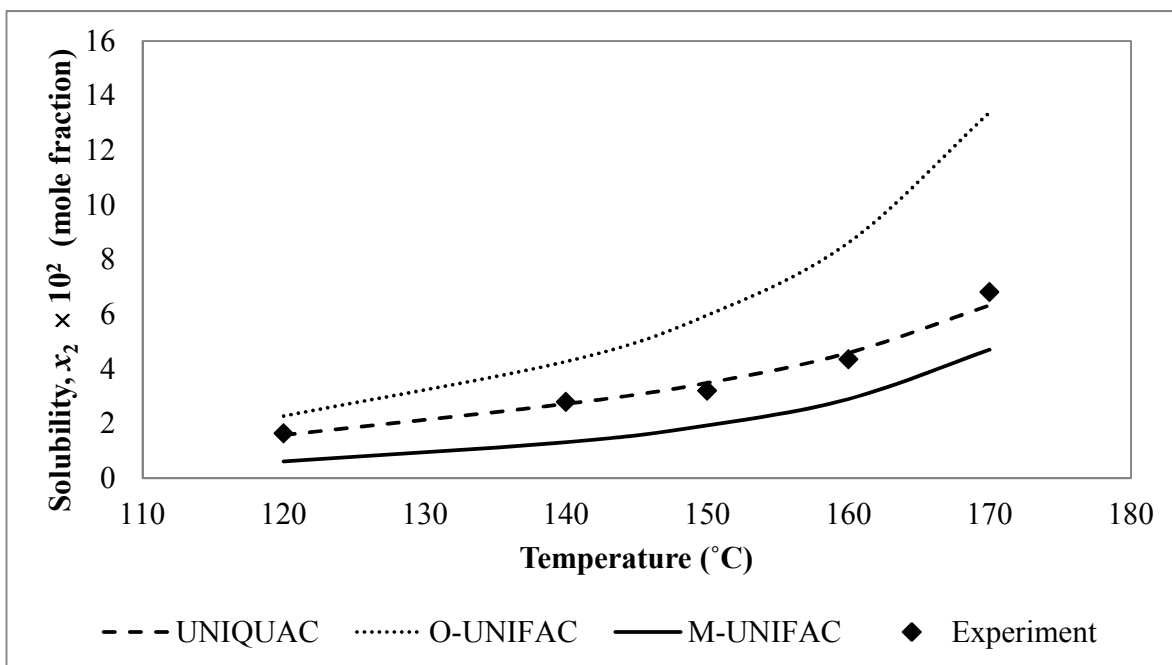


Figure 5.52: Anthracene solubility in subcritical ethanol calculated from various models and in comparison with experimental data

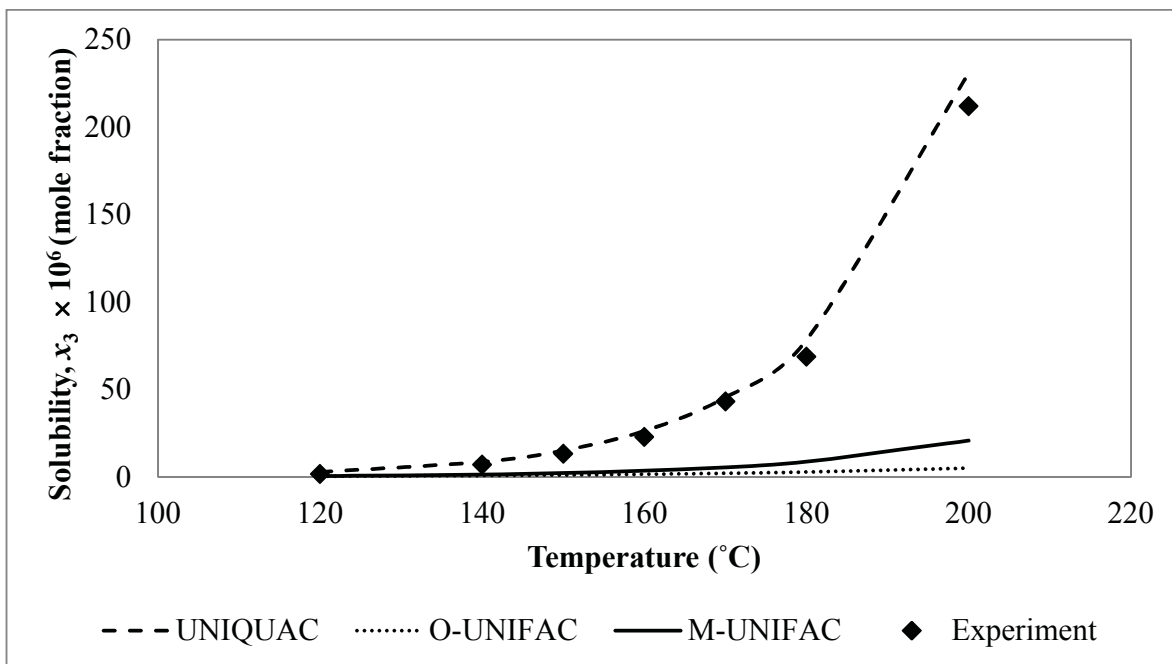


Figure 5.53: Anthracene solubility in ethanol-modified subcritical water calculated from various models and in comparison with experimental data, $f = 0.01$

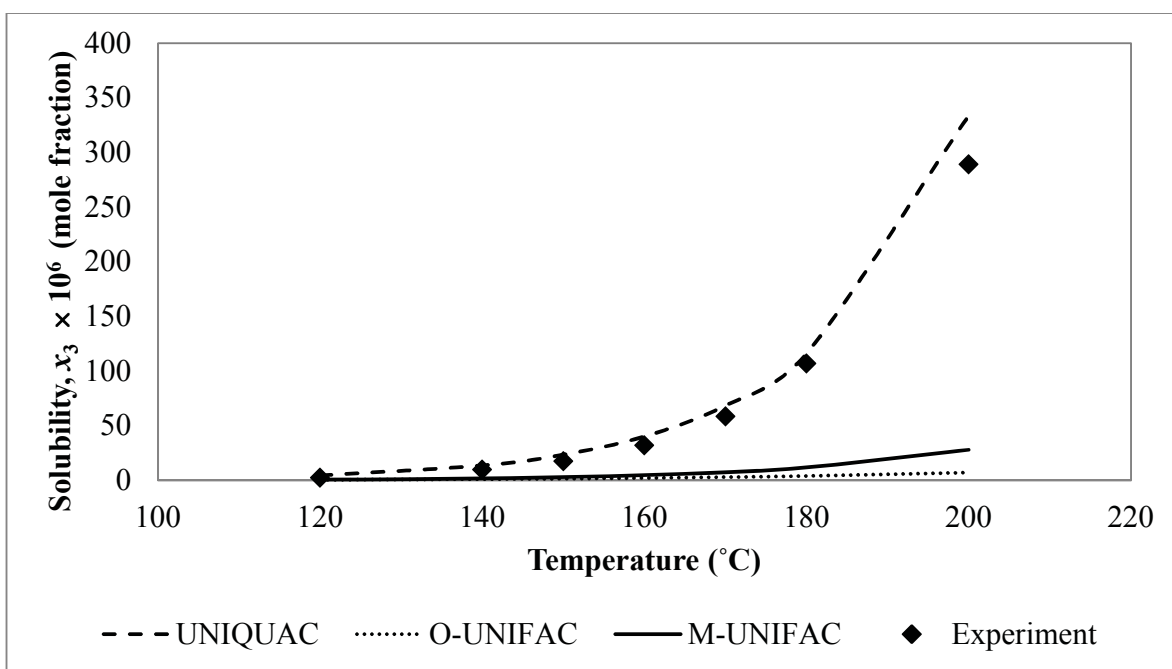


Figure 5.54: Anthracene solubility in ethanol-modified subcritical water calculated from various models and in comparison with experimental data, $f = 0.02$

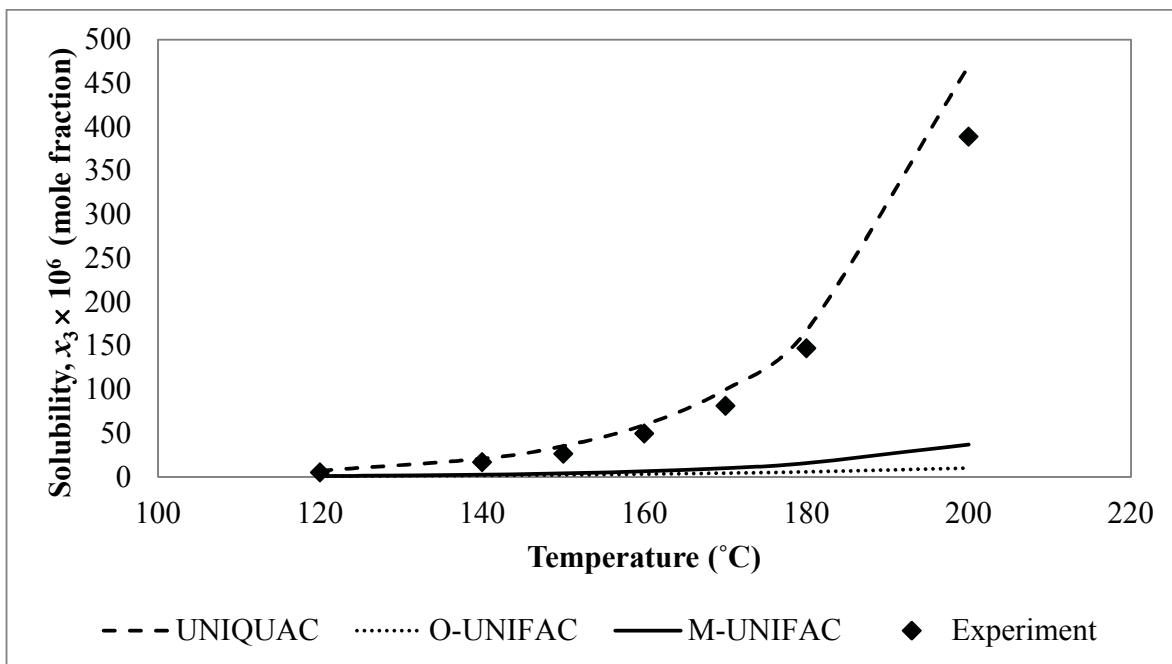


Figure 5.55: Anthracene solubility in ethanol-modified subcritical water calculated from various models and in comparison with experimental data, $f = 0.03$

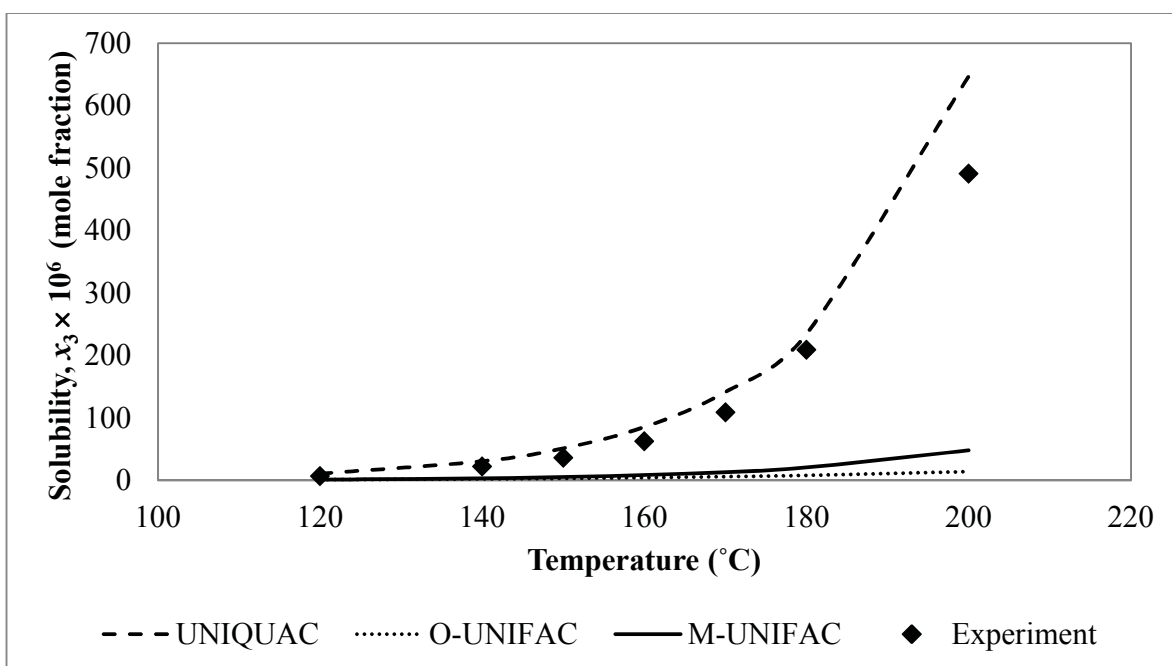


Figure 5.56: Anthracene solubility in ethanol-modified subcritical water calculated from various models and in comparison with experimental data, $f = 0.04$

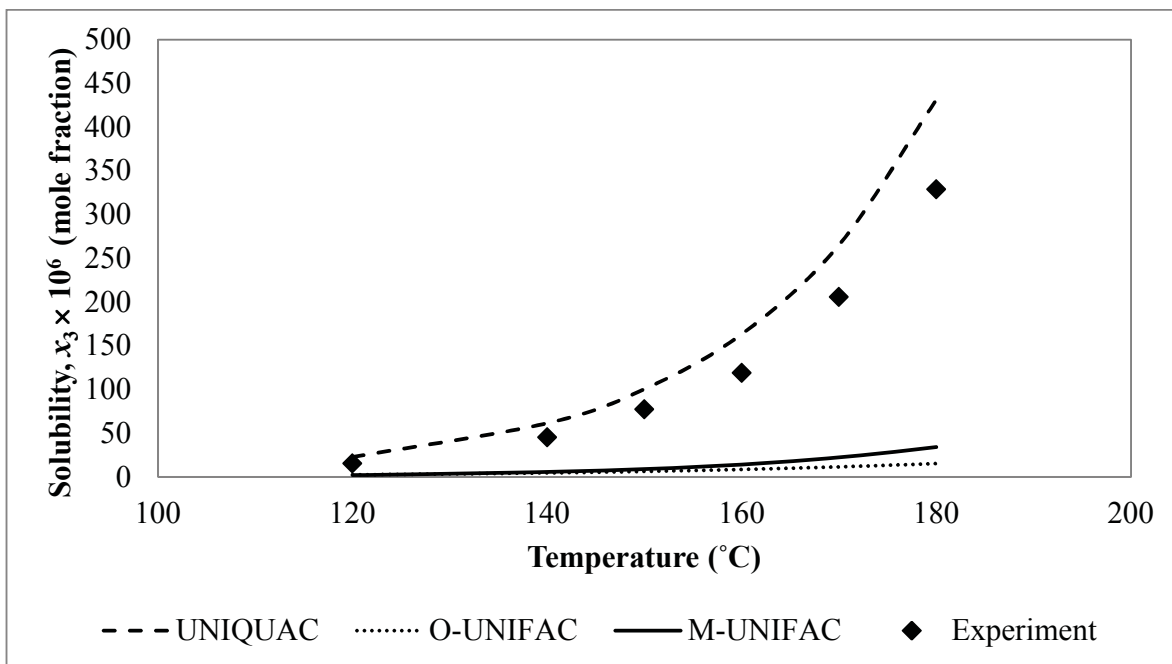


Figure 5.57: Anthracene solubility in ethanol-modified subcritical water calculated from various models and in comparison with experimental data, $f = 0.06$

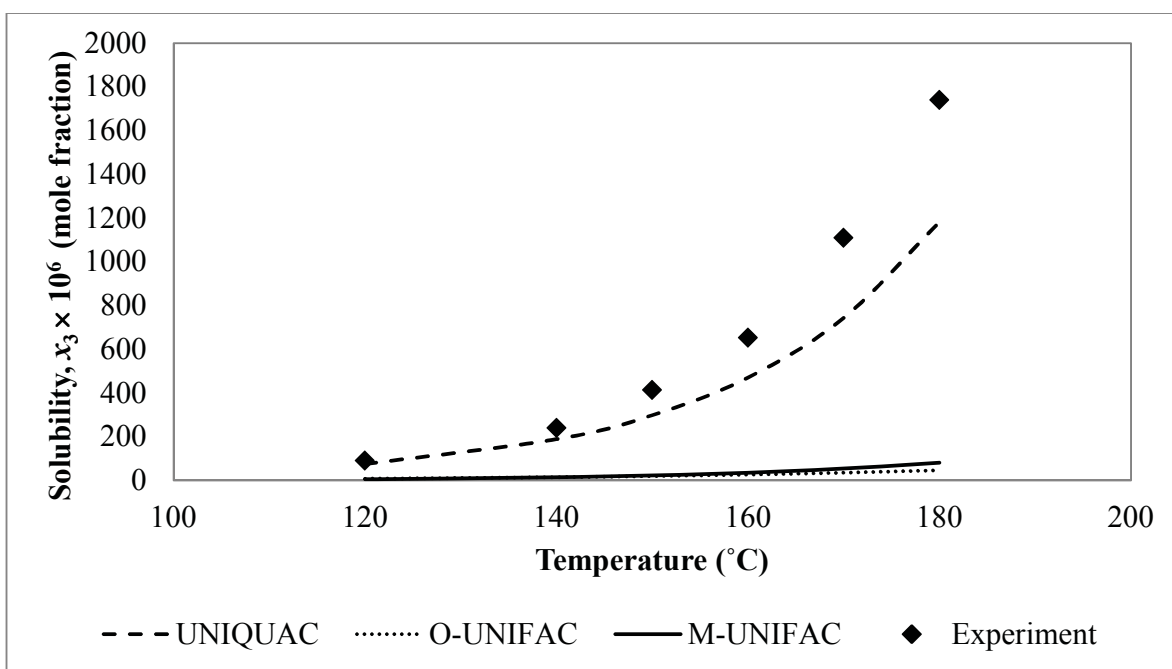


Figure 5.58: Anthracene solubility in ethanol-modified subcritical water calculated from various models and in comparison with experimental data, $f = 0.10$

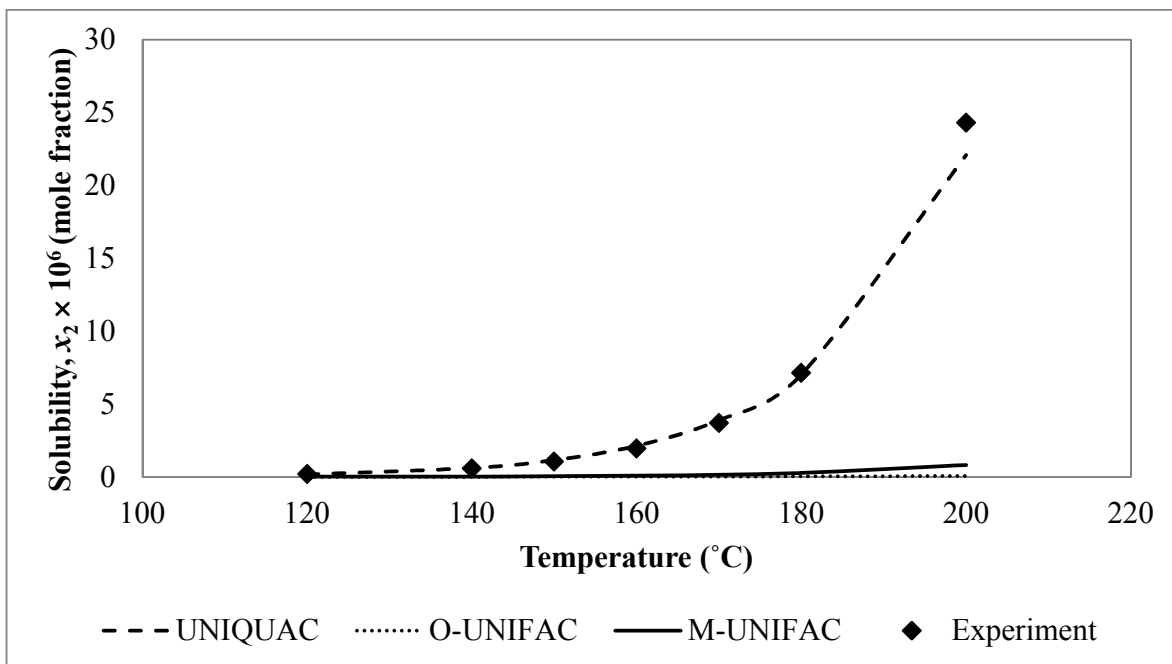


Figure 5.59: *p*-Terphenyl solubility in subcritical water calculated from various models and in comparison with experimental data

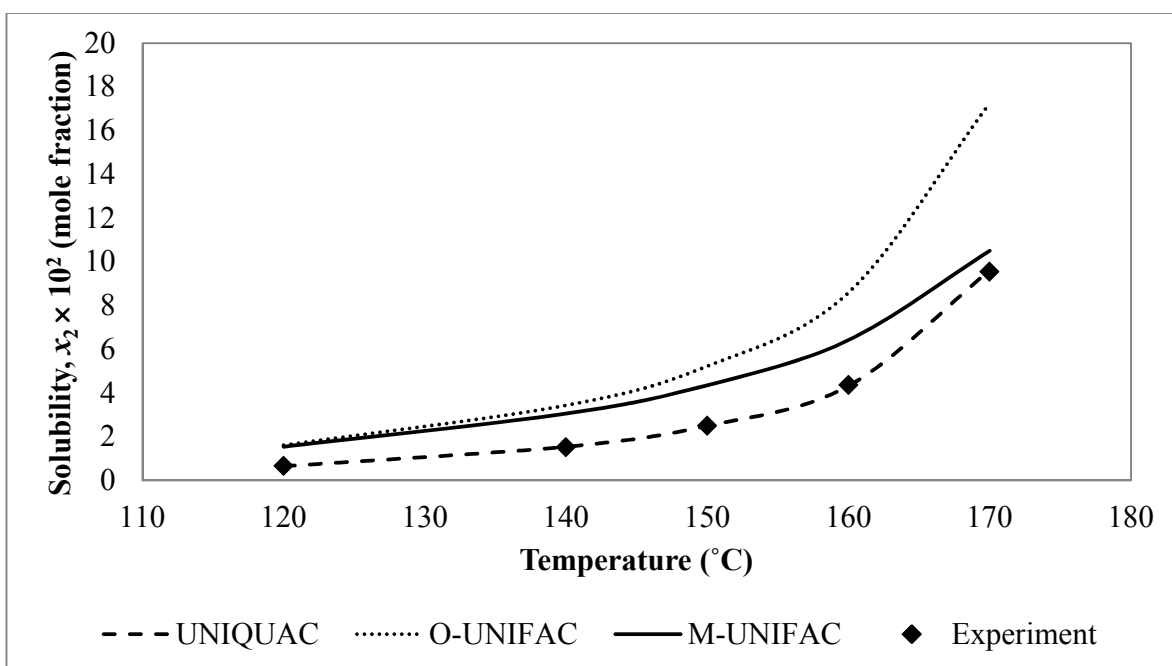


Figure 5.60: *p*-Terphenyl solubility in subcritical ethanol calculated from various models and in comparison with experimental data

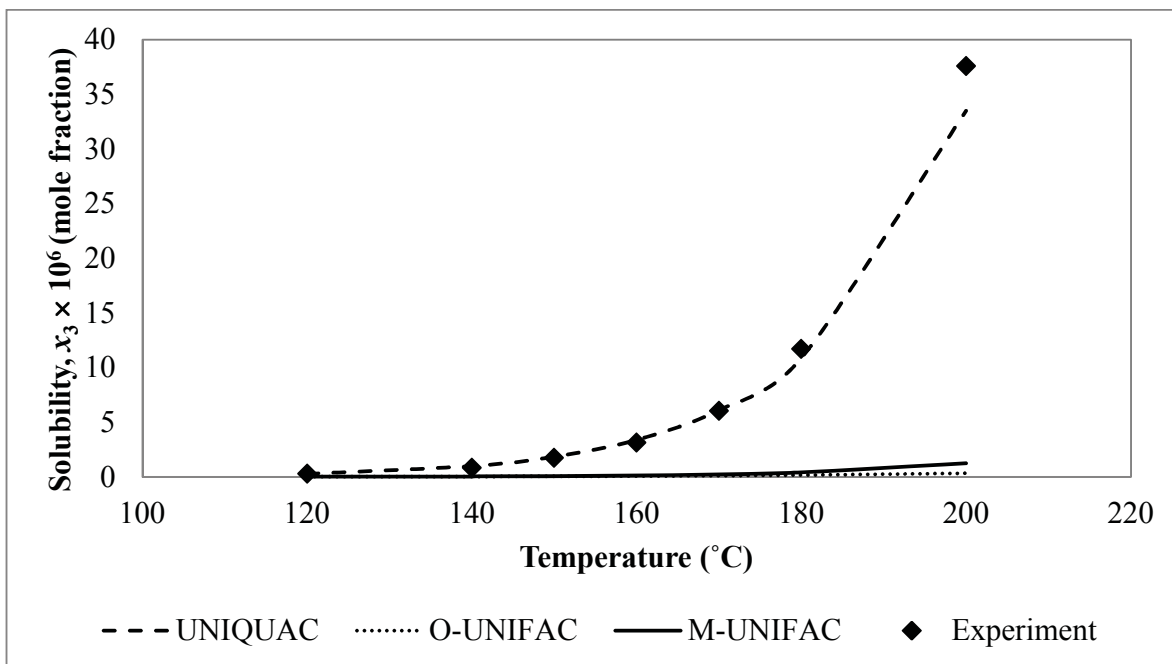


Figure 5.61: *p*-Terphenyl solubility in ethanol-modified subcritical water calculated from various models and in comparison with experimental data, $f = 0.01$

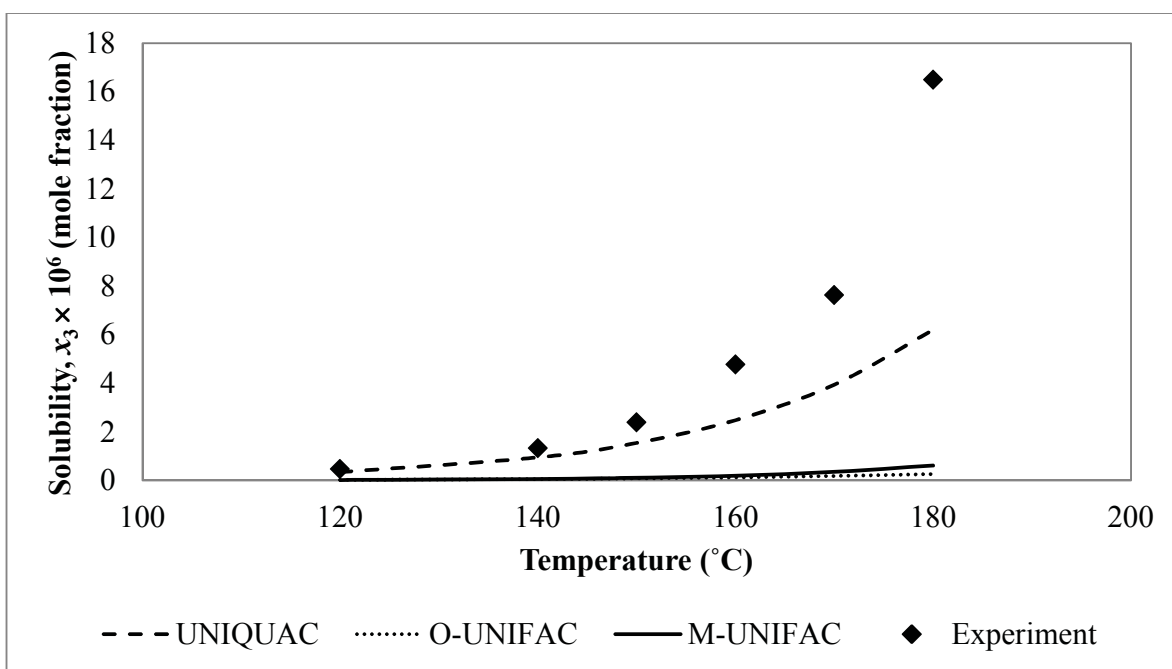


Figure 5.62: *p*-Terphenyl solubility in ethanol-modified subcritical water calculated from various models and in comparison with experimental data, $f = 0.02$

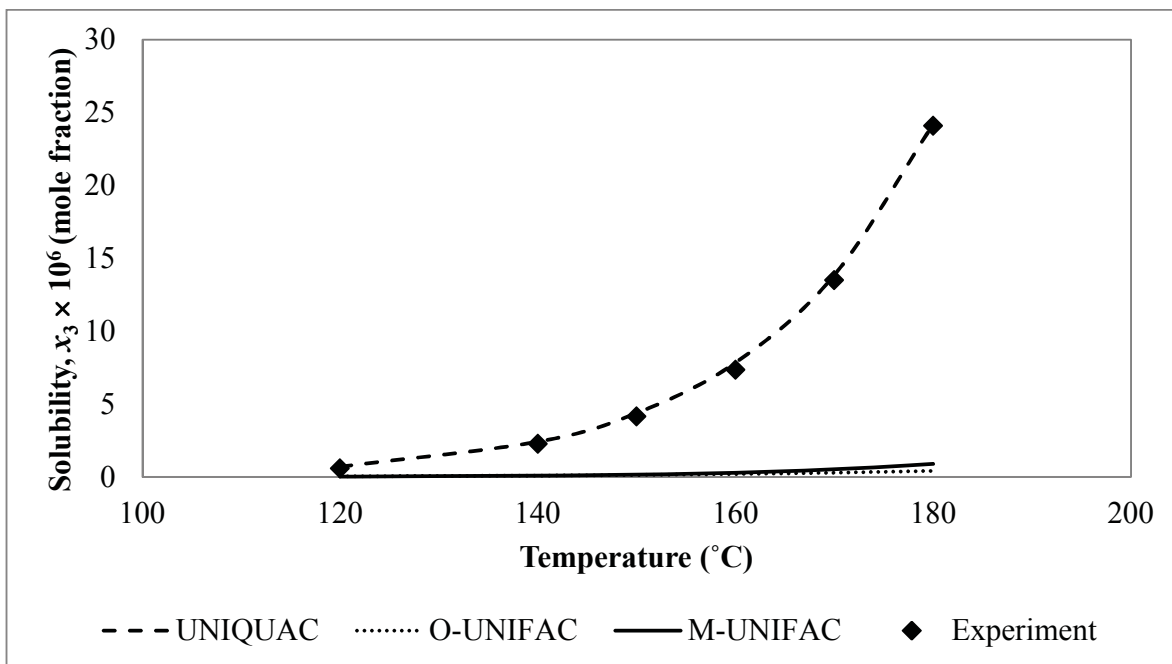


Figure 5.63: *p*-Terphenyl solubility in ethanol-modified subcritical water calculated from various models and in comparison with experimental data, $f = 0.03$

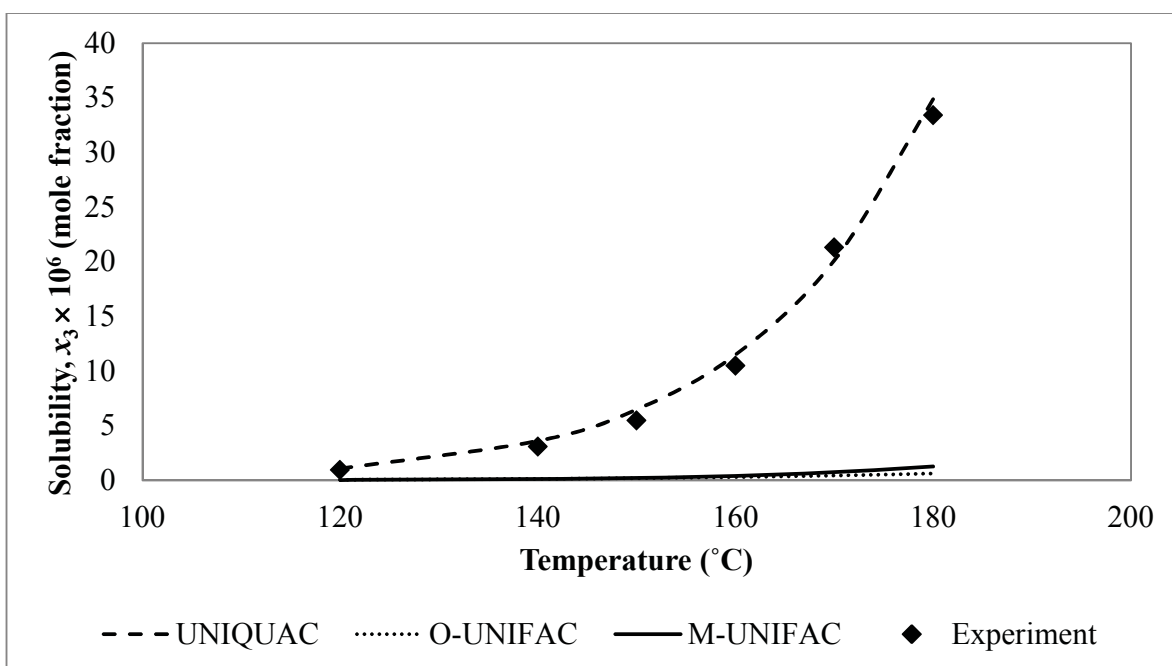


Figure 5.64: *p*-Terphenyl solubility in ethanol-modified subcritical water calculated from various models and in comparison with experimental data, $f = 0.04$

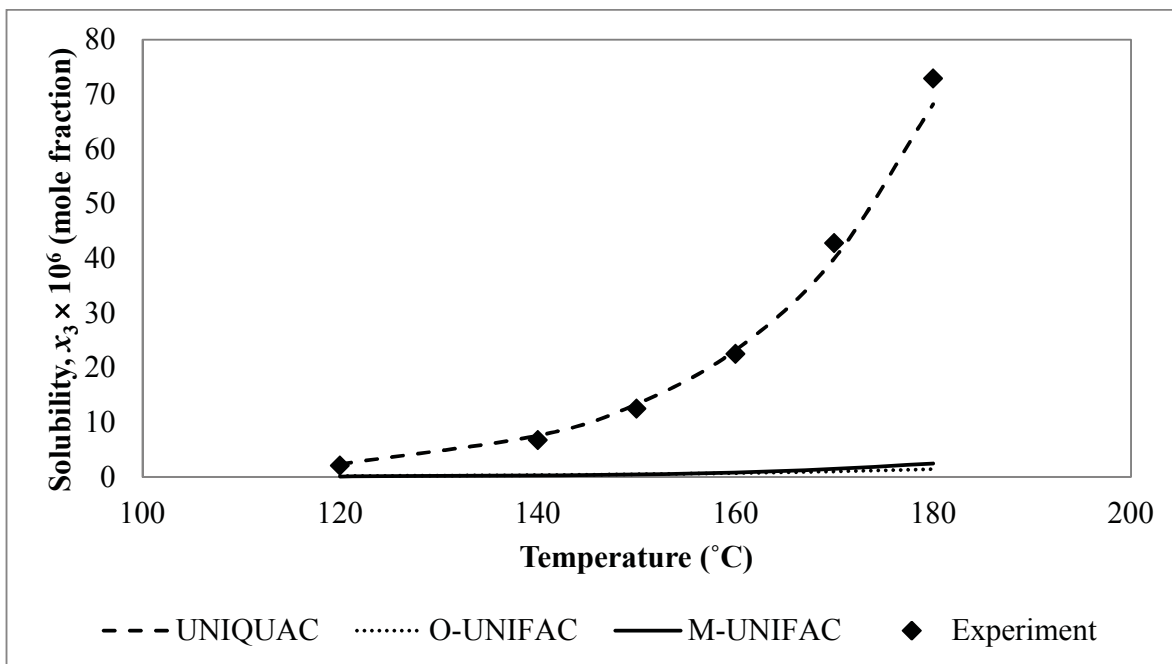


Figure 5.65: p -Terphenyl solubility in ethanol-modified subcritical water calculated from various models and in comparison with experimental data, $f = 0.06$

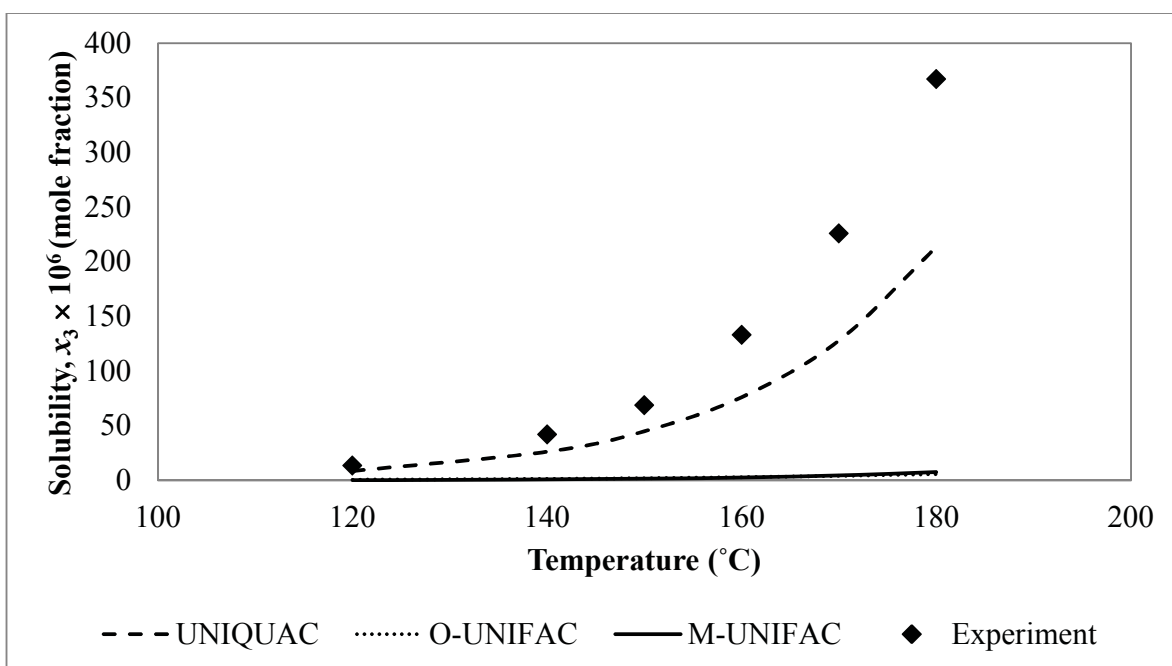


Figure 5.66: p -Terphenyl solubility in ethanol-modified subcritical water calculated from various models and in comparison with experimental data, $f = 0.10$

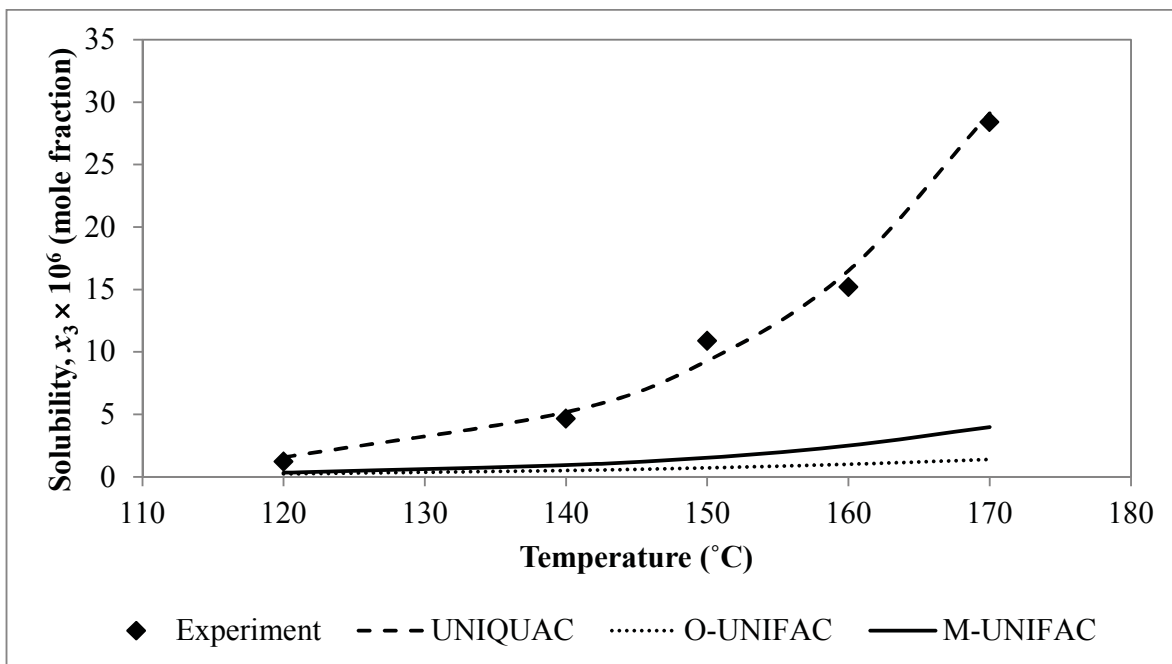


Figure 5.67: Anthracene solubility in water (1) – anthracene (2) – *p*-terphenyl (3) system calculated from various models and in comparison with experimental data

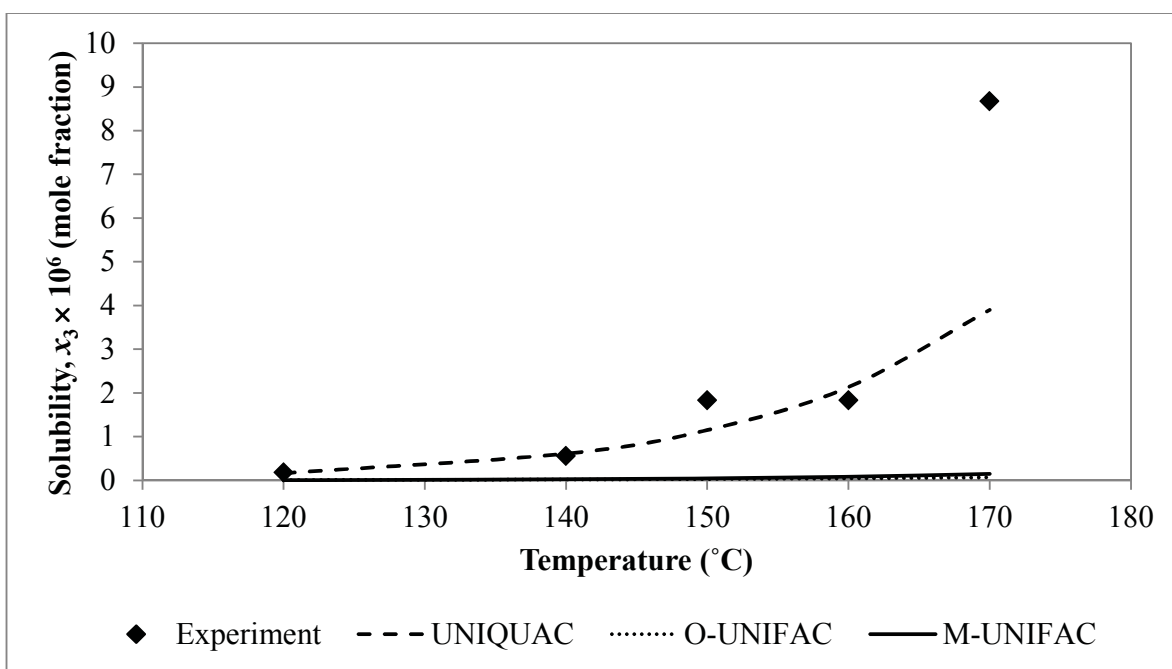
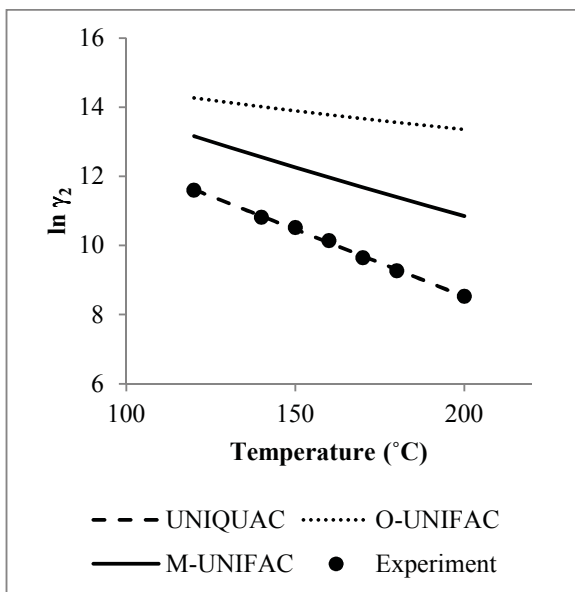
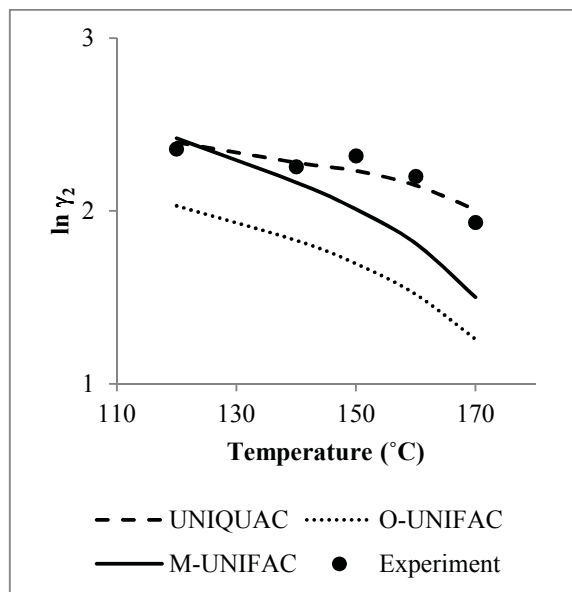


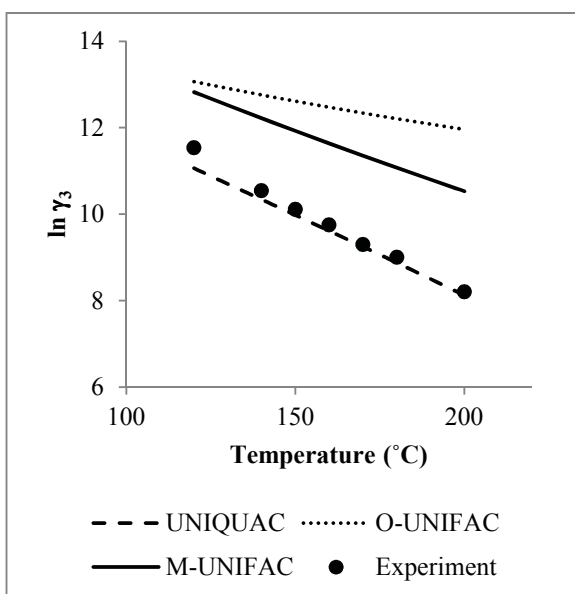
Figure 5.68: *p*-Terphenyl solubility in water (1) – anthracene (2) – *p*-terphenyl (3) system calculated from various models and in comparison with experimental data



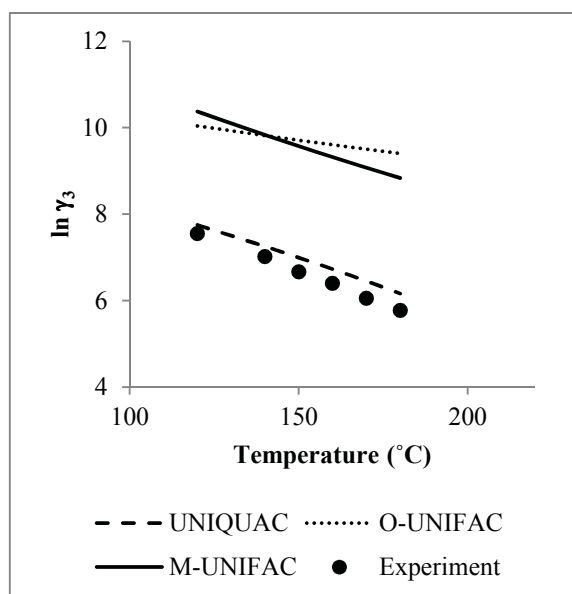
(a) subcritical water



(b) subcritical ethanol

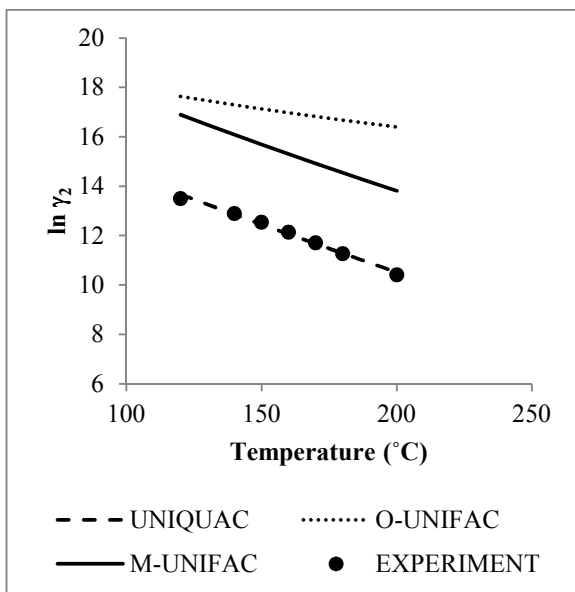


(c) subcritical water/ethanol, $f = 0.01$

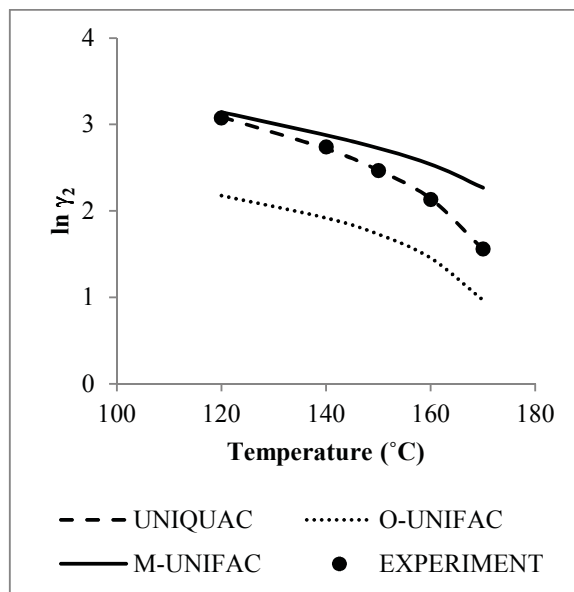


(b) subcritical water/ethanol, $f = 0.10$

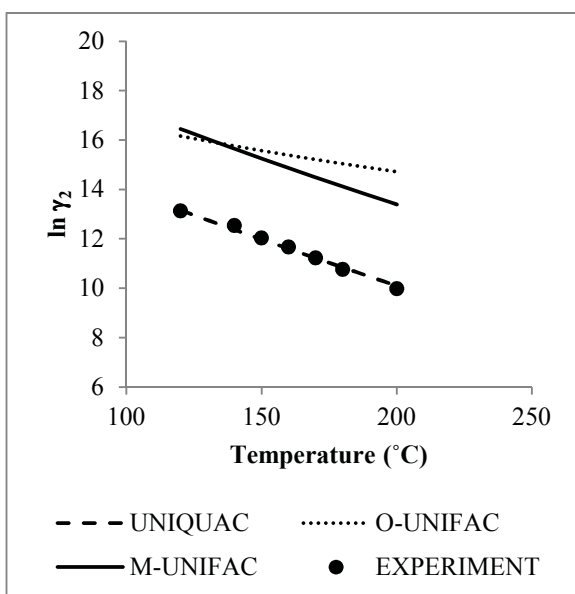
Figure 5.69 : Natural logarithm of activity coefficient as a function of temperature for anthracene in various subcritical solvent systems



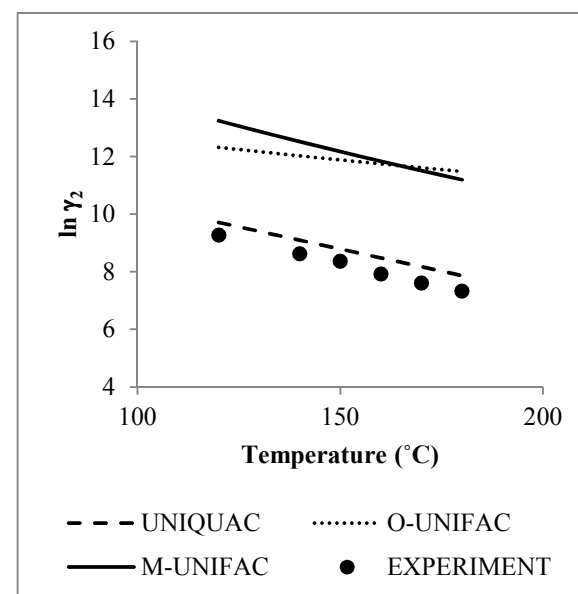
(a) subcritical water



(b) subcritical ethanol

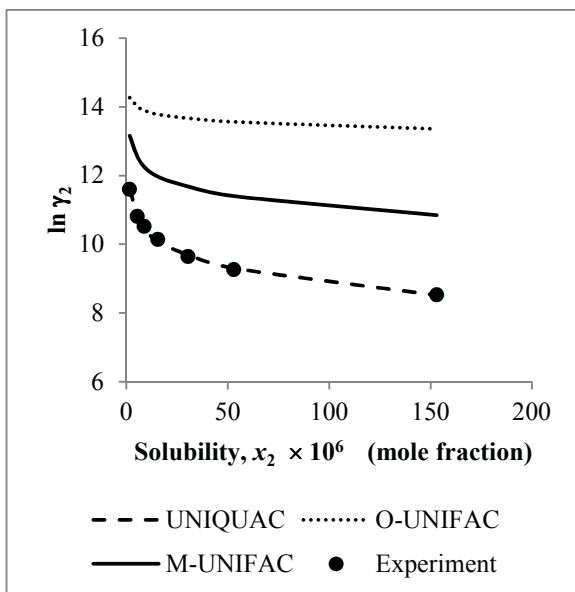


(c) subcritical water/ethanol, $f = 0.01$

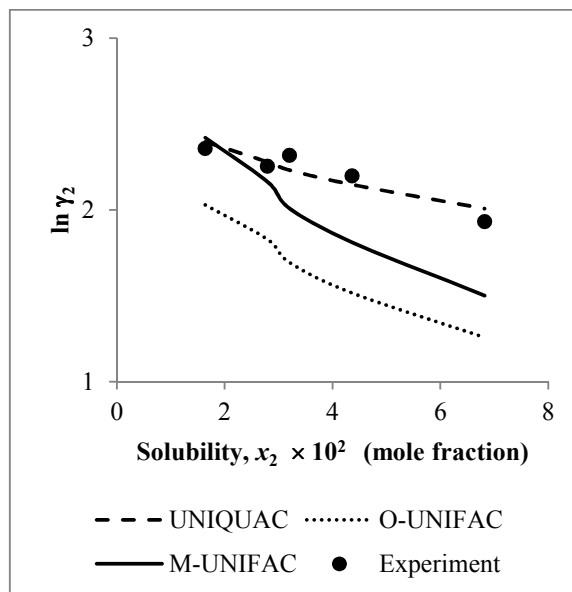


(b) subcritical water/ethanol, $f = 0.10$

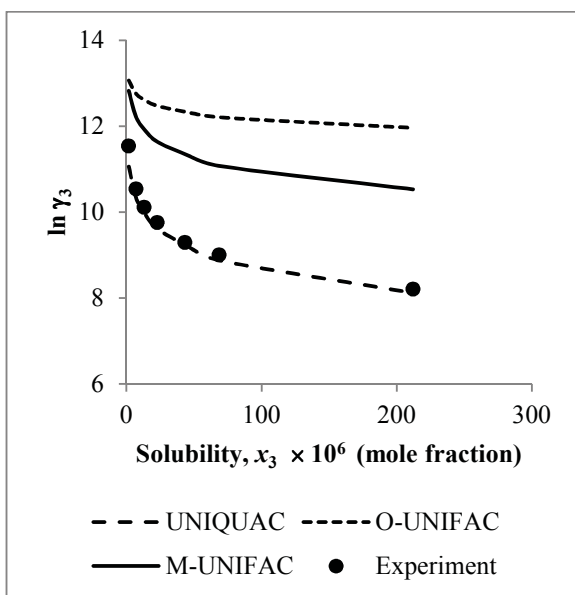
Figure 5.70: Natural logarithm of activity coefficient as a function of temperature for *p*-terphenyl in various subcritical solvent systems



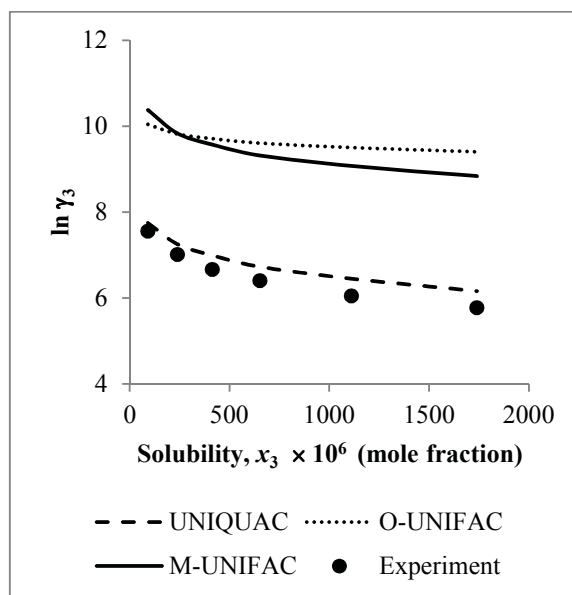
(a) subcritical water



(b) subcritical ethanol

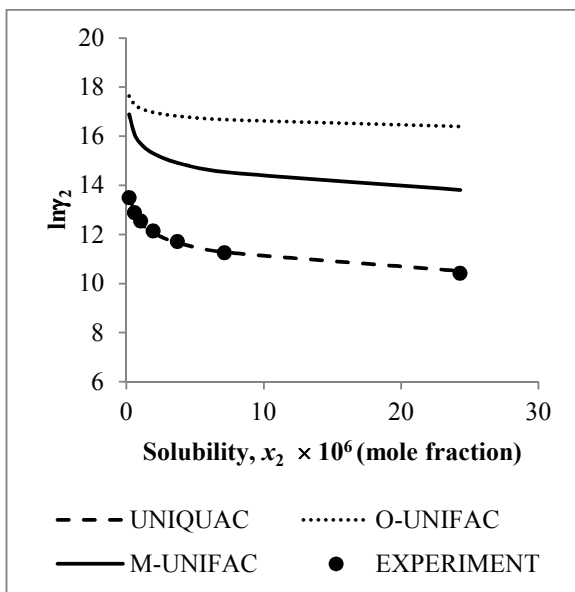


(c) subcritical water/ethanol, $f=0.01$

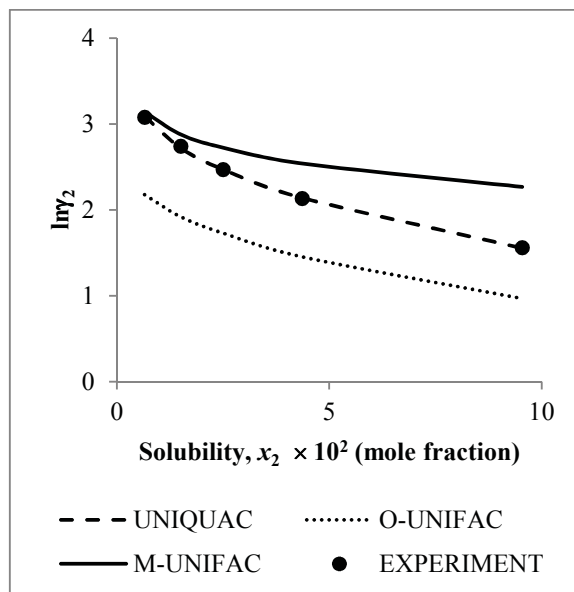


(b) subcritical water/ethanol, $f=0.10$

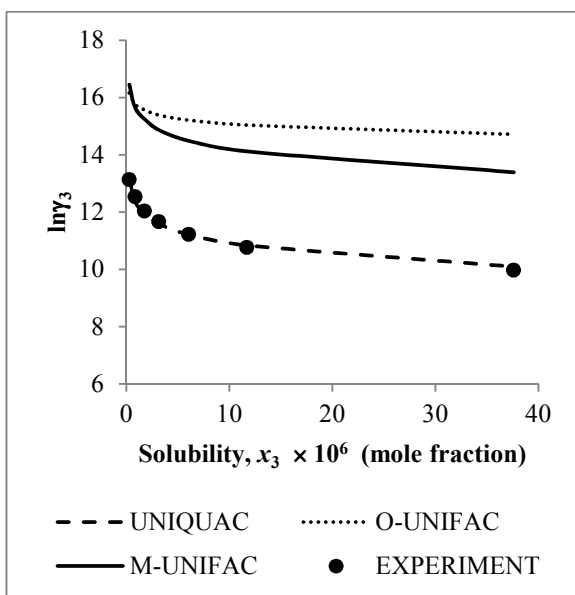
Figure 5.71: Natural logarithm of activity coefficient as a function of anthracene solubility in various subcritical solvent systems



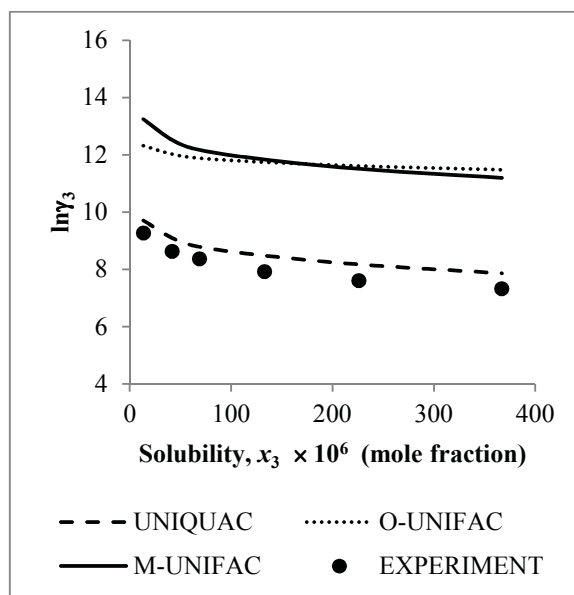
(a) subcritical water



(b) subcritical ethanol

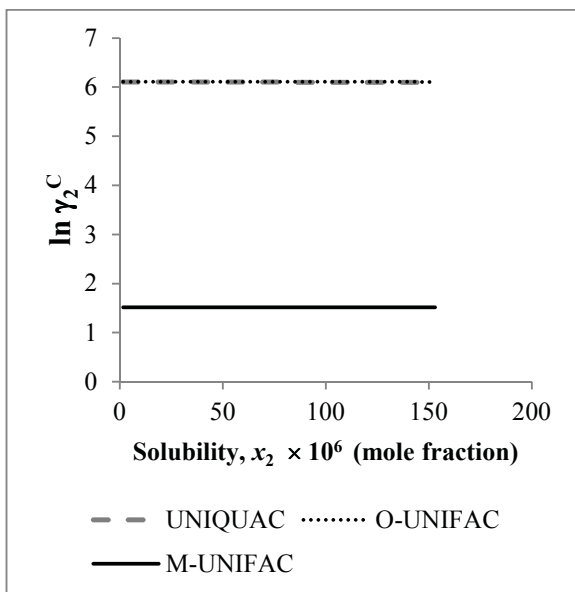


(c) subcritical water/ethanol, $f=0.01$

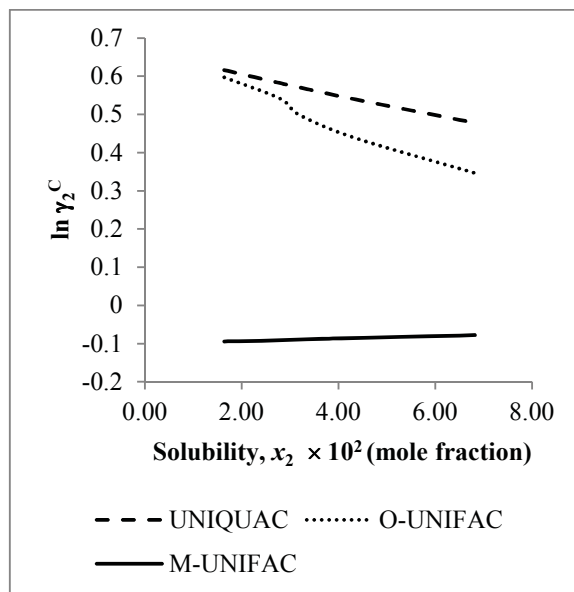


(b) subcritical water/ethanol, $f=0.10$

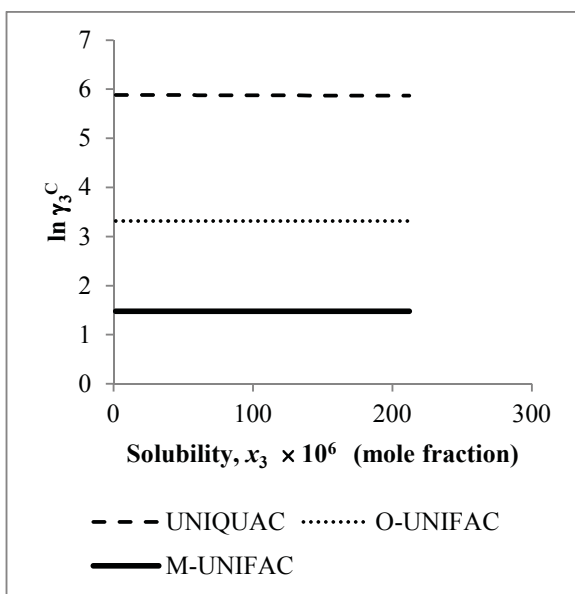
Figure 5.72 : Natural logarithm of activity coefficient as a function of *p*-terphenyl solubility in various subcritical solvent systems



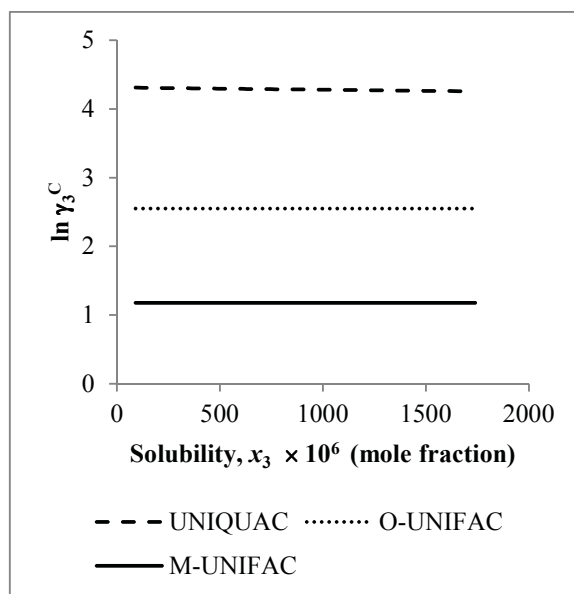
(a) subcritical water



(b) subcritical ethanol



(c) subcritical water/ethanol, $f = 0.01$



(b) subcritical water/ethanol, $f = 0.10$

Figure 5.73: $\ln \gamma^C$ as a function of anthracene solubility in various subcritical solvent systems

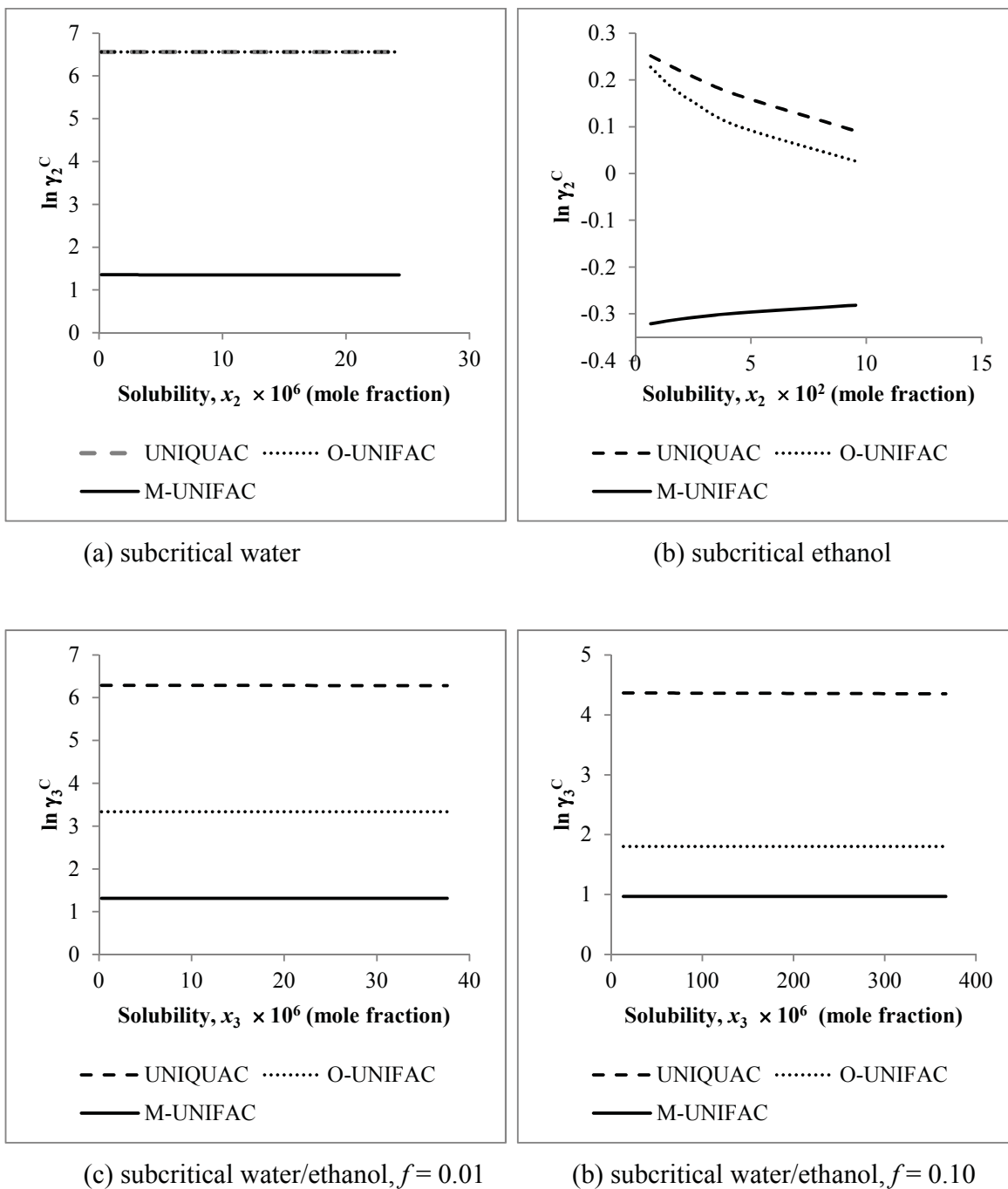


Figure 5.74: $\ln \gamma^C$ as a function of p -terphenyl solubility in various subcritical solvent systems

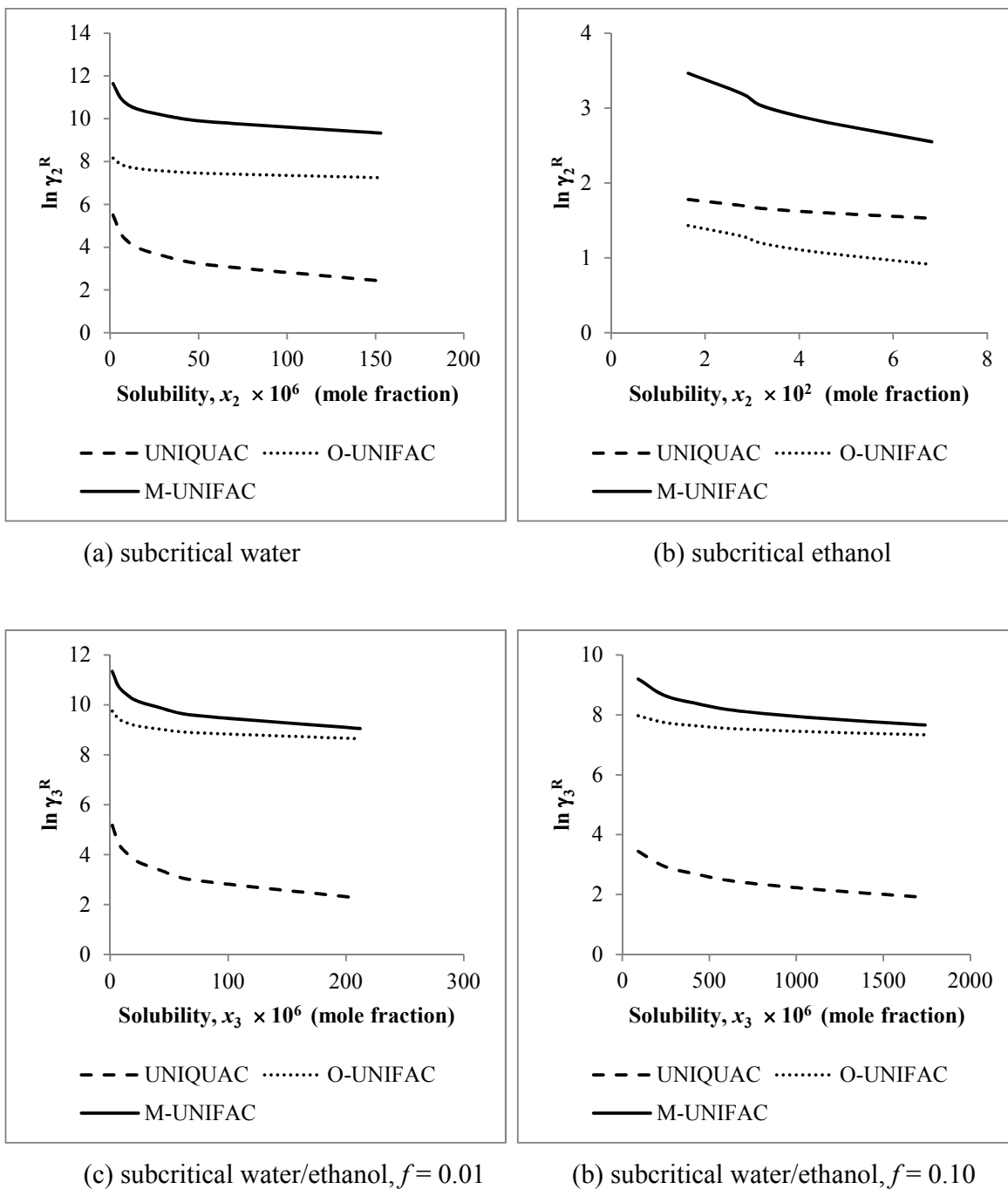


Figure 5.75: $\ln \gamma^R$ as a function of anthracene solubility in various subcritical solvent systems

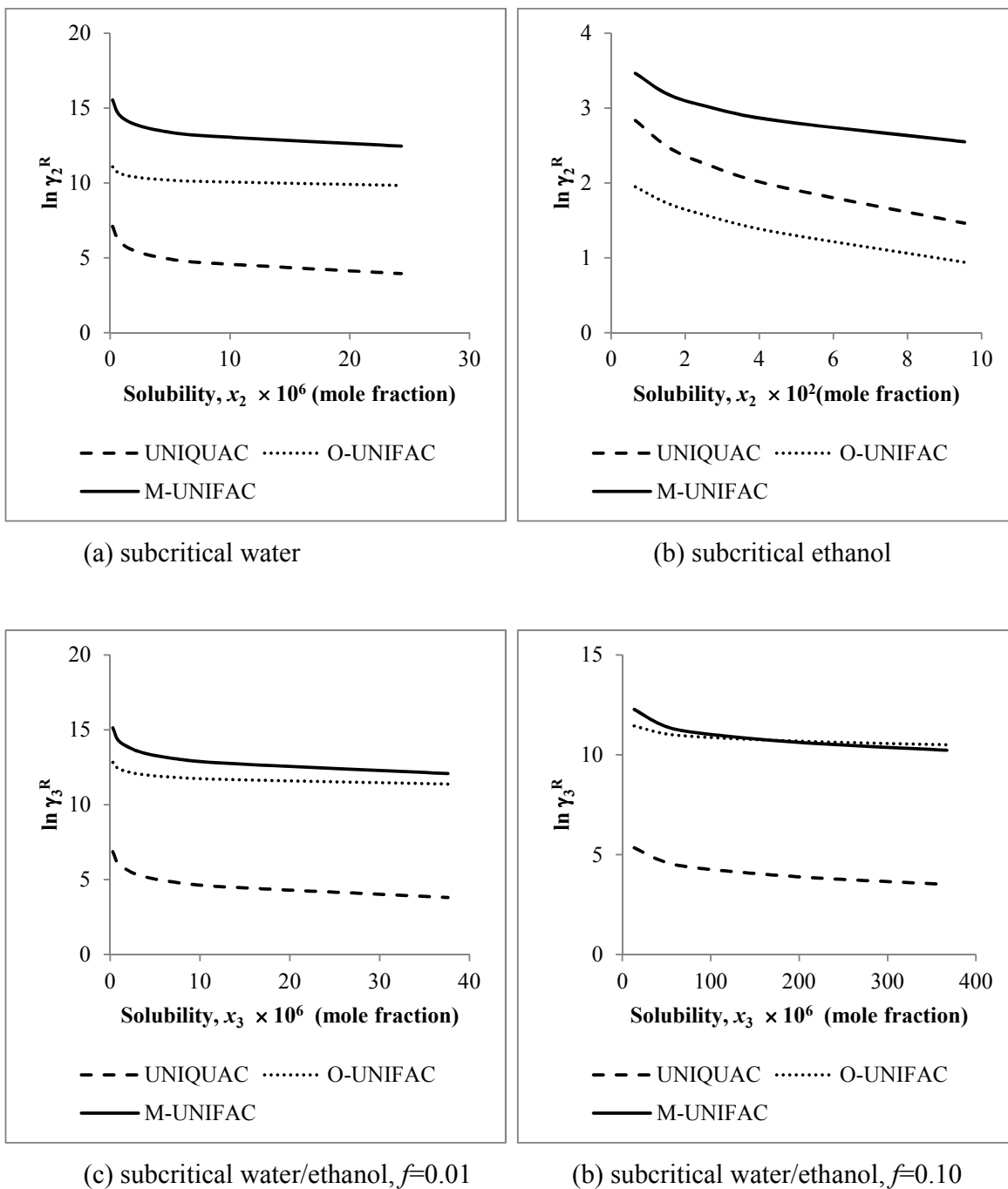


Figure 5.76: $\ln \gamma_2^R$ as a function of *p*-terphenyl solubility in various subcritical solvent systems

The systems investigated in this thesis are non-ideal, in that these systems involve non-polar solutes interacting with polar solvents that associate through hydrogen bonding. The failure of the O-UNIFAC to account for the substantial increase in solubility due to temperature change is understandable, given that the activity coefficient used in the original form of the UNIFAC model is not temperature-dependent. The M-UNIFAC model overcame this weakness with a temperature-dependent activity coefficient which, for all accounts, could reflect well the trend observed in experimental data (Figures 5.69 – 5.70). However, the M-UNIFAC model fell short in terms of its accuracy with error margins as high as 42% in comparison to experimental data. The UNIQUAC model, in its original form, shared the same energy interaction parameters with the O-UNIFAC, in which the lack of temperature-dependency of its energy parameters is already known. Thus, when the original form of the energy interaction parameters was first used in the present study together with the UNIQUAC model, the solubility trend observed was not representative of experimental data. The inclusion of a quadratic temperature function into the energy interaction parameters changed the quality of the UNIQUAC values and reduced the deviations to less than 7%. The small deviation was not surprising, since the energy interaction parameters were based on experimental data for binary systems.

In ternary systems, all three models tended to deviate further from experimental data as the concentration of ethanol increased. UNIQUAC and UNIFAC models had been shown to *not* represent the relationship between activity coefficient and concentration well [23]. The lack of concentration dependence of the group activity coefficient is reflected in this study wherein the calculated values deviate further with increasing ethanol and PAH concentrations. The reason could be that the interaction energies derived in the UNIQUAC/UNIFAC models were based on lattice theory and assumed to be concentration independent which might not describe the actual pair-distribution of solute-solvent involved over a wide concentration range [23].

All three models considered in this study are based upon the sums of two parts of activity coefficient: the combinatorial part which takes into account the difference in size and shape of the components, and the residual that takes into account the energetic effects. Of the three, the UNIQUAC model is based on interactions between *components* while the UNIFAC models are based upon interactions between functional *groups*. As both the UNIFAC models failed considerably in representing the SLE data in the highly non-ideal subcritical solvent systems, an

identification on the shortcomings of the models is necessary. Given that the UNIFAC models are to a certain extent, similar to the UNIQUAC model, in terms of being a sum of their combinatorial and residual activity coefficients, qualitative identification of the weakness in the UNIFAC models is made easier by breaking them into their combinatorial and residual terms, and by comparing them to the UNIQUAC model. Such comparison may, to a certain extent, shed light on the causality of the shortcomings; wherein molecular interactions (residual), size and shape (combinatorial), and/or additional associative factors come into question.

The UNIQUAC and the O-UNIFAC models share the same combinatorial term and identical surface and volume parameters. The combinatorial term, based upon the assumption that no association or solvation exists, takes *only* into consideration differences in size and shape. Hence, an examination on the combinatorial term of the two models found that the $\ln \gamma^C$ values calculated by the two models in subcritical *water* were almost similar [Figures 5.73(a) and 5.74(a)]. In subcritical ethanol, the $\ln \gamma^C$ of both models were quite similar at lower PAHs solubility, but diverged as the solubilities of PAHs increase [(Figures 5.73(b) and 5.74(b))]. Meanwhile, the $\ln \gamma^C$ for both models in ethanol-modified subcritical systems were found to be very far apart [(Figures 5.73(c,d) and 5.74(c,d))]. While it seems that the combinatorial activity coefficient in the UNIQUAC model is only based upon surface and volume parameters it is, in fact, affected by the residual part of the activity coefficient. It can be seen from Equations (5.13) and (5.24) that the concentration of the solutes, x_i , enters into both the combinatorial and residual parts. Since numerical iterations are involved in the calculation of solute solubility, and since solute solubility is partly affected by the residual term, the effect from the residual activity coefficient penetrates also into the combinatorial term.

For systems containing subcritical water, the residual term for the O-UNIFAC model was found to be considerably higher than the UNIQUAC model. Since it has already been established that the combinatorial terms for both O-UNIFAC and UNIQUAC are of similar values in the PAH-water system, it can only be deduced that the major cause of the shortcomings in the O-UNIFAC model comes from its residual term. In fact, the residual activity coefficient seemed to have been excessively estimated for systems containing subcritical water and PAHs. Hence, the O-UNIFAC model seemed to fail to account for molecular interactions in the mixtures, of which the H-bond and system polarity play significant roles. For PAH-subcritical water

systems, the residual term appeared to be overestimated; giving rise to lower solubility forecast. In PAH-subcritical ethanol systems, the residual term appeared to be underestimated yielding higher forecasted solubility values. Consequently, improvements to the O-UNIFAC model would require changes made to its residual term.

In the M-UNIFAC model, the combinatorial term was found to be much lower than the UNIQUAC model [Figures 5.73 -5.74]. The huge difference observed in the combinatorial term for the M-UNIFAC, in contrast to the UNIQUAC model is due to the surface and volume parameters that were dealt with empirically in the M-UNIFAC model. In contrast, the residual term for the M-UNIFAC model was found to be substantially higher than the UNIQUAC model. For water-containing systems, the sums of the combinatorial and the residual terms in the M-UNIFAC were found to exceed that of the UNIQUAC model. Meanwhile, the sums of the two activity coefficient terms in subcritical ethanol systems were found to be underestimated. Thereby, it can be deduced that the insufficiency of the residual term for both M- and O-UNIFAC in subcritical solvent systems, arose, because of their failure to account for changes in system polarity and the interaction between the components at higher temperature. Hence, the residual term in the M-UNIFAC model, as was in the case of the O-UNIFAC, requires a revision/modification.

Modifications to the UNIFAC models would require changes made to the residual term, or to include an additional term to account for system polarity and the associative effect among the solute and solvent molecules. Various modifications to the UNIFAC models have been undertaken along with many variations that adopted an association based activity coefficient term. Further investigation into the associative activity coefficient term would be required in the near future. However, as suggested by Fornari et al. [8], the association term would require a temperature-dependent term to provide substantial improvement to the UNIFAC models.

5.4 Conclusion

The results obtained show that the UNIQUAC model provides a good representation of the solubility of anthracene and *p*-terphenyl in ternary systems. Both the O-UNIFAC and the M-UNIFAC models performed poorly, mainly due to the inadequacy of the residual component of the activity coefficient. In ternary systems, all three models showed increasing deviations from experimental data as ethanol concentration increases. Further work is required to find a suitable non-empirical thermodynamic model for solubility calculation of PAHs in subcritical conditions.

5.5 Bibliography

- [1] Karasek P, Planeta J, Roth M. Solubility of solid polycyclic aromatic hydrocarbons in pressurized hot water at temperatures from 313K to the melting point. *Industrial & Engineering Chemistry Research* 2006;45 (12):4454-60.
- [2] Miller DJ, Hawthorne SB, Gizir AM, Clifford AA. Solubility of polycyclic aromatic hydrocarbons in subcritical water from 298 K to 498 K. *Journal of Chemical & Engineering Data* 1998;43 (6):1043-7.
- [3] Mathis J, Gizir AM, Yang Y. Solubility of alkylbenzenes and a model for predicting the solubility of liquid organics in high-temperature water. *Journal of Chemical & Engineering Data* 2004;49 (5):1269-72.
- [4] Abrams DS, Prausnitz JM. Statistical thermodynamics of liquid mixtures: A new expression for the excess Gibbs energy of partly or completely miscible systems. *AIChE Journal* 1975;21 (1):116-28.
- [5] Aage Fredenslund RLJMP. Group-contribution estimation of activity coefficients in nonideal liquid mixtures. *AIChE Journal* 1975;21 (6):1086-99.
- [6] Anderson TF, Prausnitz JM. Application of the UNIQUAC Equation to Calculation of Multicomponent Phase Equilibria. 1. Vapor-Liquid Equilibria. *Industrial & Engineering Chemistry Process Design and Development* 1978;17 (4):552-61.
- [7] Weidlich U, Gmehling J. A modified UNIFAC model. 1. Prediction of VLE, hE, and γ_{∞} . *Industrial & Engineering Chemistry Research* 1987;26 (7):1372-81.
- [8] Fornari T, Stateva RP, Señorans FJ, Reglero G, Ibañez E. Applying UNIFAC-based models to predict the solubility of solids in subcritical water. *The Journal of Supercritical Fluids* 2008;46 (3):245-51.
- [9] Arbuckle WB. Using UNIFAC to calculate aqueous solubilities. *Environmental Science & Technology* 1986;20 (10):1060-4.
- [10] Kikic I, Alessi P, Rasmussen P, Fredenslund A. On the combinatorial part of the UNIFAC and UNIQUAC models. *The Canadian Journal of Chemical Engineering* 1980;58 (2):253-8.
- [11] Gmehling J, Li J, Schiller M. A modified UNIFAC model. 2. Present parameter matrix and results for different thermodynamic properties. *Industrial & Engineering Chemistry Research* 1993;32 (1):178-93.
- [12] Gmehling Jr, Lohmann Jr, Jakob A, Li J, Joh R. A modified UNIFAC (Dortmund) model. 3. Revision and extension. *Industrial & Engineering Chemistry Research* 1998;37 (12):4876-82.
- [13] Gmehling J, Wittig R, Lohmann J, Joh R. A modified UNIFAC (Dortmund) model. 4. Revision and extension. *Industrial & Engineering Chemistry Research* 2002;41 (6):1678-88.
- [14] Prausnitz JM, Lichtenthaler RN, de Azevedo EG. *Molecular thermodynamics of fluid-phase equilibria*. Englewood Cliffs, N.J.: Prentice-Hall Inc., 1969.
- [15] Poling BE, Prausnitz JM, O'Connell JP. *The properties of gases and liquids*. New York: McGraw-Hill, 2001.
- [16] Zhao H, Unhannanant P, Hanshaw W, Chickos JS. Enthalpies of vaporization and vapor pressures of some deuterated hydrocarbons. Liquid-vapor pressure isotope effects. *J. Chem. Eng. Data* 2008;53:1545-56.

- [17] Gmehling J, Onken U. Vapor-liquid equilibrium data collection. Frankfurt: Dechema, 1977.
- [18] Gmehling JrG, Anderson TF, Prausnitz JM. Solid-liquid equilibria using UNIFAC. *Industrial & Engineering Chemistry Fundamentals* 1978;17 (4):269-73.
- [19] Lasdon LS, Waren AD, Jain A, Ratner M. Design and Testing of a Generalized Reduced Gradient Code for Nonlinear Programming. *ACM Trans. Math. Softw.* 1978;4 (1):34-50.
- [20] Voutsas EC, Pamouktsis C, Argyris D, Pappa GD. Measurements and thermodynamic modeling of the ethanol–water system with emphasis to the azeotropic region. *Fluid Phase Equilibria* 2011;308 (1–2):135-41.
- [21] Suzuki K, Sue H, Inomata H, Arai K, Saito S. The significant structure model equation of state extended to mixtures. *Fluid Phase Equilibria* 1990;58 (3):239-64.
- [22] Skjold-Jørgensen S, Rasmussen P, Fredenslund AA. On the temperature dependence of the UNIQUAC/UNIFAC models. *Chemical Engineering Science* 1980;35 (12):2389-403.
- [23] Skjold-Jørgensen S, Rasmussen P, Fredenslund A. On the concentration dependence of the UNIQUAC/UNIFAC models. *Chemical Engineering Science* 1982;37 (1):99-111.

6 Conclusion and Recommendations

A static analytical equilibrium method was utilized to measure the solubilities of anthracene and *p*-terphenyl in subcritical water and ethanol based mixtures. Highly reproducible solubility results were obtained. The solubilities of anthracene and *p*-terphenyl in subcritical water and ethanol based mixtures have been established to be highly dependent on temperature. In binary systems, the solubilities of PAHs in subcritical water and subcritical ethanol increase exponentially with temperature. In ternary systems involving the addition of ethanol as a modifier, the solubilities of PAHs were also found to increase exponentially with temperature and ethanol composition. In ethanol-modified subcritical water systems, sharp increases in solubility were observed between 140 °C and 160 °C, and at ethanol mole fraction, $f \geq 0.06$. In a ternary mixture consisting of two solids (anthracene and *p*-terphenyl in subcritical water), solubility depression was observed for anthracene at all temperatures, except at 150 °C, while solubility depression was observed for *p*-terphenyl at 120 °C and 140 °C.

The change in solubility with pressure for all subcritical water and ethanol-modified water systems considered in this study was insignificant in the range of pressures considered (50 – 150 bar) and the combined effect from temperature and pressure change was also negligible. It has also been shown that the sublimation pressure of the solid solutes influence their solubility in subcritical conditions while the dielectric constant of the solvent plays a secondary role. In all systems investigated, the solubility of *p*-terphenyl increased with temperature at a higher rate than anthracene. The rate with which the solubility of *p*-terphenyl increased with temperature in subcritical ethanol was found to be higher than in subcritical water while anthracene showed a lower rate in ethanol than in water. The difference in the rate of solubility increase with temperature for anthracene and *p*-terphenyl would allow for the specific extraction of compounds, by tuning both the subcritical solvents and temperature used.

Of the three activity coefficient-based thermodynamic models considered, the UNIQUAC model was found to provide the best representation of PAHs solubilities in subcritical water and ethanol mixtures. However, the highly predictive quality of the UNIQUAC model could only be realized with the inclusion of a quadratic temperature function into the energy interaction

parameters. Both the O-UNIFAC and the M-UNIFAC models performed poorly in all systems considered, mainly due to the inadequacy in the residual component of the activity coefficient. In subcritical water systems, both models rarely fall within the same order of magnitude as experimental data and could not account for the dramatic increase in solubility with temperature. A lack of temperature-dependent activity coefficient also contributed to the inability of the O-UNIFAC model to account for the dramatic rise in solubility with temperature. While all three models showed increasing deviation from experimental data with increasing ethanol concentration, the UNIQUAC model was found to be well within an average absolute standard deviation of 7%.

The deficiencies of the UNIFAC models would require improvement made to the residual terms with, perhaps an inclusion of an association based activity coefficient term. However, the associative term would require a temperature dependent component to provide for substantial improvement. While the UNIQUAC model provided good representation of experimental data, it is an empirical model that cannot be extended to other solutes or solvents beyond those considered here unless experimental data are available. Hence, further work is required to find a suitable non-empirical thermodynamic model for solubility calculations of organic solutes in subcritical conditions. Among others, the thermodynamic models considered must be able to account for the high pressure required in subcritical systems, and the hydrogen bonding that occurs within the solvent and solute molecules. Hence, equations of state with various mixing rules that account for associating hydrogen bonding can be used to test for their suitability in subcritical water and ethanol based systems.

The thermodynamic database for anthracene and *p*-terphenyl is extended in this thesis with the inclusion of ternary systems. The evaluation of PAHs solubilities in ternary systems is a step forward in understanding their behaviour in real life. However, a polluted matrix generally consists of tens to hundreds of components. Therefore, further investigation into higher order systems is required.

Appendix A

FT-IR Spectra

Appendix A1: FT-IR spectra of anthracene prior to, and after being subjected to experimental conditions

The IR spectra were recorded with a Thermo Nicolet 370 FTIR spectrometer on a KBr disc. The FTIR spectra of anthracene pre- and post-solubility measurements shown in Figures A.1 – A.4 do not show noticeable degradation of anthracene. The IR spectra for anthracene at 140 °C, 150 °C, 160 °C and 170 °C were not conducted. The reason being that the total mixing time for these temperatures are almost similar to that at 180 °C and, if no noticeable changes were observed at 180 °C, it was assumed that similar spectra would be observed for temperatures lower than 180 °C.

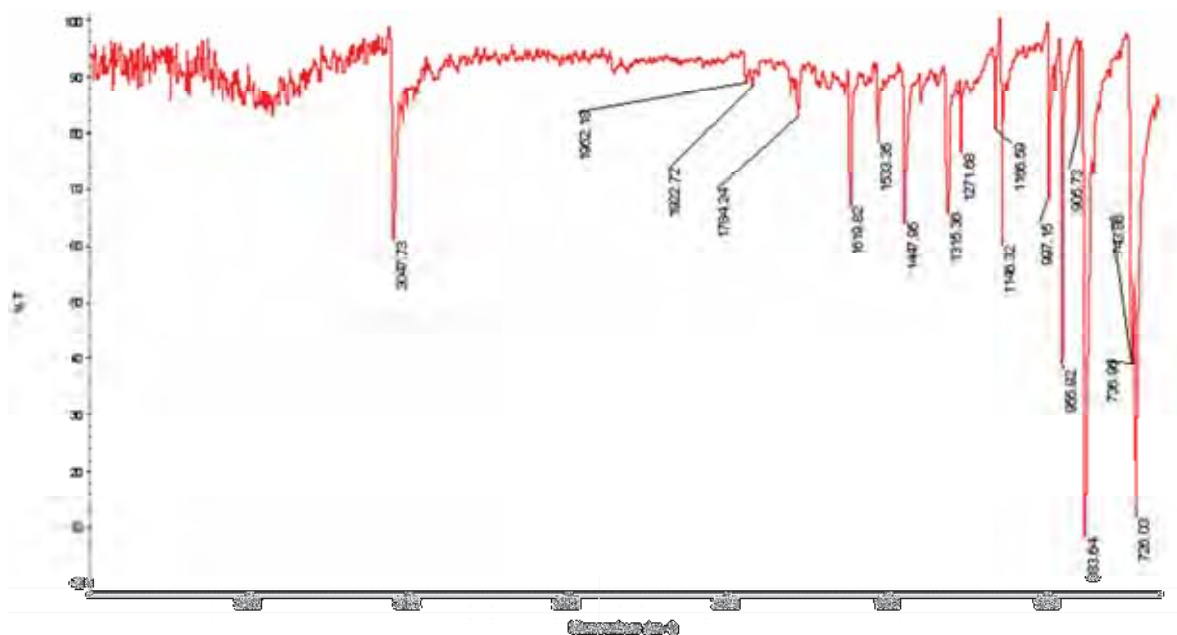


Figure A.1: FT-IR spectra of raw anthracene

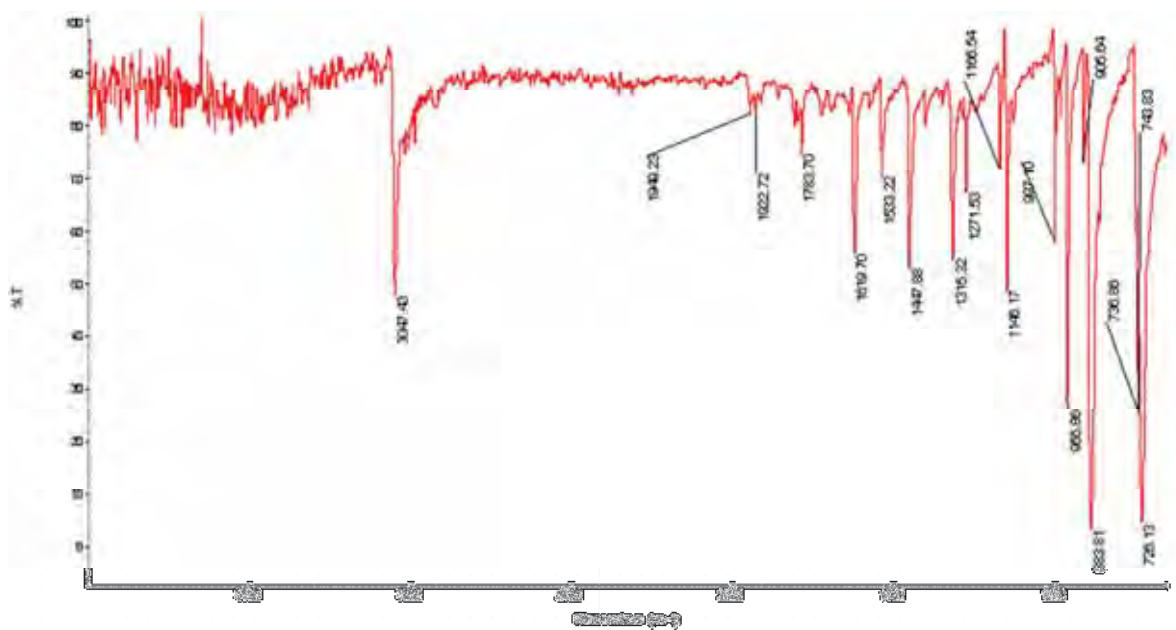


Figure A.2: FT-IR spectra of anthracene post solubility measurement in subcritical water at 120 °C, 50 bar and 197 minutes

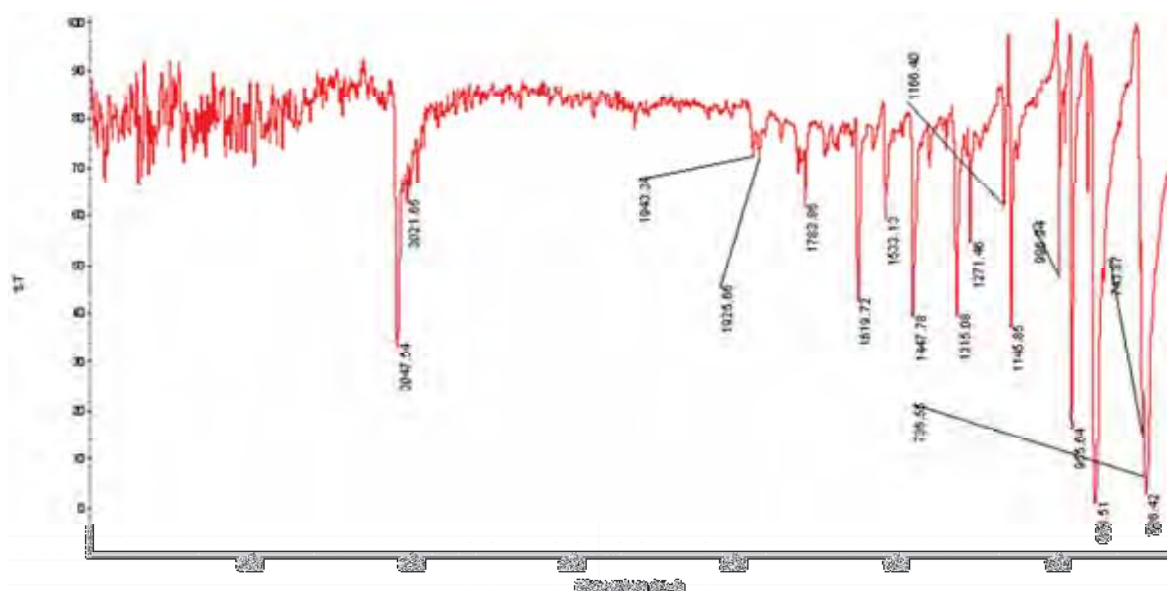


Figure A.3: FT-IR spectra of anthracene post solubility measurement in subcritical water at 180 °C, 50 bar and 63 minutes

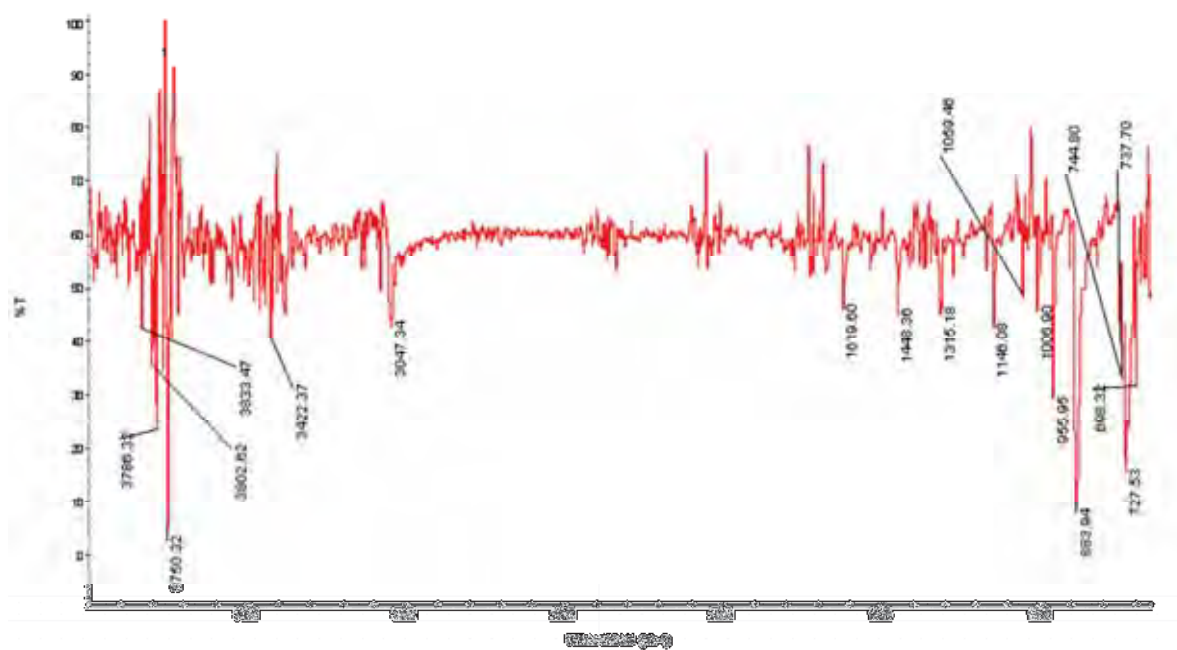


Figure A.4: FT-IR spectra of anthracene post solubility measurement in subcritical water at 200 °C, 50 bar and 50 minutes

Appendix A2: FT-IR spectra of *p*-terphenyl prior to, and after being subjected to experimental conditions

The IR spectra were recorded with a Thermo Nicolet 370 FTIR spectrometer on a KBr disc. The FTIR spectra of *p*-terphenyl pre- and post-solubility measurements shown in Figures A.5 – A.8 do not show noticeable degradation of *p*-terphenyl. The IR spectra for *p*-terphenyl at 140 °C, 150 °C, 160 °C and 170 °C were not conducted. The reason being that the total mixing time for these temperatures are almost similar to that at 180 °C and, if no noticeable changes were observed at 180 °C, it was assumed that similar spectra would be observed for temperatures lower than 180 °C.

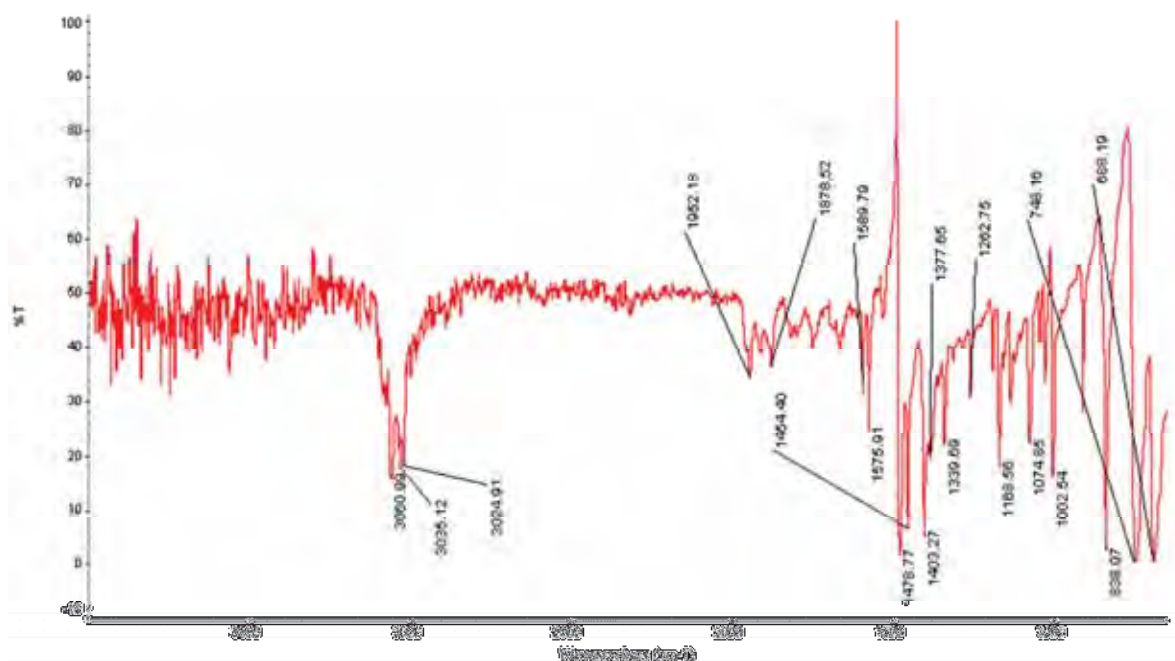


Figure A.5: FT-IR spectra of raw *p*-terphenyl

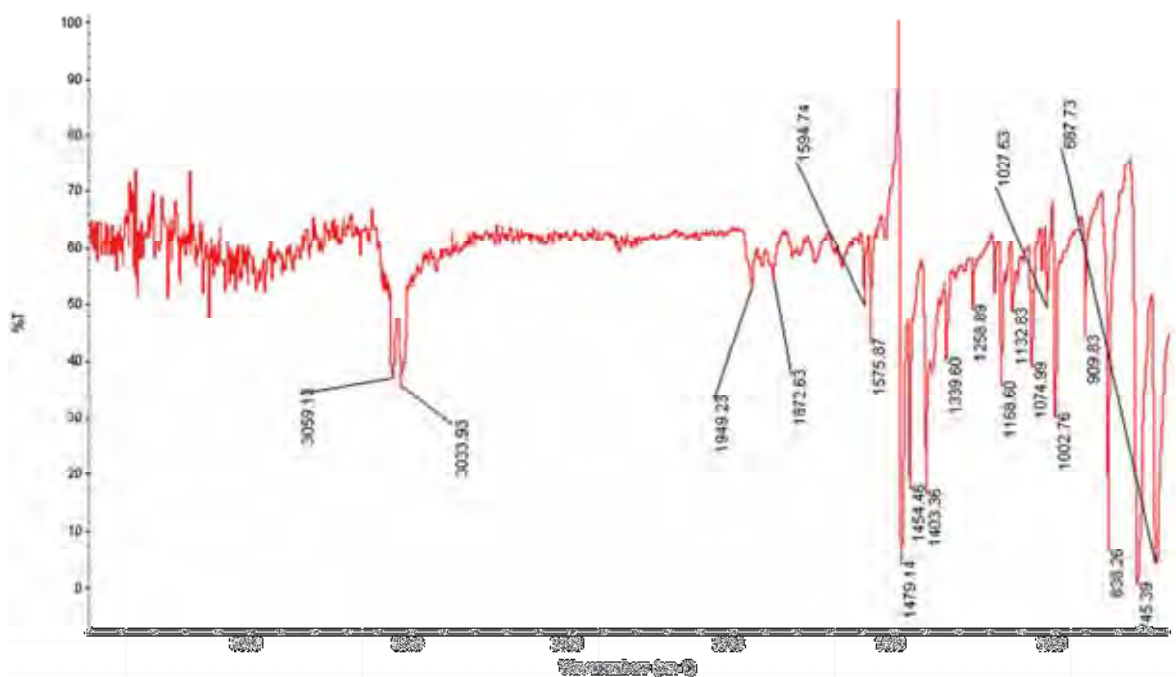


Figure A.6: FT-IR spectra of *p*-terphenyl post solubility measurement in subcritical water at 120 °C, 50 bar and 197 minutes

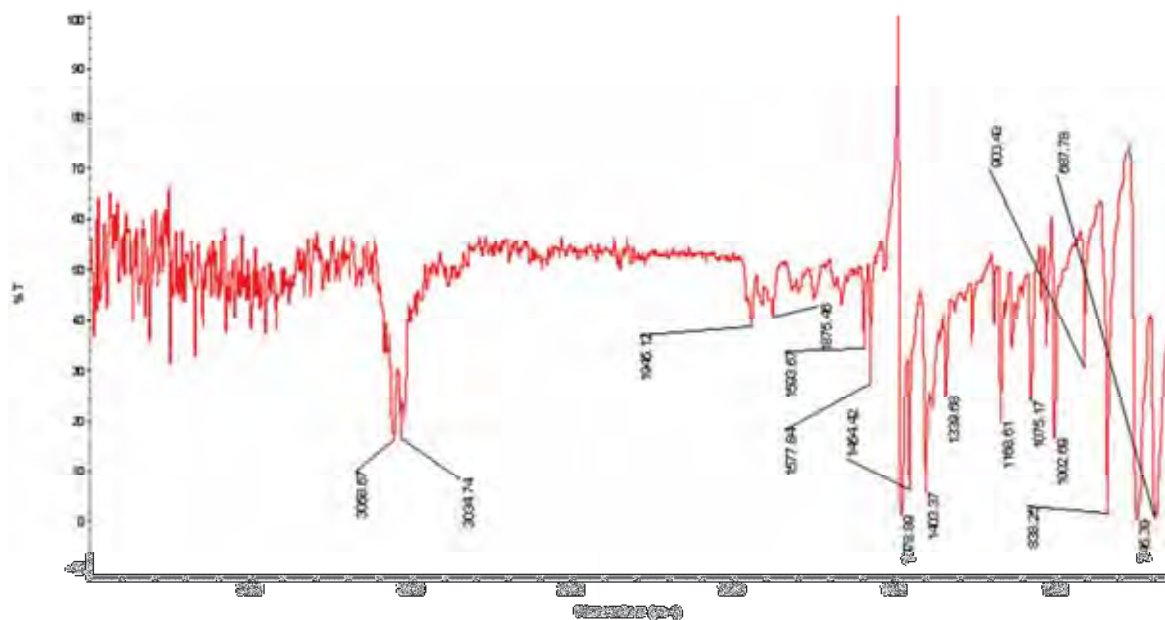


Figure A.7: FT-IR spectra of *p*-terphenyl post solubility measurement in subcritical water at 180 °C, 50 bar and 63 minutes

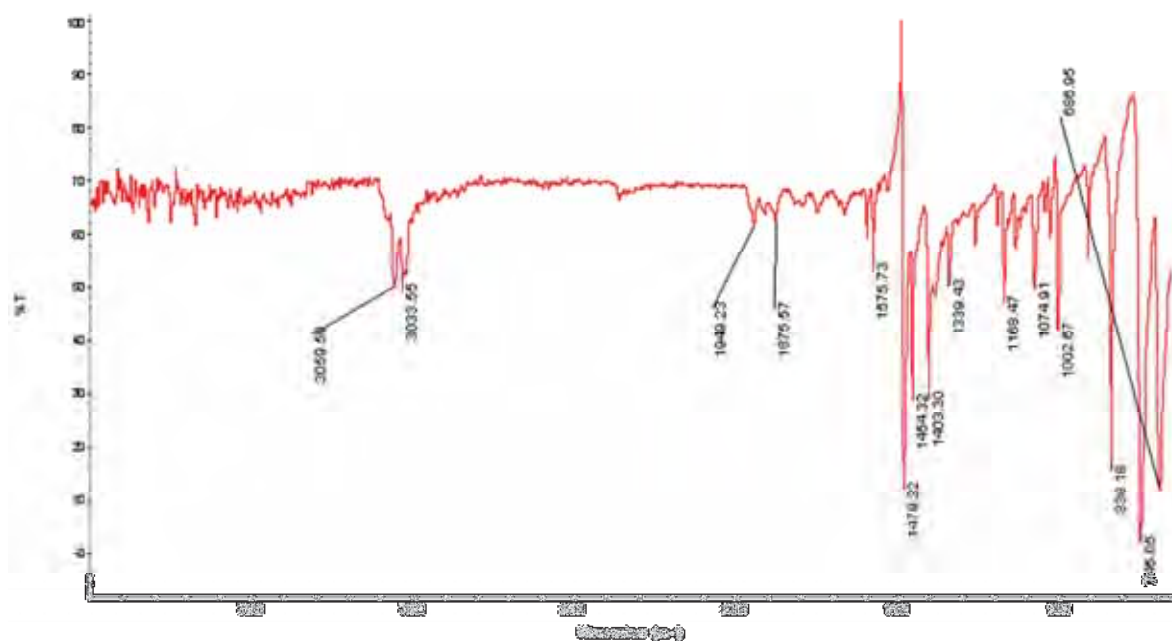


Figure A.8: FT-IR spectra of *p*-terphenyl post solubility measurement in subcritical water at 200 °C, 50 bar and 50 minutes

Appendix B

Calibration curves

Appendix B1: UV-VIS calibration curve generated for anthracene in methanol

The following Figure B.1 is a five-point calibration curve generated to determine the amount of anthracene collected for solubility measurement. The calibration curve for anthracene dissolved in analytical grade methanol was obtained based on the 356 nm peak absorbance.

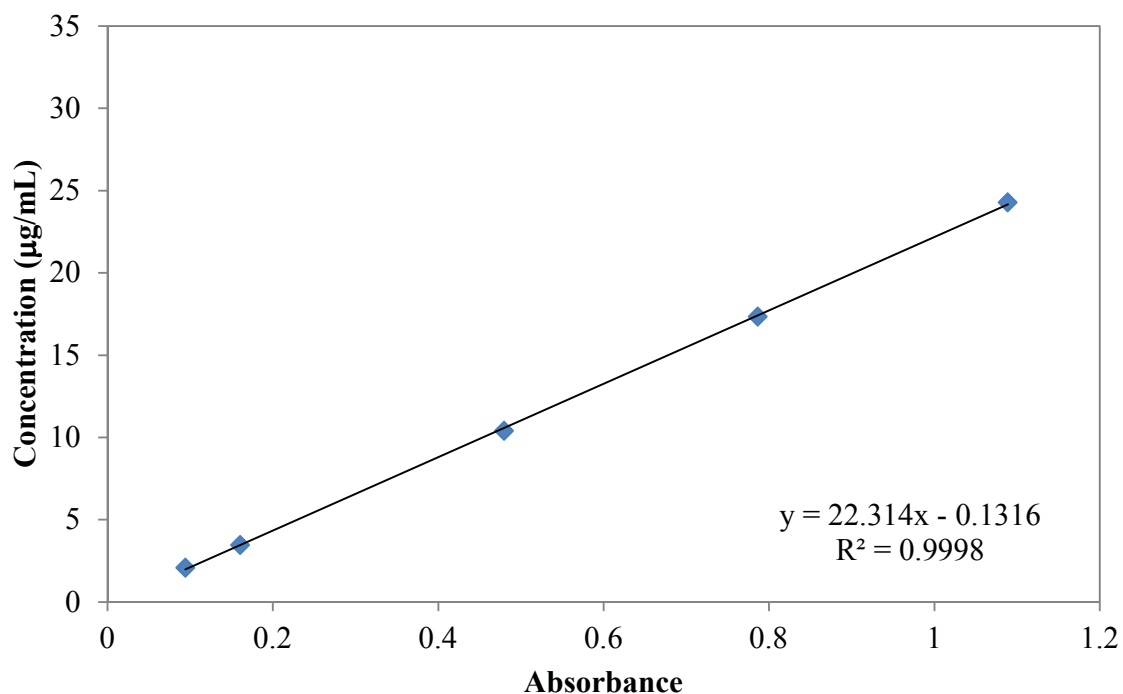


Figure B.1: Calibration curve of anthracene in methanol at 356 nm

Appendix B2: UV-VIS calibration curve generated for *p*-terphenyl in methanol

The following Figure B.2 is a five-point calibration curve generated to determine the amount of *p*-terphenyl collected in the collection vessel. *p*-Terphenyl was dissolved in analytical grade methanol with the calibration curve based on the 278 nm peak absorbance.

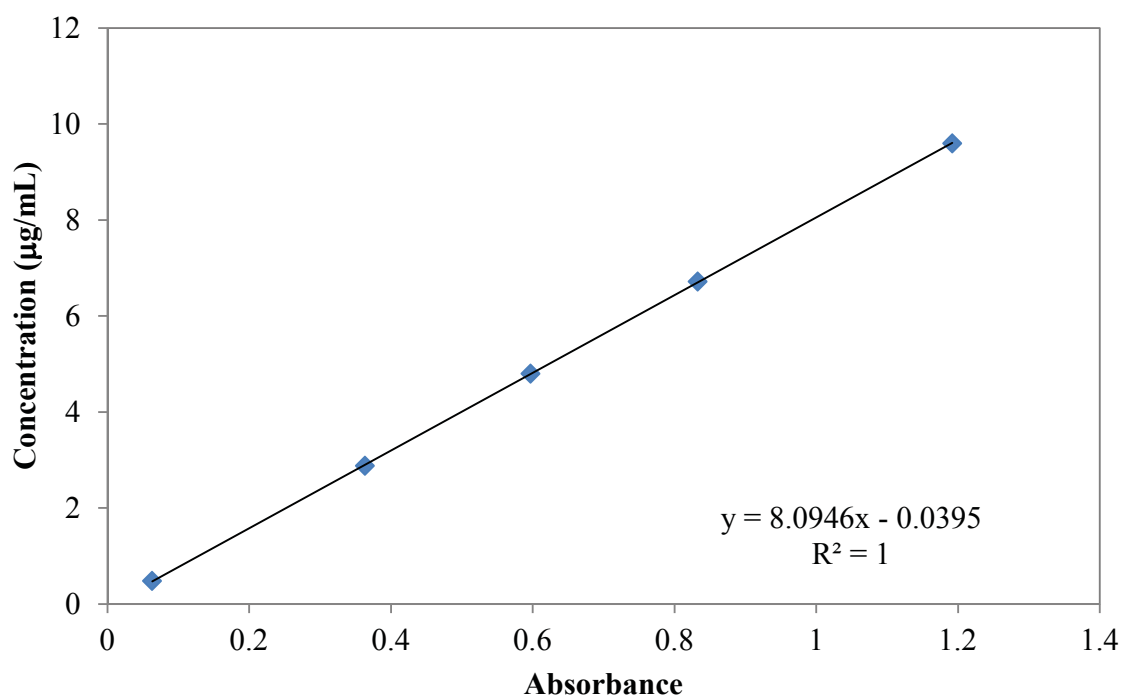


Figure B.2: Calibration curve of *p*-terphenyl in methanol at 278 nm

Appendix B3: RP-HPLC calibration curve for anthracene dissolved in acetonitrile

Figure B.3 is a five-point calibration curve generated to determine the amounts of anthracene collected in the ternary solubility studies of anthracene and *p*-terphenyl in subcritical water. The calibration curve is based on the 357 nm peak absorbance area of anthracene.

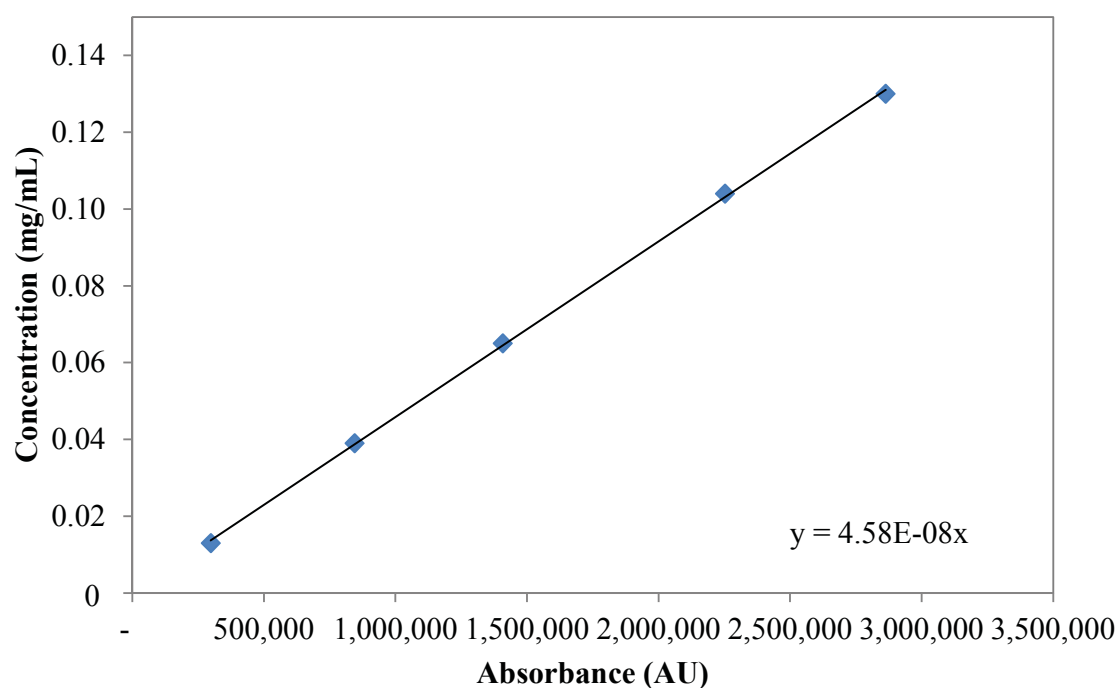


Figure B.3: Calibration curve of anthracene in acetonitrile at 357 nm

Appendix B4: RP-HPLC calibration curve generated for *p*-terphenyl dissolved in acetonitrile

Figure B.4 shows the point calibration curve generated to determine the amount of *p*-terphenyl dissolved in HPLC-grade acetonitrile. The calibration curve was based on the 298 nm peak absorbance area.

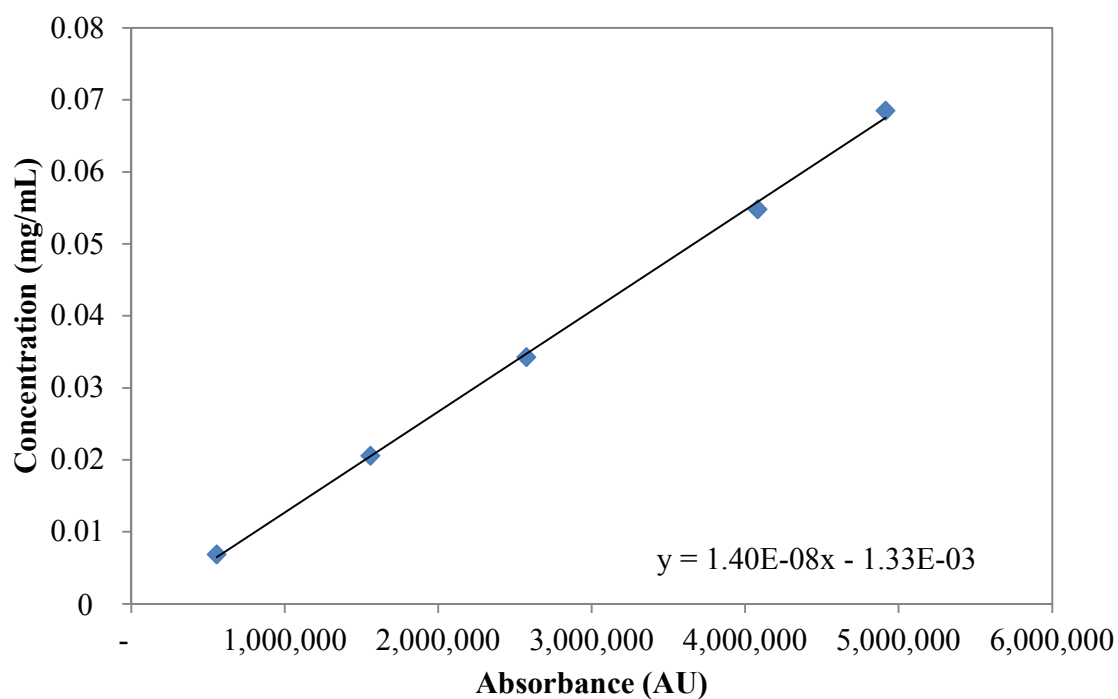


Figure B.4: Calibration curve of *p*-terphenyl in acetonitrile at 279 nm